

CHAPTER 2: STRUCTURAL EVALUATION

This chapter presents a synopsis of the evaluations carried out to establish the mechanical and structural characteristics of the HI-STAR 100 package as they pertain to demonstrating compliance with the provisions of 10CFR71. All required structural design analyses of the packaging, components, and systems Important to Safety (ITS) pursuant to the provisions of 10CFR71 are documented in this chapter. The objectives of this chapter are twofold:

- a. To demonstrate that the structural performance of the HI-STAR 100 package has been adequately evaluated for the conditions specified under normal conditions of transport and hypothetical accident conditions.
- b. To demonstrate that the HI-STAR 100 package design has adequate structural integrity to meet the regulatory requirements of 10CFR71 [2.1.1].

To facilitate regulatory review, the assumptions and conservatism inherent in the analyses are identified along with a complete description of the analytical methods, models, and acceptance criteria. A summary of other considerations germane to satisfactory structural performance, such as corrosion and material fracture toughness is also provided.

~~Detailed numerical computations supporting the conclusions in the main body of this chapter are further supplemented through a series of appendices. Where appropriate, the text within the chapter makes reference to the information contained in the appendices. Section 2.10 contains the complete list of appendices that support this chapter.~~

This SAR is written to conform to the requirements of NUREG-1617 and 10CFR71 and follows the format of Regulatory Guide 7.9 [1.0.3]. It is noted that the areas of NRC staff technical inquiries with respect to 10CFR71 structural compliance span a wide array of technical topics within and beyond the material in this chapter. To facilitate the staff's review, Table 2.0.1 "Matrix of NUREG-1617/10CFR71 Compliance - Structural Review", is included in this chapter. A comprehensive cross-reference of the topical areas set forth in Section 2.3.2 (Regulatory Requirements) of the draft Regulatory Guide 1617, along with the sponsoring paragraphs in 10CFR71, and the location of the required compliance information, within this SAR, is contained in Table 2.0.1.

Section 2.10.2 contains a summary of the evaluation findings derived from the technical information presented in this chapter.

TABLE 2.0.1- MATRIX OF NUREG-1617/10CFR71 COMPLIANCE – STRUCTURAL REVIEW†

SECTION IN NUREG-1617 AND APPLICABLE 10CFR71/REG.GUIDE (R.G.) SECTIONS	NUREG-1617/10CFR71 COMPLIANCE ITEM	LOCATION IN SAR CHAPTER 2	LOCATION OUTSIDE OF SAR CHAPTER
2.3.1 Description of Structural Design			
10CFR71.31(a)(1); 10CFR71.33	Description of Structural Design	2.1	1.2.3
10CFR71.33	Drawings		1.4
10CFR71.33	Weights and Center of Gravity	2.2	
10CFR71.31(c)	Applicable Codes/Standards		1.3
2.3.2 Material Properties			
10CFR71.33	Materials and Material Specifications	2.3	
10CFR71.33	Prevention of Chemical, Galvanic, or Other Reactions	2.4	
10CFR71.43(d)	Effects of Radiation on Materials	2.4.4	

TABLE 2.0.1- MATRIX OF NUREG-1617/10CFR71 COMPLIANCE – STRUCTURAL REVIEW (Continued)

SECTION IN NUREG-1617 AND APPLICABLE 10CFR71/REG.GUIDE (R.G.) SECTIONS	NUREG-1617/10CFR71 COMPLIANCE ITEM	LOCATION IN SAR CHAPTER 2	LOCATION OUTSIDE OF SAR CHAPTER
R.G 7.11, 7.12	Brittle Fracture	2.1.2.3	
2.3.3 Lifting and Tie Down Standards for All Packages			
10CFR71.45(a)	Lifting Devices	2.5; 2.A; 2.B; 2.S; 2.T; 2.AG	1.4
10CFR71.45(b)	Tie-Down Devices	2.5; 2.C; 2.R	1.4
2.3.4 General Considerations for Structural Evaluation of Packaging			
10CFR71, Subpart E,F	Evaluation by Analysis		
10CFR71.35(a), 71.41(a)	• Models, Methods, and Results	2.6, 2.7.1, 2.7.2	
10CFR71, Subpart E,F	• Material Properties	2.3	
“	• Boundary Conditions	2.6	
“	• Dynamic Amplifiers	2.K 2.6, 2.7	
“	• Load Combinations	2.1	
“	• Margins of Safety	2.5, 2.6, 2.7	

TABLE 2.0.1- MATRIX OF NUREG-1617/10CFR71 COMPLIANCE – STRUCTURAL REVIEW (Continued)

SECTION IN NUREG-1617 AND APPLICABLE 10CFR71/REG.GUIDE (R.G.) SECTIONS	NUREG-1617/10CFR71 COMPLIANCE ITEM	LOCATION IN SAR CHAPTER 2	LOCATION OUTSIDE OF SAR CHAPTER
10CFR71, Subparts E,F	Evaluation by Test		
10CFR71.73(a)	• Procedures for Impact Testing	2.7.1; 2.H 2.A	
“	• Test Specimens	2.7.1; 2.H 2.A	
10CFR71.73(c)(1)	• Drop Orientations	2.7.1; 2.H 2.A	
“	• Conclusions	2.7.1; 2.H 2.A	
2.3.5 Normal Conditions of Transport			
10CFR71.71 with reference to 10CFR71 sections 71.35(a), 71.43(f), 71.51(a)(1), 71.55(d)(4)	Heat	2.6.1; 2.D ; 2.E ; 2.F ; 2.J ; 2.L ; 2.N ; 2.O ; 2.Q ; 2.U ; 2.AC ; 2.AE	
“	Cold	2.6.2; 2.AE ; 2.AI ; 2.AJ ; 2.AK	
“	Reduced External Pressure	2.6.3	
“	Increased External Pressure	2.6.4	
“	Vibration	2.6.5	
“	Water Spray	2.6.6	
“	Free Drop	2.6.1; 2.6.2; 2.6.7 ; 2.AE	
“	Corner Drop	NA	NA
“	Compression	NA	NA
“	Penetration	NA	NA

TABLE 2.0.1- MATRIX OF 10CFR71 COMPLIANCE – STRUCTURAL REVIEW (Continued)

SECTION IN NUREG-1617 AND APPLICABLE 10CFR71/REG.GUIDE (R.G.) SECTIONS	NUREG-1617/10CFR71 COMPLIANCE ITEM	LOCATION IN SAR CHAPTER 2	LOCATION OUTSIDE OF SAR CHAPTER
2.3.6 Hypothetical Accident Conditions			
10CFR71.73(c)(1)	Free Drop	2.7.1, 2.A; 2.I; 2.J; 2.L; 2.N; 2.O; 2.U; 2.AC; 2.AE; 2.AF; 2.AH; 2.AO	
10CFR71.73(c)(2)	Crush	NA	NA
10CFR71.73(c)(3)	Puncture	2.7.2; 2.U	
10CFR71.73(c)(4)	Thermal	2.7.3; 2.G; 2.J; 2.L; 2.N	
10CFR71.73(c)(5)	Immersion-Fissile Material	2.7.4	NA
10CFR71.73(c)(6)	Immersion – All Material	2.7.5; 2.J	
2.3.7 Special Requirements for Irradiated Nuclear Fuel Shipments			
10CFR71.61	Elastic Stability of Containment	2.7.5; 2.J	
“	Closure Seal Region Below Yield Stress	2.7.12.AE	
2.3.8 Internal Pressure Test			
10CFR71.85(b)	Internal Pressure Test – All stresses below yield	2.6.1.4.3	8.1

TABLE 2.0.1- MATRIX OF 10CFR71 COMPLIANCE – STRUCTURAL REVIEW (Continued)

SECTION IN 10CFR71	10CFR71 COMPLIANCE ITEM	LOCATION IN SAR CHAPTER 2	LOCATION OUTSIDE OF SAR CHAPTER
Appendices			
	Supplemental Information	2.10	

† Legend for Table 2.0.1

Per the nomenclature defined in Chapter 1, the first digit refers to the chapter number, the second digit is the section number within the chapter; an alphabetic character in the second place means it is an appendix to the chapter.

NA Not Applicable for this item

2.1 STRUCTURAL DESIGN

2.1.1 Discussion

The HI-STAR 100 System (also designated as the HI-STAR 100 Package) consists of three principal components: the multi-purpose canister (MPC), the overpack assembly, and a set of impact limiters. The overpack confines the MPC and provides the containment boundary for transport conditions. The MPC is a hermetically sealed, welded structure of cylindrical profile with flat ends and an internal honeycomb fuel basket for SNF. A complete description of the HI-STAR MPC is provided in Section 1.2.1.2.2 wherein its design and fabrication details are presented with the aid of figures. A detailed discussion of the HI-STAR 100 overpack is presented in Subsection 1.2.1.2.1. Detailed *drawings* for the HI-STAR 100 System are provided in Section 1.4. In this section, the discussion is directed to characterizing and establishing the structural features of the MPC and the transport overpack.

The design of the HI-STAR 100 MPC seeks to attain three objectives that are central to its functional adequacy, namely;

- **Ability to Dissipate Heat:** The thermal energy produced by the spent fuel must be transported to the outside surface of the MPC such that the prescribed temperature limits for the fuel cladding and the fuel basket metal walls are not exceeded.
- **Ability to Withstand Large Impact Loads:** The MPC with its payload of nuclear fuel must be sufficiently robust to withstand large impact loads associated with the hypothetical accident conditions during transportation of the system. Furthermore, the strength of the MPC must be sufficiently isotropic to assure structural qualification under a wide variety of drop orientations.
- **Restraint of Free End Expansion:** The membrane and bending stresses produced by restraint of free end expansion of the fuel basket are conservatively categorized as primary stresses. In view of the concentration of heat generation in the fuel basket, it is necessary to ensure that structural constraints to its external expansion do not exist.

Where the first two criteria call for extensive inter-cell connections, the last criterion requires the opposite. The design of the HI-STAR 100 MPC seeks to realize all of the above three criteria in an optimal manner.

As the description presented in Chapter 1 indicates, the MPC enclosure vessel is a spent nuclear fuel (SNF) pressure vessel designed to meet ASME Code, Section III, Subsection NB stress limits. The enveloping canister shell, the MPC baseplate, and the closure lid system form a complete closed pressure vessel referred to as the "enclosure vessel". This enclosure vessel serves as the helium retention boundary when the HI-STAR 100 is within the purview of 10CFR71. Within this cylindrical vessel is an integrally welded assemblage of cells of square cross sectional openings, referred to herein as the "fuel basket". The fuel basket is analyzed under the provisions of Subsection NG of Section III of the ASME Code. There are different multi-purpose canisters that are exactly alike in their external dimensions. The essential difference between the MPCs lies in the fuel baskets. Each fuel storage MPC is designed to house fuel assemblies with

different characteristics. Although all HI-STAR 100 MPC fuel baskets are configured to maximize structural ruggedness through extensive inter-cell connectivity, they are sufficiently dissimilar in structural details to warrant separate evaluations. Therefore, analyses for the different MPC types are presented, as appropriate, throughout this chapter.

The HI-STAR 100 overpack provides the containment function for the stored SNF. There is an undivided reliance on the structural integrity of this containment vessel to maintain complete isolation of its contained radioactive contents from the environment under all postulated accident scenarios, even though the MPC is a completely autonomous, ASME Section III Class 1 pressure vessel which provides an unbreachable enclosure for the fuel. The containment boundary is made up of the inner shell, the bottom plate, the top flange, and the closure plate.

Components of the HI-STAR 100 System that are important to safety and their applicable design codes are defined in Chapter 1.

The structural function of the MPC in the transport mode is:

1. To maintain position of the fuel in a sub-critical configuration.
2. To maintain a helium confinement boundary.

The structural function of the overpack in the transport mode is:

1. To serve as a penetration and puncture barrier for the MPC.
2. To provide a containment boundary.
3. To provide a structurally robust support for the radiation shielding.

The structural function of the impact limiters in the transport mode is:

1. To cushion the HI-STAR 100 overpack and the contained MPC with fuel during normal transport handling and in the event of a hypothetical drop accident during transport.

Some structural features of the MPCs that allow the system to perform their structural functions are summarized below:

- There are no external or gasketed ports or openings in the MPC. The MPC does not rely on any sealing arrangement except welding. The absence of any gasketed or flanged joints precludes joint leaks. The MPC enclosure vessel contains no valves or other pressure relief devices.
- The closure system for the MPCs consists of two components, namely, the MPC lid and the closure ring. The MPC lid is a thick circular plate continuously welded to the MPC shell along its

circumference. The MPC closure system is shown in the ~~Design Drawings~~ *drawings* in Section 1.4. The MPC lid-to-MPC shell weld is a J-groove weld that is subject to root and final pass liquid penetrant examinations and finally, a volumetric examination to ensure the absence of unacceptable flaws and indications. The MPC lid is equipped with vent and drain ports which are utilized for evacuating moisture and air from the MPC following fuel loading and subsequent backfilling with an inert gas (helium) in a specified quantity. The vent and drain ports are covered by a cover plate and welded before the closure ring is installed. The closure ring is a thin circular annular plate edge-welded to the MPC shell and to the MPC lid. Lift points for the MPC are provided in the MPC lid.

- The MPC fuel basket consists of an array of interconnecting plates. The number of storage cells formed by this interconnection process varies depending on the type of fuel being transported. Basket designs for different PWR and BWR cell configurations have been designed and are explained in detail in Subsection 1.2. All baskets are designed to fit into the same MPC shell. Welding the plates along their edges essentially renders the fuel basket into a multi-flange beam. For example, Figure 2.1.1 provides an isometric illustration of a fuel basket for the MPC-68 design.
- The MPC basket is separated from the longitudinal supports installed in the enclosure vessel by a small gap. The gap size decreases as a result of thermal expansion (depending on the magnitude of internal heat generation from the stored spent fuel). The provision of a small gap between the basket and the basket support structure is consistent with the natural thermal characteristics of the MPC. The planar temperature distribution across the basket, as shown in Chapter 3, approximates a shallow parabolic profile. This profile will create high thermal stresses unless structural constraints at the interface between the basket and the basket support structure are removed.

The MPCs will be loaded with fuel assemblies with widely varying heat generation rates. The basket/basket support structure gap tends to be reduced for higher heat generation rates due to increased thermal expansion rates. The basket/basket support structure gap tends to be reduced due to thermal expansion from decay heat generation. Gaps between the fuel basket and the basket support structure are specified to be sufficiently large such that a gap exists around the periphery under all normal or accident conditions of transport.

A small number of optional flexible thermal conduction elements (thin aluminum tubes) may be interposed between the basket and the MPC shell. The elements are designed to be resilient. They do not provide structural support for the basket, and thus their resistance to thermal growth is negligible.

Structural features of the overpack that allow the HI-STAR 100 package to perform its safety function are summarized below:

- The overpack features a thick inner shell welded to a bottom plate which forms a load bearing surface for the HI-STAR 100 System. A solid metal top flange welded at the top of the inner shell provides the attachment location for the lifting trunnions. The top flange is designed to provide a recessed ledge for the closure plate to protect the bolts from direct shear loading resulting from an impulsive load at the top edge of the overpack (Figure 2.1.2). In the transport mode the overpack

inner shell, bottom plate, top flange, and closure plate with metallic seals constitute the containment boundary for the HI-STAR 100 System. The HI-STAR 100 overpack is subject to the stress limits of the ASME Code, Section III, Subsection NB [2.1.5].

- The inner shell (containment boundary) is reinforced by multi-layered intermediate shells. The multi-layer approach eliminates the potential for a crack in any one layer, developed by any postulated mechanical loading or material flaw, to travel uninterrupted through the vessel wall. The intermediate shells also buttress the overpack inner shell against buckling. The intermediate shells of the HI-STAR 100 overpack are subject to the stress limits of the ASME Code, Section III, Subsection NF, Class 3 [2.1.7].
- To facilitate handling of the loaded package, the HI-STAR 100 overpack is equipped with two lifting trunnions at the top of the overpack. ~~and may be equipped with two optional pocket trunnions near the base. The initial seven HI-STAR 100 overpacks are equipped with The optional pocket trunnions, are embedded in the overpack intermediate shells, just above the bottom plate. HI-STAR 100 overpacks fabricated after the initial seven do not have pocket trunnions (see Subsection 2.5 for further discussion). The centerline through the pocket trunnion is offset from a vertical plane containing the overpack's center of gravity to ensure a stable rotation direction if the pocket trunnions are employed for upending and downending.~~ Lifting trunnions are conservatively designed to meet the design safety factor requirements of NUREG-0612 [2.1.9] and ANSI N14.6-1993 [2.1.10] for single failure proof lifting equipment.
- A circular recess is incorporated on the inner surface of the overpack closure plate. The purpose of this recess is to reduce the moment applied to the flanged joint from MPC impact during a hypothetical top end drop accident. During a hypothetical drop accident where the top end of the overpack impacts first, the MPC contacts the inner surface of the overpack closure plate. Because of the recess, the MPC will only contact an annular region of the inner surface of the overpack closure plate. Thus, the load on the overpack closure plate from the MPC is located closer to the bolt circle, and the moment on the flanged joint is reduced.
- A small circular gap between the MPC external surface and the inside surface of the overpack is provided to allow insertion and removal of the MPC. This gap diminishes monotonically with the increase in the heat generation rate in the MPC, but is sized to avoid metal-to-metal contact between the MPC and the overpack cylindrical surface as a result of thermal expansion under the most adverse thermal conditions.
- There are no valves in the HI-STAR 100 overpack containment boundary. The vent and drain ports used during HI-STAR 100 overpack loading and unloading operations are closed with port plugs and metallic seals. The port plugs are recessed and are suitably protected with a cover plate with seal. These small penetrations equipped with dual seals are not deemed to be particularly vulnerable locations in the HI-STAR 100 System.

The HI-STAR 100 System is equipped with a set of impact limiters (AL-STAR) attached to the top and bottom ends of the overpack. The structural function of the impact limiters is to cushion the HI-STAR 100 overpack and the contained MPC with fuel in the event of a hypothetical drop accident during transport, and to provide the necessary resistance to the longitudinal decelerations experienced during normal rail transport. The design of the impact limiter is independent of the design of the MPC and overpack. This is achieved by establishing design basis deceleration limits for normal transport and for the hypothetical 30-foot drop accident and demonstrating that impact limiter performance limits the deceleration levels imposed on the cask.

Table 1.3.3 provides a listing of the applicable design codes for all structures, systems, and components that are designated as Important to Safety (ITS).

2.1.2 Design Criteria

Regulatory Guide 7.6 provides design criteria for the structural analysis of shipping casks [2.1.4]. Loading conditions and load combinations that must be considered for transport are defined in 10CFR71 [2.1.1] and in USNRC Regulatory Guide 7.8 [2.1.2]. Consistent with the provisions of these documents, the central objective of the structural analysis presented in this chapter is to ensure that the HI-STAR 100 System possesses sufficient structural capability to meet the demands of normal conditions and hypothetical accident conditions of transport.

The following table provides a synoptic matrix to demonstrate our explicit compliance with the seven regulatory positions stated in Regulatory Guide 7.6.

REGULATORY GUIDE 7.6 COMPLIANCE	
Regulatory Position	Compliance in HI-STAR 100 SAR
1. Material properties, design stress intensities, and fatigue curves are obtained from the ASME Code	Tables 2.1.12-2.1.20 for allowable stresses/stress intensities and Tables 2.3.1-2.3.5 for material properties are obtained from the ASME Code (the 1995 Code tables are used). Section 2.6.1.3.3 uses the appropriate fatigue data from the Code.
2. Under normal conditions of transport, the limits on stress intensity are those limits defined by the ASME Code for primary membrane and for primary membrane plus bending for Level A conditions.	Tables 2.1.3-2.1.5 define the correct stress intensity limits for normal conditions of transport as stated in the ASME Code for Level A conditions.
3. Perform fatigue analysis for normal conditions of transport using ASME Code Section III methodology (NB) and appropriate fatigue curves.	Section 2.6.1.3.3 considers the potential for fatigue using accepted ASME Code methodology and fatigue data from the ASME Code.
4. The stress intensity S_n associated with the range of primary plus secondary stresses under normal conditions should be less than $3S_m$ where S_m is the primary membrane stress intensity from the Code.	Section 2.6.1.3.3 considers the fatigue potential of the HI-STAR 100 Package based on the $3S_m$ limit.

REGULATORY GUIDE 7.6 COMPLIANCE	
Regulatory Position	Compliance in HI-STAR 100 SAR
5. Buckling of the containment vessel should not occur under normal or accident conditions.	The methodology used is Code Case N-284; this has been accepted by the NRC as an appropriate vehicle to evaluate buckling of the containment.
6. Under accident conditions, the values of primary membrane stress intensity should not exceed the lesser of $2.4S_m$ and $0.7S_u$ (ultimate strength), and primary membrane plus bending stress intensity should not exceed the lesser of $3.6S_m$ and S_u .	Tables 2.1.3-2.1.5 of the SAR state these requirements.
7. The extreme total stress intensity range should be less than S_a at 10 cycles as given by the appropriate fatigue curves.	Subsection 2.6.1.3.3 demonstrates compliance by conservatively bounding the total stress intensity range and demonstrating that the bounding value is less than S_a at 10 cycles as given by the appropriate fatigue curves.

Note that Regulatory Guide 7.6 references ASME Code Sections in the 1977 code year. This SAR has been prepared using the identical information on allowable stress intensities and fatigue data as listed in the 1995 ASME Code.

Table 1.3.1, in Chapter 1, summarizes the ASME pressure vessel code applicability to HI-STAR 100 components. Table 1.3.2 in Chapter 1 provides a statement of exceptions taken to the ASME Code requirements.

Stresses arise in the components of the HI-STAR 100 System due to various loads that originate under normal and hypothetical accident conditions of transport. These individual loads are combined to form load combinations. Stresses and stress intensities resulting from the load combinations are compared to allowable stresses and stress intensities. The following subsections present loads, load combinations, and allowable strengths for use in the structural analyses of the MPC and the HI-STAR 100 overpack.

2.1.2.1 Loading and Load Combinations

10CFR71 and Regulatory Guide 7.6 define two conditions that must be considered for qualification of a transport package. These are defined as "Normal Conditions of Transport" and "Hypothetical Accident Conditions", which are related herein to the ASME Code Service Levels for the purposes of quantifying allowable stress limits. In terms of the ASME terminology, the following parallels are applicable.

Normal Conditions of Transport = ASME Design Condition and ASME Level A or B Service Condition

Hypothetical Accident Condition = ASME Level D Service Condition

To establish the appropriate loadings and load combinations that require evaluation, the pressure and temperatures used for the design analyses must be defined. Table 2.1.1 establishes the design pressures for the two transport conditions that must be evaluated. Table 2.1.2 establishes reference hot temperature limits

for the two conditions of transport. The ASME Code does not prescribe a metal temperature limit for Level D (also called "faulted") conditions. Under the provisions of the ASME Code, large strains (such as deformations resulting from a thermal shock) are acceptable if the post-event structural configuration of the component is within the limits prescribed for it subsequent to the faulted event (ASME Code Section III, Subsection NCA-2142.4). In the case of the cask, *it iswe required* that the containment boundary continues to perform its function and that the outer skin continues to provide an enclosure for the radiation shielding. For conservatism, the peak metal bulk temperature during and after the fire transient in the overpack containment structure is required to be limited to the maximum temperature limit prescribed in the ASME Section II Part D allowable stress /stress intensity tables. That is, the maximum bulk metal temperature is equal to the maximum temperature for which the allowable stress intensity, S_m , is listed in the Code for the applicable Code Class. For the external skin of the overpack that is directly exposed to the fire no specific temperature limits are enforced by the governing documents. The performance expectation of the HI-STAR 100 package, however, is that the skin does not melt, slump, or sever from the overpack structure. This performance objective is considered to be fulfilled with adequate margin if the metal temperature of the enclosure shell at any section does not exceed 50% of the melting point of the shell material. Tables 2.1.3 and 2.1.4 set forth the allowable strength bases for the two conditions of transport based on their designation as Level A, B, or D.

For its qualification as an acceptable packaging component, the following types of loads are defined for the HI-STAR 100 MPC.

- Dead load (lb.), D ;
- Internal design pressure (psi), P_i ;
- External design pressure (psi), P_o ;
- Accident internal pressure (psi), P_i^* ;
- Accident external pressure (psi), P_o^* ;
- Thermal load due to design basis heat generation in the MPC, T , and under most adverse external environmental conditions, T' ;
- Side drop at 0° basket circumferential orientation under normal conditions of transport, H ;
- Side drop at 45° basket circumferential orientation under normal conditions of transport, H ;
- Drop at 0° fuel basket circumferential orientation under design basis deceleration for hypothetical accident conditions, H' (angle of inclination that the package longitudinal axis makes with the horizontal plane varies);

- Drop at 45° fuel basket circumferential orientation under design basis deceleration for hypothetical accidental conditions, H'(angle of inclination that the package longitudinal axis makes with the horizontal plane varies);
- Vertical drop under design basis deceleration for hypothetical accident conditions, H'.

Insofar as the fuel basket is not radially symmetric, the orientation of the basket cross section with respect to the direction of side drop will affect the state of stress induced by the deceleration produced by the impact. Heretofore, two horizontal drop circumferential orientations are considered which are referred to as the 0 degree drop and 45 degree drop, respectively. *Figures 2.1.3 and 2.1.4, showing an MPC-68 fuel basket, illustrate the two orientations.* In the 0-degree drop, the basket drops with its two sets of panels, respectively, parallel and normal to the vertical (Figure 2.1.3). The 45-degree drop implies that the basket's honeycomb section is rotated meridionally by 45 degrees (Figure 2.1.4).

For the above loads, a series of load combinations for the fuel baskets and the enclosure vessel are compiled in Tables 2.1.6 and 2.1.7, respectively. These load combinations represent both normal conditions of transport and the hypothetical accident conditions.

The loadings and load combinations applicable to the overpack are more numerous, because all external loads directly bear on it and several potentially limiting oblique drop orientations exist. In the following, each individual overpack loading which enters in subsequent load combinations is explained.

- **Internal Design Pressure, P_i :** An internal design pressure is defined for the containment cavity of the overpack pressure vessel (Figure 2.1.5). The coincident external pressure is assumed to be atmospheric (0 psig) (Table 2.1.1). ~~The design value is based on conservatively assuming that the MPC enclosure vessel is breached.~~
- **External Design Pressure, P_o :** An external design pressure with the cavity depressurized (0 psig) is defined for the overpack pressure vessel as the second design condition loading (Figure 2.1.6),(Table 2.1.1).
- **Accident External Pressure, P_o^* :** An external accident design pressure with cavity depressurized (Figure 2.1.6)(Table 2.1.1). This loading in conjunction with the buckling analysis of the overpack inner shell, is intended to demonstrate that the containment boundary is in compliance with the requirements of 10CFR71.61. This loading condition bounds the external pressure specified by 10CFR71.73(c)(5) and (6).
- **Accident Internal Pressure, P_i^* :** An internal accident design pressure is defined for the containment cavity of the overpack pressure vessel (Figure 2.1.5). The coincident external pressure is assumed to be atmospheric (0 psig) (Table 2.1.1). ~~The design value is based on conservatively assuming that the MPC enclosure vessel is breached.~~

- **Thermal Conditions:** Thermal conditions pertain to the stresses that develop due to thermal gradient in the overpack. The temperature field in the overpack under the maximum heat generation scenario is developed in Chapter 3. The effect of this temperature field, T_h , is included in all load cases, as appropriate.

The condition where the overpack is subject to a -40°F ambient environment and maximum decay heat is labeled as T_s . Likewise, the condition when the overpack is subject to a -20°F ambient environment is denoted by T_c . Finally, the thermal load during and after 30 minutes of exposure to a 1475°F enveloping fire is referred to as T_f .

- **Overpack Joint Sealing Load, W_s :** The pre-load applied to the overpack closure plate bolts seat the metallic seals and create a contact pressure on the inside land which serves to protect the joint from leakage under postulated impact loading events. The bolt pre-load, however, produces a state of stress in the overpack top closure plate, the overpack top flange, and the overpack inner and intermediate shell region adjacent to the flange. The pre-load, W_s , is, therefore, treated as a distinct loading type.
- **Fabrication Loads, F:** The internal loads induced due to the method of fabrication employed in building the overpack are included in the load combinations.
- **Bottom End Drop, D_{ba} :** This is the first of six drop accident scenarios, wherein the packaging is assumed to drop vertically with its overpack bottom plate sustaining the impulsive load transmitted through the bottom impact limiter. The weight of the package is included in all drop load cases. A schematic of the external forces working on the overpack under this drop scenario is illustrated in Figure 2.1.7. The deceleration load under the 30 ft drop event (accident event) is labeled D_{ba} . (The design basis deceleration is given in Table 2.1.10).
- **Top End Drop, D_{ta} :** This drop condition is the opposite of the preceding case. The top closure plate withstands the impact load transmitted through the impact limiter. This loading is illustrated in Figure 2.1.8. The design basis deceleration is given in Table 2.1.10.
- **Side Drop, D_{sn} and D_{sa} :** The overpack along with its contents drops with its longitudinal axis horizontal. The loaded MPC bears down on the overpack as it decelerates under the resistance offered by the two impact limiters pressing against an essentially unyielding surface (Figure 2.1.9). The subscripts "n" and "a" denote normal transport and hypothetical accident conditions, respectively. The design basis deceleration is given in Table 2.1.10.
- **Bottom C.G.-Over-the-Corner Drop, D_{ca} :** In this drop scenario, the HI-STAR 100 System is assumed to impact an essentially unyielding surface with its center-of-gravity directly above its bottom corner (Figure 2.1.10) under the hypothetical drop accident condition. The design basis deceleration is given in Table 2.1.10.

- **Top Center-of-Gravity Over-the-Corner Drop, D_{ga} :** This loading case is identical to the preceding case, except that the package is assumed to be dropping with its top end down and its center-of-gravity is aligned with the corner of the top closure plate (Figure 2.1.11). The design basis deceleration is given in Table 2.1.10.
- **Side Puncture Force Event, P_s :** This event consists of a free drop of the packaging for 1 meter (40 in.) on to a stationary and vertical mild steel bar of 6 in. diameter with its leading edge (top edge) rounded to 1/4 in. radius. The bar is assumed to be of such a length as to cause maximum damage to the overpack. The package is assumed to be dropping horizontally with the penetrant force being applied at the mid-length of the cask (Figure 2.1.12).
- **Top End Puncture Force, P_t :** This event is similar to the preceding case except the penetrant force is assumed to act at the center of the top closure plate (Figure 2.1.13).
- **Bottom End Puncture Force, P_b :** This is the third of the bar puncture events configured to create a condition of maximum damage to the package. The loading event is identical to the preceding two cases, except that the puncture load acts on the center of the bottom plate of the overpack (Figure 2.1.14).
- **Vibration and Shock, V :** Vibration and shock loads arise during transport of the packaging. The vibratory loads transmitted to the HI-STAR 100 System will produce negligibly small stresses in comparison with stresses that will be produced by the loadings described previously. Therefore, this loading is neglected in the analyses performed herein.

The foregoing loadings are combined in the manner of Table 1 of Regulatory Guide 7.8 to form four (4) distinct load combinations for the normal condition of transport and nineteen (19) load combinations for the hypothetical accident conditions. These load combinations are summarized in Tables 2.1.8 and 2.1.9.

Two concluding observations are relevant with respect to a Flange Seating Condition and to the External Pressure Condition:

- **Flange Seating Condition:** The stress field in the overpack under the bolt pre-stress load condition is evaluated with the elastic constants of the finite element gridwork in the overpack set at its coincident hot environment condition (100°F ambient). The bolt pre-load and material elastic constants under the cold environment condition (-20°F) will be different, resulting in a slightly different stress field. However, the consequence of this refinement is considered to be a second order effect and is, therefore, neglected.
- **External Pressure Condition:** The condition of 20 psia external pressure in Table 1 of Regulatory Guide 7.8 is conservatively bounded by the deep submergence pressure under 200 meters of water. Likewise, the internal design pressure of 100 psig with outside at ambient is assumed to conservatively bound the minimum external pressure (3.5 psia) service condition.

In the load cases considered (Tables 2.1.6-2.1.9), material behavior is always considered to be linearly elastic. To facilitate review, the following matrix is provided to relate the load combinations specifically addressed in Table 1 of Regulatory Guide 7.8 to the load combinations defined in this SAR by Tables 2.1.6-2.1.9. Also included in the matrix are locations in the SAR where particular results are presented that are germane to demonstrating compliance with the intent of Regulatory Guide 7.8.

Compliance of HI-STAR 100 SAR With Regulatory Guide 7.8 Load Combinations		
Reg. Guide Load Combination	HI-STAR 100 Explicit Load Combination (Tables 2.1.6-2.1.9)	Location in SAR for Results
NORMAL CONDITIONS		
Hot Environment	Table 2.1.7(Case E1.c) Table 2.1.8(Case 1)	2.6.1.3.1.2; Tables 2.6.6,2.6.7 Table 2.6.5; Table 2.6.9
Cold Environment	Table 2.1.8(Case 2)	Table 2.6.12
Increased External Pressure	Table 2.1.9 (Case 18 bounds)	2.6.4
Minimum External Pressure	---	2.6.3
Vibration and Shock	---	2.6.5
One-Foot Free Drop	Table 2.1.6(Case F2) Table 2.1.7(Case E2) Table 2.1.8(Cases 3,4)	Tables 2.6.2,2.6.8 Table 2.6.3 Tables 2.6.9,2.6.12
ACCIDENT CONDITIONS		
Thirty-Foot Free Drop	Table 2.1.6(Case F3) Table 2.1.7(Case E3) Table 2.1.9(Cases 1-5;9-13)	Tables 2.7.1,2.7.4,2.7.7 Tables 2.7.2,2.7.4,2.7.7 Tables 2.7.3,2.7.5,2.7.6-2.7.8
Puncture by Bar	Table 2.1.9(Cases 6-8;14-16)	Tables 2.7.3,2.7.5,2.7.6-2.7.8
Fire Accident	Table 2.1.9(Cases 17,19)	Tables 2.7.3,2.7.8

2.1.2.2 Allowables

Components of the HI-STAR 100 System Important to Safety (ITS) are listed in Table 1.3.3. Allowable stresses are tabulated for these components for all applicable service levels. The applicable service level from the ASME Code for determination of allowables is listed in Subsection 2.1.2.1.2.1.2.1.

Allowable stress limits for the overpack containment structure and for the MPC enclosure vessel are obtained from the ASME Code, Section III, Division 1, Subsection NB [2.1.5]. The MPC fuel basket is subject to the stress limits of ASME Section III, Division 1, Subsection NG [2.1.6].

All noncontainment parts of the overpack (e.g., intermediate shells, outer enclosure shells, radial channels), are subject to the stress limits of ASME Section III, Subsection NF [2.1.7] for mechanical loadings. The overpack containment boundary and the MPC enclosure vessel are also evaluated for stability in accordance with ASME Code Case N-284 [2.1.8]. Overpack closure bolts are subject to the stress limits of ASME Section III, Subsection NB. Finally, lifting trunnions and other lifting components are subject to the stress limits of NUREG-0612 [2.1.9], which references ANSI N14.6 [2.1.10].

Allowable stresses and stress intensities are calculated using the data provided in the ASME Code, Section II, Part D [2.1.11] and Tables 2.1.3 through 2.1.5. Tables 2.1.11 through 2.1.20 contain numerical values of the allowable stresses/stress intensities for all MPC and overpack load-bearing materials as a function of temperature.

In all tables, the terms S_m , S_y , and S_u , respectively, denote the design stress intensity, minimum yield strength, and the ultimate strength. Property values at intermediate temperatures that are not reported in the ASME Code are obtained by linear interpolation as allowed by paragraph NB-3229. Property values are not extrapolated beyond the limits of the Code in any structural analysis.

Additional terms relevant to the analyses are extracted from the ASME Code (Figure NB-3222-1) as follows.

<u>Symbol</u>	<u>Description</u>	<u>Notes</u>
P_m	Average primary stress across a solid section.	Excludes effects of discontinuities and concentrations. Produced by pressure and mechanical loads.
P_L	Average stress across any solid section.	Considers effects of discontinuities but not concentrations. Produced by pressure and mechanical loads, including inertia earthquake effects.
P_b	Primary bending stress.	Component of primary stress proportional to the distance from the centroid of a solid section. Excludes the effects of discontinuities and concentrations. Produced by pressure and mechanical loads, including inertia earthquake effects.
P_e	Secondary expansion stress.	Stresses which result from the constraint of free-end displacement. Considers effects of discontinuities but not local stress concentration. (Not applicable to vessels.)
Q	Secondary membrane plus bending stress.	Self-equilibrating stress necessary to satisfy continuity of structure. Occurs at structural discontinuities. Can be caused by pressure, mechanical loads, or differential thermal expansion.
F	Peak stress.	Increment added to primary or secondary stress by a concentration (notch), or, certain thermal stresses that may cause fatigue but not distortion. This value is not used in the tables.

It is shown in this report that there is no interference between component parts due to free thermal expansion. Therefore, P_e does not develop within any HI-STAR 100 component. A summary of the allowable limits for normal conditions of transport and for the hypothetical accident conditions as they apply to various components of the package is presented in Table 2.1.3 for the overpack and MPC enclosure vessel (shell, lid, and baseplate), in Table 2.1.4 for the MPC fuel basket, and in Table 2.1.5 for the noncontainment parts of the overpack.

It is recognized that the planar temperature distribution in the fuel basket and the overpack under the maximum heat load condition is the highest at the cask center and drops monotonically, reaching its lowest value at the outside surface. Strictly speaking, the allowable stresses/stress intensities at any location in the basket, the enclosure vessel, or the overpack should be based on the coincident metal temperature under the specific operating condition. However, in the interest of conservatism, reference temperatures may be established for each component that are upper bounds on the metal temperature for each situational condition. Table 2.1.21 provides the reference temperatures for the MPC and the overpack and, utilizing Tables 2.1.11 through 2.1.20, provides conservative numerical limits for the stresses and stress intensities for all loading cases.

Summarizing the previous discussions, in accordance with the Regulatory Guide 7.6 and with ASME Code Section III, Subsection NB, the allowable stress limits for the overpack containment boundary are based on design stress intensities (S_m), yield strengths (S_y) and ultimate strengths (S_u). These limits govern the design of the overpack (including the inner shell, the top flange, the bottom plate, and the closure plate), and also govern the design of the MPC enclosure vessel. The stress limits for the MPC fuel basket are based on stress intensities as set forth in ASME, Section III, Subsection NG. For applicable accident conditions, Appendix F of the ASME Code applies [2.1.12]. Stress limits for closure bolts conform to those given in Table 2.1.24.

The lifting devices in the HI-STAR 100 overpack and the multi-purpose canisters, collectively referred to as "trunnions", are subject to specific limits set forth by NUREG-0612: the primary stresses in a trunnion must be less than the smaller of 1/10 of the material ultimate strength and 1/6 of the material yield strength while loaded by the lifted load that includes an appropriate dynamic load amplifier.

The region around the trunnion is part of the NF structure in HI-STAR 100 and an NB pressure boundary in the MPC, and as such, must satisfy the applicable stress (or stress intensity) limits for the load combination. In addition to meeting the applicable Code limits, it is further required that the local primary stresses at the trunnion/mother structure interface must not exceed the material yield stress at three times the handling condition load. This criterion eliminates the potential of local yielding at the trunnion/structure interface.

Impact limiters are not designed to any stress or deformation criteria. Rather, their function is solely to absorb the impact energy by plastic deformation. The impact limiter must perform its energy absorption function over the range of environmental temperatures.

Allowable stresses derived from other authoritative sources are summarized in Table 2.1.24.

2.1.2.3 Brittle Fracture Failure

The MPC canister and basket are constructed from a series of stainless steels termed Alloy X. These stainless steel materials do not undergo a ductile-to-brittle transition in the minimum temperature range of the HI-STAR 100 System. Therefore, brittle fracture is not a concern for the MPC components. However, the HI-STAR 100 overpack is composed of ferritic steel materials, which will be subject to impact loading in a cold environment and, therefore, must be evaluated and/or subjected to impact testing in accordance with the ASME Code to ensure protection against brittle fracture.

Tables 2.1.22 and 2.1.23 provide the fracture toughness test criteria for the HI-STAR 100 overpack components in accordance with the applicable ASME Codes and Regulatory Guide requirements for prevention of brittle fracture. Regulatory Guides 7.11 [2.1.13] and 7.12 [2.1.14] are used to determine drop test requirements for the containment boundary components, as discussed below.

All containment boundary materials subject to impact loading in a cold environment must be evaluated and/or tested for their propensity for brittle fracture. The overpack baseplate, top flange, and closure plate have thicknesses greater than four inches. Table 1 of Regulatory Guide 7.12 requires that the Nil Ductility Transition temperature, T_{NDT} (for the lowest service temperature of -20°F), be -129°F for 6-inch thick material, and linear interpolation of the table shows that for 7-inch thick material, the T_{NDT} is -132°F . SA350-LF3 has been selected as the material for these overpack components based on the material's capability to perform at low temperatures with excellent ductility properties.

The overpack inner shell has a thickness of 2.5 inches. SA203-E has been selected as the material for this item due to its capability to perform at low temperatures (Table A1.15 of ASME Section IIA. Regulatory Guide 7.11 requires that the T_{NDT} for this material be less than -70°F (at the lowest service temperature of -20°F).

The overpack closure plate bolts are fabricated from SB-637 Grade N07718, a high strength nickel alloy material. Section 5 of NUREG/CR-1815 [2.1.15] indicates that bolts are generally not considered a fracture critical component. Nevertheless, this material has a high resistance to fracture at low temperatures, as can be shown by calculating the transition temperature of the material and assessing its performance as indicated in NUREG/CR-1815.

The Aerospace Structural Metals Handbook [2.1.16] shows that minimum impact absorption energy for SB-637 Grade N07718 at -320°F is 18.5 ft-lb. This may be transferred into a fracture toughness value by using the relationship (presented in Section 4.2 of NUREG/CR-1815) between Charpy impact measurement, C_v (ft-lb), and dynamic fracture toughness, K_{ID} (psi $\sqrt{\text{in.}}$)

$$K_{ID} = (5 E C_v)^{1/2}$$

where $E = 31 \times 10^6$ psi at -320°F and C_v (minimum) = 18.5 ft-lb.

Therefore,

$$K_{ID} = 53.5 \text{ ksi}\sqrt{\text{in.}}$$

Using Figure 2 of NUREG/CR-1815 yields

$$(T - T_{NDT}) = 32 \text{ degrees F}$$

Since the data used is for $T = -320^{\circ}\text{F}$, then $T_{NDT} = -320^{\circ}\text{F} - 32^{\circ}\text{F} = -352^{\circ}\text{F}$

Using Figure 3 of NUREG/CR-1815 where thickness is defined as the bolt diameter (1.5 inch), and $\sigma/\sigma_{yd} = 1$ per Regulatory Guide 7.11, A (degrees F) is found to be 60 degrees F. Therefore, the required maximum nil ductility transition temperature per NUREG/CR-1815 for the closure bolts is:

$$\begin{aligned} T_{NDT} &= T_{LT} - A \\ &= -40^{\circ} - 60^{\circ} = -100^{\circ}\text{F} \end{aligned}$$

where T_{LT} = lowest temperature of -40°F (conservatively below the lowest service temperature).

The large margin between the calculated T_{NDT} and the required maximum Nil Ductility Transition temperature leads to the conclusion that SB-637 Grade N07718 possesses appropriate fracture toughness for use as closure lid bolting.

ASME Code Section III, Subsection NF requires Charpy V-notch tests for materials of certain noncontainment components of the overpack. The intermediate shells used for gamma shielding are fabricated from normalized SA516-70. Table A1.15 of ASME Section IIA shows that normalized SA516-70 should have minimum energy absorption of 12 ft-lb at -40°F for a Charpy V-notch test. The lowest anticipated temperature the overpack is to experience is conservatively set at -40°F . Therefore, these tests on the normalized SA516-70 materials of the intermediate shells will confirm the minimum energy absorption of 12 ft-lb at -40°F and the ability of the intermediate shells to perform their intended function at the lowest service temperature.

The pocket trunnions *in the initial seven HI-STAR 100 overpacks* are fabricated from 17-4PH (or equivalent) material that is precipitation hardened to condition H1150. ARMCO Product Data Bulletin S-22 [2.1.17] shows that Charpy V-notch testing of 17-4PH H1150 material at -110°F gives energy absorption values of approximately 48 ft-lbs. Using the same methodology as used for the closure bolts,

$$K_{ID} = 83 \text{ ksi}\sqrt{\text{in.}}$$

where $E = 28.7 \times 10^6$ psi and $C_v = 48$ ft-lbs.

Using Figure 2 of NUREG/CR-1815 yields

$$T - T_{NDT} = 65^{\circ}\text{F}$$

and therefore

$$T_{\text{NDT}} = -110^{\circ}\text{F} - 65^{\circ}\text{F} = -175^{\circ}\text{F}$$

While the optional pocket trunnions are not part of the containment for the overpack, Regulatory Guide 7.12 is used to define the required T_{NDT} for the trunnion pocket thickness ($T_{\text{NDT}} = -140^{\circ}\text{F}$). The 35°F margin between the calculated T_{NDT} and the T_{NDT} defined in Regulatory Guide 7.12 provides assurance that brittle fracture failure of the 17-4 material will not occur at the lowest service temperature.

2.1.2.4 Impact Limiter

The impact limiters are designed as energy absorbers to ensure that the maximum impact deceleration applied to the package is limited to values less than the design basis deceleration, as applicable.

2.1.2.5 Buckling

Certain load combinations subject structural sections with relatively large slenderness ratios (such as the MPC enclosure vessel shell) to compressive stresses that may actuate buckling instability before the allowable stress is reached. Tables 2.1.7 and 2.1.9 list load combinations for the MPC enclosure vessel and the HI-STAR 100 overpack structure; the cases that warrant stability (buckling) check are listed therein.

Table 2.1.1

DESIGN PRESSURES

Pressure Location	Condition	Pressure (psig)
MPC Internal Pressure	Normal Condition of Transport	100
	Hypothetical Accident	125 [†]
MPC External Pressure	Normal Condition of Transport	40
	Hypothetical Accident	60 [†]
Overpack External Pressure	Normal Condition of Transport	(0) Ambient
	Hypothetical Accident	300
Overpack Internal Pressure	Normal Condition of Transport	100
	Hypothetical Accident	125
Overpack Enclosure Shell Internal Pressure	Normal Condition of Transport	30
	Hypothetical Accident	30

[†] For ~~the~~ transport, this represents the differential pressure limit for elastic/plastic stability calculations.

Table 2.1.2

NORMAL REFERENCE TEMPERATURES AND ACCIDENT BULK METAL TEMPERATURE
LIMITS

HI-STAR 100 Component	Normal Operating Condition Reference Temp. Limits [†] (Deg.F)	Hypothetical Accident Condition Metal Bulk Temp. Limits ^{††} (Deg.F)
MPC shell	450	550
MPC basket	725	950
MPC lid	550	775
MPC closure ring	400	775
MPC baseplate	400	775
MPC Boral	800	950
MPC heat conduction elements	725	950
Overpack inner shell	400	500
Overpack bottom plate	350	700
Overpack closure plate	400	700
Overpack top flange	400	700
Overpack closure plate seals	400	1200
Overpack closure plate bolts	350	600
Port plug seals (vent and drain)	400	1600
Port cover seals (vent and drain)	400	932
Neutron shielding	300	†††
Overpack Intermediate Shells	350	700
Overpack Outer Enclosure Shell	350	1350
Optional Pocket Trunnion	200	700
Impact Limiter	150	1105

[†] These temperatures are maximum possible temperatures for the normal operating condition. They bound the actual calculated temperatures.

^{††} These temperatures are maximum possible temperatures for the postulated fire accident. They must bound the actual calculated temperatures.

^{†††} For shielding analysis, the neutron shield is conservatively assumed to be lost during the fire accident.

Table 2.1.3

OVERPACK CONTAINMENT STRUCTURE AND MPC ENCLOSURE VESSEL STRESS INTENSITY LIMITS
FOR DIFFERENT LOADING CONDITIONS (ELASTIC ANALYSIS PER NB-3220)[†]

STRESS CATEGORY	NORMAL CONDITIONS OF TRANSPORT	HYPOTHETICAL ACCIDENT ^{††}
Primary Membrane, P_m	S_m	AMIN ($2.4S_{mb}$, $.7S_u$)
Local Membrane, P_L	$1.5S_m$	150% of P_m Limit
Membrane plus Primary Bending	$1.5S_m$	150% of P_m Limit
Primary Membrane plus Primary Bending	$1.5S_m$	150% of P_m Limit
Membrane plus Primary Bending plus Secondary	$3S_m$	N/A
Average ^{†††} Primary Shear (Section in Pure Shear)	$0.6S_m$	$0.42S_u$

[†] Stress combinations including F (peak stress) apply to fatigue evaluations only.

^{††} Governed by Appendix F, Paragraph F-1331 of the ASME Code, Section III. Stress limited to S_u

^{†††} Governed by NB-3227.2 or F-1331.1(d) of the ASME Code, Section III (NB or Appendix F)

Table 2.1.4

MPC BASKET STRESS INTENSITY LIMITS
FOR DIFFERENT LOADING CONDITIONS (ELASTIC ANALYSIS PER NG-3220)

STRESS CATEGORY	NORMAL CONDITIONS OF TRANSPORT	HYPOTHETICAL ACCIDENT [†]
Primary Membrane, P_m	S_m	AMIN ($2.4S_{mb}$, $.7S_u$) ^{††}
Primary Membrane plus Primary Bending	$1.5S_m$	150% of P_m Limit (Limited to S_u)
Primary Membrane plus Primary Bending plus Secondary	$3S_m$	N/A

[†] Governed by Appendix F, Paragraph F-1331 of the ASME Code, Section III.

^{††} Average primary shear stress across a section loaded in pure shear shall not exceed $0.42S_u$.

Table 2.1.5

STRESS INTENSITY LIMITS FOR DIFFERENT
LOADING CONDITIONS FOR THE EXTERNAL STRUCTURALS IN THE HI-STAR OVERPACK
(ELASTIC ANALYSIS PER NF-3260 - CLASS 3)
(ELASTIC ANALYSIS PER NF-3220 - CLASS 1)

STRESS CATEGORY	NORMAL CONDITION OF TRANSPORT [†]	HYPOTHETICAL ACCIDENT ^{††}
Primary Membrane, P_m	S (Class 3) S_m (Class 1)	AMAX ($1.2S_y, 1.5S_m$) but $< .7S_u$
Primary Membrane, P_m , plus Primary Bending, P_b	1.5S (Class 3) 1.5 S_m (Class 1)	150% of P_m (Limited to S_u)
Shear Stress	N/A (Class 3) .6 S_m (Class 1)	$< 0.42S_u$

Definitions:

- S = Allowable Stress Value for Table 1A, ASME Section II, Part D
- S_m = Allowable Stress Intensity Value from Table 2A, ASME Section II, Part D
- S_u = Ultimate Strength

[†] Limits for Normal Condition of Transport are on stress for Class 3 and on stress intensity for Class 1, upper value in column is for Class 3; lower value in column is for Class 3.

^{††} Governed by Appendix F, Paragraph F-1332 of the ASME Code, Section III. Class 1 and Class 3 use same stress intensity limits.

Table 2.1.6

LOADING CASES FOR THE MPC FUEL BASKET

Case Number	Load Combination [†]	Notes
F1	T or T'	Demonstrate that the most adverse of the temperature distributions in the basket will not cause fuel basket to expand and contact the enclosure vessel wall. Compute the stress intensity and show that it is less than allowable.
F2		
F2.a	D+H	1 ft. side drop, 0 degrees circumferential orientation (Figure 2.1.3)
F2.b	D+H	1 ft. side drop, 45 degrees circumferential orientation (Figure 2.1.4)
F3		
F3.a	D + H'	30 ft. vertical axis drop
F3.b	D + H'	30 ft. side Drop, 0 degrees circumferential orientation (Figure 2.1.3)
F3.c	D + H'	30 ft. side Drop, 45 degrees circumferential orientation (Figure 2.1.4)

[†] The symbols used for loads are defined in Subsection 2.1.2.1.4.2.1.

Table 2.1.7

LOADING CASES FOR THE MPC ENCLOSURE VESSEL

Case Number	Load Combination [†]	Notes
E1		
E1.a	Design internal pressure, P_i	Primary Stress intensity
E1.b	Design external pressure, P_o	Primary stress intensity limits, buckling stability
E1.c	Design internal pressure plus Temperature, $P_i + T$	Primary plus secondary stress intensity under Level A condition
E2		
E2.a	$(P_i, P_o) + D + H$	1 ft. side drop, 0° circumferential orientation (Figure 2.1.3)
E2.b	$(P_i, P_o) + D + H$	1 ft. side drop, 45° circumferential orientation (Figure 2.1.4)

[†] The symbols used for loads are defined in Subsection 2.1.2.1.1. Note that in the analyses, the bounding pressure (P_i, P_o) is applied, e.g., in stability calculations P_o is bounding, whereas in stress calculations both P_o and P_i are appropriate.

Table 2.1.7 (continued)

Case Number	Load Combination [†]	Notes
E3		
E3.a	$D + H' + P_o$ (Stability of the shell considers internal pressure plus drop deceleration)	30 ft. vertical axis drop
E3.b	$D + H' + P_i$	30 ft. side drop, 0° circumferential orientation (Figure 2.1.3)
E3.c	$D + H' + P_i$	30 ft. side drop, 45° circumferential orientation (Figure 2.1.4)
E4	T or T'	Demonstrate that interference with the overpack will not develop for T
E5	$(P_i^*, P_o^*) + D + T'$	Demonstrate compliance with level D stress limits - buckling stability

[†] The symbols used for loads are defined in Subsection 2.1.2.1.1. Note that in the analyses, the bounding pressure (P_i, P_o) is applied, e.g., in stability calculations P_o is bounding, whereas in stress calculations both P_o and P_i are appropriate.

Table 2.1.8

OVERPACK LOAD CASES FOR NORMAL CONDITION OF TRANSPORT

Case Number	Load Combination*	Notes
1	$T_h + P_i + F + W_s$	Hot Environment
2	$T_s + P_o + F + W_s$	Super-Cold Environment
3	$T_h + D_{sn} + P_i + F + W_s$	Free One Foot Side Drop - Hot Environment
4	$T_c + D_{sn} + P_o + F + W_s$	Free One Foot Side Drop - Cold Environment
5	T_c and $T_h + P_i + V$	Rapid Ambient Temperature Change

Note that load case 5 is outside of the load combinations of Reg. Guide 7.8

† The symbols used here are defined in Subsection 2.1.2.1.1.

Table 2.1.9

OVERPACK LOAD CASES FOR HYPOTHETICAL ACCIDENT CONDITIONS OF TRANSPORT

Case Number	Load Combination†	Notes
1	$T_h + D_{ba} + P_i + F + W_s$	Bottom End 30 ft. Drop - Hot
2	$T_h + D_{ta} + P_i + F + W_s$	Top End 30 ft Drop - Hot
3	$T_h + D_{sa} + P_i + F + W_s$	Side 30 ft Drop - Hot
4	$T_h + D_{ea} + P_i + F + W_s$	30 ft C.G. Over-the-Bottom-Corner Drop - Hot
5	$T_h + D_{ga} + P_i + F + W_s$	30 ft C.G. Over-the-Top-Corner Drop Hot
6	$T_h + P_s + P_i + F + W_s$	Side Puncture - Hot
7	$T_h + P_t + P_i + F + W_s$	Top End Puncture - Hot
8	$T_h + P_b + P_i + F + W_s$	Bottom End Puncture - Hot
9	$T_c + D_{ba} + P_o + F + W_s$	Case 1 - Cold
10	$T_c + D_{ta} + P_o + F + W_s$	Case 2 - Cold
11	$T_c + D_{sa} + P_o + F + W_s$	Case 3 - Cold
12	$T_c + D_{ea} + P_o + F + W_s$	Case 4 - Cold
13	$T_c + D_{ga} + P_o + F + W_s$	Case 5 - Cold
14	$T_c + P_s + P_o + F + W_s$	Case 6 - Cold
15	$T_c + P_t + P_o + F + W_s$	Case 7 - Cold
16	$T_c + P_b + P_o + F + W_s$	Case 8 - Cold
17	$T_f + P_i + F + W_s$	Fire Event (Bolt unloading)
18	P_o^*	Containment Stability - Hot Deep Submergence
19	$P_i^* + T_f + F + W_s$	Fire Accident Internal Pressure - Hot
20	$T_h + D_{ga} + P_i + F + W_s$	30 ft C.G. Oblique Drop (30 Degree) on Top Forging - Hot
21	$T_c + D_{ga} + P_i + F + W_s$	30 ft C.G. Oblique Drop (30 Degree) on Top Forging - Cold
22	$T_c + D_{ga} + P_i + F + W_s$	30 ft Drop -Slapdown Secondary Impact Limiter at Top Forging - Hot

† The symbols used here are defined in Subsection 2.1.2.1.1

Table 2.1.10
BOUNDING DECELERATIONS FOR DROP EVENTS

Event	Deceleration Value (in multiples of acceleration due to gravity)
Normal conditions of transport, drop from 1 ft. height (any circumferential orientations)	17
Transport hypothetical accident conditions; drop from 30 ft. height (any axial and circumferential orientations)	60

Table 2.1.11

DESIGN, LEVELS A AND B: STRESS INTENSITY

Code: ASME NB
 Material: SA203-E
 Service Conditions: Normal Conditions of Transport
 Item: Stress Intensity

Temp. (degree F)	Classification and Value (ksi)					
	S_m	P_m^\dagger	P_L^\dagger	$P_L + P_b^\dagger$	$P_L + P_b + Q$	$P_e^{\dagger\dagger}$
-20 to 100	23.3	23.3	35.0	35.0	69.9	69.9
200	23.3	23.3	35.0	35.0	69.9	69.9
300	23.3	23.3	35.0	35.0	69.9	69.9
400	22.9	22.9	34.4	34.4	68.7	68.7
500	21.6	21.6	32.4	32.4	64.8	64.8

Definitions:

- S_m = Stress intensity values per ASME Code
- P_m = Primary membrane stress intensity
- P_L = Local membrane stress intensity
- P_b = Primary bending stress intensity
- P_e = Expansion stress
- Q = Secondary stress
- $P_L + P_b$ = Either primary or local membrane plus primary bending

Definitions for Table 2.1.11 apply to all following tables unless modified.

Notes:

1. ~~Limits on values are presented in Table 2.1.3.~~

[†] Evaluation required for Design condition only.

^{††} P_e not applicable to vessels.

Table 2.1.12

LEVEL D: STRESS INTENSITY

Code: ASME NB
 Material: SA203-E
 Service Condition: Hypothetical Accident
 Item: Stress Intensity

Temp. (degree F)	Classification and Value (ksi)		
	P_m	P_L	$P_L + P_b$
-20 to 100	49.0	70.0	70.0
200	49.0	70.0	70.0
300	49.0	70.0	70.0
400	48.2	68.8	68.8
500	45.4	64.9	64.9

Notes:

1. Level D allowables per NB-3225 and Appendix F, Paragraph F-1331.
2. Average primary shear stress across a section loaded in pure shear may not exceed $0.42 S_u$.
3. Limits on values are presented in Table 2.1.3.

Table 2.1.13

DESIGN, LEVELS A AND B: STRESS INTENSITY

Code: ASME NB
 Material: SA350-LF3
 Service Conditions: Normal Conditions of Transport
 Item: Stress Intensity

Temp. (degree F)	Classification and Value (ksi)					
	S_m	P_m^\dagger	P_L^\dagger	$P_L + P_b^\dagger$	$P_L + P_b + Q$	P_e^{**}
-20 to 100	23.3	23.3	35.0	35.0	69.9	69.9
200	22.8	22.8	34.2	34.2	68.4	68.4
300	22.2	22.2	33.3	33.3	66.6	66.6
400	21.5	21.5	32.3	32.3	64.5	64.5
500	20.2	20.2	30.3	30.3	60.6	60.6
600	18.5	18.5	27.75	27.75	55.5	55.5
700	16.8	16.8	25.2	25.2	50.4	50.4

Notes:

1. Source for S_m is ASME Code.
2. Limits on values are presented in Table 2.1.3.

[†] Evaluation required for Design condition only.

^{**} P_e not applicable to vessels.

Table 2.1.14

LEVEL D, STRESS INTENSITY

Code: ASME NB
 Material: SA350-LF3
 Service Conditions: Hypothetical Accident
 Item: Stress Intensity

Temp. (degreeF)	Classification and Value (ksi)		
	P_m	P_L	$P_L + P_b$
-20 to 100	49.0	70.0	70.0
200	48.0	68.5	68.5
300	46.7	66.7	66.7
400	45.2	64.6	64.6
500	42.5	60.7	60.7
600	38.9	58.4	58.4
700	35.3	53.1	53.1

Notes:

1. Level D allowables per NB-3225 and Appendix F, Paragraph F-1331.
2. Average primary shear stress across a section loaded in pure shear may not exceed $0.42 S_u$.
3. Limits on values are presented in Table 2.1.3.

Table 2.1.15
DESIGN AND LEVEL A: STRESS AND STRESS INTENSITY

Code:	ASME NF (Class 3)	ASME NF (Class1)
Material:	SA515, Grade 70	SA515, Grade 70
	SA516, Grade 70	SA516, Grade 70
Service Conditions:	Normal Conditions of Transport	Normal Conditions of Transport
Item:	Stress	Stress Intensity

Temp. (degreeF)	Classification and Value (ksi)					
	S (Class 3)	S _m (Class 1)	Membrane Stress (Class 3)	P _m (Class 1)	Membrane plus Bending Stress (Class 3)	P _m +P _b (Class 1)
-20 to 100	17.5	23.3	17.5	23.3	26.3	34.95
200	17.5	23.1	17.5	23.1	26.3	34.65
300	17.5	22.5	17.5	22.5	26.3	33.75
400	17.5	21.7	17.5	21.7	26.3	32.55
500	17.5	20.5	17.5	20.5	26.3	30.75
600	17.5	18.7	17.5	18.7	26.3	28.05
650	17.5	18.4	17.5	18.4	26.3	27.6
700	16.6	18.3	16.6	18.3	24.9	27.45

Notes:

1. S = Maximum allowable stress values from Table 1A of ASME Code, Section II, Part D.
2. Stress classification per Paragraph NF-3260.
3. Limits on values are presented in Table 2.1.5.
4. Level A allowable stress intensities per NF.3221.1.
5. S_m = Stress intensity values per Table 2A of ASME, Section II, Part D.
6. Limits on values are presented in Table 2.1.5.

Table 2.1.16

LEVEL D: STRESS INTENSITY

Code: ASME NF
 Material: SA515, Grade 70
 SA516, Grade 70
 Service Conditions: Hypothetical Accident
 Item: Stress Intensity

Temp. (degree F)	Classification and Value (ksi)		
	S_m	P_m	$P_m + P_b$
-20 to 100	23.3	45.6	68.4
200	23.1	41.5	62.3
300	22.5	40.4	60.6
400	21.7	39.1	58.7
500	20.5	36.8	55.3
600	18.7	33.7	50.6
650	18.4	33.1	49.7
700	18.3	32.9	49.3

Notes:

1. Level D allowable stress intensities per Appendix F, Paragraph F-1332.
2. S_m = Stress intensity values per Table 2A of ASME, Section II, Part D.
3. Limits on values are presented in Table 2.1.5.

Table 2.1.17
DESIGN, LEVELS A AND B: STRESS INTENSITY

Code: ASME NB
 Material: Alloy X
 Service Conditions: Normal Conditions of Transport
 Item: Stress Intensity

Temp. (degree F)	Classification and Numerical Value					
	S_m	P_m^\dagger	P_L^\dagger	$P_L + P_b^\dagger$	$P_L + P_b + Q$	$P_e^{\dagger\dagger}$
-20 to 100	20.0	20.0	30.0	30.0	60.0	60.0
200	20.0	20.0	30.0	30.0	60.0	60.0
300	20.0	20.0	30.0	30.0	60.0	60.0
400	18.7	18.7	28.1	28.1	56.1	56.1
500	17.5	17.5	26.3	26.3	52.5	52.5
600	16.4	16.4	24.6	24.6	49.2	49.2
650	16.0	16.0	24.0	24.0	48.0	48.0
700	15.6	15.6	23.4	23.4	46.8	46.8
750	15.2	15.2	22.8	22.8	45.6	45.6
800	14.9	14.9	22.4	22.4	44.7	44.7

Notes:

1. S_m = Stress intensity values per Table 2A of ASME II, Part D.
2. Alloy X S_m values are the lowest values for each of the candidate materials at temperature.
3. Stress classification per NB-3220.
4. Limits on values are presented in Table 2.1.3.

[†] Evaluation required for Design condition only.

^{††} P_e not applicable to vessels.

Table 2.1.18
LEVEL D: STRESS INTENSITY

Code: ASME NB
 Material: Alloy X
 Service Conditions: Hypothetical Accident
 Item: Stress Intensity

Temp. (degree F)	Classification and Value (ksi)		
	P_m	P_L	$P_L + P_b$
-20 to 100	48.0	72.0	72.0
200	48.0	72.0	72.0
300	46.2	69.3	69.3
400	44.9	67.4	67.4
500	42.0	63.0	63.0
600	39.4	59.1	59.1
650	38.4	57.6	57.6
700	37.4	56.1	56.1
750	36.5	54.8	54.8
800	35.8	53.7	53.7

Notes:

1. Level D stress intensities per ASME NB-3225 and Appendix F, Paragraph F-1331.
2. The average primary shear strength across a section loaded in pure shear may not exceed $0.42 S_u$.
3. Limits on values are presented in Table 2.1.3.

Table 2.1.19
DESIGN, LEVELS A AND B: STRESS INTENSITY

Code: ASME NG
 Material: Alloy X
 Service Conditions: Normal Conditions of Transport
 Item: Stress Intensity

Temp. (degree F)	Classification and Value (ksi)				
	S_m	P_m	P_m+P_B	P_m+P_b +Q	P_e
-20 to 100	20.0	20.0	30.0	60.0	60.0
200	20.0	20.0	30.0	60.0	60.0
300	20.0	20.0	30.0	60.0	60.0
400	18.7	18.7	28.1	56.1	56.1
500	17.5	17.5	26.3	52.5	52.5
600	16.4	16.4	24.6	49.2	49.2
650	16.0	16.0	24.0	48.0	48.0
700	15.6	15.6	23.4	46.8	46.8
750	15.2	15.2	22.8	45.6	45.6
800	14.9	14.9	22.4	44.7	44.7

Notes:

1. S_m = Stress intensity values per Table 2A of ASME, Section II, Part D.
2. Alloy X S_m values are the lowest values for each of the candidate materials at temperature.
3. Classifications per NG-3220.
4. Limits on values are presented in Table 2.1.4.

Table 2.1.20

LEVEL D: STRESS INTENSITY

Code: ASME NG
 Material: Alloy X
 Service Conditions: Hypothetical Accident
 Item: Stress Intensity

Temp. (degrees F)	Classification and Value (ksi)		
	P_m	P_L	$P_L + P_b$
-20 to 100	48.0	72.0	72.0
200	48.0	72.0	72.0
300	46.2	69.3	69.3
400	44.9	67.4	67.4
500	42.0	63.0	63.0
600	39.4	59.1	59.1
650	38.4	57.6	57.6
700	37.4	56.1	56.1
750	36.5	54.8	54.8
800	35.8	53.7	53.7

Notes:

1. Level D stress intensities per ASME NG-3225 and Appendix F, Paragraph F-1331.
2. The average primary shear strength across a section loaded in pure shear may not exceed $0.42 S_u$.
3. Limits on values are presented in Table 2.1.4.

Table 2.1.21

REFERENCE TEMPERATURES AND STRESS LIMITS
FOR THE VARIOUS LOAD CASES

Load Case Number	Material	Reference Temperature [†] , (°F)	Stress Intensity Allowables, ksi		
			P _m	P _L + P _b	P _L + P _b + Q
F1	Alloy X	725	15.4	23.1	46.2
F2	Alloy X	725	15.4	23.1	46.2
F3	Alloy X	725	36.9	55.4	NL ^{††}
E1	Alloy X	450 ^{†††}	18.1	27.2	NL
E2	Alloy X	450 ^{†††}	18.1	27.2	54.3
E3	Alloy X	450 ^{†††}	43.4	65.2	NL
E4	Alloy X	450 ^{†††}	18.1	27.2	54.3
E5	Alloy X	775 ^{†††}	36.15	54.25	NL

[†] Values for reference temperatures are taken as the design temperatures (Table 2.1.2).

^{††} NL: No specific limit in the Code.

^{†††} Levels used for enclosure vessel top closure and baseplate only.

Table 2.1.21 (continued)
REFERENCE TEMPERATURES AND STRESS LIMITS
FOR THE VARIOUS LOAD CASES

Condition	Material	Reference Temperature, (°F)	Stress Intensity Allowables, ksi		
			P _m	P _L + P _b	P _L + P _b + Q
Normal	SA203-E	400 [†]	22.9	34.4	68.7
	SA350-LF3	400 [†]	21.5	32.3	64.5
	SA516 Gr. 70 SA515 Gr. 70	400 [†]	17.5	26.3	52.5
	SA203-E	-20	23.3	35.0	69.9
	SA350-LF3	-20	23.3	35.0	69.9
	SA516 Gr. 70 SA515 Gr. 70	-20	17.5	26.3	52.5
Hypothetical Accident - Mechanical Loads	SA203-E	400 [†]	48.2	68.8	NL ^{††}
	SA350-LF3	400 [†]	45.2	64.6	NL
	SA516 Gr. 70 SA515 Gr. 70	400 [†]	39.1	58.7	NL
	SA203-E	-20	49.0	70.0	NL
	SA350-LF3	-20	49.0	70.0	NL
	SA516 Gr. 70 SA515 Gr. 70	-20	45.6	68.4	NL
Fire	SA203-E	500	45.4	64.9	NL
	SA350-LF3	700	35.3	53.1	NL
	SA516 Gr. 70	700	32.9	49.3	NL

[†] Values for reference temperatures are taken as the design temperatures (Table 2.1.2).

^{††} NL: No limit specified in the Code.

Table 2.1.22

FRACTURE TOUGHNESS TEST CRITERIA: CONTAINMENT BOUNDARY

Item	Material	Thickness (in.)	Charpy V-Notch Temperature [†]	Drop Test Temperature ^{††}
Weld Metal for NB Welds	As required	NA	As required per ASME Section III, Subsection NB, Article NB-2430 and Article NB-2330 Min. test temperature = -40°F	As required per ASME Section III, Subsection NB, Articles NB-2430 and Article NB-2330
Shell	SA203E	2-1/2	$T_{NDT} \leq -70^{\circ}\text{F}$ with testing and acceptance criteria per ASME Section III, Subsection NB, Article NB-2330	$T_{NDT} \leq -70^{\circ}\text{F}$ per Reg. Guide 7.11
Top Flange	SA350-LF3	8-3/4	$T_{NDT} \leq -136^{\circ}\text{F}$ with testing and acceptance criteria per ASME Section III, Subsection NB, Article NB-2330	$T_{NDT} \leq -136^{\circ}\text{F}$ per Reg. Guide 7.12

[†] Temperature is T_{NDT} unless noted.

^{††} Materials to be tested in accordance with ASTM E208-87a.

Table 2.1.22 (Continued)

FRACTURE TOUGHNESS TEST CRITERIA: CONTAINMENT BOUNDARY

Item	Material	Thickness (in.)	Charpy V-Notch Temperature [†]	Drop Test Temperature ^{**}
Bottom Plate	SA350-LF3	6	$T_{NDT} \leq -129^{\circ}\text{F}$ with testing and acceptance criteria per ASME Section III, Subsection NB, Article NB-2330	$T_{NDT} \leq -129^{\circ}\text{F}$ per Reg. Guide 7.12
Closure Plate	SA350-LF3	6	$T_{NDT} \leq -129^{\circ}\text{F}$ with testing and acceptance criteria per ASME Section III, Subsection NB, Article NB-2330	$T_{NDT} \leq -129^{\circ}\text{F}$ per Reg. Guide 7.12

[†] Temperature is T_{NDT} unless noted.

^{**} Materials to be tested in accordance with ASTM E208-87a.

Table 2.1.23
FRACTURE TOUGHNESS TEST CRITERIA: MISCELLANEOUS ITEMS

Item	Material	Thickness (in.)	Charpy V-Notch Temperature [†]	Drop Test Temperature
Intermediate Shells	SA516 Grade 70	1-1/4 and 1	Test temperature = -40 Deg. F with acceptance criteria per ASME Section III, Subsection NF, Table NF- 2331(a)-3 and Figure NF-2331(a)-2, except BOM items 15 & 16 shall meet Table NF-2331(a)-1 and NF-2331 (a)- 4	Not Required
Port Cover Plates	SA203-E	1-1/2	Test temperature = -40 Deg. F with acceptance criteria per ASME Section III, Subsection NF, Table NF- 2331(a)-3 and Figure NF-2331(a)-2	Not Required
Weld Metal for NF Welds	As required	NA	As required per ASME Section III, Subsection NF, Article NF-2430 and Article NF-2330 Test temperature = -40 Deg. F	Not Required

[†] Temperature is T_{NDT} unless noted.

Table 2.1.24

ALLOWABLE STRESS CRITERIA FROM OTHER SOURCES

OVERPACK CLOSURE BOLTS[†]:

STRESS CATEGORY	NORMAL CONDITIONS OF TRANSPORT	HYPOTHETICAL ACCIDENT
Average Tensile Stress	$2/3 S_y$	$\text{AMIN}(S_y, 0.7 S_u)$
Average Shear Stress	$0.6 (2/3 S_y)$	$\text{AMIN}(0.6 S_y, 0.42 S_u)$
Combined Tensile and Shear Stress ^{††}	$R_t^2 + R_s^2 < 1.0$	$R_t^2 + R_s^2 < 1.0$

IMPACT LIMITER ATTACHMENT BOLTS:

STRESS CATEGORY	NORMAL CONDITIONS OF TRANSPORT	HYPOTHETICAL ACCIDENT
Average Tensile Stress	$2/3 S_y$	S_u
Average Shear Stress	$0.6 (2/3 S_y)$	S_u
Combined Tensile and Shear Stress	$R_t^2 + R_s^2 < 1.0$	$R_t^2 + R_s^2 < 1.0$

LIFTING TRUNNIONS AND LIFTING BOLTS:

The lifting trunnions and the lifting bolts, for the overpack closure plate and for the MPC lid, are designed in accordance with NUREG-0612 and ANSI N14.6. Specifically, the design must meet factors of safety of six based on the material yield stress and ten based on the material ultimate stress for non-redundant lifting devices.

[†] The overpack closure bolts are designed in accordance with NUREG/CR-6007, "Stress Analysis of Closure Bolts for

^{††} R_t and R_s are the ratios of actual stress to shear stress, respectively.

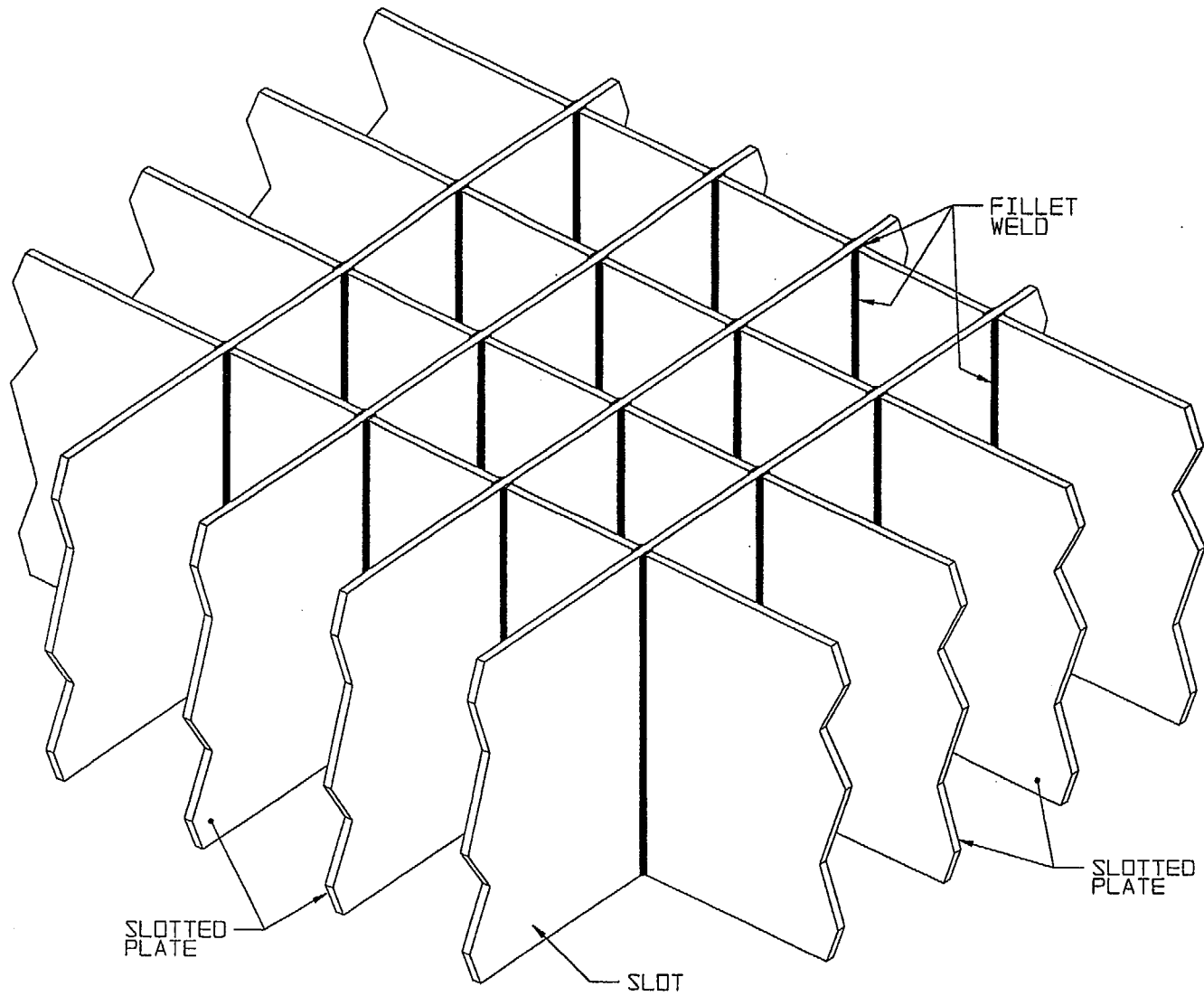


FIGURE 2.1.1; MPC FUEL BASKET GEOMETRY

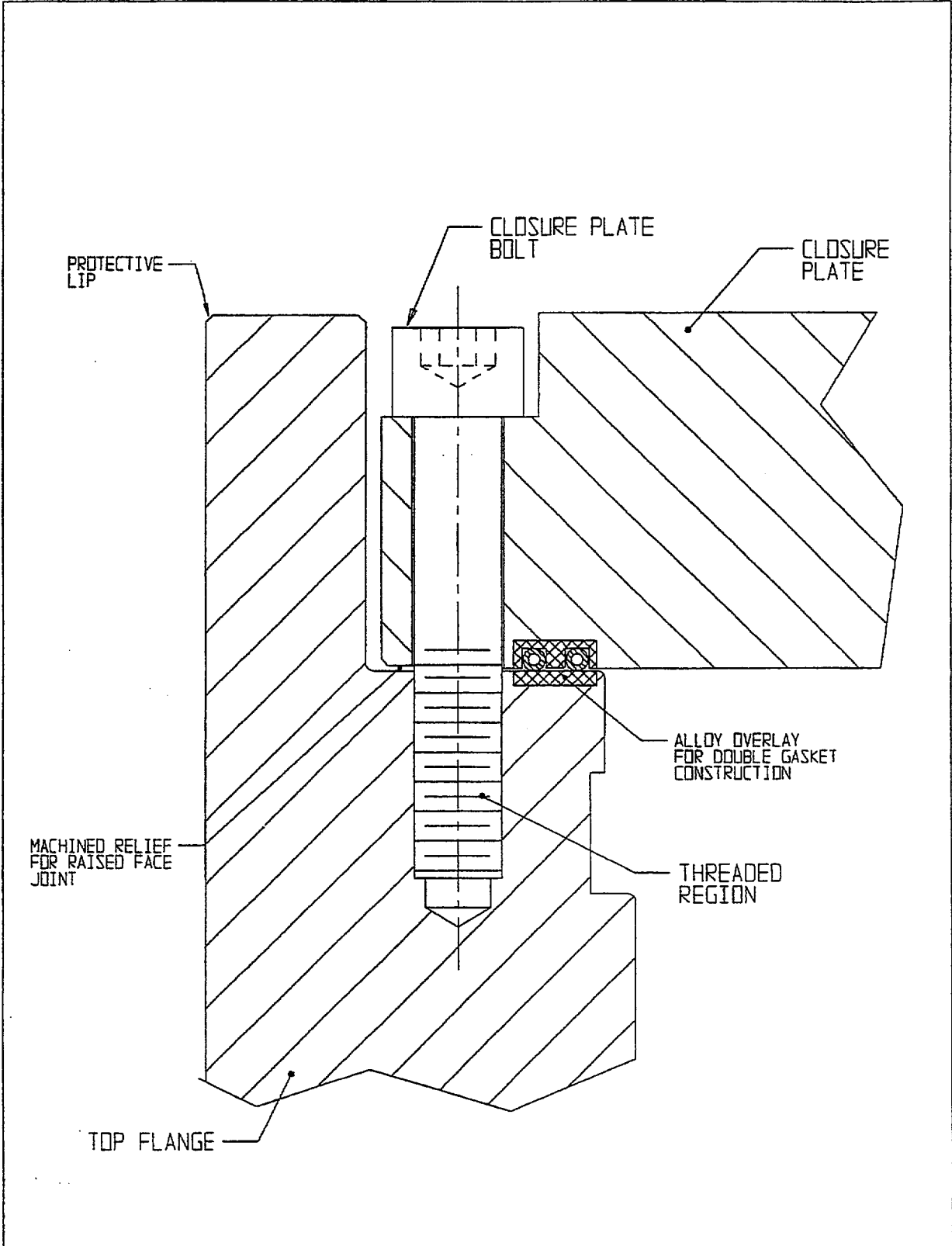


FIGURE 2.1.2; SCHEMATIC OF CLOSURE PLATE BOLTED JOINT

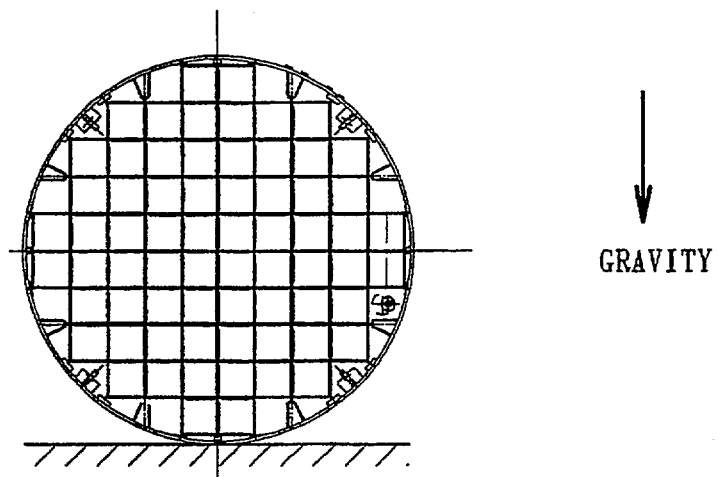


FIGURE 2.1.3; 0° DROP ORIENTATION FOR THE MPCs

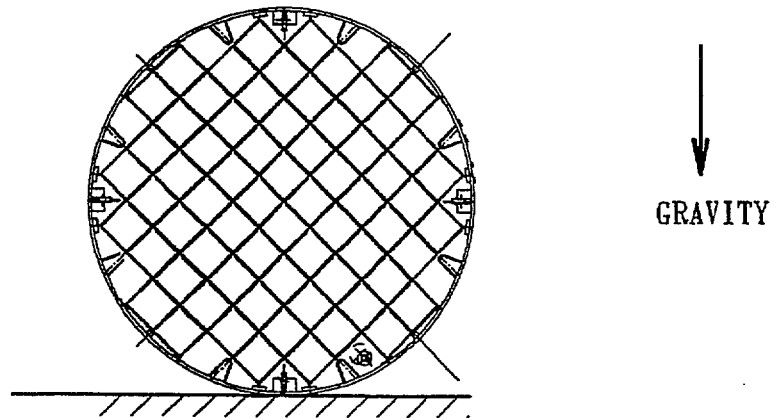


FIGURE 2.1.4; 45° DROP ORIENTATION FOR THE MPCs

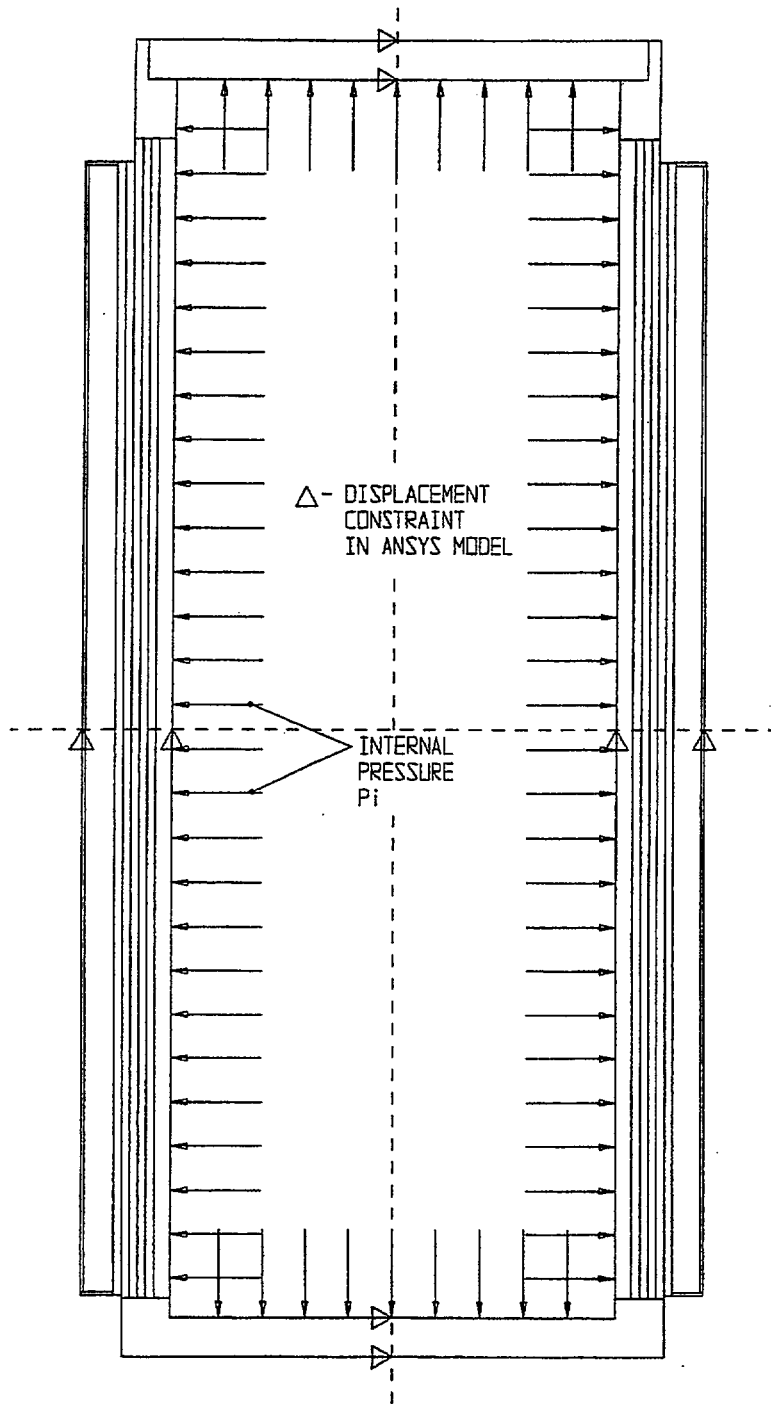


FIGURE 2.1.5; FREE BODY DIAGRAM OF OVERPACK - INTERNAL PRESSURE

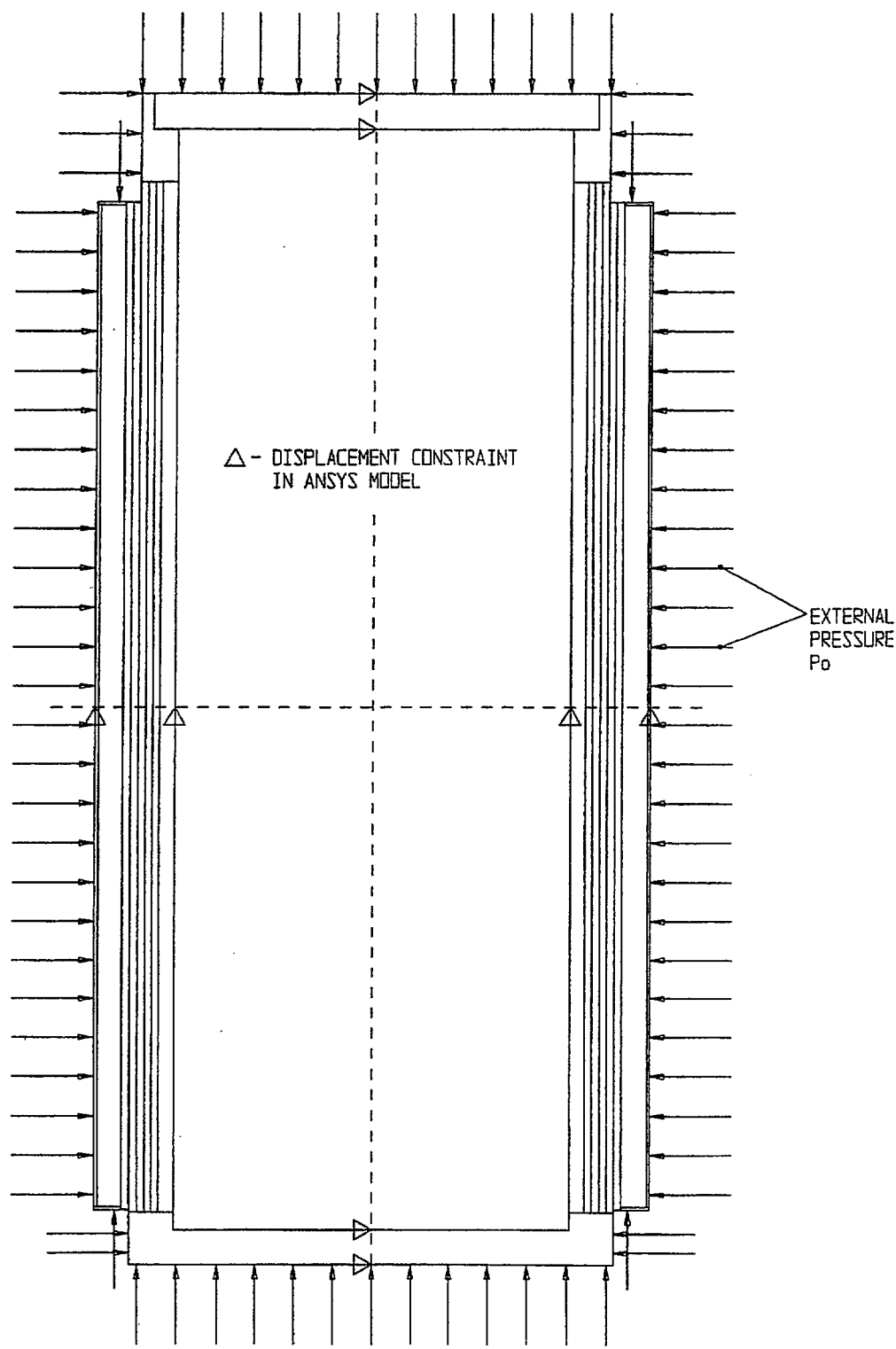


FIGURE 2.1.6; FREE BODY DIAGRAM OF OVERPACK - EXTERNAL PRESSURE

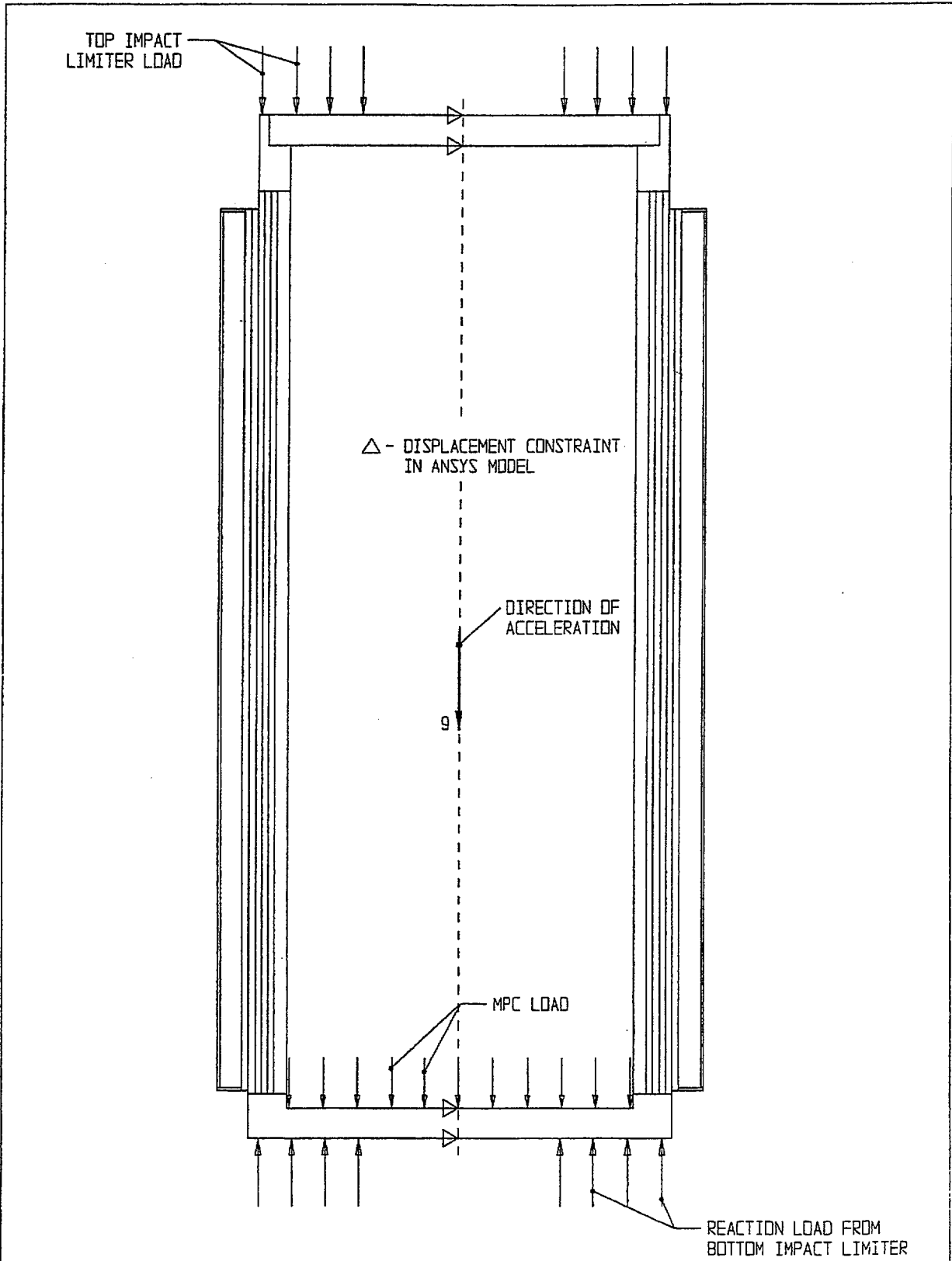


FIGURE 2.1.7; FREE BODY DIAGRAM OF OVERPACK - BOTTOM END DROP

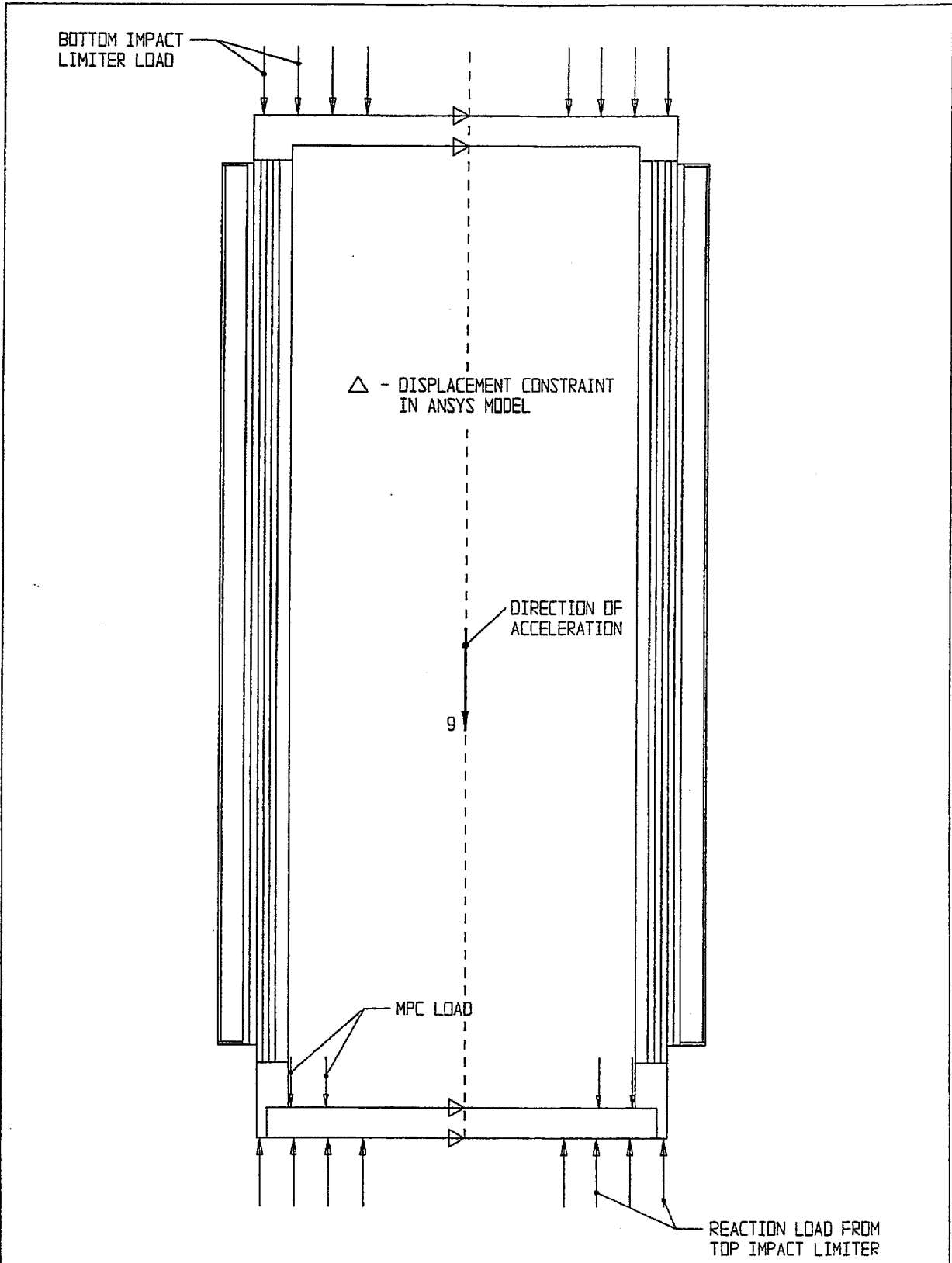


FIGURE 2.1.8; FREE BODY DIAGRAM OF OVERPACK - TOP END DROP

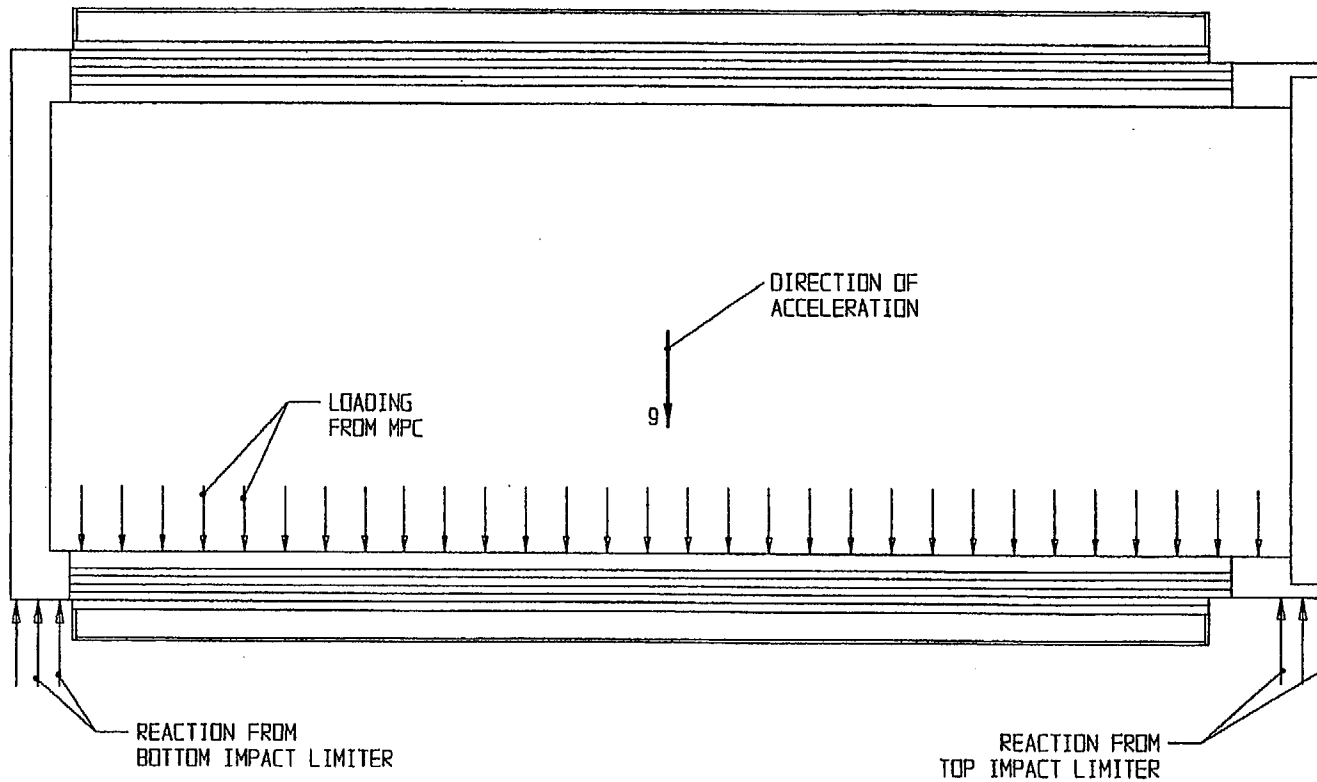


FIGURE 2.1.9; FREE BODY DIAGRAM OF OVERPACK - SIDE DROP

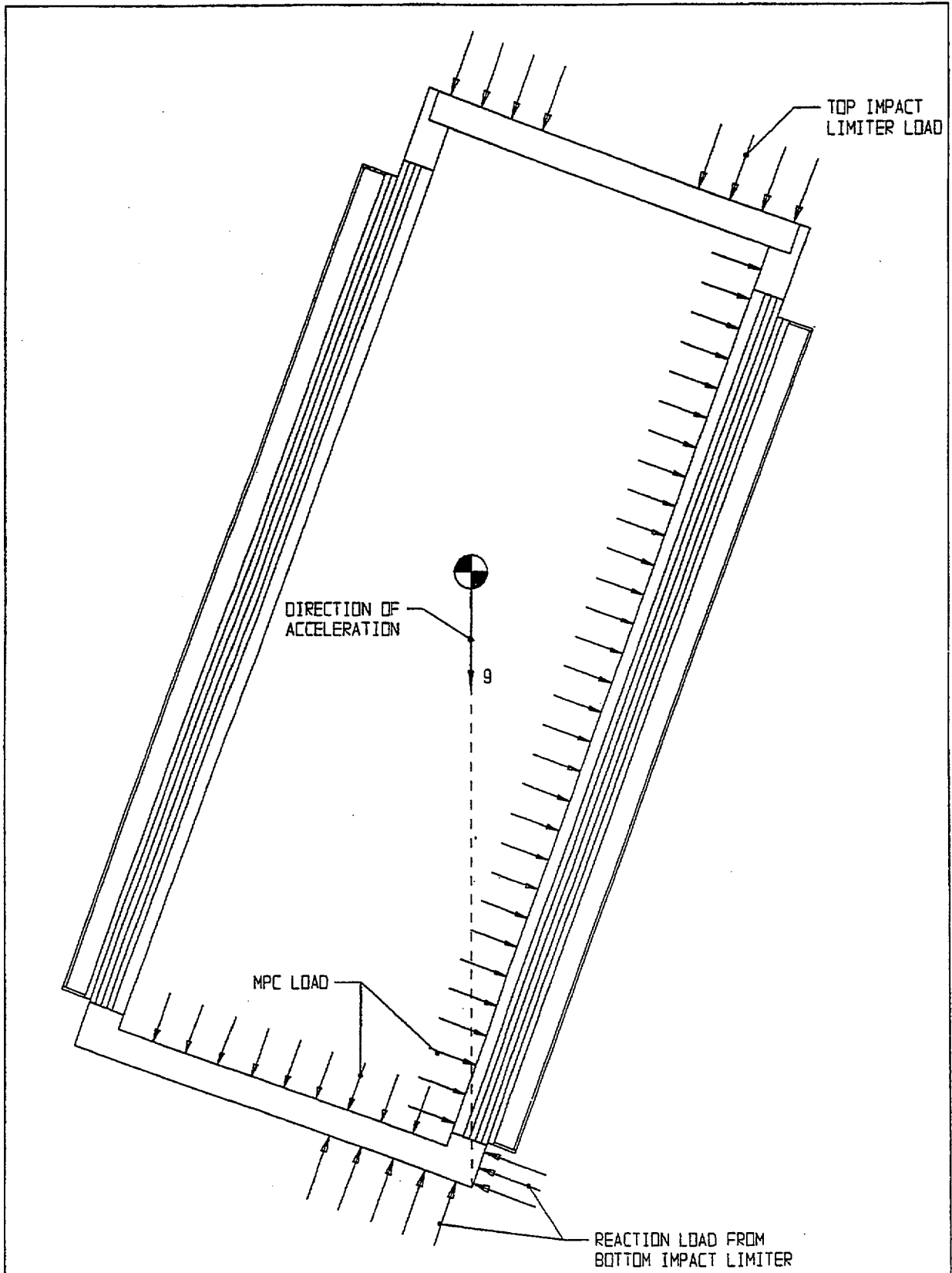


FIGURE 2.110 ; FREE BODY DIAGRAM FOR BOTTOM CG - OVER - CORNER DROP

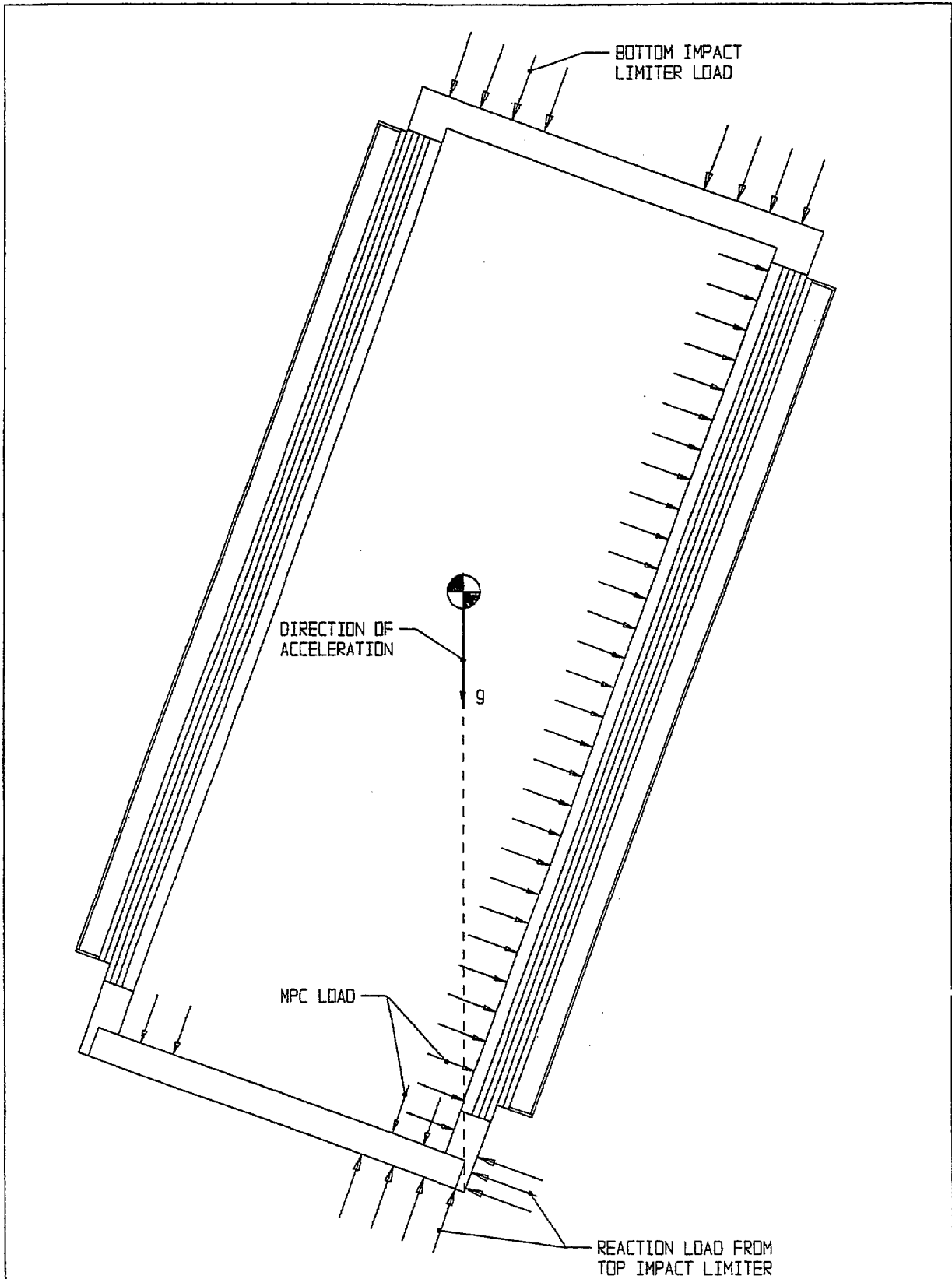


FIGURE 2.1.11; FREE BODY DIAGRAM FOR TOP CG - OVER - CORNER DROP

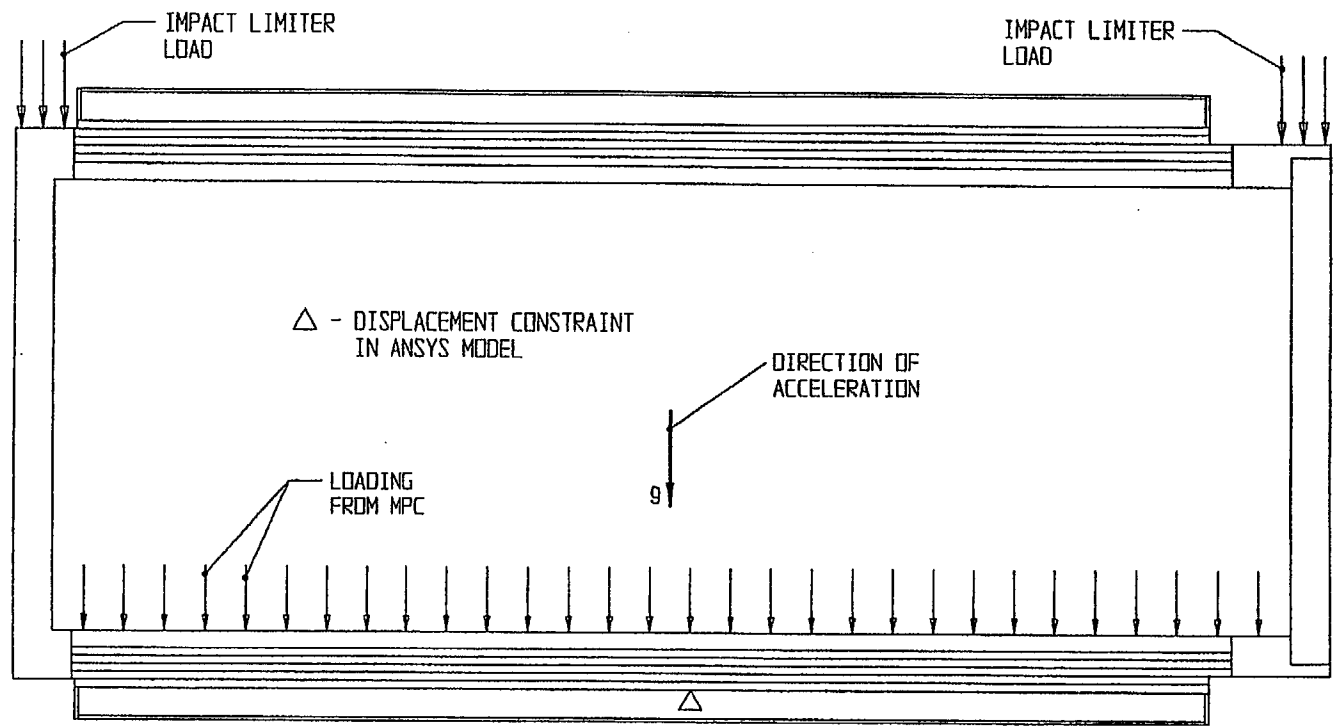


FIGURE 2.1.12; FREE BODY DIAGRAM FOR PUNCTURE DROP ONTO BAR - SIDE

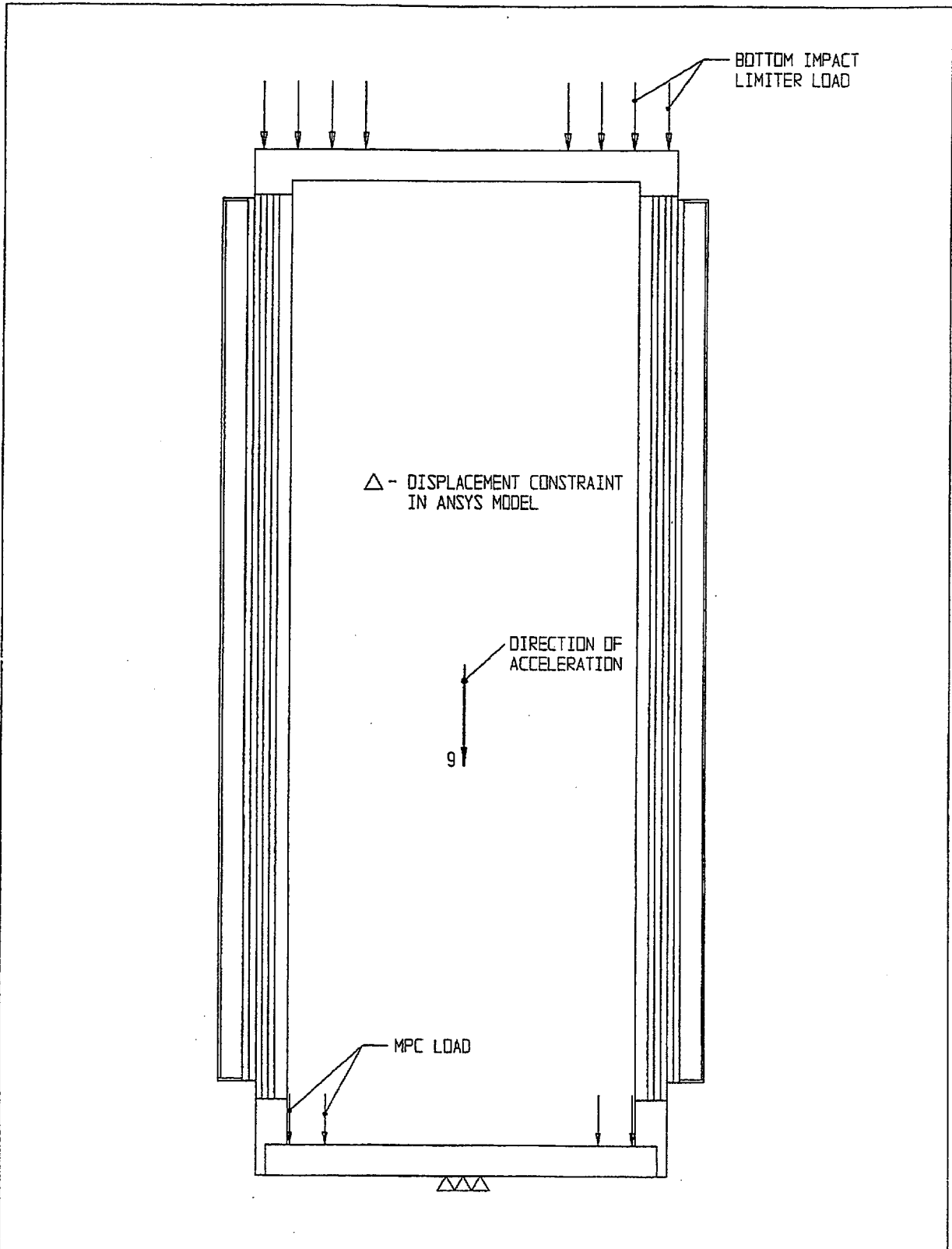


FIGURE 2.1.13; FREE BODY DIAGRAM FOR PUNCTURE DROP ONTO BAR - TOP END

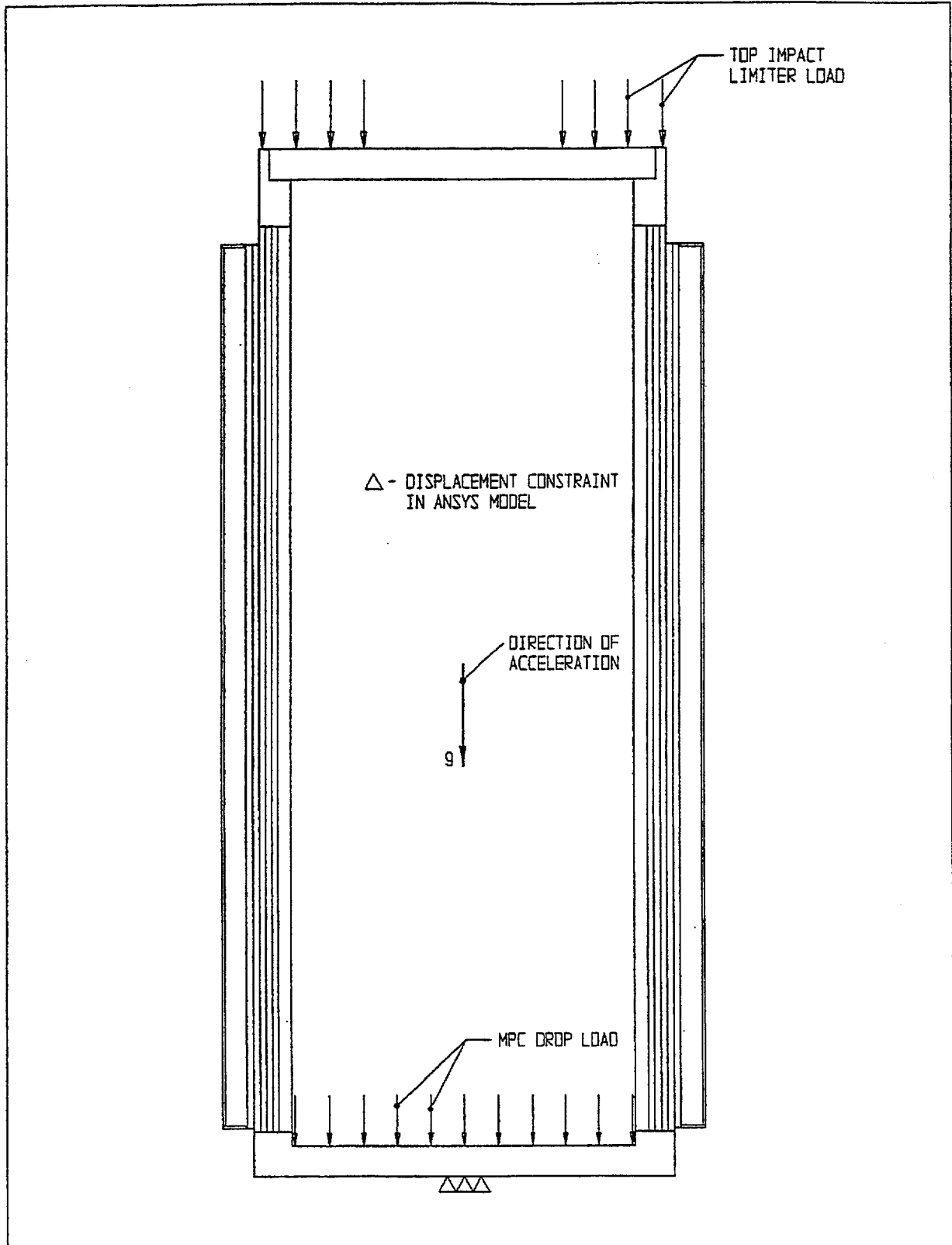


FIGURE 2.114; FREE BODY DIAGRAM FOR PUNCTURE DROP ONTO BAR - BOTTOM END

Table 2.2.1 provides the weights of the individual HI-STAR 100 components as well as the total system weights. The weight of the impact limiter is also provided.

The locations of the calculated centers of gravity (CGs) are presented in Table 2.2.2 per the locations described in Figure 2.2.1. All centers of gravity are located on the cask centerline since the non-axisymmetry effects of the cask system plus contents are negligible.

Table 2.2.3 provides the lift weight for the HI-STAR 100 System when the heaviest fully loaded MPC is lifted from the fuel pool. The effect of buoyancy is neglected, and the weight of rigging is set at a conservative value.

Table 2.2.4 provides a table of bounding weights that may be used in calculations where additional conservatism is introduced by increasing the weight.

Table 2.2.1
HI-STAR 100 CALCULATED WEIGHT DATA[†]

Item	Component Weight (lb)	Component Weight (lb)	Total Weight (lb)
Overpack ^{††}	153,710		
— Overpack closure plate	7,984	7,984	153,710
Bottom impact limiter			17,231
Top impact limiter			19,187
MPC Weights ^{†††}	Fuel Basket	Basket + Shell Without SNF	Fully Loaded with SNF and Fuel Spacers
MPC-68	16,240		
— MPC-24			
— Fuel Basket	17,045	37,591	87,171
— Without SNF	39,667		
— Fully loaded with SNF	79,987		
MPC-24	20,842		
— Overpack with loaded MPC-24	223,607	40,868	82,494
MPC-32	12,340	34,507	89,765
MPC-24E/EF	23,535	43,561	85,188
Trojan MPC-24E/EF ^{††††}	21,284	40,643	80,963
Overpack with loaded MPC-68/68F			
— MPC-68	15,263		
— Fuel Basket	39,641		240,881
— Without SNF	87,241		
— Fully loaded with SNF			
— Overpack with fully loaded MPC-2468	240,951		236,204
Overpack with loaded MPC-32			243,745
Overpack with loaded MPC-24E/EF			238,898
Overpack with loaded MPC-24E/EF (Trojan)			235,283
— Overpack with minimum weight MPC without SNF	189,007	187,500	
Total weight of transport package			
— With MPC-68/68F ^{††}	277,29970,115		
— With MPC-24	272,62277,269		
— With MPC-32	279,893		
— With MPC-24E/EF	275,316		
— With Trojan MPC-24E/EF	271,701		

[†] All calculated weights are rounded up to the nearest whole number.

^{††} Including overpack closure plate.

^{†††} MPC vessel (shell, baseplate, and lid) weights include a 4% upward adjustment; fuel weight is design basis, including all non-fuel components and DFC (i.e., 1680 lbs for PWR and 700 lbs for BWR).

^{††††} MPC vessel weight used is for MPC-24, which bounds shell weight for Trojan MPC-24E/EF due to height difference. Trojan MPC weight includes MPC spacer.

Table 2.2.2

CENTERS OF GRAVITY OF HI-STAR 100 CONFIGURATIONS

Component	Height of CG Above Datum, inches
Overpack empty	99.7
MPC-6824 empty	111.508.9
MPC-2468 empty	109.009.9
MPC-32 empty	113.2
MPC-24E/EF empty	107.8
Trojan MPC-24E/EF	104.2
MPC-6824 with fuel in overpack	102.51.8
MPC-2468 with fuel in overpack	102.31.8
MPC-32 with fuel in overpack	102.1
MPC-24E/EF with fuel in overpack	102.2
Trojan MPC-24E/EF with fuel in overpack	101.0

NOTE:

The datum used for calculations involving the overpack is the bottom of the overpack bottom plate. The datum used for calculations involving the MPC only is the bottom of MPC baseplate (Figure 2.2.1).

The location of the loaded Trojan centroid includes top spacer ring above MPC top lid.

Table 2.2.3

CALCULATED MAXIMUM LIFT WEIGHT ON CRANE HOOK ABOVE POOL

Item	Weight (lb)
Total weight of overpack	153,710
Total weight of MPC(upper bound) + fuel	89,057 [†]
Overpack closure plate	-7,984
Water in MPC and overpack	16,384
Lift yoke	3,600
Inflatable annulus seal	50
TOTAL	254,816^{††}

[†] Includes MPC closure rings.

^{††} Trunnions are rated to lift 250,000 lbs. For weight exceeding 250,000 lbs, weight can be reduced by partial draining of the MPC. See Chapter 7 for operational controls.

Table 2.2.4

COMPONENT WEIGHTS AND DIMENSIONS FOR ANALYTIC CALCULATIONS*

Component	Weight (lbs)
MPC baseplate	3,000
MPC closure lid	10,400
MPC shell	5,900
MPC miscellaneous parts	3,700
Fuel basket	24,000/16,400 (PWR/BWR)13,000
Fuel	54,000
Total MPC	90,000
Overpack baseplate	10,000
Overpack closure plate	8,000
Overpack shell	137,000
Total overpack	155,000
Total HI-STAR 100 lift weight	250,000
Impact limiters	37,000
HI-STAR with limiters	282,000
<i>Item</i>	<i>Dimension (inch)</i>
<i>Overpack Outer Diameter</i>	<i>96</i>
<i>Overpack Length</i>	<i>203.125</i>
<i>MPC Outer Diameter</i>	<i>68.375</i>
<i>MPC Length</i>	<i>190.5</i>
<i>Overpack Inner Diameter</i>	<i>68.75</i>

Note: Analytical calculations may use weights and dimensions in Table 2.2.4 or actual weights and dimensions for conservatism in calculation of safety factors. Finite element analyses may use weights calculated based on input weight densities.

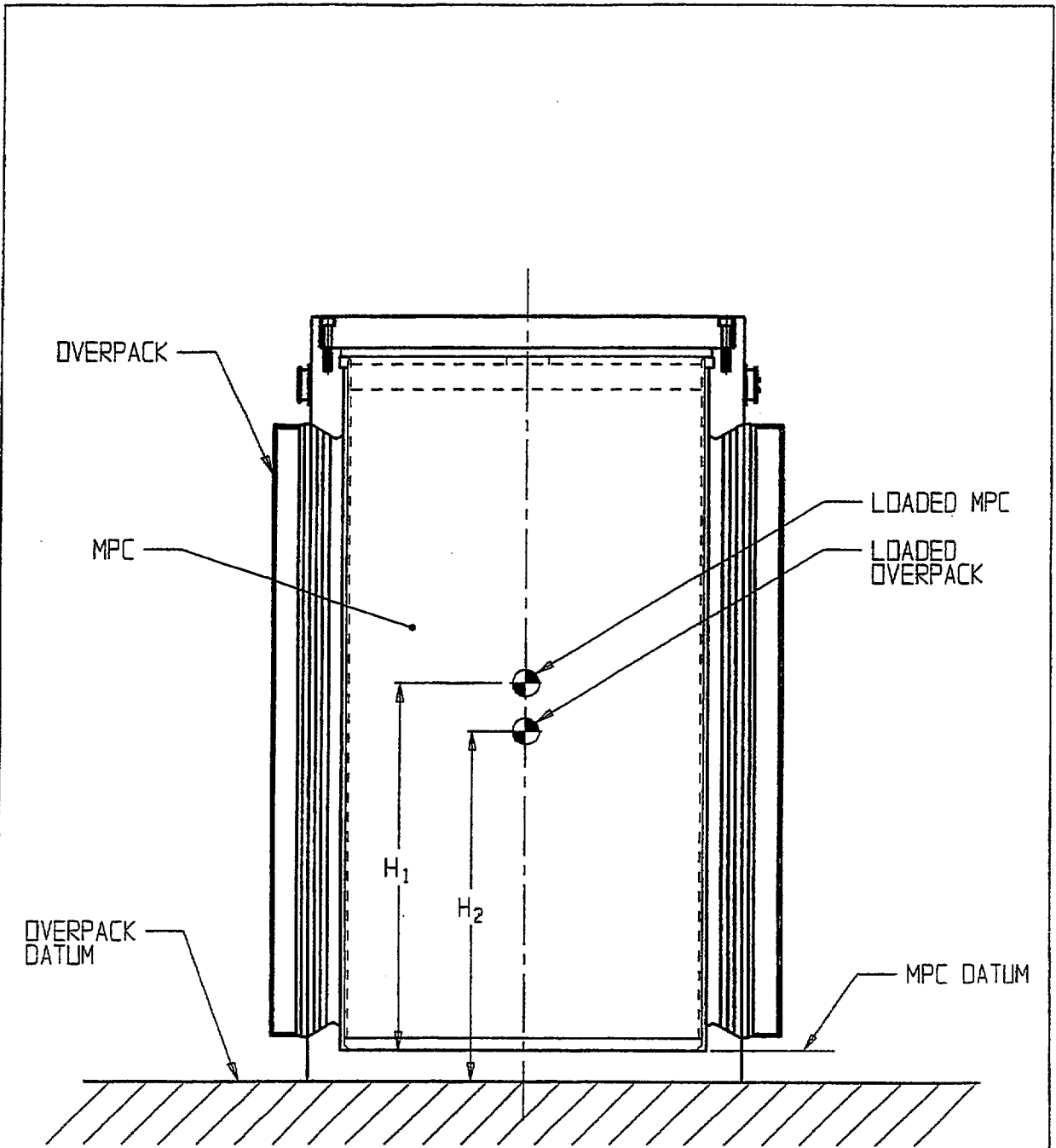


FIGURE 2.2.1; HI-STAR 100 DATUM DEFINITION FOR TABLE 2.2.2

2.3 MECHANICAL PROPERTIES OF MATERIALS

This section provides the mechanical properties used in the structural evaluation. The properties include yield stress, ultimate stress, modulus of elasticity, Poisson's ratio, weight density, and coefficient of thermal expansion. The property values are presented for a range of temperatures for which structural calculations are performed.

The materials selected for use in the HI-STAR 100 MPC and overpack are presented in the Bills-of-Materials in Chapter 1, Section 1.4. In this chapter, the materials are divided into two categories, structural and nonstructural. Structural materials are those that serve a load bearing function. Materials that do not support mechanical loads are considered nonstructural. For example, the overpack inner shell is a structural material, while Holtite-A (neutron shield) is a nonstructural material.

2.3.1 Structural Materials

2.3.1.1 Alloy X

A hypothetical material termed Alloy X is defined for all MPC structural components. The material properties of Alloy X are the least favorable values from the set of candidate stainless alloys. The purpose of a "least favorable" material definition is to ensure that all structural analyses are conservative, regardless of the actual MPC material. For example, when evaluating the stresses in the MPC, it is conservative to work with the minimum values for yield strength and ultimate strength. This guarantees that the material used for fabrication of the MPC is of equal or greater strength than the hypothetical material used in the analysis. In the structural evaluation, the only property for which it is not always conservative to use the minimum values is the coefficient of thermal expansion. Two sets of values for the coefficient of thermal expansion are specified, a minimum set and a maximum set. For each analysis, the set of coefficients, minimum or maximum that causes the more severe load on the cask system is used. Table 2.3.1 lists the numerical values for the material properties of Alloy X versus temperature. These values, taken from the ASME Code, Section II, Part D [2.1.11], are used to complete all structural analyses. The maximum temperatures in MPC components may exceed the allowable limits of temperature during short time duration events. However, under no scenario does the maximum temperature of Alloy X material used in the helium confinement boundary exceed 1000°F. As shown in ASME Code Case N-47-33 (Class 1 Components in Elevated Temperature Service, 1995 Code Cases, Nuclear Components), the strength properties of austenitic stainless steels do not change due to exposure to 1000 °F temperature for up to 10,000 hours. Therefore, there is no significant effect on mechanical properties of the helium confinement boundary or fuel basket material during the short time duration loading. Further description of Alloy X, including the materials from which it is derived, is provided in Appendix 1.A.

Two properties of Alloy X which are not included in Table 2.3.1 are weight density and Poisson's ratio. These properties are assumed constant for all structural analyses, regardless of the temperature. The values used are shown in the table below.

PROPERTY	VALUE
Weight Density (lb./in ³)	0.290
Poisson's Ratio	0.30

2.3.1.2 Carbon Steel, Low-Alloy, and Nickel Alloy Steel

The carbon steels used in the HI-STAR 100 System are SA516 Grade 70, SA515 Grade 70. These steels are not constituents of Alloy X. The material properties of SA516 Grade 70 and SA515 Grade 70 are shown in Tables 2.3.2 and 2.3.3, respectively. The nickel alloy and low-alloy steels are SA203-E and SA350-LF3, respectively. The material properties of SA203-E and SA350-LF3 are given in Table 2.3.4.

Two properties of these steels which are not included in Tables 2.3.2 through 2.3.4 are weight density and Poisson's ratio. These properties are assumed constant for all structural analyses. The values used are shown in the table below.

PROPERTY	VALUE
Weight Density (lb./in ³)	0.283
Poisson's Ratio	0.30

2.3.1.3 Bolting Materials

Material properties of the bolting materials used in the HI-STAR System are given in Table 2.3.5.

2.3.1.4 Weld Material

All weld filler materials utilized in the welding of the Code components will comply with the provisions of the appropriate ASME subsection (e.g., Subsection NB for the overpack and enclosure vessel) and Section IX. All non-Code welds shall also be made using weld procedures which meet Section IX of the ASME Code. All non-code welds shall also be made using weld procedures which meet Section IX of the ASME Code. The minimum tensile strength of the weld wire and filler material (where applicable) will be equal to or greater than the tensile strength of the base metal listed in the ASME Code.

2.3.1.5 Impact Limiter

The Impact Limiter for the HI-STAR 100 System has been named AL-STAR™. AL-STAR is composed of cross core and uni-directional aluminum honeycomb made by layering corrugated sheets of aluminum (alloy 5052). For the cross core material, alternate layers of corrugated aluminum sheets are laid in orthogonal direction to each other (Figure 2.3.1). The layers are bonded together by a high-temperature epoxy. The Holtec drawing-1765 in Section 1.4 illustrates

the arrangement of the cross core and uni-directional honeycomb sectors in AL-STAR to realize adequate crush moduli in all potential impact modes. The external surface of AL-STAR consists of a stainless steel skin to provide long-term protection against weather and environmental conditions.

Rail transport considerations limit the maximum diameter of the impact limiter to 128 inches. The axial dimension of AL-STAR is limited by the considerations of maximum permissible packaging weight for rail transport. Within the limitations of space and weight, AL-STAR must possess sufficient energy absorption capacity so as to meet the design basis rigid body deceleration limits (Table 2.1.10) under all postulated drop orientations. The sizing of the AL-STAR internal structure is principally guided by the above considerations. For example, in order to ensure that a sufficient portion of the honeycomb structure participates in lateral impacts, a thick carbon steel shell buttressed with gussets (~~Drawing 1765~~) provides a hard backing surface for the aluminum honeycomb to crush against.

Two properties of the cross core honeycomb germane to its function are the crush strength and the nominal density. The crush strength of AL-STAR is the more important of the two properties; the density is significant in establishing the total weight of the package. The crush strength increases monotonically with density. For example, the cross core honeycomb of 2500 psi crush strength has a nominal density of 27 lb. per cubic foot. At 2,000 psi crush strength, the change in aluminum honeycomb parameters lowers the density to approximately 22 lb. per cubic foot. The crush strength of the honeycomb can be varied within a rather wide range by adjusting the aluminum foil thickness and corrugation size. *Drawings in Section 1.4* ~~Drawing 1765~~ shows the required crush strengths of the honeycomb sectors in the various regions of AL-STAR.

Like all manufactured materials, the crush strength and density of the honeycomb material are subject to slight variation within a manufactured lot. The crush strength will be held to a tolerance of approximately 15% (a nominal crush strength $\pm 7.5\%$).

Hexcel Corporation's publication TSB 120, "Mechanical Properties of Hexcel Honeycomb Materials", [2.3.1] provides detailed information on the mechanical characteristics of aluminum honeycomb materials. Hexcel's experimental data shows that the load-deflection curve of aluminum honeycomb simulates the shape of elastic-perfectly plastic materials. The honeycomb crushes at a nearly uniform load (slowly applied) until a solidity in the range of 30 to 40% is reached. It is the crushing at constant load characteristic of aluminum honeycomb along with its excellent crush strength-to-weight ratio that makes it an ideal energy absorption material. The cross layered honeycomb (cross-core) has an identical crush strength in two orthogonal directions. In other words, from a load-deflection standpoint, the cross-layered honeycomb is a transversely isotropic material.

A typical honeycomb pressure-strain curve is illustrated in Figure 2.4H.2.1 in Appendix 2.4H wherein additional discussion on the crush properties of the honeycomb material is provided.

However, three key properties of the honeycomb material which are central to its function as a near-ideal impact limiter crush material are summarized below.

- i. The honeycomb material can be used in the "un-crushed" or "pre-crushed" condition. The difference is in the initial "bump" in the pressure-strain curve shown in Figure 2.4H.2.1. By pre-crushing the honeycomb, its pressure-strain relationship simulates that of an ideal elastic-perfectly-plastic material, which is most desirable in limiting abrupt peaks in the deceleration of the package under drop events.
- ii. Irrespective of the crush strength, under quasi-static loading, all honeycomb materials begin to strain harden at about 60% strain and lock up at about 70%. Thus, a 10-inch thick honeycomb column will crush down to a thickness of 4 inches at near constant force; crushing further will require progressively greater compression force. The six inches of available crush distance is referred to as the available "stroke" in the lexicon of impact limiter design technology.
- iii. Because the crush material is made entirely out of one of the most cryogenically competent industrial metals available, aluminum, the pressure-crush behavior of the ALSTAR honeycomb material is insensitive to the environmental temperature range germane to Part 71 transport (-20 degrees F to 100 degrees F). Table Y-1 of the ASME Code [2.1.11] lists the yield strength of the material (Alloy 5052) to be constant in the range -20 degrees F to 350 degrees F.

Independent confirmation of the invariance of the ALSTAR's crush properties with temperature in the range of temperatures applicable to the HI-STAR 100 packaging was provided by experiments conducted by Holtec International in June 1998 [2.3.2] using sample material obtained from Hexcell. The test objective was to evaluate the temperature sensitivity, if any, of the static compression strength of the honeycomb material. To that end, test specimens were cut from the sample material and were subject to static compression testing using a Q.A. validated procedure.

A series of specimens of two different strengths were tested at three different temperatures. The specimens were tested at -29 degrees C, 23 degrees C and 80 degrees C which represent "Cold", "Ambient", and "Heat" environmental conditions. Ten specimens were prepared for each crush strength, to allow for multiple data points at each test temperature. The specimens were not pre-crushed so the static compression-crush curves exhibited an initial peak. After discounting the initial peaks in the static force-crush curve, the constant force range for each specimen could be identified from the test data and a crush pressure for the specimen defined by dividing this constant force by the measured specimen loaded area.

The computed crush pressures showed no significant trending that could be ascribed to environmental effects. Figure 2.3.2 is a plot of the test results and plots the average of the calculated test crush pressures from the series of specimens at each of the three temperatures. The results for individual test samples at any given temperature were within manufacturing tolerance. It is clear from the plotted results that the effect of temperature is well within the data scatter due to manufacturing tolerance. Therefore, within the temperature range germane to the ALSTAR impact limiter, the force-crush characteristic is expected to be essentially unaffected by the coincident honeycomb metal temperature. This leads to the ~~us to~~ conclusion that environmental temperature effects will not influence impact limiter performance predictions.

Appendix 2.4H contains further information on the AL-STAR honeycomb and its performance characteristics. The sensitivity of the package performance to variations in compression strength of the aluminum honeycomb is evaluated in Appendix 2.4H.

In summary, the AL-STAR impact limiter is composed of a carbon steel inner shell structure, an assemblage of cross core and uni-directional aluminum honeycombs and a stainless steel external sheathing.

None of the structural materials has a low melting point or is flammable. A Holtite-A layer is situated deep in the honeycomb in such a manner that it does not participate in the crushing process, but provides neutron shielding in the axial direction.

2.3.2 Nonstructural Materials

2.3.2.1 Neutron Shield

The neutron shield in the overpack is not considered as a structural member of the HI-STAR 100 System. Its load carrying capacity is neglected in all structural analyses except where such omission would be nonconservative. The only material property of the neutron shield which is important to the structural evaluation is weight density (1.63 g/cm^2).

2.3.2.2 BoralTM Neutron Absorber

Boral is not a structural member of the HI-STAR 100 System. Its load carrying capacity is neglected in all structural analyses. The only material property of Boral which is important to the structural evaluation is weight density. As the MPC fuel baskets can be constructed with Boral panels of variable areal density, the weight that produces the most severe cask load is assumed in each analysis. (Density 2.644 g/cm^3).

2.3.2.3 Aluminum Heat Conduction Elements

The aluminum heat conduction elements are located between the fuel basket and MPC vessel in several of the early vintage MPC-68s and MPC-68Fs. They have since been removed from the MPC design and none were installed in the PWR MPCs. They are thin, flexible elements whose sole function is to transmit heat from the basket. They are not credited with any structural load capacity and are shaped to provide negligible resistance to basket thermal expansion. The total weight of the aluminum heat conduction elements is less than 1,000 lb. per MPC.

Table 2.3.1

ALLOY X MATERIAL PROPERTIES

Temp. (°F)	Alloy X				
	S_y	S_u	α_{min}	α_{max}	E
-40	30.0	75.0	8.54	8.55	28.8214
100	30.0	75.0	8.54	8.55	28.14
150	27.5	73.0	8.64	8.67	27.87
200	25.0	71.0	8.76	8.79	27.6
250	23.75	68.5	8.88	8.9	27.3
300	22.5	66.0	8.97	9.0	27.0
350	21.6	65.2	9.10	9.11	26.75
400	20.7	64.4	9.19	9.21	26.5
450	20.05	64.0	9.28	9.32	26.15
500	19.4	63.5	9.37	9.42	25.8
550	18.8	63.3	9.45	9.50	25.55
600	18.2	63.1	9.53	9.6	25.3
650	17.8	62.8	9.61	9.69	25.05
700	17.3	62.5	9.69	9.76	24.8
750	16.9	62.2	9.76	9.81	24.45
800	16.6	61.7	9.82	9.90	24.1

Definitions:

S_y = Yield Stress (ksi)

α = Mean Coefficient of thermal expansion (in./in. per degree F x 10^{-6})

S_u = Ultimate Stress (ksi)

E = Young's Modulus (psi x 10^6)

Notes:

1. Source for S_y values is Table Y-1 of [2.1.11].
2. Source for S_u values is Table U of [2.1.11].
3. Source for α_{min} and α_{max} values is Table TE-1 of [2.1.11].
4. Source for E values is material group G in Table TM-1 of [2.1.11].

Table 2.3.2
SA516, GRADE 70 MATERIAL PROPERTIES

Temp. (°F)	SA516, Grade 70			
	S _y	S _u	á	E
-40	38.0	70.0	5.53	29.34
100	38.0	70.0	5.53	29.34
150	36.3	70.0	5.71	29.1
200	34.6	70.0	5.89	28.8
250	34.15	70.0	6.09	28.6
300	33.7	70.0	6.26	28.3
350	33.15	70.0	6.43	28.0
400	32.6	70.0	6.61	27.7
450	31.65	70.0	6.77	27.5
500	30.7	70.0	6.91	27.3
550	29.4	70.0	7.06	27.0
600	28.1	70.0	7.17	26.7
650	27.6	70.0	7.30	26.1
700	27.4	70.0	7.41	25.5
750	26.5	69.3	7.50	24.85

Definitions:

S_y = Yield Stress (ksi)

α = Mean Coefficient of thermal expansion (in./in. per degree F x 10⁻⁶)

S_u = Ultimate Stress (ksi)

E = Young's Modulus (psi x 10⁶)

Notes:

1. Source for S_y values is Table Y-1 of [2.1.11].
2. Source for S_u values is Table U of [2.1.11].
3. Source for á values is material group C in Table TE-1 of [2.1.11].
4. Source for E values is "Carbon steels with C ≤ 0.30%" in Table TM-1 of [2.1.11].

Table 2.3.3
SA515, GRADE 70 MATERIAL PROPERTIES

Temp. (°F)	SA515, Grade 70			
	S_y	S_u	α	E
-40	38.0	70.0	5.53	29.34
100	38.0	70.0	5.53	29.34
150	36.3	70.0	5.71	29.1
200	34.6	70.0	5.89	28.8
250	34.15	70.0	6.09	28.6
300	33.7	70.0	6.26	28.3
350	33.15	70.0	6.43	28.0
400	32.6	70.0	6.61	27.7
450	31.65	70.0	6.77	27.5
500	30.7	70.0	6.91	27.3
550	29.4	70.0	7.06	27.0
600	28.1	70.0	7.17	26.7
650	27.6	70.0	7.30	26.1
700	27.4	70.0	7.41	25.5
750	26.5	69.3	7.50	24.85

Definitions:

S_y = Yield Stress (ksi)

α = Mean Coefficient of thermal expansion (in./in. per degree F x 10^{-6})

S_u = Ultimate Stress (ksi)

E = Young's Modulus (psi x 10^6)

Notes:

1. Source for S_y values is Table Y-1 of [2.1.11].
2. Source for S_u values is Table U of [2.1.11].
3. Source for α values is material group C in Table TE-1 of [2.1.11].
4. Source for E values is "Carbon steels with C \leq 0.30%" in Table TM-1 of [2.1.11].

Table 2.3.4
SA350-LF3 AND SA203-E MATERIAL PROPERTIES

Temp. (°F)	SA350-LF3			SA350-LF3/SA203-E		SA203-E		
	S _m	S _y	S _u	E	α	S _m	S _y	S _u
-100	23.3	37.5	70.0	28.5	6.20	23.3	40.0	70.0
100	23.3	37.5	70.0	27.6	6.27	23.3	40.0	70.0
200	22.8	34.2	68.5	27.1	6.54	23.3	36.5	70.0
300	22.2	33.2	66.7	26.7	6.78	23.3	35.4	70.0
400	21.5	32.2	64.6	26.1	6.98	22.9	34.3	68.8
500	20.2	30.3	60.7	25.7	7.16	21.6	32.4	64.9
600	18.5	-	-	-	-	-	-	-
700	16.8	-	-	-	-	-	-	-

Definitions:

- S_m = Design Stress Intensity (ksi)
- S_y = Yield Stress (ksi)
- S_u = Ultimate Stress (ksi)
- α = Coefficient of Thermal Expansion (in./in. per degree F x 10⁻⁶)
- E = Young's Modulus (psi x 10⁶)

Notes:

1. Source for S_m values is Table 2A of [2.1.11].
2. Source for S_y values is Table Y-1 of [2.1.11].
3. Source for S_u values is ratioing S_m values.
4. Source for α values is material group E in Table TE-1 of [2.1.11].
5. Source for E values is material group B in Table TM-1 of [2.1.11].

Table 2.3.5
SB637-N07718, SA564-630, AND SA705-630 MATERIAL PROPERTIES

Temp. (°F)	SB637-N07718				
	S _y	S _u	E	α	S _m
-100	150.0	185.0	29.9	---	50.0
-20	150.0	185.0	---	---	50.0
70	150.0	185.0	29.0	7.0567	50.0
100	150.0	185.0	---	7.08	50.0
200	144.0	177.6	28.3	7.22	48.0
300	140.7	173.5	27.8	7.33	46.9
400	138.3	170.6	27.6	7.45	46.1
500	136.8	168.7	27.1	7.57	45.6
600	135.3	166.9	26.8	7.67	45.1
SA705-630/SA564-630 (Age Hardened at 1075°F)					
Temp. (°F)	S _y	S _u	E	α	-
200	115.6	145.0	28.5	5.9	-
300	110.7	145.0	27.9	5.9	-
400	106.7	141	-	-	-
500	103.5	140	-	-	-
SA705-630/SA564-630 (Age Hardened at 1150°F)					
200	97.1	135.0	28.5	5.9	-
300	93.0	135.0	27.9	5.9	-
400	89.8	131.4	-	-	-
500	87	128.5	-	-	-

Definitions

S_m = Design Stress Intensity (ksi)

S_y = Yield Stress (ksi)

α = Mean Coefficient of thermal expansion (in./in. per degree F x 10⁻⁶)

S_u = Ultimate Stress (ksi)

E = Young's Modulus (psi x 10⁶)

Notes:

1. Source for S_m values is Table 4 of [2.1.11].
2. Source for S_y, S_u values is ratioing design stress intensity values.
3. Source for α values is Tables TE-1 and TE-4 of [2.1.11], as applicable.
4. Source for E values is Table TM-1 of [2.1.11].

Table 2.3.6

YIELD STRENGTH OF SA-193-B8S IMPACT LIMITER ATTACHMENT BOLTS

Yield Stress for Attachment Bolt Calculations [†]	
Item	Yield Stress (psi)
Yield Stress	50,000

[†] Source for stress is Table 3 of [2.1.11].

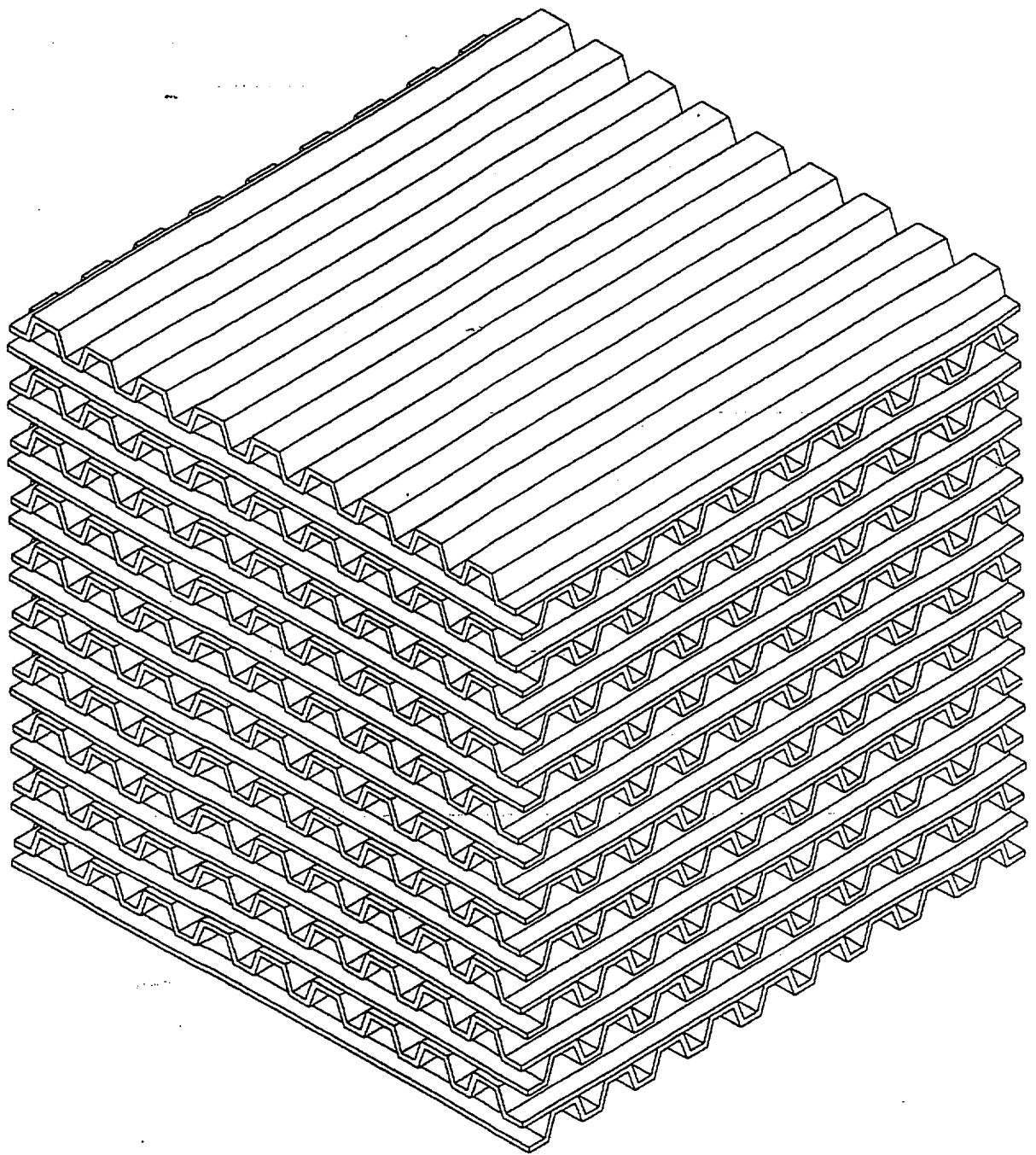


FIGURE 2.3.1; CROSS LAYERED ALUMINUM HONEYCOMB

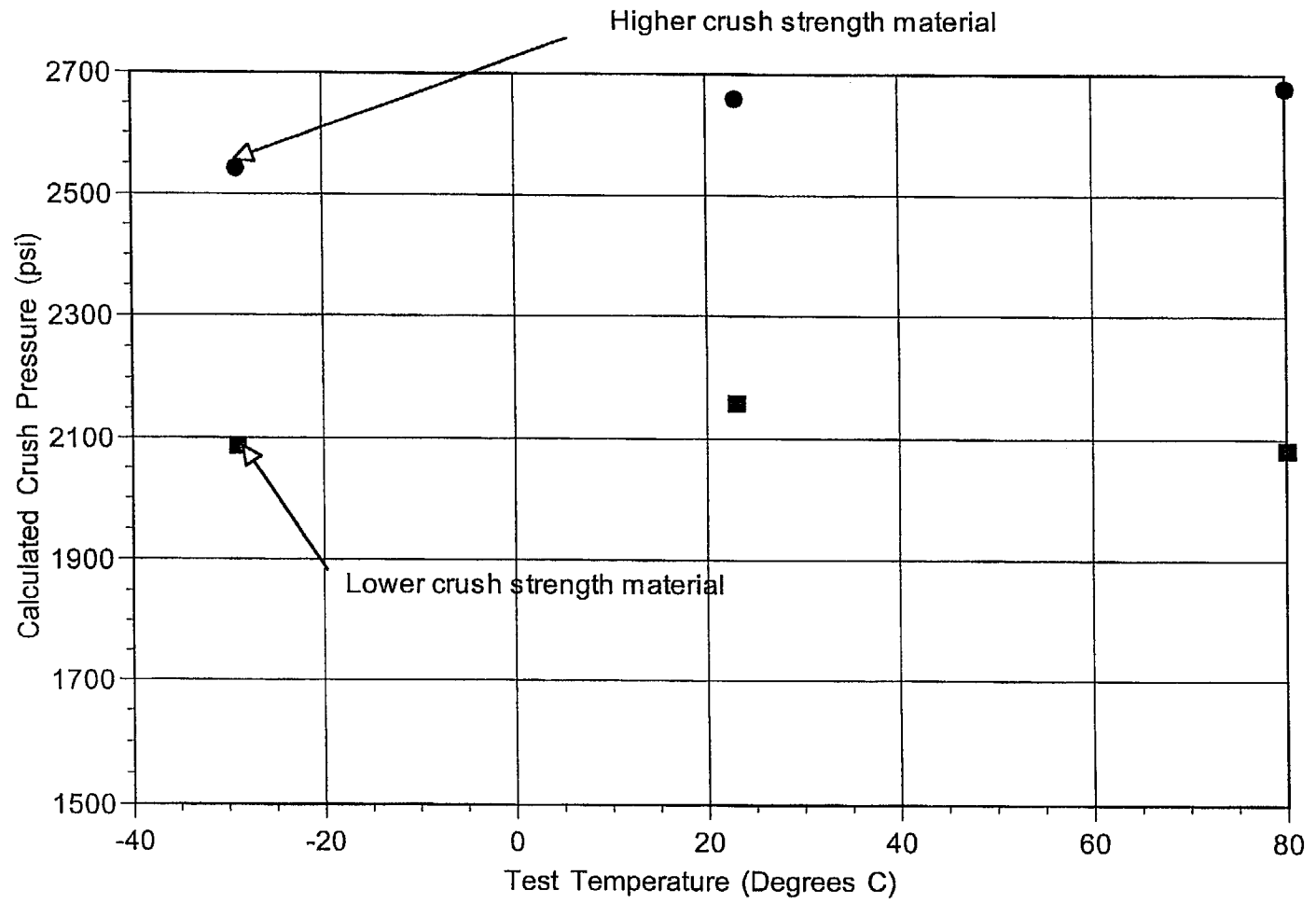


FIGURE 2.3.2 Average Crush Strength of Tested Specimens vs Test Temperature

2.4 GENERAL STANDARDS FOR ALL PACKAGES

The compliance of the HI-STAR 100 System to the general standards for all packaging, specified in 10CFR71.43, is demonstrated in the following paragraphs.

2.4.1 Minimum Package Size

The HI-STAR 100 package meets the requirements of 10CFR71.43(a); the outer diameter of the overpack is approximately 96" and its length is approximately 203".

2.4.2 Tamperproof Feature

During transport operations, a wire tamper seal with a stamped identifier will be attached between the lower base of the upper impact limiter shell and the head of one of the impact limiter attachment bolts for the purpose of indicating possible tampering. In order to access the radioactive contents of the overpack, the upper impact limiter is required to be removed to access the closure plate bolting. This tamper seal satisfies the requirements of 10CFR71.43(b). A second wire tamper seal will be attached between the lower impact limiter and an attachment bolt head to indicate tampering. This seal will prevent access to the drain port. The assembly drawing in Section 1.4 depicts the security seals.

2.4.3 Positive Closure

There are no quick-connect/disconnect valves in the containment boundary of the HI-STAR 100 packaging. The only access to the overpack internals is through the closure plate on the overpack which weighs over 7000 pounds and the overpack vent and drain ports which are sealed and protected by bolted cover plates. This closure plate is fastened to the overpack flange with heavy bolts which are torqued to closure values in Table 7.1.2. Opening of the overpack vent and drain port would require removal of the bolted cover plate and unthreading of the port plug. Inadvertent opening of the overpack is not feasible; opening an overpack requires mobilization of special tools and a source of power. The overpack containment boundary is analyzed for normal and accident condition internal pressure and demonstrates integrity under both conditions.

2.4.4 Chemical and Galvanic Reactions

There is no credible mechanism for chemical or galvanic reactions in the HI-STAR 100 MPC. The MPC, which is filled with helium, provides a nonaqueous and inert environment. Insofar as corrosion is a long-term time-dependent phenomenon, the inert gas environment in the MPC precludes the incidence of corrosion during transport. Furthermore, the only dissimilar material groups in the MPC are: (1) BoralTM and stainless steel and (2) aluminum and stainless steel. Boral and stainless steel have been used in close proximity in wet storage for over 30 years. Many spent fuel pools at nuclear plants contain fuel racks, which are fabricated from Boral and stainless steel materials, with geometries similar to the HI-STAR 100 MPC. Not one case of

chemical or galvanic degradation has been found in fuel racks built by Holtec. This experience provides a sound basis to conclude that corrosion will not occur in these materials. Additionally, the aluminum heat conduction elements and stainless steel basket are very close on the galvanic series chart. Aluminum, like other metals of its genre (e.g., titanium and magnesium) rapidly passivates in an aqueous environment, leading to a thin ceramic (Al_2O_3) barrier which renders the material essentially inert and corrosion-free over long periods of application. The physical properties of the material, e.g., thermal expansion coefficient, diffusivity, and thermal conductivity, are essentially unaltered by the exposure of the aluminum metal stock to an aqueous environment. In order to eliminate the incidence of aluminum water reaction inside the MPC during fuel loading operation (when the MPC is flooded with pool water) all aluminum surfaces will be pre-passivated or anodized before installation of Boral or conduction inserts in the MPC (see the ~~Drawings and Bills of Materials in~~ Section 1.4).

The HI-STAR 100 overpack combines low-alloy and nickel alloy steels, carbon steels, neutron and gamma shielding, thermal expansion foam, and bolting materials. All of these materials have a long history of nongalvanic behavior within close proximity of each other. The internal and external carbon steel surfaces of the overpack and closure plates are sandblasted and coated to preclude surface oxidation. The coating does not chemically react with borated water. Therefore, chemical or galvanic reactions involving the overpack materials are highly unlikely and are not expected.

The interfacing seating surfaces of the closure plate metallic seals are clad with stainless steel to assure long-term sealing performance and to eliminate the potential for localized corrosion of the seal seating surfaces.

In accordance with NRC Bulletin 96-04, a review of the potential for chemical, galvanic, or other reactions among the materials of the HI-STAR 100 System, its contents and the operating environment which may produce adverse reactions has been performed. Table 2.4.1 provides a listing of the materials of fabrication for the HI-STAR 100 System and evaluates the performance of the material in the expected operating environments during short-term loading/unloading operations and transport operations. As a result of this review, no operations were identified which could produce adverse reactions beyond those conditions already analyzed in this SAR.

The HI-STAR 100 System is composed of materials with a long proven history of use in the nuclear industry. The materials are not affected by the radiation levels caused by the spent nuclear fuel. Gamma radiation damage to metals (e.g., aluminum, stainless steel, and carbon steel) does not occur until the dose reaches 1018 rads or more. The gamma dose from the spent nuclear fuel transported in the HI-STAR 100 System is on the order of 1010 rads. Moreover, significant radiation damage due to neutron exposure does not occur for neutron fluences below approximately 10^{19} n/cm² [2.4.1, 2.4.2], which is far greater than the neutron fluence for which components of the HI-STAR 100 System will be exposed.

Table 2.4.1

HI-STAR 100 SYSTEM MATERIAL COMPATIBILITY
WITH OPERATING ENVIRONMENTS

Material/Component	Fuel Pool (Borated and Unborated Water) ¹	Transport (Open to Environment)
Alloy X: -MPC Fuel Basket -MPC Baseplate -MPC Shell -MPC Lid -MPC Fuel Spacers	Stainless steels have been extensively used in spent fuel storage pools with both borated and unborated water with no adverse reactions or interactions with spent fuel.	The MPC internal and external environment will be inert (helium) atmosphere. No adverse interactions identified.
Aluminum -Conduction Inserts	Aluminum and stainless steels form a galvanic couple. However, they are very close on the galvanic series chart and aluminum rapidly passivates in an aqueous environment forming a thin ceramic (Al ₂ O ₃) barrier. The aluminum will be installed in a passivated condition. Therefore, during the short time they are exposed to fuel pool water, corrosion is not expected.	In a non-aqueous atmosphere galvanic corrosion is not expected.
Boral: -Neutron Absorber	The Boral will be used in passivated condition. Extensive in-pool experience on spent fuel racks with no adverse reactions.	The Boral will be in a helium environment. No adverse reactions identified.

¹ HI-STAR 100 System short-term operating environment during loading and unloading.

Table 2.4.1 (continued)

HI-STAR 100 SYSTEM MATERIAL COMPATIBILITY
WITH OPERATING ENVIRONMENTS

Material/Component	Fuel Pool (Borated and Unborated Water) ²	Transport (Open to Environment)
<p>Steels:</p> <ul style="list-style-type: none"> -SA350-LF3 -SA203-E -SA515 Grade 70 -SA516 Grade 70 -SA750 630 17-4 PH -SA564 630 17-4 PH -SA106 -SA193-B7 <p>Overpack Body</p>	<p>All exposed steel surfaces (except seal areas, pocket trunnions, and bolt locations) will be coated with paint specifically selected for performance in the operating environments. Even without coating, no adverse reactions (other than nominal corrosion) have been identified.</p>	<p>Internal surfaces of the overpack will be painted and maintained in an inert atmosphere. Exposed external surfaces (except those listed in fuel pool column) will be painted and will be maintained with a fully painted surface. No adverse reactions identified.</p>
<p>Stainless Steels:</p> <ul style="list-style-type: none"> -SA240 304 -SA193 Grade B8 -18-8 S/S <p>Miscellaneous Components</p>	<p>Stainless steels have been extensively used in spent fuel storage pools with both borated and unborated water with no adverse reactions.</p>	<p>Stainless steel has a long proven history of corrosion resistance when exposed to the atmosphere. These materials are used for bolts and threaded inserts. No adverse reactions with steel have been identified. No impact on performance.</p>

² HI-STAR 100 System short-term operating environment during loading and unloading.

Table 2.4.1 (continued)
 HI-STAR 100 SYSTEM MATERIAL COMPATIBILITY
 WITH OPERATING ENVIRONMENTS

Material/Component	Fuel Pool (Borated and Unborated Water) ³	Transport (Open to Environment)
Nickel Alloy: -SB637-NO7718 Bolting	Bolts are not used in pool.	Exposed to weathering effects. No adverse reactions with overpack closure plate. No impact on performance.
Brass: -Rupture Disk	Small surface of rupture disk will be exposed. No significant adverse impact identified.	Exposed to external weathering. No loss of function expected. Disks inspected prior to transport.
Holtite-A: -Neutron Shield	The neutron shield is fully enclosed by the outer enclosure. No adverse reaction identified. No adverse reactions with thermal expansion foam or steel.	The neutron shield is fully enclosed in the outer enclosure. No adverse reaction identified. No adverse reactions with thermal expansion foam or steel.
Silicone Foam: -Thermal Expansion Foam	Fully enclosed in the outer enclosure. No adverse reaction identified. No adverse reactions with neutron shield or steel.	Foam is fully enclosed in outer enclosure. No adverse reaction identified. No adverse reactions with neutron shield or steel.

³ HI-STAR 100 System short-term operating environment during loading and unloading.

Table 2.4.1 (continued)

HI-STAR 100 SYSTEM MATERIAL COMPATIBILITY
WITH OPERATING ENVIRONMENTS

Material/Component	Fuel Pool (Borated and Unborated Water) ⁴	Transport (Open to Environment)
<p><u>Paint:</u></p> <ul style="list-style-type: none"> - Carboline 890 - Thermaline 450 	<p>Carboline 890 used for exterior surfaces. Acceptable performance for short-term exposure in mild borated pool water.</p> <p>Thermaline 450 selected for excellent high temperature resistance properties. Will only be exposed to demineralized water during in-pool operations as annulus is filled prior to placement in the spent fuel pool and the inflatable seal prevents fuel pool water in-leakage. No adverse interaction identified which could affect MPC/fuel assembly performance.</p>	<p>Good performance on exterior surfaces. Discoloration is not a concern.</p> <p>During transport, internal overpack surfaces will operate in an inert (helium) atmosphere. No adverse reaction identified.</p>
<p><u>Metallic Seals:</u></p> <ul style="list-style-type: none"> - Alloy X750 - 304 S/S 	<p>Not installed or exposed during in-pool handling.</p>	<p>Seals enclosed by closure plate or port cover plates.</p> <p>Closure plate seals seat against stainless steel overlay surfaces. No degradation of seal integrity due to corrosion is expected.</p>

⁴ HI-STAR 100 System short-term operating environment during loading and unloading.

2.5 LIFTING AND TIE-DOWN STANDARDS

2.5.1 Lifting Devices

As required by Reg. Guide 7.9, in this subsection, analyses for all lifting operations applicable to the transport of a HI-STAR 100 package are presented to demonstrate compliance with the requirements of paragraph 71.45(a) of 10CFR71.

The HI-STAR 100 System has the following types of lifting devices: lifting trunnions located on the overpack top flange and threaded holes for eye bolts to lift the overpack closure plate. Lifting devices associated with movement of the MPC are not considered here; MPC lifting is addressed in a companion HI-STAR100 document (*FSAR*, Docket 72-1008), and summarized in Subsection 2.5.1.3.

The evaluation of the adequacy of the lifting devices entails careful consideration of the applied loading and associated stress limits. The load combination $D+H$, where H is the "handling load", is the generic case for all lifting adequacy assessments. The term D denotes the dead load. Quite obviously, D must be taken as the bounding value of the dead load of the component being lifted. Table 2.2.4 gives bounding weights. In all lifting analyses considered in this document, the handling load H is assumed to be equal to $0.15D$. In other words, the inertia amplifier during the lifting operation is assumed to be equal to $0.15g$. This value is consistent with the guidelines of the Crane Manufacturer's Association of America (CMAA), Specification No. 70, 1988, Section 3.3, which stipulates a dynamic factor equal to 0.15 for slowly executed lifts. Thus, the "apparent dead load" of the component for stress analysis purposes is $D^* = 1.15D$. Unless otherwise stated, all lifting analyses in this section use the "apparent dead load", D^* , in the lifting analysis.

Analysis methodology to evaluate the adequacy of the lifting device may be analytical or numerical. For the analysis of the trunnion, an accepted conservative technique for computing the bending stress is to assume that the lifting force is applied at the tip of the trunnion "cantilever" and that the stress state is fully developed at the base of the cantilever. This conservative technique, recommended in NUREG-1536 for use in a storage *FSAR*, is applied to the trunnion analyses presented in this SAR.

The lifting trunnions are designed to meet the requirements of 10CFR71.45(a). The lifting attachments that are part of the HI-STAR 100 package also meet the design requirements of NUREG-0612 [2.1.9], which defines specific additional safety margins to ensure safe handling of heavy loads in critical regions of nuclear power plants. Satisfying the more conservative design requirements of NUREG-0612 ensures that the design requirements of 10CFR71.45(a) are met.

In general, the stress analysis to establish safety in lifting, pursuant to NUREG-0612, 10CFR71.45(a), and the ASME Code, requires evaluation of three discrete zones which may be referred to as (i) the trunnion, (ii) the trunnion/component interface, hereinafter referred to as Region A, and (iii) the rest of the component, specifically the stressed metal zone adjacent to Region A, herein referred to as Region B.

Stress limits germane to each of the above three areas are discussed below:

- i. Trunnion: NUREG-0612 requires that under the "apparent dead load", D^* , the maximum primary stress in the trunnion be less than 10% of the trunnion material ultimate strength *and* less than 1/6th of the trunnion material yield strength. In other words, the maximum moment and shear force developed in the trunnion cantilever is less than 1/6 of the moment and shear force corresponding to incipient plasticity, and less than 1/10 of the flexural collapse moment or ultimate shear force for the section.
- ii. Region A: Trunnion/Component Interface: Stresses in Region A must meet ASME Code Level A limits under applied load D^* . Additionally, paragraph 71.45(a) of 10CFR71 requires that the maximum primary stress under $3D^*$ be less than the yield strength of the weaker of the two materials at the trunnion/component interface. In cases involving section bending, the developed section moment must be compared against the plastic moment at yield. Typically, the stresses in the component in the vicinity of the trunnion/component interface are higher than elsewhere. However, exceptional situations exist. For example, when lifting a loaded MPC, the overpack baseplate, which supports the entire weight of the loaded MPC, is a candidate location for high stress even though it is far removed from the lifting location (which is located in the top lid).
- iii. Region B: This region constitutes the remainder of the component where the stress limits under the concurrent action of the apparent dead load D^* and other mechanical loads that may be present during handling (e.g. internal pressure) are required to meet Level A Service Limits under normal conditions of transport.

In summary, both Region A and Region B are required to meet the stress limits corresponding to ASME Level A under the load D^* . Additionally, portions of the component that may experience high stress during the lift are subject to the stress criterion of paragraph 71.45(a) of 10CFR71, which requires satisfaction of yield strength as the limit when the sole applied load is $3D^*$. In general, all locations of high stress in the component under D^* must also be checked for compliance with ASME Code Level A stress limits.

Unless explicitly stated otherwise, all analyses of lifting operations presented in this report follow the load definition and allowable stress provisions of the foregoing. Consistent with the practice adopted throughout this chapter, results are presented in dimensionless form, as safety factors, defined as SF, where

$$SF = (\text{Allowable Stress in the Region Considered}) / (\text{Computed Maximum Stress in the Region})$$

It should be emphasized that the safety factor, SF, defined in the foregoing, represents the additional margin that is over and beyond the margin built into NUREG 0612 (e.g. a factor of 10 on ultimate strength or 6 on yield strength).

In the following subsections, each of the lifting analyses performed to demonstrate compliance with regulations *is described*. Summary results are presented for each of the analyses.

It is recognized from the discussion in the foregoing that stresses in Region A are subject to two distinct criteria, namely Level A stress limits under D* and any other loading that may be present (such as pressure) and yield strength at 3D*. The "3D*" identifier *is used* whenever the paragraph 71.45(a) load case (the stresses must be bounded by the yield point at 3D*) is the applied loading.

The HI-STAR 100 System has two types of lifting devices that are used during handling and loading operations. Two lifting trunnions are located on the overpack top flange for vertical package handling operations. There are also four lifting eyeholes for handling of the overpack closure plate. Four lifting eyes are installed in the holes for connection to lifting slings.

The two lifting trunnions on the overpack top flange are spaced at 180-degree intervals. Trunnion analysis results are presented in Subsection 2.5.1.1.

The four threaded holes of the overpack closure plate accommodate lifting eyes that are used only for installation or removal of the overpack closure plate.

2.5.1.1 Overpack Trunnion Analysis

The lifting trunnion for the HI-STAR 100 overpack is presented in *the* Holtec Drawings (Section 1.4). The two lifting trunnions for HI-STAR 100 are circumferentially spaced at 180 degrees. The trunnions are designed for a two-point lift and are sized to satisfy the aforementioned NUREG-0612 criteria. The trunnion material is SB-637-N07718 bolt material, which is the same high strength material used for the closure plate bolts.

Each trunnion is initially threaded into the outer wall of the overpack top flange and is held in place by a locking pad. During a lifting operation, the moment and shear force are resisted by bearing and shearing stresses in the threaded connection.

The embedded trunnion is analyzed as a cantilever beam subjected to a uniformly distributed load applied over a short span of surface at the outer edge of the trunnion. *Calculations demonstrate* that the stresses in the trunnions, computed in the manner of the foregoing, comply with NUREG-0612 provisions.

Specifically, the following results are obtained:

Safety Factors from HI-STAR 100 Lifting Trunnion Stress Analysis [†]			
Item	Value (ksi) or (lb.) or (lb.-in.)	Allowable (ksi) or (lb) or (lb.-in.)	Safety Factor
Bending stress (Comparison with Yield Stress/6)	17.3	24.5	1.41
Shear stress (Comparison with Yield Stress/6)	7.4	14.7	1.99
Bending Moment (Comparison with Ultimate Moment/10)	323,000	574,600	1.78
Shear Force (Comparison with Ultimate Force/10)	144,000	282,000	1.97

[†] The bounding lifted load is 250,000 lb. (per Table 2.2.4).

We note from the above that all safety factors are greater than 1.0. A factor of safety of exactly 1.0 means that the maximum stress, under apparent lift load D*, is equal to the yield stress in tension or shear divided by 6, or that the section moment or shear force is equal to the ultimate section moment capacity or section force capacity divided by 10.

It is also important to note that safety factors associated with satisfaction of 10CFR71.45(a) are double those reported in the table since 10CFR71.45 only requires a factor of safety of 3 on the yield strength.

2.5.1.2 Stresses in the Overpack Closure Plate, Main Flange, and Baseplate During Lifting

2.5.1.2.1 Analysis of Closure Plate Lifting Holes and Eyes

The closure plate of the HI-STAR 100 overpack is lifted using four wire rope slings. The slings are attached to the closure plate using clevis eyebolts threaded into four holes in the closure plate.

10CFR71.45(a) requires a safety factor of 3 (based on yield strength) for the stress qualification of the clevis eyebolts. Lid lifting will normally be carried out with a lift angle of 90 degrees. However, to be conservative, the analysis assumes a minimum lift angle of 45 degrees.

The eyebolts are sized for a bounding weight of 9,200 lbs. (a value that includes a 15% dynamic amplifier). The working capacity of standard eyebolts is specified with a safety factor of four. Accordingly, its bolt size

is selected such that it has a working capacity of approximately 17,000 lb. (vertical). This results in a safety factor of greater than 7.0 calculated against the clevis ultimate load capacity. *The tapped holes and specified bolts in the closure plate are analyzed and it is demonstrated that adequate thread strength and engagement length exists using allowable stresses in accordance with NUREG-0612 requirements (which are more severe than 10CFR71.45(a) requirements)*

Minimum safety factors are summarized in the table below where we note that a safety factor of 1.0 means that the stress is the lessor of yield stress/6 or ultimate stress/10.

Overpack Top Closure B Minimum Safety Factors			
Item	Value (lb.)	Capacity (lb.)	Minimum Safety Factor
Overpack Top Closure Lifting Bolt Shear	9,200	12,080	1.31
Overpack Top Closure Lifting Bolt Tension	9,200	15,390	1.67

2.5.1.2.2 Top Flange

- ASME Service Condition (Region B)

During lifting of a loaded HI-STAR 100, the top flange of the overpack (in which the lift trunnions are located) is identified as a potential location for high stress levels.

The top flange interface with the trunnion under the lifted load D is analyzed using simplified strength of materials models that focus on the local stress state in the immediate vicinity of the connection that develops to react the applied trunnion load. The bending moment that is transferred from the trunnion to the top forging is reacted by a shear stress distribution on the threads. Figure 2.5.1 shows a schematic of the distribution used to react the applied moment by thread shear. The top flange is considered a NB component subject to the lifted load and internal pressure. The membrane stress intensity due to both components of load is computed at the interface and compared to the allowable local membrane stress intensity. The interface region is also conservatively considered as subject to the provisions of NUREG-0612 and the thread shear stress and bearing stress are compared to 1/6 of the top forging yield stress in shear or compression. The following table summarizes the results:*

Top Flange B Minimum Safety Factors (Interface with Trunnion)			
Item	Value (ksi)	Allowable (ksi)	Safety Factor
Bearing Stress (NUREG-0612 Comparison)	3.808	5.975	1.57
Thread Shear Stress (NUREG-0612 Comparison)	3.376	3.585	1.06
Stress Intensity (NB Comparison)	7.857	34.6	4.4

It is noted from the above that all safety factors are greater than 1.0 and that the safety factors for bearing stress and thread shear stress represent the *additional* margin over the factor of safety *inherent in the member by virtue of the load multiplier mandated in NUREG-0612.*

- Overpack Top Flange and Baseplate Under 3D*

Analyses are performed for the components of the HI-STAR 100 structure that are considered as Region A (namely, the top flange region and baseplate) and evaluated for safety under three times the apparent lifted load (3D). A one-quarter symmetry finite element model of the top section of the HI-STAR, without the lid has been constructed. The model is assumed constrained at 36" below the top of the top flange. Contact elements are used to model the interface between the trunnion and the top flange and the material behavior is assumed to be elastic-plastic in nature (i.e. a bi-linear stress strain curve is input into the finite element analysis model). The analysis seeks to demonstrate that under 3 times the lifted load, the maximum primary membrane stress across any section in the immediate vicinity of the trunnion is below the material yield strength and the primary membrane plus primary bending stress across any section does not exceed 1.5 times yield. The overpack baseplate is also analyzed using formulas from classical plate theory, conservatively assuming that the allowable strengths are determined at the component design temperature rather than at the lower normal operating conditions.*

The results are summarized in the table below:

Overpack Top Flange and Baseplate Minimum Safety Factors (10CFR71.45(a) Loading)			
Item	Value (ksi)	Allowable (ksi)	Safety Factor
Top Flange Membrane Stress Intensity (3D*)	27.44	32.2	1.17
Top Flange Membrane plus Bending Stress Intensity (3D*)	30.0	48.3	1.61
Baseplate Membrane plus Bending Stress Intensity (3D*)	1.452	32.2	22.2

The safety factors are all greater than 1.0 indicating that the requirements of 10CFR71.45(a) are satisfied in the top flange and baseplate of the HI-STAR 100 overpack.

2.5.1.3 MPC Lifting Analyses

The MPC can be inserted or removed from an overpack by lifting bolts that are designed for installation into threaded holes in the top lid. The HI-STAR 100 FSAR (Docket 72-1008) contains analyses of the components of the MPC that are considered as lifting devices. The strength requirements of the bolts and base metal are examined in based on the requirements of NUREG 0612. For a conservative analysis, we impose the requirements of NUREG-0612 on the closure lid material, which are more severe than the 10CFR71.45(a) requirements. A conservative analysis of the MPC baseplate under the 3D* loading is also performed. The MPC baseplate is modeled as a simply supported plate subject to the load from the fuel basket and the fuel.

The following table summarizes the results from these analyses also performed for the HI-STAR 100 FSAR. As stated earlier, safety factors tabulated in this section represent margins that are over and beyond those implied by the loading magnification mandated in NUREG 0612 or 10CFR71.45(a), as appropriate.

Summary of MPC Lifting Analyses-Minimum Safety Factors			
Item	Value of Stress (ksi) or Load (lb.)	Allowable (ksi) or Capacity (lb.)	Safety Factor
MPC Lifting Bolt Load B NUREG 0612	103,500	111,300	1.08
Baseplate Bending Stress B (3D*)	13.26	20.7	1.56

We note that all factors of safety are greater than 1.0 as required.

2.5.1.4.1 Lifting of Damaged Fuel Canisters

All damaged fuel canisters suitable for deployment in the HI-STAR 100 Package are analyzed for structural integrity during a lifting operation. Appendix 2.B describes the analyses undertaken and summarizes the results obtained.

In conclusion, the synopses of lifting device, device/component interface, and component stresses, under all contemplated lifting operations for the HI-STAR 100 overpack and MPC have been presented in the foregoing *and show that all factors of safety are greater than 1.0.*

2.5.2 Tie-Down Devices

2.5.2.1 Discussion

The initial design of the HI-STAR 100 Systems envisioned a shear ring located on the top flange and pocket trunnions located near the bottom of the outer enclosure shell to serve as locations for tie-down. Accordingly, previous issues of the SAR included analyses to qualify the shear ring/pocket trunnion components as tie-down devices complying with the requirements of 10CFR71.45(b).

The pair of semi-obround recesses referred to as pocket trunnions were originally incorporated into the HI-STAR design to permit the cask to be upended (or downended) by using circular shafts inserted in the "pockets" to serve as rotation pivots. Recent handling experience with the seven HI-STAR 100 overpacks manufactured thus far (ca. April 2002) and the HI-TRAC transfer casks (which are similar in overall dimensions and weight) has shown that utilizing an L-shaped cradle, designed as an ancillary under Part 72 regulations for the upending and downending operations, is a more robust method of cask handling. The cradle method of handling Holtec's overpacks and MPCs has garnered considerable experience through ISFSI implementation operations at several sites. Because the cradle method of upending and downending does not require the pocket trunnions, and because the recesses to incorporate the pocket trunnions lead to increased local dose, the pocket trunnions are being henceforth eliminated from the HI-STAR design. All HI-STAR 100 overpacks (except the first seven units already manufactured) shall be fabricated without the twin pocket trunnions; even in the first seven units that have the shear ring and pocket trunnions, these locations are no longer designated as tie-down locations.

In lieu of relying on the pocket trunnions for tie-down, the revised tie-down arrangement for HI-STAR 100 secures the overpack to the transport vehicles in such a manner that the longitudinal inertia forces (the most frequent mode of motion-induced loading the package during transport) do not exert an overturning moment on the cask (as is the case with a pocket trunnion-based fastening means). In fact, the revised tie-down device seeks to eliminate or minimize all localized loadings on the body of the overpack, thus incorporating an additional element of safety in the transport

package.

The new tie-down configuration, pictorially illustrated in Figure 1.2.8, essentially consists of a near-full-length saddle integral to the bed of the transport vehicle to react the lateral and vertical loads, and a pair of End-Restraints, also integral to the transport vehicle, that save for a small calibrated axial clearance to provide for differential thermal expansion, provide a complete axial confinement to the overpack. The details of the design of the tie-down structure are governed by the reaction forces computed using static equilibrium relationships for inertia loads corresponding to §72.45(b) and reported in this SAR.

To comply with the requirements of 10CFR71.45(b), it must be shown by test or analysis that all devices used for package tie-down are acceptable. Therefore, in this section, we present the load analyses of the HI-STAR 100 tie-down system. The HI-STAR 100 System is shown in a transport orientation in Drawing C1782 and in Figure 1.2.8.

To summarize, HI-STAR 100 is secured to the transport vehicle in a horizontal position by the following components (no additional support structure is permanently attached to the cask for transport tie-down):

- a. A long saddle support, bearing on the overpack outer enclosure shell and enclosure shell panels, over an angle of approximately 140 degrees. Multiple tie-down straps, sized to support uplift loads, secure the HI-STAR 100 to the saddle. The saddle resists lateral loads and vertical downward oriented loads through its extensive interface with the body of the HI-STAR overpack. Vertical upward directed loads are reacted by the tie-down straps.*
- b. Longitudinal loads in either direction are transmitted to the End-Restraint by the sacrificial disc on each impact limiter that is specifically designed to resist normal handling decelerations of 17g without impairing the performance of the impact limiters during the mandated Accident Conditions of Transport drop configurations. Because the axial transport loads are bounded by the 10g's in either longitudinal direction, the aluminum honeycomb discs are quite adequate to transmit axial loads without crushing.*

In accordance with 10CFR71.45(b), the inertia forces, applied at the center of gravity of the loaded HI-STAR 100, arise from:

- a. a horizontal component along the longitudinal axis of $\pm 10g$
- b. a vertical component of $\pm 2g$
- c. a lateral component of $\pm 5g$

These accelerations are referred to as the first set of load amplifiers. These forces are applied simultaneously in the respective directions with their lines of action selected to maximize the reactions. In the following, "load combinations" are identified by assembling the three loads with appropriate plus or

minus signs to reflect the fact that the lateral load can be in either direction, the vertical load can be in either direction, and the longitudinal load is uni-directional.

As required by the governing regulations, the components of the cask that are used for tie-down must be capable of withstanding the force combinations without generating stress in the cask components in excess of the material yield strength.

The saddle support under the enclosure shell, the slings, and the front and rear end structures that resist longitudinal load are not part of the HI-STAR 100 package and therefore, are not part of this submittal. The loads used to design these components are determined using the load amplifiers given by the American Association of Railroads (AAR) Field Manual, Rule 88. These amplifiers, henceforth called the second set of load amplifiers, are:

- $\pm 7.5g$'s longitudinal
- $\pm 2.0 g$'s vertical
- $\pm 2.0 g$'s lateral

In what follows, the equations of equilibrium for the packaging subject to three orthogonal inertia loads *are set down*. Tie-down reactions using either set of load amplifiers are determined from the same equilibrium equations. Numerical results are obtained for both sets of input load amplifiers and presented at the end of this section as Tables 2.5.1 and 2.5.2.

Figure 1.2.8 shows a schematic of the tie-down; Figure 2.5.2 shows a partial free-body diagram of the transport package on the railcar. The following steps to comply with the provisions of 10CFR71.45(b) are carried out:

- *Develop the general equilibrium equations to solve for the tie-down forces.*
- *Apply the equations to develop numerical results for the tie-down forces. Results are provided for the load multipliers specified in 10CFR71.45(b) and for the load multipliers in the AAR Field Manual.*
- *The tie-down force values with the 10CFR71.45(b) load amplifiers are used to evaluate the structural integrity of the cask components affected by the tie-down devices. Tie-down reactions obtained using the AAR Field Manual amplifiers for are reported for information only (for future use in designing the tie-down members of the railroad car).*

2.5.2.2 Equilibrium Equations to Determine the Tie-Down Forces

For longitudinal loading, the applied load, amplified by the imposed deceleration, is reacted directly by either the top or bottom impact limiter. The protruding donut shaped annular portion of the impact limiter is designed to mitigate the results from a 1' free end drop in accordance with regulatory requirements. The impact limiter material crush strength limits the deceleration to 17g's or less (Table 2.1.10), and it is shown in Subsection 2.6 that all components of the HI-STAR 100 package in this load path meet ASME Level A stress limits. Therefore, by suitable choice of support structure on the railcar, the HI-STAR 100 Package is assured of meeting regulatory requirements under the mandated longitudinal transport load of 10g's in either direction

For vertical loading, the resultant vertical force on the saddle is reacted by a symmetric bearing pressure, or by developing a reacting tension in the tie-down strap. Figure 2.5.12 shows a free body at a saddle support. The vertical load is conservatively assumed resisted by a radial component only, with no credit assumed for any shear stresses arising from friction at the interface. The radial pressure, p_v , is assumed to vary with circumferential location using a cosine function, with peak pressure occurring under the overpack centerline.

For lateral loading, the resultant force is conservatively assumed reacted only by a radial bearing pressure, p_h , distributed on one side of the saddle and varying around the periphery in accordance with a sine function (shear stresses due to frictional effects are conservatively neglected). Figure 2.5.13 shows the appropriate free-body. Since the radial pressure distribution corresponds to both a vertical and lateral force resultant, an opposing vertical force is developed in the tie-down strap. This vertical force is proportional to the applied lateral force, and ensures equilibrium. For the evaluation of lateral force equilibrium, it is also necessary to determine the vertical and horizontal location of the center of pressure of the radial bearing force on the enclosure shell and shell panels. This location is designated by the coordinates y_2 and z_2 in Figure 2.5.2 and in Figure 2.5.13 and ensures that there is no net moment (around the cask centerline longitudinal axis) produced by the bearing pressure.

For the geometry associated with the HI-STAR 100 transport saddles, the induced vertical upward force in the tie-down straps from the application of a lateral load is approximately equal to the magnitude of the lateral load. Thus, for a combination of lateral load and upward vertical load, there are two contributions to the total load in the tie-down sling.

- Equilibrium Equations for Tie-Down

The equilibrium equations necessary to solve for the tie-down forces under the postulated loads will be written using classical vector algebra. There are three loading cases that govern the *analysis* of the tie-down components: longitudinal (x), vertical (y), and lateral (z). The reaction forces for each loading case are determined by the equations of force and moment equilibrium. The general equations of force and moment equilibrium are developed following the *partial* free body diagram shown in Figure 2.5.2. Figure 2.5.2 defines the following force vectors: F_c , F_b , and F_t are the applied loads from the cask, and from the bottom and top impact limiters, respectively. S_i ($i=1,2,3$) are the three reaction forces at the locations

on the saddle support where tie-down straps are located. For all tie-down force calculations to determine the restraint forces, the following bounding values (for a 1g load) are ascribed to the cask and to the overpack (Table 2.2.1).

HI-STAR 100 – 250,000 lb.

Top Impact Limiter – 20,000 lb.

Bottom Impact Limiter – 18,000 lb

Results from numerical computations are summarized in tabular form at the end of this section. In the following sub-sections, discussion of the various loads and the method by which they are reacted, is presented

2.5.2.3 Longitudinal Loading

The longitudinal load is directly resisted by the impact limiters at the top and bottom of the cask. The two impact limiters have an annular region with impact limiting material chosen to resist normal handling loads up to 17g (Table 2.1.10). Therefore, they can resist normal transport longitudinal loads without loss of function in the event of a cask drop accident. The HI-STAR overpack is shown in Subsection 2.6 to meet Level A ASME Code stress limits.

2.5.2.4 Vertical Load

The vertical loads, directed either upwards or downwards, are resisted by the tie-down straps or the saddle support at the three locations shown in Figures 1.2.8 and 2.5.2. Planer equilibrium equations for force and moment equilibrium have the form (refer to Figure 2.5.2):

$$\sum_i S_i = G$$

$$\sum_i x_i S_i = M$$

where $G = F_t + F_c + F_b$ and $M = F_t x_t + F_c x_c - F_b x_b$

These two equations, coupled with the assumption that the cask is rigid, yields the solution for the three tie-down reactions; the magnitude of the three vertical reactions are determined in the form:

$$S_{i(\text{vertical})} = f_i F + g_i M \quad i = 1,2,3$$

The detailed numerical computations leading to the results reported in tabular form at the end of this subsection conservatively assume that the outermost tie-down straps are located so that their

centerlines are approximately 1' from the upper and lower edge of the outer enclosure panels. In the above equation, F is the total vertical applied force and M is the total moment, about a horizontal axis through the base of the cask, from the vertical components of the applied force. The applied forces are the weights of the cask, and the top and bottom impact limiters, amplified by the appropriate "g" value and located at the centroid of the components (per Figure 2.5.2). When the applied load is directed downward, the reactions at the saddle supports are distributed bearing pressures at the saddle/enclosure shell interface, as shown in Figure 2.5.12; when the applied load is directed upward, the reactions are provided by tensile loads in the tie-down straps, which are distributed to the enclosure shell as a radial pressure.

2.5.2.5 Lateral Load

For this load case, lateral loads, in either direction, are distributed to each saddle support location where tie-down straps are present, and are resisted by a radial bearing pressure distribution at the saddle/enclosure shell interface. The radial pressure distribution has a lateral and vertical resultant force. The lateral component of the reaction load at each saddle/enclosure shell interface is computed from force and moment equilibrium and the same form of solution is achieved as given for the vertical loads. In this case, however, since the resultant resisting force is directed through the cask longitudinal centerline at each support location, at each of the support locations, there is an induced vertical force in the tie-down strap that develops to balance the vertical component of the force between the overpack and the support at each location. Figure 2.5.13 shows how the forces are distributed so that at each location, the vertical force from the interface pressure is balanced by the induced load in the tie-down strap, while the horizontal net force from the interface pressure balances the lateral reaction force at that location. The location of the resultant force at the saddle/enclosure shell interface ensures that there is no net moment at the support. That is, the relation between the lateral load, the induced vertical load, and the center of pressure coordinates y_2 and z_2 is:

$$F(\text{lateral}) \times (y_2) = F(\text{induced vertical}) \times (z_2)$$

The saddle support angle is chosen to ensure that the resultant force is inclined approximately 45 degrees to the vertical, so that the applied lateral force induces a vertical force of the same magnitude that is resisted by the tie-down straps.

2.5.2.6 Numerical Results for Tie-Down Reactions

The longitudinal load in either direction is reacted by the impact limiters and does not impose any load on the saddle support or the tie-down straps. The lateral load and vertical load results in a bearing pressure between the saddle support and the enclosure shell and a tensile load in the tie-down strap. The only directional effect leading to different results is the direction of the applied

vertical load. Therefore, the load combinations to be considered are:

- (1) Longitudinal load, +lateral load, +vertical load upward*
- (2) Longitudinal load +lateral load, + vertical load downward*

The results for the tie-down reactions due to each individual load and due to the defined load combinations are presented in Table 2.5.1.

As noted earlier, the AAR Field Manual, Rule 88 specifies a set of load amplifiers that are appropriate for designing the saddle and the trunnion support but are not part of the packaging qualification effort. For information purposes only, *results* for the tie-down reactions *are provided* for the load case combinations using the load amplifiers (defined earlier as the second set) given by the AAR Field Manual, Rule 88. Results are given in Table 2.5.2.

To comply with the governing requirements (10CFR71.45(b)(1)), it should be demonstrated that under the tie-down loads, no part of the cask experience stresses in excess of the material yield strength. It has been noted earlier that the impact limiters are capable of resisting longitudinal loads in excess of the regulatory requirements for transport. Therefore, only transport loads in the vertical and lateral direction need be assessed for their affect on cask stress. The only loads transmitted to the overpack from lateral and vertical loads are radial pressures on the overpack outer enclosure. The enclosure shell is backed by the Holtite-A material, which, in reality, can resist some compression and transfer the load to the intermediate shells. However, since no structural credit is assumed for Holtite-A, it is conservatively considered that the radial loads from the tie-down forces are transmitted only through the radial channel legs connecting the outer enclosure shell to the overpack intermediate shells. The following simplified analysis serves to ensure that the cask components do not exceed their yield stress under the combined action of lateral and vertical tie-down loads.

An examination of the bounding loads from Table 2.5.1 concludes that the most demand on the cask structure occurs when the tie-down strap load, from both lateral and vertical transport forces, is assumed reacted over 180 degrees and therefore, transmitted to the overpack intermediate shells as a compressive direct load in nineteen (19) radial channel legs (see applicable drawing in Section 1.4 showing the radial channels). This enables the determination of a minimum length of contact between the tie-down straps and the enclosure shell to ensure that the direct stress in the radial channels remains below the yield strength. Conservatively evaluating the yield strength of the radial channels at 400 degrees F per Table 2.1.2, Tables 2.3.2 and 2.3.3 give:

$$S_y = 32,600 \text{ psi}$$

The average direct stress, "St", in a channel is computed by first determining the equivalent uniform radial pressure developed at the interface between the tie-down strap and the enclosure shell. From simple equilibrium, this radial pressure is determined by the formula:

$$p = 2T/DL$$

T is the load in the tie-down strap, D is the outer diameter of the enclosure shell, and L is the length of enclosure shell under pressure.

The pressure, p, is related to the direct compressive load, "G", in one of the channel legs, by the following equation:

$$G = p \times (sL) \quad \text{where the span between channel legs is approximated as } s = (3.14159 \times (D/2))/19$$

Finally, the stress in the channel leg, "St", is given as:

$$St = G/(tL) \quad \text{where } t \text{ is the channel leg thickness.}$$

$$\text{Setting } St = Sy \text{ and solving for "L", gives: } L = (3.14159/19) \times (T/t \times Sy)$$

The minimum length L is computed using $T = 647,000 \text{ lb.}/2$, and $t=0.5"$, to obtain:

$$L = 3.282"$$

Since the minimum sling length needed to support the load is 6" (or greater), it is seen that the cask stress developed to resist the lateral and vertical transport loads is much less than the yield stress of the channel legs; therefore, the governing regulatory requirement of 10CFR71.45(b)(1) is satisfied.

2.5.2.7 Structural Integrity of Pocket Trunnions on Applicable HI-STAR 100 Systems

The summary of results provided in tabular form, herein, is applicable only to the units that have been previously manufactured and, therefore, have pocket trunnions. The structural function of the pocket trunnions on applicable HI-STAR 100 Systems is limited to supporting the HI-STAR overpack during upending /downending operations if a separate downending cradle is not employed. If the pocket trunnion recess is utilized as a loaded pivot point during downending, the applied load for this operation is conservatively considered as the loaded weight of the package without impact limiters (250,000 lb.), amplified by a 15% inertia load factor. This load can be applied in any direction as the package is rotated 90 degrees. Results of structural integrity analyses, performed to qualify the rotation trunnion recess on the affected units, are summarized below.

Analyses are performed to evaluate the structural performance of various portions of the pocket trunnion under the stated total load, divided equally between the two trunnions. Since the trunnions are not utilized as tie-down devices, they are not considered as ASME Code items; nevertheless, their performance is evaluated by comparing calculated stresses against yield strengths (to conform to the methodology employed in the HI-STAR 100 FSAR). Analyses for bearing stress levels, primary stress levels in the trunnion recess body, and weld stress in the weld group that attaches the recess forging to the intermediate shells. The methods of analysis include both simple strength of materials evaluation and finite element analysis of the pocket trunnion body. For the bearing stress analysis, the average bearing stress is computed based on the diameter of the male trunnion that would fit the trunnion pocket. For the general primary stress state in the trunnion forging, a finite element model of the trunnion recess is developed. Finally, for the analysis of the weld stress distribution, simple strength of materials equilibrium analysis is used with weld sizes appropriate to the minimum weld configuration in-place on the affected HI-STARs. The maximum weld stress is computed accounting for the weld material between the trunnion recess and the intermediate shells and between the pocket trunnion and the outer enclosure shell.

The results of the pocket trunnion recess analyses for an upending/downending load equal to 125,000 lb. x 1.15, are summarized in the following table:

<i>Structural Integrity Results for HI-STAR Systems Equipped with Pocket Trunnions</i>			
<i>Item</i>	<i>Calculated Stress (ksi)</i>	<i>Allowable Stress (ksi)</i>	<i>Safety Factor = $\frac{\text{Allowable Value}}{\text{Calculated Value}}$</i>
<i>Bearing Stress</i>	6.183	97.1	15.71 (based on material yield strength)
<i>Pocket Recess Primary Membrane + Primary Bending Stress</i>	14.17	32.33	2.282 (based on 1/3 of trunnion material yield strength)
<i>Maximum Weld Stress</i>	2.399	14.533	4.802 (based on 1/3 of base metal yield strength)

2.5.3 Failure of Lifting and Tie-Down Devices

10CFR71.45 establishes criteria for minimum safety factors for lifting attachments, and provides input design loads for tie-down devices. 10CFR71.45 also requires that the lifting attachments and tie-down devices *permanently attached to the cask*, be designed in a manner such that a structural failure during lifting or transport will not impair the ability of the transportation package to meet other requirements of Part 10CFR71. In this section of the SAR, the issues concerning a structural failure during lifting or tie-down during transport are addressed. Specifically, the following issues are considered and resolved below:

a. Lifting Attachments:

Analyses are performed, *using simple strength of materials concepts and evaluations* to demonstrate that the ultimate load carrying capacity of the lifting trunnions is governed by the cross section of the trunnion external to the overpack top forging rather than by any section within the top forging. Detailed calculations that compare the ultimate load capacity of the shank of the lifting trunnion (the external cylindrical portion extending outside of the overpack top forging) to the ultimate load capacity of the top forging *are performed*. The ultimate load carrying capacity of the trunnion shank is based on an examination of the ultimate capacity of the section in both shear and bending. The ultimate load capacity of the top forging is determined by its capacity to resist moment by thread shear at the trunnion/forging threaded interface and to equilibrate the lifting load by bearing action at the trunnion forging bearing surface interface. It is concluded that the trunnion shank reaches ultimate load capacity limit prior to the top forging reaches its corresponding ultimate load capacity limit. Loss of the external shank of the lifting trunnion will not cause loss of any other structural or shielding function of the HI-STAR 100 overpack; therefore, the requirement imposed by 10CFR71.45(a) is satisfied.

The following safety factors *are established*:

$$\frac{\text{(Ultimate Bearing Capacity at Trunnion/Top Forging Interface)}}{\text{(Ultimate Trunnion Load)}} = 1.16$$

$$\frac{\text{(Ultimate Moment Capacity at Trunnion/Top Forging Thread Interface)}}{\text{(Ultimate Trunnion Moment Capacity)}} = 1.57$$

b. Tie-Down Devices

There are no tie-down devices that are permanently attached to the cask; therefore, no analyses are required to demonstrate that the requirements of 10CFR71.45(b)(3) are satisfied.

2.5.4 Conclusions

Lifting devices have been considered in Subsection 2.5.1 and Tie-Down devices have been considered in Subsection 2.5.2. It is shown that requirements of 10CFR71.45(a)(lifting devices) and 10CFR71.45(b)(tie-down devices) are satisfied. *All safety factors exceed 1.0.*

No tie-down device is a permanent part of the cask. All tie-down devices (saddle, tie-down straps, and fore and aft impact limiter targets, are part of the rail car and accordingly are not designed in this SAR. The maximum loads imposed on these items are recorded for subsequent design efforts.

Table 2.5.1
TIE-DOWN REACTIONS[†] - 10CFR71 LOAD RESULTS

<i>Item</i>	<i>Component</i>	<i>Load Combination 1 (kips)</i>	<i>Load Combination 2 (kips)</i>
<i>Impact Limiter Target</i>	<i>Longitudinal</i>	2,880	2,880
<i>Top End Saddle -1</i>	<i>Lateral</i>	420.85	420.85
	<i>Vertical - Saddle</i>	420.85	252.51 + 420.85
	<i>Vertical - Tie-Down Strap</i>	84.17 + 420.85	420.85
<i>Intermediate Saddle-2</i>	<i>Lateral</i>	480.15	480.15
	<i>Vertical - Saddle</i>	480.15	288.09 + 480.15
	<i>Vertical - Tie-Down Strap</i>	96.03 + 480.15	480.15
<i>Bottom End Saddle -3</i>	<i>Lateral</i>	539	539
	<i>Vertical - Saddle</i>	539	323.4 + 539
	<i>Vertical - Tie-Down Strap</i>	107.8 + 539	539

[†] See Figure 2.5.2 for definition of the symbols for the reaction loads.

Table 2.5.2

TIE-DOWN REACTIONS[†] - AAR RULE 88 LOAD RESULTS

<i>Item</i>	<i>Component</i>	<i>Load Combination 1 (kips)</i>	<i>Load Combination 2 (kips)</i>
<i>Impact Limiter Target</i>	<i>Longitudinal</i>	<i>2,160</i>	<i>2,160</i>
<i>Top End Saddle -1</i>	<i>Lateral</i>	<i>168.34</i>	<i>168.34</i>
	<i>Vertical - Saddle</i>	<i>168.34</i>	<i>252.51 + 168.34</i>
	<i>Vertical - Tie-Down Strap</i>	<i>84.17 + 168.34</i>	<i>168.34</i>
<i>Intermediate Saddle-2</i>	<i>Lateral</i>	<i>192.06</i>	<i>192.06</i>
	<i>Vertical - Saddle</i>	<i>192.06</i>	<i>288.09 + 192.06</i>
	<i>Vertical - Tie-Down Strap</i>	<i>96.03 + 192.06</i>	<i>192.06</i>
<i>Bottom End Saddle -3</i>	<i>Lateral</i>	<i>215.6</i>	<i>215.6</i>
	<i>Vertical - Saddle</i>	<i>215.6</i>	<i>323.4 + 215.6</i>
	<i>Vertical - Tie-Down Strap</i>	<i>107.8 + 215.6</i>	<i>215.6</i>

[†] See Figure 2.5.2 for definition of the symbols for the reaction loads.

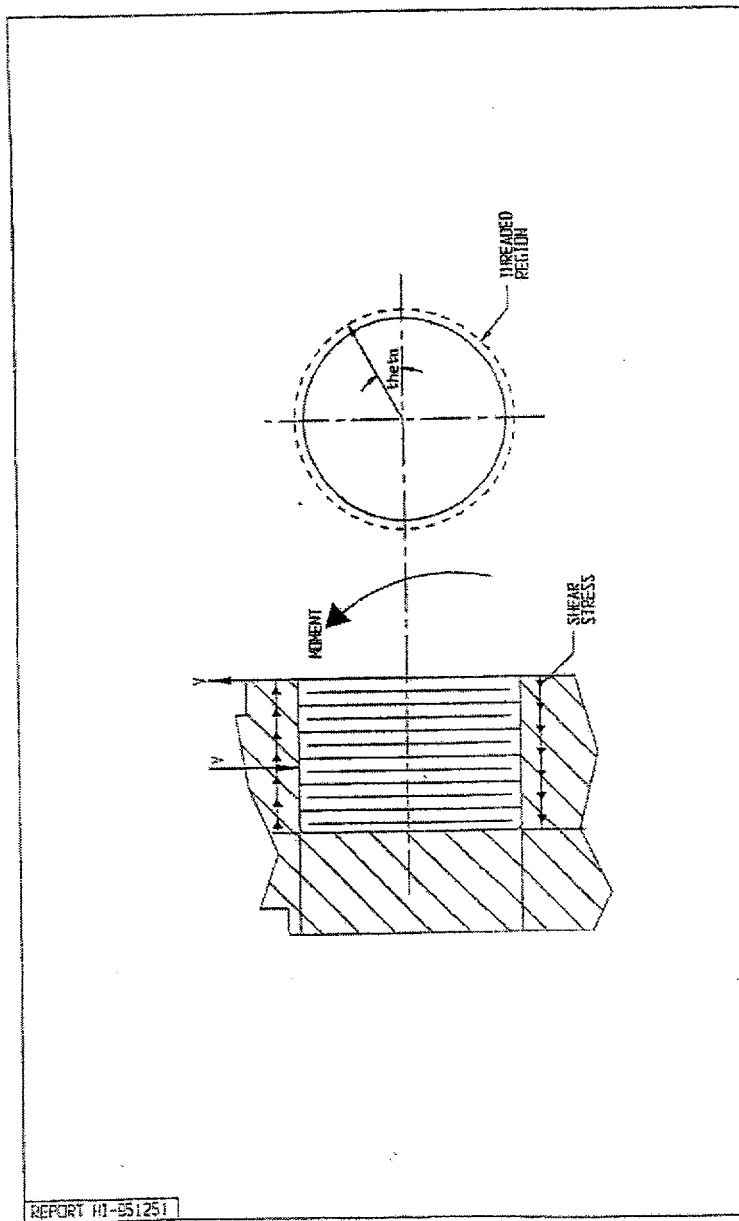
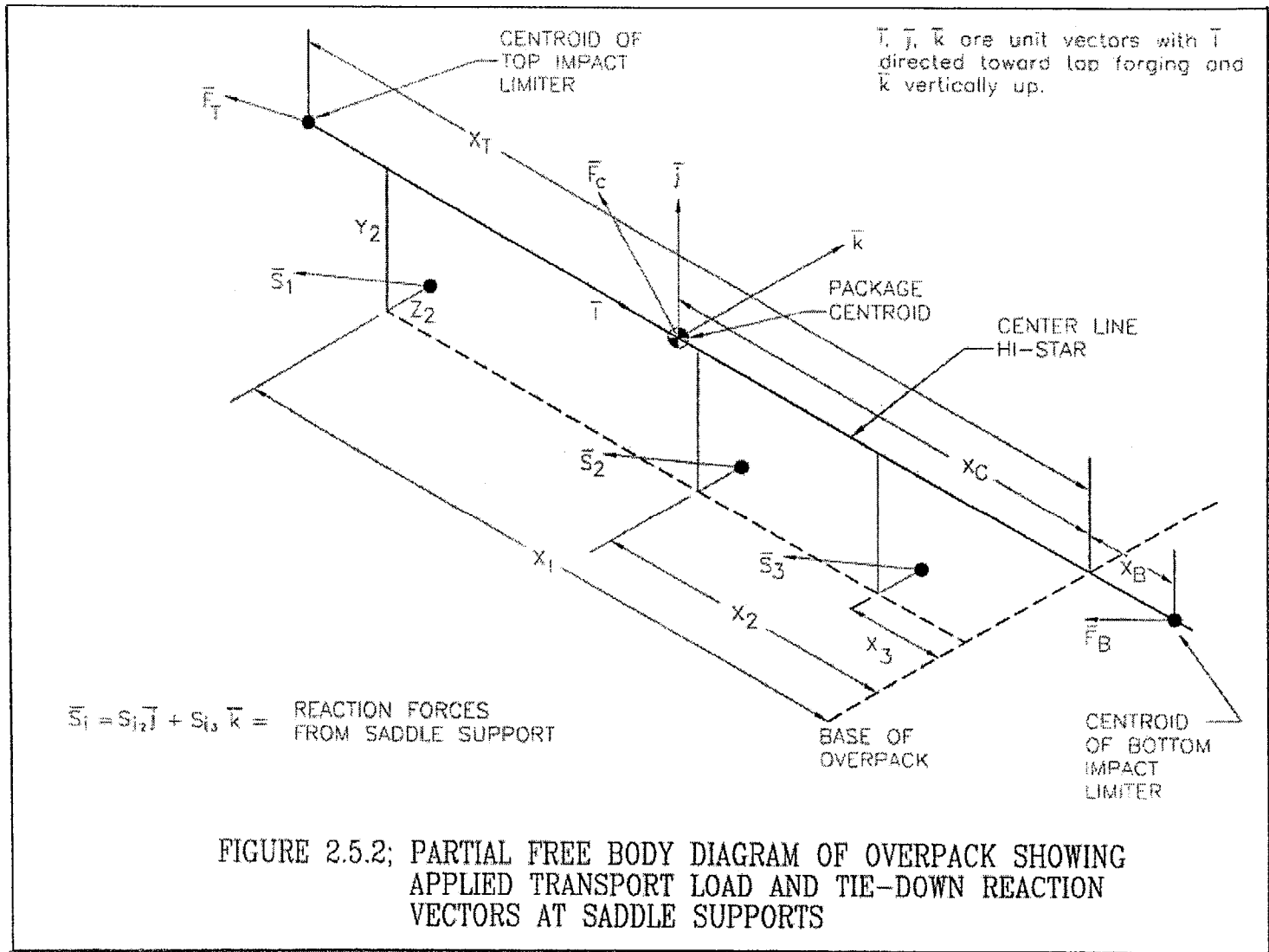


FIGURE 2.5.1; FREE BODY SKETCH OF LIFTING TRUNNION THREADED REGION SHOWING MOMENT BALANCE BY SHEAR STRESS



FIGURES 2.5.3 THROUGH 2.5.11 DELETED

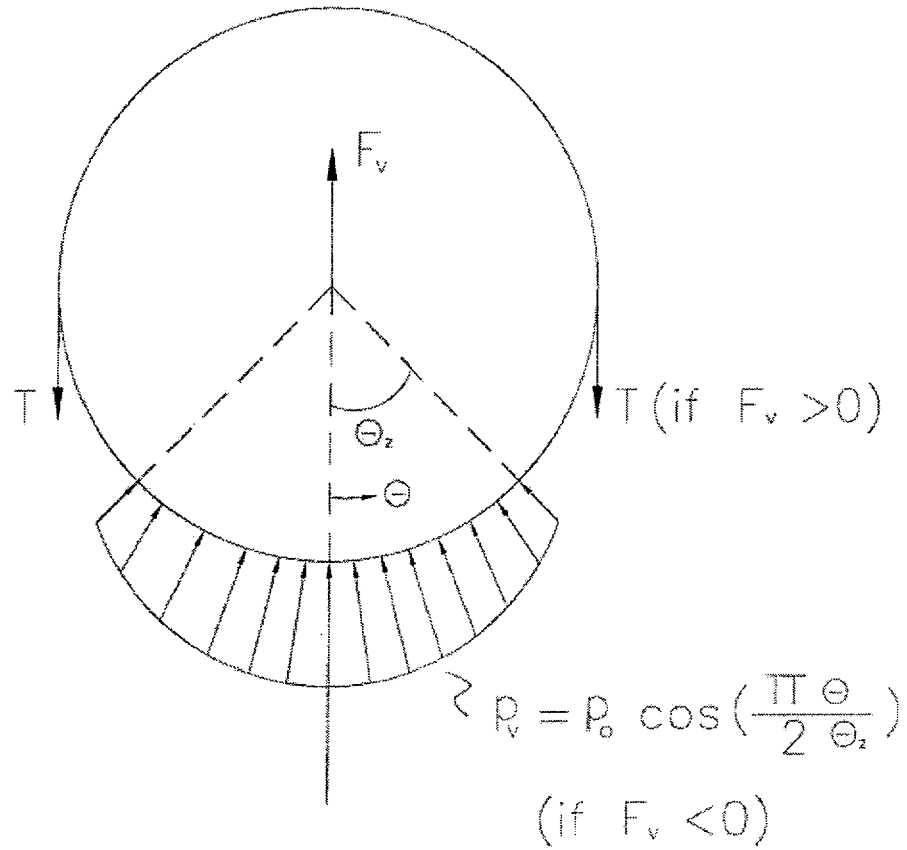
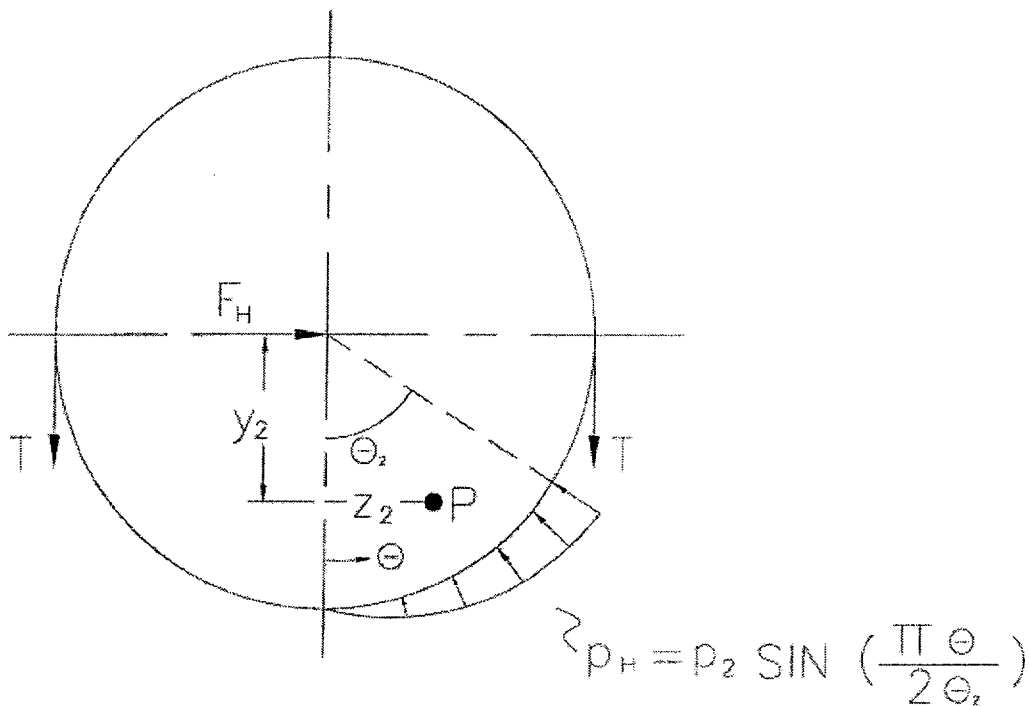


FIGURE 2.5.12; FREE-BODY AT TIE DOWN LOCATION
WITH SADDLE SUPPORT AND
TIE-DOWN STRAP-VERTICAL REACTION
LOAD



$$2T = f(\Theta_2) F_H = F_v \quad \left(\begin{array}{l} \text{Vertical resultant} \\ \text{on saddle} \end{array} \right)$$

PT. P IS LOCATION OF CENTER OF PRESSURE

FIGURE 2.5.13; FREE-BODY AT TIE-DOWN LOCATION WITH SADDLE SUPPORT AND TIE-DOWN STRAP-LATERAL REACTION LOAD

2.6 NORMAL CONDITIONS OF TRANSPORT

The HI-STAR 100 package, when subjected to the normal conditions of transport specified in 10CFR71.71, meets the design criteria in Subsection 2.1.2 (derived from the stipulations in 10CFR71.43 and 10CFR71.51) as demonstrated in the following section.

2.6.1 Heat

Subsection 2.6.1, labeled "Heat" in Regulatory Guide 7.9, is required to contain information on all structural (including thermoelastic) analyses performed on the cask to demonstrate positive safety margins, except for lifting operations that are covered in the preceding Section 2.5. Accordingly, this subsection contains all necessary information on the applied loadings, differential thermal expansion considerations, stress analysis models, and results for all normal conditions of transport. Assessment of potential malfunction under "Cold" conditions is required to be presented in Subsection 2.6.2.

Consistent with Regulatory Guide 7.9, the thermal evaluation of the HI-STAR 100 Package is reported in Chapter 3. The thermal evaluation also establishes the material temperatures, which are used in the structural evaluations discussed in this section and in Section 2.7.

2.6.1.1 Summary of Pressures and Temperatures

Design pressures and design temperatures for all conditions of transport are listed in Tables 2.1.1 and 2.1.2, respectively.

Load cases F1 (Table 2.1.6) and E4 (Table 2.1.7) are defined to study the effect of differential thermal expansion among the constituent components in the HI-STAR 100 Package. Figures 2.6.1 and 2.6.2 provide the defining bounding temperature distributions used for the MPC and overpack finite element thermal stress calculations to maximize stresses that develop due to temperature gradients. The distribution T is applied conservatively to analyze its effect on the fuel basket, the enclosure vessel (helium retention boundary), and the overpack.

2.6.1.2 Differential Thermal Expansion

In addition to the finite element solutions for free expansion stress (due to temperature gradients), simplified closed form calculations are independently performed to demonstrate that a physical interference will not develop between the overpack and the MPC canister, and between the MPC canister and the fuel basket due to unconstrained thermal expansion of each component during normal conditions of transport. To assess this in the most conservative manner, the thermal solutions computed in Chapter 3 are surveyed for the following information.

- The radial temperature distribution in each of the fuel baskets at the location of peak center metal temperature.

- The highest and lowest mean temperatures of the canister shell for the hot environment condition.
- The inner and outer surface temperature of the overpack shell (inner shell, intermediate shells, neutron shield, and outer closure) at the location of highest and lowest surface temperature (which will produce the lowest mean temperature).

The thermal evaluation is performed in Chapter 3. Tables 3.4.17 and 3.4.18 present the resulting temperatures used in the deflection evaluation.

Using the temperature information in the above-mentioned tables, simplified thermoelastic solutions of equivalent axisymmetric problems are used to obtain conservative estimates of gap closures. The following procedure, which conservatively neglects axial variations in temperature distribution, is utilized.

1. Use the surface temperature information for the fuel basket to define a parabolic distribution in the fuel basket that bounds (from above) the actual temperature distribution. Using this result, generate a conservatively high estimate of the radial and axial growth of the different fuel baskets using classical closed form solutions for thermoelastic deformation in cylindrical bodies.
2. Use the temperatures obtained for the canister to predict an estimate of the radial and axial growth of the canister to check the canister-to-basket gaps.
3. Use the temperatures obtained for the canister to predict an estimate of the radial and axial growth of the canister to check the canister-to-overpack gaps.
4. Use the overpack surface temperatures to construct a logarithmic temperature distribution (characteristic of a thick walled cylinder) at the location used for canister thermal growth calculations; and use this distribution to predict an estimate of overpack radial and axial growth.
5. For given initial clearances, compute the operating clearances.

~~The calculational procedure outlined is presented in Appendices 2.D and 2.F for the different fuel baskets, (HI-STAR 100 overpack with MPC 24 and MPC 68, respectively).~~

The results are summarized in the tables given below for normal conditions of transport.

THERMOELASTIC DISPLACEMENTS IN THE MPC AND OVERPACK UNDER HOT TEMPERATURE ENVIRONMENT CONDITION				
CANISTER - FUEL BASKET				
	Radial Direction (in.)		Axial Direction (in.)	
Unit	Initial Clearance	Final Gap	Initial Clearance	Final Gap
All PWR MPCs-24	0.1875	0.101	2.0	1.57
MPC-68	0.1875	0.104	2.0(min)	1.586(min)
CANISTER - OVERPACK				
	Radial Direction (in.)		Axial Direction (in.)	
Unit	Initial Clearance	Final Gap	Initial Clearance	Final Gap
All PWR MPCs-24	0.09375	0.058	0.625	0.422
MPC-68	0.09375	0.059	0.625	0.429

It can be verified by referring to the Design Drawings provided in Section 1.4 of this report, and the foregoing table, that the clearances between the MPC basket and canister structure, as well as those between the MPC shell and overpack inside surface, are sufficient to preclude a temperature induced interference from the thermal expansions listed above.

~~It is concluded~~~~We conclude~~ that the HI-STAR 100 package meets the requirement that there be no restraint of free thermal expansion in any of the constituent components (i.e, the fuel basket, the enclosure vessel, and the overpack structure).

2.6.1.3 Stress Calculations

In this subsection, ~~we consider~~ the normal conditions of transport associated with the thermal environment designated as "Heat" ~~are considered~~. ~~We calculate~~ The stresses due to the combined effect of pressure, mechanical loads, and thermal gradient ~~are evaluated~~. Within this subsection, ~~we also consider~~ the effects of fatigue and structure elastic/plastic stability under compression and lateral loading ~~are also considered~~. Included in the subsection is a complete description of the finite element models developed to assess

package performance under various loads. A two-dimensional finite element model of the fuel basket and the MPC enclosure shell is developed to evaluate the effect of pressure, radial temperature gradients and lateral deceleration induced inertia loads. A three-dimensional model of the overpack is also developed in this section to assess performance of the overpack under all load cases. Since both of these finite element models are used again in Section 2.7, where ~~we examine~~ hypothetical accident conditions of transport *are examined*, the explanation of the features of the model is presented herein in a general manner. Included in this description of the features of the model is a discussion of the loads applied, how they are chosen, and the methodology used to insure satisfaction of equilibrium. Where the loads, assumptions, geometry, etc. are common to both normal conditions of transport analyses and to hypothetical accident conditions of transport, the detailed description is presented in this section. Where the descriptions and discussions are relevant only for the hypothetical accident condition of transport, the detailed descriptions required for full understanding of the analysis are presented in Section 2.7.

This subsection presents the methodology for calculation of the stresses in the different components of the HI-STAR 100 Package from the load cases assembled in Section 2.1. Where the results are finite element based the methodology and the model is described in detail in this section. Results of finite element stress analyses are ~~documented in two appendices that are used as source appendices~~ for the comparison with allowable stresses performed in Subsection 2.6.1.4. Loading cases for the MPC fuel basket, the MPC enclosure vessel, and the HI-STAR 100 storage overpack are listed in Tables 2.1.6 through 2.1.8, respectively, for normal conditions of transport. ~~Detailed analyses for the load cases are presented in labeled appendices that are listed in the load case tables.~~ An abbreviated description of each of the analyses is presented in the body of the chapter.

In general, as required by Regulatory Guide 7.9, the comparison of the calculated stresses with their corresponding allowables is presented in Subsection 2.6.1.4. However, for clarity in the narrative in this subsection (2.6.1.3), unnumbered summary tables are presented within the text. The key stress comparisons are subsequently reproduced in numbered tables in Subsection 2.6.1.4 to provide strict compliance with Regulatory Guide 7.9.

For all stress evaluations, the allowable stresses and stress intensities for the various HI-STAR 100 System components are based on bounding high metal temperatures to provide additional conservatism (Table 2.1.21 for the MPC basket and shell, for example). Elastic behavior is assumed for all stress analyses. Elastic analysis is based on the assumption of a linear relationship between stress and strain.

In Section 2.7, the same analytical models described here for normal conditions of transport are used to assess package performance under the hypothetical accident conditions. Therefore, the description of the models provided below is also applicable to the analysis performed in Section 2.7 except as previously noted.

In addition to the loading cases germane to stress evaluations mentioned above, cases pertaining to the elastic stability of the overpack are also considered.

The specific finite element models and component calculations described and reported in this subsection are:

1. MPC stress and stability calculations
2. HI-STAR 100 overpack stress and stability calculations

MPC stress and elastic stability analyses are considered in Subsection 2.6.1.3.1 wherein load cases from Tables 2.1.6 and 2.1.7 appropriate to normal conditions of transport are considered. The following analyses for the MPC are performed:

- a. Finite element analysis of the MPC fuel basket and MPC helium retention shell under lateral loads from handling loads during normal transport.
- b. Finite element and analytical analysis of the helium retention vessel (enclosure vessel) as an ASME Code pressure vessel.
- c. Analysis of the fuel support spacers under longitudinal inertia compression load appropriate to normal conditions of transport.
- d. Elastic stability and yielding of the MPC enclosure shell under axial and lateral loads arising from normal handling and external pressure.

Overpack stress and elastic stability analyses are considered in Subsection 2.6.1.3.2. Load cases from Table 2.1.8 are considered. The following analyses are performed to establish the structural adequacy of the overpack:

- a. Three-dimensional finite element analysis of the overpack subjected to load cases listed in Table 2.1.8 for normal conditions of transport.
- b. Consideration of fabrication stresses.
- c. Structural analysis of the closure bolting for normal condition of transport.
- d. Stress Analysis of overpack enclosure shell and return.

2.6.1.3.1 MPC Stress Calculations

The structural function of the MPC in the transport mode is stated in Section 2.1. The calculations presented here demonstrate the ability of the MPC to perform its structural function. Analyses are performed for each of the MPC designs, ~~namely: the MPC 24, and the MPC 68.~~ The following subsections describe the model, individual loads, load combinations, and analysis procedures applicable to the MPC.

The load cases considered herein pertain to lateral loading on the MPC components, namely the fuel basket and the enclosure vessel. For this purpose, a finite element model of the MPC is necessary. During normal conditions of transport, a bounding handling load is simulated by applying a deceleration induced inertia load from a 1' drop with impact limiters installed. During hypothetical accident conditions (see Section 2.7), the MPC is subject to the design basis decelerations from a 30' drop. The finite element model used to simulate both load cases is described here and is used for analyses for normal conditions of transport and later in Section 2.7 is used for the hypothetical accident analyses.

- Description of Finite Element Models of the MPCs under Lateral Loading

A finite element model of each MPC is used to assess the effects of normal and accident conditions of transport. The models are constructed using ANSYS [2.6.4], and they are identical to the models used in HI-STAR's 10CFR72 submittal under Docket Number 72-1008. The following model description is common to all MPCs.

The MPC structural model is two-dimensional. It represents a one-inch long cross section of the fuel basket and the MPC canister.

The MPC model includes the fuel basket, the basket support structures, and the MPC shell. A basket support is defined as any structural member that is welded to the inside surface of the MPC shell. A portion of the overpack inner surface is modeled to provide the correct boundary conditions for the MPC. Figures 2.6.3 through 2.6.11 show the MPC models. ~~Detailed element numbers for the fuel basket and the enclosure vessel are provided in six Appendices, 2.W through 2.Z, 2.AA, and 2.AB.~~

The fuel basket support structure shown in the figures here, and in the design drawings in Section 1.4, is a multi-plate structure consisting of solid shims or support members having two separate compressive load supporting members. For conservatism in the finite element model some dual path compression members (i.e., "V" angles) ~~angles~~ are simulated as single columns. Therefore, the calculated stress intensities in the fuel basket supports, ~~reported in Appendix 2.AC~~ from the finite element solution, are conservatively overestimated in some locations.

The ANSYS model is not intended to resolve the detailed stress distributions in weld areas. Individual welds are not included in the finite element model. ~~A separate analysis for basket welds and for the basket support "V" angles is contained in Appendix 2.AD.~~

No credit is taken for any load support offered by the Boral panels, sheathing, and the *optional* aluminum heat conduction elements. Therefore, these so-called non-structural members are not represented in the model. The bounding MPC weight used, however, does include the mass contributions of these non-structural components.

The model is built using five ANSYS element types: BEAM3, PLANE82, CONTAC12, CONTAC26, and COMBIN14. The fuel basket and MPC shell are modeled entirely with two-dimensional beam elements (BEAM3). Plate-type basket supports are also modeled with BEAM3 elements. Eight-noded plane elements (PLANE82) are used for the solid-type basket supports. The gaps between the fuel basket and the basket supports are represented by two-dimensional point-to-point contact elements (CONTAC12). Contact between the MPC shell and the overpack is modeled using two-dimensional point-to-ground contact elements (CONTAC26) with an appropriate clearance gap.

For each MPC type, three variations of the finite element model were prepared. The basic model includes only the fuel basket and the enclosure shell (Figures 2.6.3 through 2.6.5 show representative configurations) and is used only to study the free thermal expansion due to the temperature field developed in the system. The other two models include a representation of the overpack and are used for the two drop cases considered. Two orientations of the deceleration vector are considered. The 0-degree drop model includes the overpack-MPC interface in the basket orientation illustrated in Figures 2.6.6 through 2.6.8. The 45-degree drop model represents the overpack interface with the basket oriented in the manner shown in Figures 2.6.9 through 2.6.11. Table 2.6.1 lists the element types and number of elements for all three models for all fuel storage MPC types.

A contact surface is provided in the models used for drop analyses to represent the overpack inner shell. As the MPC makes contact with the overpack, the MPC shell deforms to mate with the inside surface of the inner shell. The nodes that define the elements representing the fuel basket and the MPC shell are located along the centerline of the plate material. As a result, the line of nodes that forms the perimeter of the MPC shell is inset from the real boundary by a distance that is equal to half of the shell thickness. In order to maintain the specified MPC shell/overpack gap dimension, the radius of the overpack inner shell is decreased by an equal amount in the model.

Contact is simulated using two-dimensional point-to-ground elements (CONTAC26). The surface is tangent to the MPC shell at the initial point of impact and extends approximately 135144 degrees on both sides. This is sufficient to capture the full extent of contact between the MPC and the overpack.

The three discrete components of the HI-STAR System, namely the fuel basket, the MPC shell, and the overpack, are engineered with small diametral clearances that which are large enough to permit unconstrained thermal expansion of the three components under the rated (maximum) heat duty condition. A small diametral gap under ambient conditions is also necessary to assemble the system without physical interference between the contiguous surfaces of the three components. The required gap to ensure unrestricted thermal expansion between the basket and the MPC shell is less than 0.1 inch. This gap, too, will decrease under maximum heat load conditions, but will introduce a physical nonlinearity in the structural events involving lateral loadings (such as side drop of the system) under ambient conditions. It is evident from the system design drawings that the fuel basket, which is non-radially symmetric, is in proximate contact with the MPC shell at a discrete number of locations along the circumferences. At these locations, the MPC shell, backed by the massive overpack weldment, provides a virtually rigid support line to the fuel basket during lateral drop events. Because the fuel basket, the MPC shell, and the overpack are all three-dimensional structural weldments, their inter-body clearances may be somewhat uneven at different

azimuthal locations. As the lateral loading is increased, clearances close at the support locations, resulting in the activation of the support from the overpack.

The bending stresses in the basket and the MPC shell at low lateral loading levels, which are too small to close the support location clearances, are secondary stresses since further increase in the loading will activate the overpack's support action, mitigating further increase in the stress. Therefore, to compute primary stresses in the basket and the MPC shell under lateral drop events, the gaps should be assumed to be closed. However, for conservatism, it is assumed that an initial gap of 0.1875" exists, in the direction of the applied deceleration, at all support locations between the basket and the shell, and the diametral gap between the shell and the overpack at the support locations is 3/32". All stresses produced by the applied loading on this configuration are compared with primary stress levels even though the self-limiting stresses should be considered secondary in the strict definition of the ASME Code. Therefore, many of the reported safety factors for conditions of normal transport are conservative in that secondary stress allowables are ignored in the computation of safety factors. Similarly, in Section 2.7, the safety factors reported for the hypothetical accident conditions will also be conservative since ~~we do not separate out~~ the secondary stresses *is contained in the result*.

- Description of Individual Loads and Boundary Conditions Applied to the MPCs

The method of applying each individual load to the MPC model is described in this subsection. The individual loads and the load combinations are shown in Tables 2.1.6 and 2.1.7. *As an example, a* free-body diagram of the MPC-68 corresponding to each individual load is given in Figures 2.6.12 through 2.6.14. In the following discussion, reference to vertical and horizontal orientations *is*are made. -Vertical refers to the direction along the cask axis, and horizontal refers to a radial direction.

Quasi-static structural analysis methods are used. The effect of any dynamic load factors (DLFs) is included in the final evaluation of safety factors. All analyses are carried out using the design basis decelerations in Table 2.1.10.

The MPC models used for side drop evaluations are shown in Figures 2.6.6 through 2.6.11. In each model, the fuel basket and the enclosure vessel are constrained to move only in the direction that is parallel to the acceleration vector. The overpack inner shell, which is defined by three nodes needed to represent the contact surface, is fixed in all degrees of freedom. The fuel basket, enclosure vessel, and overpack inner shell are all connected at one location by linear springs (see Figure 2.6.6, for example).

(a) Accelerations (Load Case F2 (Table 2.1.6) and E2 (Table 2.1.7))

During a side impact event, the stored fuel is directly supported by the cell walls in the fuel basket. Depending on the orientation of the drop, 0 or 45 degrees (see Figures 2.1.3 and 2.1.4), either one or two walls support the fuel. The effect of deceleration on the fuel basket and canister metal structure is accounted for by amplifying the gravity field in the appropriate direction. In the finite element model this load is introduced by applying a uniformly distributed pressure over the full span of the supporting walls. Figure 2.6.15 shows the pressure load on a typical cell for both the 0 degree and the 45 degree drop cases. The

magnitude of the pressure is determined by the weight of the fuel assembly (Table 1.2.13), the axial length of the fuel basket support structure, the width of the cell wall, and the impact acceleration. It is assumed that the load is evenly distributed along an axial length of basket equal to the fuel basket support structure. For example, the pressure applied to an impacted cell wall during a 0-degree side drop event is calculated as follows:

$$p = \frac{a_v W}{L \ell}$$

where:

- p = pressure
- a_v = ratio of the impact acceleration to the gravitational acceleration
- W = weight of a stored fuel assembly
- L = axial length of the fuel basket support structure
- ℓ = width of a cell wall

For the case of a 45-degree side drop the pressure on any cell wall equals p (defined above) divided by the square root of two. Figures 2.6.13, 2.6.14, and 2.6.15 show the details of the fuel assembly pressure load on the fuel basket.

(b) Internal/External Pressure (Load Case E1 (Table 2.1.7))

Design internal pressure in the MPC model is applied by specifying pressure on the inside surface of the enclosure vessel. The magnitude of the internal pressure applied to the model is taken from Table 2.1.1.

For this load condition, the center of the fuel basket is fixed in all degrees of freedom.

(c) Temperature (Load Cases F1 (Table 2.1.6) and E4 (Table 2.1.7))

Temperature distributions are developed in Chapter 3 and applied as nodal temperatures to the finite element model of the MPC enclosure vessel (confinement boundary). Maximum design heat load has been used to develop the temperature distribution used to demonstrate compliance with ASME Code stress intensity levels. A plot of the applied temperature distribution as a function of radius is shown in Figure 2.6.1. Figure 2.6.12 shows the MPC-68 with the typical boundary conditions for all thermal and pressure load cases.

- Analysis Procedure

The analysis procedure for this set of load cases is as follows:

1. The stress intensity and deformation field due to the combined loads is determined by the finite element solution. Results are *then subject to post-processing and listed in Appendix 2.A.C.*
2. The results for each load combination are compared to allowables. The comparison with allowable values is made in Subsection 2.6.1.4.

2.6.1.3.1.2 Analysis of Load Cases E1.a and E1.c (Table 2.1.7)

Load Cases E1.a and E1.c pertain to the performance of the helium retention boundary structure (enclosure vessel) considered as an ASME Section III, Subsection NB pressure vessel.

Since the MPC shell is a pressure vessel, the classical Lame's calculations should be performed to demonstrate the shell's performance as a pressure vessel. ~~We note that dead load has an insignificant effect on this stress state. We first perform C~~calculations for the shell under internal pressure *are performed initially*. Subsequently, ~~we perform a~~ finite element analysis on the entire helium retention boundary as a pressure vessel subject to both internal pressure and temperature gradients *is performed*. Finally, ~~we perform~~ confirmatory hand calculations *are performed* to gain confidence in the finite element predictions,

- Lames Solution for the MPC Shell

The stress from internal pressure is found ~~for normal and accident pressures conditions~~ using classical formulas:

~~W~~e define the following quantities:

P = pressure, r = MPC radius, and t = shell thickness.

Using classical thin shell theory, the circumferential stress, $\sigma_1 = Pr/t$, the axial stress $\sigma_2 = Pr/2t$, and the radial stress $\sigma_3 = -P$ are computed for both normal and accident internal pressures. The results are given in the following table:

Classical Shell Theory Results for Normal and Accident Internal Pressures				
Item	σ_1 (psi)	σ_2 (psi)	σ_3 (psi)	$\sigma_1 - \sigma_3$ (psi)
P= 100 psi	6,838	3,419	-100	6,938
P= 200125 psi	13,6778,548	6,8384,274	-200125	13,8778,673

Table 2.1.21 provides the allowable membrane stress for Load Case E1 for Alloy X under normal conditions of transport. It is seen ~~We see~~ that a safety factor greater than 1.0 exists for the case of normal and accident pressures. Subsection 2.7.3.3.1 develops the corresponding safety factor for the case of accident pressure.

$$FS = \frac{18.1 \text{ ksi}}{6.938 \text{ ksi}} = 2.6$$

- Finite Element Analysis (Load Case E1.a and E1.c of Table 2.1.7)

Having performed the classical “thin shell under pressure” evaluation, ~~we now proceed to perform~~ a finite element analysis *is performed* where the interaction between the end closures and the MPC shell is rigorously modeled.

The MPC shell, the top lid, and the baseplate together form the helium retention boundary (enclosure vessel) for storage of spent nuclear fuel. In this section, ~~we evaluate~~ the operating condition consisting of dead weight, internal pressure, and thermal effects for the normal heat condition of transport *is evaluated*. The top and bottom plates of the MPC enclosure vessel (EV) are modeled using plane axisymmetric elements, while the shell is modeled using the axisymmetric thin shell element. The thickness of the top lid varies in the MPC types *and can be either a single thick lid, or two dual lids, welded around their common periphery*; ~~for conservative results~~, the minimum thickness top lid is modeled *in the finite element analysis*. *As applicable, the results for the MPC top lid are modified to account for the fact that in the dual lid configuration, the two lids act independently under mechanical loading*. The temperature distributions for all MPC constructions are nearly identical in magnitude and gradient. Temperature differences across the thickness of both the baseplate and the top lid exist during HI-STAR 100's operations. There is also a thermal gradient from the center of the top lid and baseplate out to the shell wall. The metal temperature profile is essentially parabolic from the centerline of the MPC out to the MPC shell. There is also a parabolic temperature profile along the length of the MPC canister. Figure 2.6.20 shows a sketch of the confinement boundary structure with identifiers A-I (also called locating points) where temperature input data is used to represent a continuous temperature distribution for analysis purposes. The overall dimensions of the confinement boundary are also shown in the figure.

~~Section 3.4~~ ~~Table 3.4.22~~ provides the desired temperatures for thermal stress analysis of the helium retention boundary. From the tables (3.4.22 and 3.4.23), ~~it is seen that we see that~~ the distribution ~~from~~ ~~the PWRs MPC-24~~ provides the largest temperature gradients in the baseplate (from centerline to outer edge) and in the shell (from the joint at the baseplate to the half-height of the cask). It will be shown later that stress intensities are greatest in these components of the vessel. ~~Therefore, detailed stress analyses are performed only for the MPC-24~~ *Because of the intimate contact between the two lid plates when the MPC lid is a two-piece unit, there is no significant thermal discontinuity through the thickness; thermal stresses arising in the MPC top lid will be bounding when there is only a single lid.*

Therefore, for thermal stresses, results from the analysis

that considers the lid as a one-piece unit are used and are amplified to reflect the increase in stress in the dual lid configuration.

Figure 2.6.21 shows details of the finite element model of the top lid (considered as a single piece), canister shell, and baseplate. The top lid is modeled with 40 axisymmetric quadrilateral elements; the weld connecting the lid to the shell is modeled by a single element solely to capture the effect of the top lid attachment to the canister offset from the middle surface of the top lid. The MPC canister is modeled by 50 axisymmetric shell elements, with 20 elements concentrated in a short length of shell appropriate to capture the so-called "bending boundary layer" at both the top and bottom ends of the canister. The remaining 10 shell elements model the MPC canister structure away from the shell ends in the region where stress gradients are lower (from the physics of the problem). The baseplate is modeled by 20 axisymmetric quadrilateral elements. Deformation compatibility at the connections is enforced at the top by the single weld element, and deformation and rotation compatibility at the bottom by additional shell elements between nodes 106-107 and 107-108.

The geometry of the model is listed below (terms are defined in Figure 2.6.21):

$$\begin{aligned} H_t &= 9.5'' \text{ (the minimum total thickness lid is assumed)} \\ R_L &= 0.5 \times 67.25'' \text{ (Bill of Materials for Top Lid, MPC drawing in Section 1.4)} \\ L_{MPC} &= 190.5'' \text{ (MPC drawing in Section 1.4 Drawing 1393, Sheet 1)} \\ t_s &= 0.5'' \\ R_S &= 0.5 \times 68.375'' \\ t_{BP} &= 2.5'' \\ \beta L &= 2\sqrt{R_s t_s} \approx 12'' \text{ (The bending boundary layer)} \end{aligned}$$

Stress analyses are carried out for two cases as follows:

- a. internal pressure = 100 psi
- b. internal pressure = 100 psi, plus applied temperature field for the MPC 24

~~The We note that~~ the dead weight of the top lid reduces the stresses due to pressure. For example, the equivalent pressure simulating the effect of the weight of the top lid is an external pressure of 3 psi, which reduces the pressure difference across the top lid to 97 psi. Thus, for conservatism, dead weight of the top

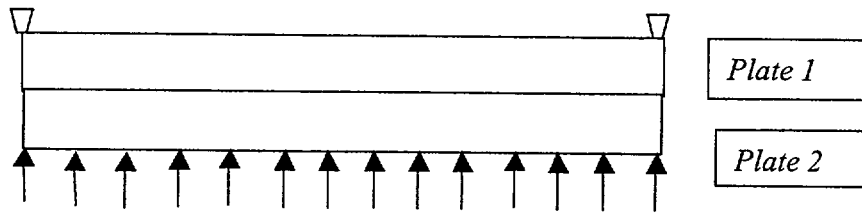
lid is neglected to provide additional conservatism in the results. The dead weight of the baseplate, however, adds approximately 0.73 psi to the effective internal pressure acting on the base. The effect of dead weight is still insignificant compared to the 100 psi design pressure, and is therefore neglected. The thermal loading in the confinement vessel is obtained by developing a parabolic temperature profile to the entire length of the MPC canister and to the top lid and baseplate. The temperature data provided at locations A-I in Figures 2.6.20 and 2.6.21 are sufficient to establish the profiles. Through-thickness temperatures are assumed linearly interpolated between top and bottom surfaces of the top lid and baseplate. All material properties and expansion coefficients are considered to be temperature-dependent in the model.

Results for stress intensity are reported for the case of internal pressure alone and for the combined loading of pressure plus temperature (Load Case E1.c in Table 2.1.7). Tables 2.6.6 and 2.6.7 report results at the inside and outside surfaces of the top lid and baseplate at the centerline and at the extreme radius. Canister results are reported in the "bending boundary layer" and at a location near mid-length of the MPC canister. In the tables, the calculated value is the value from the finite element analysis, the categories are P_m = primary membrane; $P_L + P_b$ = local membrane plus primary bending; and $P_L + P_b + Q$ = primary plus secondary stress intensity. The allowable stress intensity value is obtained from the appropriate table in Section 2.1 for Level A conditions, and the safety factor SF is defined as the allowable strength divided by the calculated value. Allowable stresses for Alloy X are taken at 300° F, which bounds the normal heat condition of transport temperatures everywhere except at the mid-length position of the MPC shell (Location I in Figure 2.6.20) during the normal operation. At Location I, the allowable strength is taken at 400°F. The results given in Tables 2.6.6 and 2.6.7 demonstrate the ruggedness of the MPC as a confinement boundary. *Since mechanically induced stresses in the top lid are increased when a dual lid configuration is considered, the stress results obtained from an analysis of a single top lid must be corrected to reflect the maximum stress state when a dual lid configuration is considered. The modifications required are based on the following logic:*

Consider the case of a simply supported circular plate of thickness h under uniform lateral pressure " q ". Classical strength of materials provides the solution for the maximum stress, which occurs at the center of the plate, in the form:

$$\sigma_s = 1.225q(a/h)^2 \quad \text{where } a \text{ is the radius of the plate and } h \text{ is the plate thickness.}$$

Now consider the MPC simply supported top lid as fabricated from two plates "1" and "2", of thickness h_1 and h_2 , respectively, where the lower surface of plate 2 is subjected to the internal pressure " q ", the upper surface of plate 1 is the outer surface of the helium retention boundary, and the lower surface of plate 1 and the upper surface of plate 2 are in contact. The following sketch shows the dual lid configuration for the purposes of this discussion:



From classical plate theory, if it is assumed that the interface pressure between the two plates is uniform and that both plates deform to the same central deflection, then if

$$h_1 + h_2 = h, \text{ and if } h_2/h_1 = r$$

the following relations exist between the maximum stress in the two individual plates, σ_1 , σ_2 and the maximum stress σ_s in the single plate of thickness "h":

$$\frac{\sigma_1}{\sigma_s} = \frac{(1+r)^2}{(1+r^3)} \qquad \frac{\sigma_2}{\sigma_s} = \frac{(1+r)^2}{(1+r^3)} r$$

Since the two lid thicknesses are the same in the dual lid configuration, $r = 1.0$ so that the stresses in plates 1 and 2 are both two times larger than the maximum stress computed for the single plate lid having the same total thickness. In Tables 2.6.6 and 2.6.7, bounding results for the dual lid configuration are reported by using these ratios at all locations in the top lid.

- **Confirmatory Closed Form Solution**

The results in Table 2.6.6 and 2.6.7 also show that the baseplate and the shell connection to the baseplate are the most highly stressed regions under the action of internal pressure. To confirm the finite element results, ~~we perform~~ an alternate closed form solution *is performed* using classical plate and shell theory equations that are listed in or developed from the reference Timoshenko and Woinowsky-Krieger, Theory of Plate and Shells, McGraw Hill, Third Edition.

Assuming that the thick baseplate receives little support against rotation from the thin shell, the bending stress at the centerline is evaluated by considering a simply supported plate of radius a, and thickness h, subjected to lateral pressure p. The maximum bending stress is given by

$$\sigma = \frac{3(3+\nu)}{8} p \left(\frac{a}{h} \right)^2$$

where:

$$a = .5 \times 68.375 \text{ "in}^2$$

$$h = 2.5 \text{ "}$$

$$\nu = 0.3 \text{ (Poisson's Ratio)}$$

$$p = 100 \text{ psi}$$

Calculating the stress in the plate gives $\sigma = 23,142$ psi.

Now consider the thin MPC shell ($t = 0.5$ ") and first assume that the baseplate provides a clamped support to the shell. Under this condition, the bending stress in the thin shell at the connection to the plate is given as:

$$\sigma_{Bp} = 3p \frac{a}{t} \frac{(1-\nu/2)}{\sqrt{3(1-\nu^2)^{1/2}}} = 10,553 \text{ psi}$$

In addition to this stress, there is a component of stress in the shell due to the baseplate rotation that causes the shell to rotate. The joint rotation is essentially driven by the behavior of the baseplate as a simply supported plate; the shell offers little resistance because of the disparity in thickness and will essentially follow the rotation of the thick plate.

Using formulas from thin shell theory, the additional axial bending stress in the shell due to this rotation θ can be written in the form

$$\sigma_{B\theta} = 12 \beta D_s \frac{\theta}{t^2}$$

where

$$\theta = pa^3 / 8D (1+\nu) * \left(\frac{1}{1+\alpha} \right)$$

and

$$D = \frac{E h^3}{12(1-\nu^2)} \quad E = \text{plate Young's Modulus}$$

and

$$\alpha = \frac{2\beta a t^3}{h^3(1+\nu)}$$

$$\beta^2 = \sqrt{3(1-\nu^2)}/at$$

$$D_s = \frac{E t^3}{12(1-\nu^2)}$$

Substituting the numerical values gives

$$\sigma_{B_s} = 40,563 \text{ psi}$$

We note that the approximate solution is independent of the value chosen for Young's Modulus as long as the material properties for the plate and shell are the same.

Combining the two contributions to the shell bending stress gives the total extreme fiber stress in the longitudinal direction as 51,116 psi. We note that the same confirmatory solution can be obtained from Roark's Formulas for Stress and Strain, McGraw-Hill, 4th Edition, Table XIII. Case 30 in that text contains the solution for the bending moment at the intersection of a long cylinder and a flat plate due to internal pressures. Using the handbook formula, we obtain 53,090 psi is obtained.

The baseplate stress value, 23,142 psi, compares well with the finite element result 20,528 psi (Table 2.6.6). The shell joint stress, 51,116 psi, is greater than the finite element result (43,986 psi in Table 2.6.6). This is due to the local effects of the shell-to-baseplate connection offset. That is, the connection between shell and baseplate in the finite element model is at the surface of the baseplate, not at the middle surface of the baseplate. This offset will cause an additional bending moment that will reduce the rotation of the plate and hence, reduce the stress in the shell due to the rotation of the baseplate.

In summary, the approximate closed form solution confirms the accuracy of the finite element analysis in the MPC baseplate region.

2.6.1.3.1.3 Supplementary MPC Calculations

The MPC has been subject to extensive analysis in the companion HI-STAR 100 TSAR/FSAR (storage) submittal (Docket Number 72-1008). For completeness, certain *information appendices* from the TSAR/FSAR have been *repeatedly included* here and in Section 2.7 where the results are germane to normal conditions of transport and- to hypothetical accident conditions of transport, respectively. Because of the different requirements for storage and transport submittals, some of the results presented here may not be directly associated with a load case defined in Tables 2.1.6 and 2.1.7. Nevertheless, their inclusion here is warranted for completeness. In this subsection, ~~we summarize~~ *results are summarized* from these *analyses appendices* that pertain to normal conditions of transport. In Section 2.7, addition results pertaining to the hypothetical accident conditions of transport are reported.

- Structural Analysis of the Fuel Support Spacers (Load Case F2)

Upper and lower fuel support spacers are utilized to position the active fuel region of the spent nuclear fuel within the poisoned region of the fuel basket. It is necessary to ensure that the spacers will continue to maintain their structural integrity during normal conditions of transport. Ensuring structural integrity implies that the spacer will not buckle under the maximum compressive load, and that the maximum compressive stress will not exceed the compressive strength of the spacer material (Alloy X). Detailed calculations in ~~Appendix 2.0~~ demonstrate that large structural margins in the fuel spacers are available for the entire range of spacer lengths that may be used in HI-STAR 100 applications (for the various acceptable fuel types). *The fuel spacers are shown to meet ASME Code Subsection NG stress limits (the spacers are not, however, required to be designed to any ASME Code, however). Standard Code design formulas are used to evaluate elastic stability limits.* For normal conditions of transport (Level A Service Condition), a 10g deceleration load is applied and stress and stability issues are considered. The result ~~from Appendix 2.0~~ is summarized below:

Fuel Spacers - Minimum Safety Factors (Load Cases F2)			
Item	Load (lb.)	Capacity (lb.)	Safety Factor
Axial Load - Level A	16,800	46,446	2.76

The safety factor is greater than 1.0, which demonstrates that the fuel spacers meet the requirements of Level A Service Conditions for the normal condition of transport.

- MPC Shell Stability

The MPC shell is examined for elastic/plastic instability due to external pressure or compressive loads introduced as part of the load cases (design external pressure, normal transport). Each load component is examined separately. Design external pressure is applied to the outer surface of the enclosure vessel shell in the MPC model. The magnitude of the external pressure applied to the model is taken from Table 2.1.1. Analysis of the MPC under the external pressure is provided in Appendix 2.J. Analyses are performed using the methodology of ASME Code Case N-284 [2.1.8]. The following stability evaluations are performed in Appendix 2.J for the MPC shell for normal transport conditions:

- a. Normal Transport Deceleration Load from 10CFR71.45(b).
- b. Design external pressure plus a 1g compressive dead load.

The following table summarizes the limiting result from the calculations:

MPC Shell - Elastic/Plastic Stability (ASME Code Case N-284) - Minimum Safety Factors			
Item	Value	Allowable [†]	Safety Factor
Load Case 10CFR71.45(b) (Yield)	0.1930-174	2.0	10.3611-49
Load Case E1.b - Table 2.1.7 (Stability Interaction Curve)	0.832	1.0	1.20

Note that for the load case associated with the 10CFR71.45(b) requirement, the yield strength criteria in the Code Case N-284 method governs the "allowable" value. In this event, we include the safety factor 2.0, built into the Code Case, is included in the tabular result in order to obtain the actual safety factor with respect to the yield strength of the material.

The results demonstrate that the MPC shell meets the requirements of Code Case N-284. We note that the stability results presented above are very conservative. The stability analyses in Appendix 2.J carried out for the MPC shell assumed no axial stiffening from the fuel basket supports that run the full length of the shell. An analysis that included the effect of the stiffening (and therefore, recognized the fact that instability will most likely occur between stiffeners) will give increased safety factors for Load Case E1.b.

2.6.1.3.2

Overpack Stress Calculations

The structural functions of the overpack are stated in Section 2.1. The analyses *documented* presented here demonstrate the ability of components of the HI-STAR 100 overpack to perform their structural functions under normal conditions of transport. Load cases applicable to the structural evaluation of the HI-STAR 100 overpack under these conditions are compiled in Table 2.1.8.

In this subsection, stresses and stress intensities in the HI-STAR 100 overpack due to the combined effects of thermal gradients, pressure, and mechanical loads are presented. The results are obtained from a series of finite element analyses on the complete overpack and separate analyses on overpack components.

2.6.1.3.2.1

Finite Element Analysis - Load Cases 1 to 4 in Table 2.1.8

Load Case 1 pertains to a demonstration of the containment boundary as an ASME “NB component under Design Pressure and Level A Service Condition thermal loading. Other cases pertain to handling inertia loads imposed during normal conditions of transport and an extreme environmental condition. To analyze these load cases, a suitable finite element model of the complete overpack is required. As we noted earlier, since the identical finite element model is used in Section 2.7 to analyze the hypothetical accident conditions of transport, the following discussion refers to both sets of analyses to avoid textual repetition.

- Description of Finite Element Model (Normal Conditions and Hypothetical Accident)

The purpose of the HI-STAR 100 overpack model is to calculate stresses and stress intensities resulting from the loadings defined in Subsection 2.1 and compiled into load cases in Table 2.1.8.

A three-dimensional finite element model of the HI-STAR 100 overpack is used to assess the effects of loads associated with normal conditions of transport. The same finite element model is used in Section 2.7 to evaluate the effects of loading due to hypothetical accident scenarios. The overpack is a large structure subject to a variety of complex loads and boundary conditions. The finite element model developed for this analysis allows efficient determination of the stresses in this complex structure.

The finite element model of the overpack is constructed using ANSYS [2.6.4]. This model is duplicated in the HI-STAR 100 ~~TSAR~~FSAR (10CFR72) submittal for storage.

For structural analysis purposes, the overpack is assumed to be symmetric about a diametral mid-plane. This assumption is reasonable because the purpose of the model is to investigate global stresses in the model. The model is not intended to resolve effects due to small penetrations that produce peak stresses (which are significant only in cyclic fatigue conditions).

Element plots of the model are shown in a series of figures (Figures 2.6.16 through 2.6.19C). Figure 2.6.16 shows an overall view of half of the overpack subject to detailed finite element analysis. The view is directed

toward the internal cavity and shows the surface of symmetry. To enforce symmetry, displacements normal to the plane of symmetry at all nodes on the plane of symmetry are not permitted. Out-of-plane rotations at the nodes on the plane of symmetry are also set to zero. The basic building blocks of the finite element model are 20-node brick (SOLID95), 8-node brick (SOLID45), and 6-node tetrahedron elements (SOLID45). These are 3-D solid elements with 3 degrees of freedom at each node (three linear displacement degrees of freedom). Element densities are increased towards the top and bottom of the model in order to provide increased resolution of the stress fields in those regions.

The top flange/closure plate interface is modeled using linear spring elements (COMBIN14). The concentric seals are not modeled explicitly. The model is not intended to resolve the stress field around the grooves for the seals. The status of joint seal is ascertained by "Acompression springs" @ that which simulate the O-ring gaskets. Contact between the overpack top flange and closure plate is verified by checking the status of these spring elements. If contact between the closure plate and top flange is maintained under an applied loading (indicated by a compressive load in the "Acompression springs" @), then the integrity of the seal is determined to have been maintained under that load.

The overpack closure bolts are modeled with beam elements (BEAM4). The top of the beam elements represent the bolt head and are connected to the overpack closure plate. The bottom of the elements represents the threaded region of the bolt and is connected to nodes of elements representing the top flange. Torsional displacements of the bolts are suppressed to conform to with the degrees of freedom permitted at the nodes of the connecting solid elements.

The inner shell of the overpack is modeled with two solid element layers through the thickness of the shell.

Each of the lifting trunnions is modeled as three rigid beam elements (BEAM4) connected to the top forging. The beams extend from the forging and meet at a single node location. Trunnion stress analysis is documented in Subsection 2.5 ~~carried out in Appendix 2-B~~; the inclusion of the trunnion herein is solely to provide the appropriate offset for handling loads. The beam elements representing the trunnions are not shown on any of the figures describing the finite element model.

The neutron shield material is not a load bearing or supporting component in the finite element model. However, the weight of the neutron shield material must be included in the model in order to obtain the proper inertia loads. The neutron shield material is modeled with SOLID45 elements having a weight density that is specified in Subsection 2.3.2.1. In the model herein, ~~we include~~ the neutron shield material is included as an element set to ensure that proper accounting of total weight (and accompanying deceleration loads) occurs. Therefore, the neutron shield material must be assigned a Young's Modulus in the model. A value approximately equal to 1% of the Modulus of the steel load carrying components is assigned to the neutron shield material to insure that the neutron shield material serves as a load rather than a structural member in the model.

Figure 2.6.17 shows the finite element grid used for the bottom plate.

Figure 2.6.18 provides the details of the solid element grid for the top forging. Also shown in the figure are the line elements that represent the lid bolts. Since the lid is not shown in this figure, the upper part of the line elements is not attached to any node point.

Figure 2.6.19 shows a view from above of the overpack lid and details the element grid around the 180 degree periphery modeled.

Figure 2.6.19A shows the finite element grid for the inner shell and the five intermediate shells. The inner shell is modeled with two layers of solid elements; while each of the five intermediate shells is modeled by a single layer of solid elements sufficient to capture a linear stress distribution through the thickness.

Figure 2.6.19B presents the solid element distribution modeling the Holtite-A material. As noted previously, the structural effect of this material is neglected; the elements are included in the model to insure a proper mass distribution for the different analyses.

Finally, Figure 2.6.19C shows the shell element grid used to model the enclosure shell. Thin shell elements are used to simulate all components of the enclosure shell.

It is recognized that the layered shells of the overpack (shown in Figures 2.6.16 and 2.6.19A) are connected to each other and to the inner shell only at their top and bottom extremities. The finite element model must allow for separation between the intermediate shells in the non-connected regions under certain loading. Likewise, the intermediate shells cannot interpenetrate each other or the inner shell structure. To simulate these competing effects without making the model non-linear because of the introduction of contact elements, radial coupling of adjacent intermediate shell nodes is used in appropriate locations of the model. It is necessary to utilize physical reasoning to establish the regions where a nodal coupling is warranted because the shells can-not separate from each other. For example, radial coupling over two 60-degree spans serves to prevent interpenetration where it may occur during an impact simulation. Similarly, where physical reasoning indicates that a separation between the shell layers may occur, the nodes are left uncoupled. For example, when ovalization of the shells may occur under a specified loading, no coupling between shells is assumed. Figure 2.6.22 illustrates the nodal coupling pattern. The intermediate shell nodes that lie in the 60-degree sector between the top and bottom portions of the model remain uncoupled. The intermediate shells, in the uncoupled region, are free to separate from one another as the overpack cross section ovalizes during side impact. This modeling approach ensures that load transfer in a drop with significant lateral deceleration loads is modeled correctly. With respect to the overpack model, "bottom portion" refers to the 60-degree segment of the model closest to the point of impact. Conversely, "top portion" refers to the 60-degree sector farthest from the point of impact. This nodal coupling arrangement conservatively represents the structural behavior of the intermediate shells. In addition, no axial or circumferential nodal coupling has been used between adjacent intermediate shells. Thus, axial bending stiffness of the composite shell structure is conservatively underestimated. This underestimation of stiffness provides additional conservatism to the predicted values for safety factors.

~~The two pocket trunnions at the base of the HI-STAR 100 overpack are used for rotating the overpack from horizontal to vertical orientation and are not subjected to a large loading during the rotation process. During transport, however, these trunnions serve as restraints against longitudinal and lateral loads imposed by the action of the rail car. In particular, 10CFR71.45(b) requires that a 10g longitudinal inertia load be supported by the two pocket trunnions during transport. The rotation trunnions present in the first seven HI-STAR 100 units (see Subsection 2.5) are conservatively neglected not modeled in detail in the finite element models. Separate calculations, where applicable, are performed in appendices to this chapter and summarized later.~~

~~By the nature of the trunnion attachment, the two pocket trunnions also serve as two additional locations of support for all intermediate shell levels. In the finite element analysis of the overpack, this local attachment load path that ties all intermediate shells to the overpack baseplate is conservatively neglected.~~

Elements at locations of welds in the modeled components are assumed to have complete connectivity in all directions. Material in the model located at positions where welds exist is assumed to have material properties identical to the base material.

To summarize, the total number of nodes and elements in the overpack model are 11265 and 8642, respectively. The elements used are SOLID45, SOLID95, BEAM4, SHELL63, and COMBIN14.

For all structural analyses, material properties are obtained from the appropriate tables in Section 2.3. Property data for temperatures that are not listed in the material property tables are obtained by linear interpolation. Property values are not extrapolated beyond the limits of the code for any structural analysis.

- Description of Individual Loads and Boundary Conditions

The method of applying each individual load to the overpack model is described in this subsection. The individual loads are defined in Subsection 2.1.2.1 and are listed in Table 2.1.8 for normal conditions of transport. A free-body diagram of the overpack corresponding to each individual load is given in Figures 2.1.5 through 2.1.14. The figures presented in Section 2.1 present a general description of the loading but are lacking in specific details concerning the extent of the area exposed to the load. Therefore, in this subsection, ~~as we discuss in detail each of the applied loadings for the various cases considered is further discussed and, we provide~~ additional details on the specific application of the loads *are provided*. In the following discussion, reference to vertical and horizontal orientations ~~isare~~ made. Vertical refers to the *longitudinal* direction along the cask axis, and horizontal refers to a *lateral* ~~radial~~ direction.

Quasi-static methods of structural analysis are used. The effects of any dynamic load factors (DLF) are discussed in the final evaluation of safety factors. The load combinations are formed from the solution of individual load cases

(a) Accelerations (Used to Form Load Cases 3 and 4 in Table 2.1.8)

Table 2.1.10 provides the bounding values of the accelerations used for design basis structural evaluation. The loading is imposed by amplifying the gravity vector by the design basis deceleration. The proper distribution of the body forces induced by the accelerations is internally consistent based on the mass distribution associated with the different components of the finite element model. How these acceleration induced loadings are put in equilibrium with reaction loads from the impact limiters is discussed in detail in a later section.

In the following, ~~we discuss~~ appropriate boundary conditions for analyses for load cases associated with normal conditions of transport (Table 2.1.8) *are discussed*. However, since the same finite element model is used to evaluate hypothetical accident conditions of transport (Table 2.1.9) in Section 2.7, ~~we discuss~~ boundary conditions for Section 2.7 analyses *are discussed* here, as well, in the ongoing interest of conciseness of the presentation.

Boundary conditions for the model are as follows:

- i. End drop - In an end drop, displacement fixities are applied to the model on a cross-section through the top flange that is normal to the drop direction. Figures 2.1.7 and 2.1.8 show the free-body diagram for these load events. No reactions or internal body forces are shown. Further discussion is provided in Section 2.7.
- ii. Side drop - In a side drop, the inertia loads are reacted by the impact limiters. The overpack is in equilibrium with essentially end pinned supports. Figure 2.1.9 shows the configuration for this case. Further elaboration is provided in Section 2.7.

(b) Loads on the Overpack from the MPC

Pressures are applied on the inner surfaces of the overpack model to represent loads from the MPC for the drop loads.

- i. End drop - For a bottom end drop (Load Case 1, Hypothetical Accident, Table 2.1.9), the pressure load on the inside surface of the overpack bottom plate is assumed to be uniform and represents the load from the heaviest MPC (Figure 2.1.7). Note that this analysis conservatively assumes that the drop angle is not exactly 90° from the horizontal; attention is focussed on the overpack baseplate subject to the deceleration load from the heaviest MPC (applied as a uniform pressure) without the ameliorating effect of opposing distributed reaction from the impacted surface.

The magnitude of the pressure is the weight of the heaviest fully loaded MPC divided by the area of the faces of the elements over which the pressure is applied. The weight of

the heaviest fully loaded MPC is taken from the tables in Section 2.2, and is amplified by the design basis deceleration. Amplified loads from the MPC (weight times 60g acceleration) are applied as a pressure load to the entire inner surface of the bottom plate or the lid depending on the drop orientation. Note that for a top end drop, the MPC inertia loads act only on an outer annulus of the lid due to the raised surface deliberately introduced to act as a "landing" area for the MPC and reduce lid stress and deformation. By neglecting this raised annular area on the lid and applying the MPC load as a uniform pressure, ~~we maximize~~ stresses in the lid and the bolts *are maximized*. Further discussion is provided in Section 2.7.

- ii. Side drop - The shape and extent of the pressure distribution is determined from the results of the structural analysis of the MPC under similar orientations. In the MPC structural analysis, the extent of the support conditions of the MPC shell is determined with contact elements. In the analysis of the MPC under amplified inertia loads, the overpack is represented as a rigid circular surface. Based on results from the MPC evaluations, the loaded region is taken as 72 degrees (measured from the vertical). The MPC load on the overpack model is applied uniformly along the axial length of the inner surface of the model. Further discussion is provided in Section 2.7.
- iii. Oblique drop - Figures 2.1.10 and 2.1.11 show the balance loading applied for the oblique drop. A fixed node is defined away from the assumed impact point to insure that the package is in equilibrium under the applied loads. This drop orientation is only considered for the hypothetical accident evaluation. Therefore, a detailed discussion as to the methodology used to apply the loads and insure overall equilibrium is provided in Section 2.7 (specifically 2.7.1.3 and 2.7.1.4).

(c) Temperature (Used to Form Load Case 05 in Table 3.1.5)

Based on the results of the thermal evaluation for the normal hot environment presented in Chapter 3, a temperature distribution with a bounding gradient is applied to the overpack model. The purpose is to determine the stress intensities that develop in the overpack under the applied thermal load. A plot of the applied temperature distribution as a function of radius is shown in Figure 2.6.2.

The temperature distribution is applied to the ANSYS finite element model at discrete nodes using a parabolic curve fit of the computed distribution.

(d) Internal Pressure (Used to Form Load Cases 1 in Table 2.1.8)

Design internal pressure is applied to the overpack model. All interior overpack surfaces, including the inner shell, the bottom of the closure plate, and the top of the bottom plate are loaded with pressure. The magnitude of the internal pressure applied to the model is taken from Table 2.1.1. Figure 2.1.5 shows the displacement constraints for this load case. Figure 2.6.23 is a finite element grid plot showing the surfaces where internal pressure is applied.

(e) External Pressure (Used to Form Load Case 2 in Table 2.1.8)

Design external pressure is applied to the overpack model. External pressure is applied to the model as a uniform pressure on the outer surface of the model. The magnitude of the external pressure applied to the model is taken from Table 2.1.1. Figure 2.1.6 shows the displacement constraints for this load case. External pressures are imposed in the same manner as shown in Figure 2.6.23 except that the surfaces and magnitude are different.

(f) Bolt Pre-load (Used in all load cases in Tables 2.1.8 and 2.1.9)

The overpack closure bolts are torqued to *values predicted to preclude separation* ~~values given in Appendix 2.A~~. This torque generates a pre-load in the bolts and stresses in the closure plate and top flange in the region adjacent to the bolts. The finite element representation of the bolt elements is shown in Figure 2.6.18. The initial preload of the bolts is applied to the overpack model by applying an initial strain to the beam elements representing the bolts. This induces a tensile stress in each of the bolts and a corresponding compression in the seals (represented by spring elements). This load case is present in every load combination.

(g) Fabrication stresses

Fabrication stresses are conservatively computed for the inner shell and all of the intermediate shells. Fabrication effects are not easily introduced into the finite element model unless compression-only contact elements are used. Since the fabrication stresses are circumferential secondary stresses in the shells, the incorporation of this load case is best accomplished outside of the finite element analysis. Therefore, there is no fabrication load case associated with the finite element analyses.

~~Fabrication stresses are conservatively computed in Appendix 2.Q for the inner shell and all of the intermediate shells. Fabrication effects are not easily introduced into the finite element model unless compression-only contact elements are used. Since the fabrication stresses are circumferential secondary stresses in the shells, the incorporation of this load case is best accomplished outside of the finite element analysis. Therefore, there is no fabrication load case associated with the finite element analyses.~~

- Finite Element Analysis Solution Procedure

The analysis procedure is as follows:

1. The stress and deformation field due to each individual load is determined.
2. The results from each individual load case are combined in a postprocessor to create each load case. The load cases analyzed are listed in Table 2.1.8 for normal conditions of transport and in Table 2.1.9 for hypothetical accident conditions of transport. ~~Results are tabulated in Appendix 2.AE.~~
3. The results for each load case are compared to allowables. The calculated values are compared with allowable values in Subsection 2.6.1.4 for normal conditions of transport and in an appropriate subsection of Section 2.7 for hypothetical accident conditions.

2.6.1.3.2.2 Fabrication Stress

The fabrication stresses originate from welding operations to affix the intermediate shells in position. As the molten weld metal solidifies, it shrinks pulling the two parts of the shells together. Adjacent points at the weld location will close together after welding by an amount " δ " which is a complex function of the root opening, shape of the bevel, type of weld process, etc. The residual stresses generated by the welding process are largely confined to the weld metal and the "heat affected zone". The ASME Code recognizes the presence of residual stresses in the welds, but does not require their calculation. The Code also seeks to minimize fabrication stresses in the welds through controlled weld procedures. Nevertheless, fabrication stresses cannot be eliminated completely.

The computation of fabrication stresses is carried out to comply with the provisions of Regulatory Guide 7.8, Article C-1.5. The Regulatory Guide requires that "Fabrication and installation stresses in evaluating transportation loadings should be consistent with the joining, forming, fitting, and aligning processes employed during the construction of casks...the phrase fabrication stresses includes the stresses caused by interference fits and the shrinkage of bonded lead shielding during solidification but does not include the residual stresses due to plate formation, welding, etc."

A literal interpretation of the above-cited Regulatory Guide text exempts the HI-STAR 100 designer from computing the stresses in the containment and intermediate shells due to welding. However, in the interest of conservatism, ~~we compute and establish~~ an upper bound, on the stresses induced in the containment shell and in the intermediate shells, *is computed for* the fabrication process. ~~Detailed calculations are presented in Appendix 2.Q.~~

To calculate the so-called fabrication stresses, ~~it is~~we recalled that in affixing the intermediate shells to the cask body, the design objective does not call for a definite radial surface pressure between the layers. Rather, the objective is to ensure that the shells are not loosely installed. Fortunately, extensive experience in fabricating multi-layer shells has been acquired by the industry over the past half-century. The technology

that was developed and has matured for fabrication in older industries (such as oil and chemical) ~~is will be~~ used in HI-STAR 100 fabrication of the multi-layered shells. Mock-up tests on carbon steel coupons indicate that the total shrinkage after welding can range from 0.010" to 0.0625" for the bevel and fit-up geometry in the HI-STAR 100 design drawings. Therefore, the ~~evaluations are~~ calculations in Appendix 2.Q are carried out using the upper bound gap of 0.0625". To bound the computed stresses even further, the inter-layer friction coefficient is set equal to zero. It is intuitively apparent that increasing the friction increases the localized stresses near the "point of pull" (i.e., the weld) while mitigating the stresses elsewhere. Since ~~the our~~ object is to maximize the distributed (membrane) stress, the friction coefficient is set equal to zero in the analysis of Appendix 2.Q.

A two-dimensional finite element analysis of the inner confinement shell and the five intermediate shells is performed to establish the level of fabrication circumferential stress developing during the assembly process. A 180-degree section through the overpack, consisting of six layers of metal, is modeled. The ANSYS finite element code is used to model the fabrication process; each layer is modeled using PLANE42 four node quadrilateral elements. Contact (or lack of contact) is modeled by CONTAC48 point-to-surface elements. Symmetry boundary conditions apply at 90 degrees, and radial movement of the inner node point of the confinement layer is restrained. At 90 degrees, the inner confinement layer is restrained while the remaining layers are subject to a prescribed circumferential displacement d to stretch the layer and to simulate the shrinkage caused by the weld process. Although the actual fabrication process locates the longitudinal weld in each layer at different circumferential orientation, in the analytical simulations all layer welds are located together. This is acceptable for analysis since the stress of interest is the primary membrane component. Figure 2.6.24 shows a partial free body of a small section of one of the layers. Normal pressures p develop between each layer due to the welding process; shear stresses due to friction between the layers also develop since there is relative circumferential movement between the layers. Figure 2.6.25 shows a free body of the forces that develop on each layer.

The fabrication stress distribution is a function of the coefficient-of-friction between the layers. For a large enough coefficient-of-friction the effects of the assembly process are localized near the weld. Localized stresses are not considered as primary stresses. For a coefficient-of-friction = 0.0, the membrane hoop stress in the component shells is non-local in nature. Therefore, the fabrication stress computation conservatively considers only the case coefficient of friction (COF) = 0.0 since this will develop the largest in-plane primary membrane stress in each layer. The simulation is nonlinear in that each of the contact elements is checked for closure during increments of applied loading (the weld displacement).

The results from the analyses in Appendix 2.Q are summarized in the table below:

Fabrication Stresses in Overpack Shells ¥ –Minimum Safety Factors (Level A Service Condition at Assembly Temperature)			
Item	Value (ksi)	Allowable (ksi) (Note3)	Safety Factor
First Intermediate Shell (Note 1)	11.22	52.5	4.68
Fourth Intermediate Shell (Note 1)	7.79	52.5	6.74
Inner Shell Mid Plane (Note 2)	10.6	69.9	6.59
Inner Shell Outer Surface (Note 2)	16.27	69.9	4.30

Notes:

1. The fabrication stress is a tensile circumferential stress.
2. The fabrication stress is a compressive circumferential stress
3. Fabrication stresses are self-limiting and are therefore classified as “secondary” and are compared to 3 times the allowable membrane stress or stress intensity.

The above table leads to the conclusion that the maximum possible values for stresses resulting from HI-STAR 100 fabrication process are only a fraction of the relevant ASME Code limit.

2.6.1.3.2.3 Structural Analysis of Overpack Closure Bolting (Load Case1 - Table 2.1.8)

Stresses are developed in the closure bolts due to pre-load, pressure loads, temperature loads, and accident loads. Closure bolts are explored in detail in Reference [2.6.3] prepared for analysis of shipping casks. The analysis *herein* of the overpack closure bolts under normal conditions of transport and for the hypothetical accident conditions ~~carried out in Appendix 2.U~~ and follows *uses the methodology and the procedures defined and explained in Reference [2.6.3]; the sole exception is that some of the formulas in the reference are modified to account for the annulus on the inner surface of the overpack closure lid; this annulus exists for the sole purpose of ensuring that the interface area between the MPC lid and the overpack top closure is a peripheral ring area rather than the entire surface area of the MPC lid. This feature ensures a reduction in the computed bolt stress.*

~~The allowable stresses used for the closure bolts follows that reference.~~

The following combined load case is analyzed in Appendix 2.U for normal conditions of transport

Normal: Pressure, temperature, and pre-load loads are included (Load Case 1 in Table 2.1.8). Reference [2.6.3] reports safety factors defined as the calculated stress combination divided by the allowable stress for the load combination. This definition of safety factor is the inverse of the definition consistently used in this SAR. In summarizing the closure bolt analyses performed, in Appendix 2.U, we report results are reported using the safety factor definition of allowable stress divided by calculated stress. The following result for closure lid bolting for normal conditions of transport are obtained: from Appendix 2.U.

Overpack Closure Bolt - Safety Factor (Load Case 1 in Table 2.1.8)	
Combined Load Case	Safety Factor on Bolt Tension
Average Tensile Stress	1.441.08
Combined Tension, Shear, Bending , and Torsion	1.571.19

It is seen from the above table that the safety factor is greater than 1.0 as required. Note that the magnitude of the safety factors reflect the large magnitude of preload required for successful performance of the bolts under a hypothetical accident drop event where the demand is more severe.

2.6.1.3.2.4 Stress Analysis of Overpack Enclosure Shell

The overpack enclosure shell and the overpack enclosure return are examined for structural integrity under a bounding internal pressure in Appendix 2.AM. Flat beam strips of unit width are employed to simulate the performance of the flat panels and the flat plate return section (see drawings in Subsection 1.4). It is shown there that large safety factors exist against overstress due to an internal pressure developing from off-gassing of the neutron absorber material. The minimum safety factors are summarized below:

Location	Calculated Stress (ksi)	Allowable Stress (ksi)	Safety Factor
Enclosure Shell Return (bottom)	2.562.14	26.3	10.212.3
Enclosure Shell Return (top)	3.42	26.3	7.68
Enclosure Shell Flat Panels	5.583.72	26.3	4.717.1
Weld Shear	0.63	10.52	16.7

2.6.1.3.3 Fatigue Considerations

Regulatory Guide 2.9 requires consideration of fatigue due to cyclic loading during normal conditions of transport. Considerations of fatigue associated with long term exposure to vibratory motions associated with normal conditions of transport are considered below where individual components of the package are assessed for the potential for fatigue.

- Overpack and MPC Fatigue Considerations

The temperature and pressure cycles within the MPC and the inner shell of the overpack are entirely governed by the mechanical and thermal-hydraulic conditions presented by the fuel. The external surfaces of the overpack, however, are in direct contact with the ambient environment. The considerations of cyclic fatigue due to temperature and pressure cycling of the HI-STAR 100 System, therefore, must focus on different locations depending on the source of the cyclic stress.

As shown in the following, the overpack and the MPCs in the HI-STAR 100 System do not require a detailed fatigue analysis because all applicable loadings are well within the range ~~that~~which permits exemption from fatigue analysis per the provisions of Section III of the ASME Code. Paragraph NB-3222.4 (d) of Section III of the ASME Code provides five criteria ~~that~~which are strictly material and design condition dependent to determine whether a component can be exempted from a detailed fatigue analysis. The sixth criterion is applicable only when dissimilar materials are involved, which is not the case in the HI-STAR 100 System.

The Design Fatigue curves for the overpack and MPC materials are given in Appendix I of Section III of the ASME Code. Each of the five criteria is considered in the following:

- i. Atmospheric to Service Pressure Cycle

The number of permissible cycles, n , is bounded by $f(3S_m)$, where $f(x)$ means the number of cycles from the appropriate fatigue curve at stress amplitude of x psi. In other words

$$n < f(3S_m)$$

From Tables 2.1.11 through 2.1.20 for normal conditions, and the fatigue curves, the number of permissible cycles ~~is are~~

$$\begin{aligned} n \text{ (overpack)} &\leq 1600 \text{ (} 3S_m = 68,700 \text{ psi) (Figure I.9-1 of ASME Appendix I)} \\ n \text{ (MPC)} &\leq 40,000 \text{ (} 3S_m = 46,200 \text{ psi) (Figure I.9-2 of ASME Appendix I)} \end{aligned}$$

The MPC, which is an all-welded component, is unlikely to undergo more than one cycle, indicating that a huge margin of safety with respect to this criterion exists. The overpack, however, is potentially subject to multiple uses. However, 1000 pressurizations in the 40-year life of the overpack is an upper bound estimate. In conclusion, the projected pressurizations of the HI-STAR components do not warrant a usage factor evaluation.

ii. Normal Service Pressure Fluctuation

Fluctuations in the service pressure during normal operation of a component are considered if the total pressure excursion δ_p exceeds Δ_p .

where

$$\Delta_p = \text{Design pressure} * S / (3S_m)$$

$$S = \text{Value of } S_a \text{ for one million cycles}$$

Using the above mentioned tables and appropriate fatigue curves,

$$(\Delta p)_{\text{overpack}} = \frac{(100)(13000)}{(3)(22,900)} = 18.9 \text{ psi}$$

$$(\Delta p)_{\text{MPC}} = \frac{(100)(26000)}{(3)(16000)} = 54.2 \text{ psi}$$

During normal operation the pressure fields in the MPC and the overpack are steady state. Therefore, normal pressure fluctuations are negligibly small. Normal service pressure oscillations do not warrant a fatigue usage factor evaluation.

iii. Temperature Difference - Startup and Shutdown

Fatigue analysis is not required if the temperature difference ΔT between any two adjacent points on the component during normal service does not exceed $S_a / 2E\alpha$, where S_a is the cyclic stress amplitude for the specified number of startup and shutdown cycles. E and α are the Young's Modulus and instantaneous coefficients of thermal expansion (at the service temperature). Assuming 1000 startup and shutdown cycles, ~~we have from~~ Tables 2.3.1 and 2.3.4 and the *appropriate*

ASME fatigue curves in Appendix I or Section III, of the ASME Code give:

$$(\Delta T)_{MPC} = \frac{130,000}{(2)(25)(9.69)} = 268^{\circ}F$$

$$(\Delta T)_{overpack} = \frac{90,000}{(2)(26.1)(6.98)} = 247^{\circ}F$$

~~appropriate ASME fatigue curves in Appendix I or Section III, ASME Code.~~

There are no locations on either the overpack or MPC where ΔT between any two adjacent points approach these calculated temperatures. As reported in Tables 3.4.16-18, the maximum ΔT that occurs between two components, the MPC shell and the basket periphery, is only 115 degrees $^{\circ}F$. Therefore, it is evident this temperature criterion is satisfied for 1,000 startup and shutdown cycles.

iv. Temperature Difference - Normal Service

Significant temperature fluctuations ~~that~~ which require consideration in this criterion are those in which the range of temperature difference between any two adjacent point under normal service conditions is less than $S/2E\alpha$ where S corresponds to 10^6 cycles. Substituting ~~gives we have~~

$$(\Delta T)_{MPC} = \frac{26,000}{(2)(25)(9.69)} = 53.7^{\circ}F$$

$$(\Delta T)_{overpack} = \frac{13,000}{(2)(26.1)(6.98)} = 35.7^{\circ}F$$

During normal operation, the temperature fields in the MPC and the overpack are steady state. Therefore, normal temperature fluctuations are negligibly small. Normal temperature fluctuations do not warrant a fatigue usage factor evaluation.

v. Mechanical Loads

Mechanical loadings of appreciable cycling occur in the HI-STAR 100 System only during transportation. The stress cycling under transportation conditions is considered significant if the stress amplitude is greater than S_a corresponding to 10^6 cycles. It, therefore, follows that the stress limits which exempt the overpack and MPC are 13,000 psi and 26,000 psi, respectively.

From Subsection 2.5.2.1, g-loads typically associated with rail transport will produce stress levels in the MPC and overpack which are a small fraction of the above limits. Therefore, no potential for fatigue expenditure in the MPC and overpack materials is found to exist under transportation conditions.

In conclusion, the overpack and the MPC do not require fatigue evaluation under the exemption criteria of the ASME Code.

- Fatigue Analysis of Closure Bolts:

The maximum tensile stress developed in the overpack closure bolts during normal operating conditions *is shown by analyses not to* cannot exceed 93.0 ksi (~~Appendix 2.U and Appendix 2.A~~). The alternating stress in the bolt is equal to 1/2 of the maximum stress due to normal conditions, or 46.5 ksi. The design service temperature for the bolts per Table 2.1.2 is 350 degrees °F. Per Table 2.3.5, the Young's Modulus at 350 degrees °F is 27,000.7 million kpsi. Therefore, the effective stress intensity amplitude for calculating

$$S_a = \frac{(46.5)(4)(30e+06)}{27.7e+06} \\ = 201.4 \text{ ksi}$$

usage factor using Figure I-9.4 (ASME Code, Appendices) is (ratioing the modulus used in the figure to the modulus used here):

Using Figure I-9.4 (NB, loc. cit), the permissible number of cycles is 200.

This result indicates the main closure bolts should *not be torqued and untorqued more than 200 times. After 200 loading cycles, they must be replaced*.

The total shear area of the overpack closure bolt threads is $A_v = 9.528 \text{ in}^2$ ~~per Appendix 2.A~~. Therefore, the shear stress in the top closure bolt threads is, (~~we~~ use the limiting bolt load for normal operation and the tensile stress area of a bolt = 1.680 in^2).

$$\sigma_v = \frac{93.0 \text{ ksi} \times 1.68 \text{ in}^2}{9.528 \text{ in}^2} = 16.4 \text{ ksi}$$

The shear stress developed in the threads of the overpack closure bolts is significantly less than the stress developed in the bolt. Therefore, fatigue of the overpack closure bolts is not controlled by shear stress in

the bolt threads.

- Fatigue Considerations for Top Flange Closure Bolt Threads:

The shear area of the main flange closure bolt threads is 12.371 in.² per Appendix 2-A. Therefore, the shear stress in the flange threads under the limit load on the bolt is:

$$\sigma_v = \frac{93.0 \text{ ksi} \times 1.68 \text{ in}^2}{12.928 \text{ in}^2} = 12.6 \text{ ksi}$$

The primary membrane stress in the main flange threads is equal to twice the maximum shear stress, or 21.1 ksi. The alternating stress in the threads, S_a , is equal to 1/2 of the total stress range, or 10.56 ksi. At 400 degrees °F design temperature (per Table 2.1.2) the Young's Modulus (Table 2.3.4) is 26.1×10^6 psi.

The effective stress amplitude accounting for the fatigue strength reduction and Young's Modulus effects is given by

$$S_a = \frac{(12.6)(4)(30)}{26.1} = 57.9 \text{ ksi}$$

Using Figure I-9.4 (of NB, loc. cit), ~~we have~~ the allowable number of cycles is equal to 1,800.

Therefore, the *maximum service life of the main flange threads is 1,800 cycles* of torquing and untorquing of the overpack closure system.

- • MPC Fatigue Analysis

The maximum primary and secondary alternating stress range for normal transport conditions is conservatively assumed to be equal to the allowable alternating stress range of $0.5 \times 40,000$ psi. Conservatively using a Young's Modulus of 25×10^6 psi for the fatigue evaluation, yields

$$S = 20,000 \text{ psi} \times \frac{28.3 \times 10^6 \text{ psi}}{25 \times 10^6 \text{ psi}} = 22,640 \text{ psi}$$

Cyclic life is in excess of 1×10^6 cycles per Figure I-9.2.1 of Appendix I of the ASME Code.

- Satisfaction of Regulatory Guide 7.6 Commitment

The minimum alternating stress range, S_a , at 10 cycles from all appropriate fatigue curves is 600 ksi. All primary stresses under any of the analyses performed in this SAR under the required load combinations are shown to lead to stress intensities that are less than the ultimate strength of the containment vessel material (70 ksi). Fabrication stresses are conservatively evaluated ~~in Appendix 2.Q~~ and are summarized in Subsection 2.6.1.3.2.2. Maximum fabrication stress intensities are less than 17 ksi. Conservatively assuming a stress concentration of 4 regardless of specific location produces a stress intensity range below $4 \times (70 + 17) = 348$ ksi (< 600 ksi). Therefore, satisfaction of the Regulatory Guide 7.6 commitment is assured.

2.6.1.4 Comparison with Allowable Stresses

Consistent with the formatting guidelines of Regulatory Guide 7.9, calculated stresses and stress intensities from the finite element analyses are compared with the allowable stresses and stress intensities defined in Subsection 2.1 (Tables 2.1.11 through 2.1.21) as applicable for conditions of normal transport. The results of these comparisons are presented in the form of factors of safety (SF) defined as

$$SF = \frac{\text{Allowable Stress}}{\text{Calculated Stress}}$$

:

Safety factors associated components identified as lifting and tie-down devices have been presented in Section 2.5 as required by Regulatory Guide 7.9.

Major conservatisms are inherent in the finite element models for both the MPC fuel basket and the enclosure vessel, and for the HI-STAR 100 overpack. ~~We elucidate~~ *These conservatisms are elucidated* here with additional discussion as needed later in the text associated with each particular issue.

Conservative Assumptions in Finite Element Analyses and Evaluation of Safety Factors

1. Comparison with allowable stresses or stress intensities is made using the design temperature of the component rather than the actual operating temperature existing in the metal at that location. As an example, all comparisons with allowables for the Alloy X fuel basket material uses the allowable strength at 725 degrees F (Table 2.1.21). Under the normal heat conditions of transport, temperatures near the periphery of the fuel basket are below 450 degrees F (~~see Appendix 2.D, for example~~). High stresses in the fuel basket generally occur at the basket periphery. From Table 2.1.19, ~~we can compare~~ *the allowable stresses for primary membrane plus bending at the two temperatures are compared* to evolve the additional margin in the computed safety factor as $27.2/23.1 = 1.18$. Therefore, the reported safety factors from the analysis

have at least an additional 18% hidden component from this effect. Similar hidden margins from this kind of simplification arise in the various components of the overpack. Depending on the material, these hidden margins which increase the reported safety factor may be large or small. From Figures 3.4.17 and 3.4.18 in Chapter 3, *it is we concluded* that the normal heat condition of transport maximum inner shell temperature is less than 300 degrees F. The allowable stresses are uniformly assumed at 400 degrees F per Table 2.1.21. From Table 2.1.11, the additional hidden safety factor multiplier is computed as $35/34.4 = 1.02$. In the inner shell of the overpack, the increase in the reported safety factor from this effect is only 2% for normal conditions of transport.

2. Comparisons with primary stress allowables are made with secondary stresses included. This has an adverse effect on the reported safety factor, especially in areas near discontinuities.
3. In the modeling of the HI-STAR 100 overpack, the full structural connectivity of the intermediate shells and the inner containment shell is not included in the finite element model in order to maintain the linear elastic analysis methodology. The neglect of such interaction means that the overall bending stiffness of the overpack is underestimated; this leads to over-prediction of stresses and consequent adverse effects on reported safety factors.
4. In the modeling of the MPC fuel basket, the local reinforcement of the fuel basket panel from the fillet welds is neglected. The increase in the section modulus at the weld location is ignored leading to a decrease in stiffness of the basket panel. Consequently, under mechanical loading, the stress state is overestimated at the basket panel connection.

2.6.1.4.1 MPC Fuel Basket and Enclosure Vessel

It is recalled that the stress analyses have been performed for the load cases applicable to normal conditions of transport as assembled in Tables 2.1.6 and 2.1.7 for the fuel basket and the enclosure vessel, respectively. ~~All detailed analyses, including finite element model details and the necessary explanations to collate and interpret the voluminous numerical results have been archived are contained in appendices to this chapter. These appendices are identified in Subsection 2.10 for ease of reference. Appendix 2.AC is a compendium of finite element results for the fuel basket and enclosure vessel for each load case associated with normal conditions of transport has been developed. For ease in regulatory review, a concise set of tables have been prepared to summarize the results listed in the tables in Appendix 2.AC and in other parts of this section. Tables 2.6.6 and 2.6.7 summarize results obtained from the analyses (for all baskets) of Load Cases E1.a and E1.c defined in Table 2.1.7. Table 2.6.8 contains a synopsis of all safety factors obtained from the results in Appendix 2.AC. To further facilitate perusal of results, another level of summarization is performed in Tables 2.6.2 and 2.6.3 where the global minima of safety factor for each load case are presented. Finally, miscellaneous safety factors associated with the fuel basket and the MPC enclosure vessel are reported in Table 2.6.10.~~

The following element of information is relevant in ascertaining the safety factors under the various load cases presented in the tables.

- In the interest of simplification of presentation and conservatism, the total stress intensities under mechanical loading are considered to be of the primary genre' even though, strictly speaking, a portion can be categorized as secondary (that have much higher stress limits).

A perusal of the results for Tables 2.6.2 and 2.6.3 under different load combinations for the fuel basket and the enclosure vessel reveals that all factors of safety are above 1.0. The relatively modest factor of safety for the fuel basket under side drop events (Load Case F2.a and F2.b) in Table 2.6.2 warrants further explanation.

The wall thickness of the storage cells, which is by far the most significant variable in the fuel basket's structural strength, is significantly greater in the HI-STAR 100 MPCs than in comparable fuel baskets licensed in the past. For example, the cell wall thickness in the TN-32 basket (Docket No. 72-1021, M-56), is 0.1 inch and that in the NAC-STC basket (Docket No. 71-7235) is 0.048 inch. In contrast, the cell wall thickness in the MPC-68 is 0.25 inch. In spite of their relatively high flexural rigidities, computed margins in the HI-STAR 100 fuel baskets are rather modest. This is because of some conservative assumptions in the analysis that lead to an overstatement of the state of stress in the fuel basket. For example:

- i. The section properties of longitudinal fillet welds that attach contiguous cell walls to each other are completely neglected in the finite element model (Figure 2.6.15). The fillet welds strengthen the cell wall section modulus at the very locations where maximum stresses develop.
- ii. The radial gaps at the fuel basket-MPC shell and at the MPC shell-overpack interface are explicitly modeled. As the applied loading is incrementally increased, the MPC shell and fuel basket deform until a "rigid" backing surface of the overpack is contacted, making further unlimited deformation under lateral loading impossible. Therefore, some portion of the fuel basket and enclosure vessel (EV) stress has the characteristics of secondary stresses (which by definition, are self-limited by deformation in the structure to achieve compatibility). For conservativeness in the incremental analysis, ~~we make~~ no distinction between deformation controlled (secondary) stress and load controlled (primary) stress in the stress categorization *is made*. ~~A~~ ~~We~~ ~~treat~~ all stresses, regardless of their origin, *are considered* as primary stresses. Such a conservative interpretation of the Code has a direct (adverse) effect on the computed safety factors.

The above remarks can be illustrated simply by a simple closed-form bounding calculation. If all deformation necessary to close the gaps is eliminated from consideration, then the capacity of the fuel basket cell wall under loads which induce primary bending stress can be

ascertained by considering a clamped beam (cell wall) subject to a lateral pressure representing the amplified weight of fuel assembly plus self-weight of the cell wall (e.g., see Figure 2.6.15).

Using the cell wall thickness and *an appropriate* unsupported length for the MPC-6824, for example, the fixed edge bending stress is computed as 238.22578 psi (using the actual fuel weights, cell wall weights, cell wall thickness and unsupported length). This implies a safety factor of ~~5.7042-35~~ for a Level A event (for a 17g deceleration, $SF = 23,100/(238.22578 \times 17) = 5.7042-35$) where the allowable bending stress intensity for Alloy X at 725 degrees °F (Table 2.1.21) has been used. The above simple calculation demonstrates that the inherent safety margin under accident loading is considerably greater than is implied by the result in Table 2.6.8 ($SF=2.421-62$) for the MPC-6824 and 0-degree drop orientation. Similar conclusions can be reached for *other MPCs*, ~~the MPC-68~~ by performing scoping calculations in *a similar manner* ~~the manner just carried out for the MPC-24.~~

- iii. The SNF inertia loading on the cell panels is simulated by a uniform pressure, which is a most conservative approach for incorporating the SNF/cell wall structure interaction.

The above assumptions all act to depress the computed values of factors of safety in the fuel basket finite element analysis and render conservative results.

The reported values do not include the effect of dynamic load amplification. *Calculations Appendix 2.K* shows that, for the duration of impact and the predominant natural frequency of the basket panels under lateral hypothetical accident conditions, the dynamic load factors (DLF) are bounded by 1.05. *It is expected* ~~We would expect~~ that for the normal condition of transport 1' drop, the amplification would be reduced further.

Table 2.6.8 does not report the safety factors associated with Load Case F1 in Table 2.1.6 where *it is we* shown ~~that~~ that secondary stresses due to the thermal gradients are below the allowable secondary stress intensity limits. *A representative stress intensity level arising from fuel basket thermal gradients is 15.07 ksi* Tables 2.AC.1, 2.AC.26, and 2.AC.51 report the thermal stresses in the basket due to the radial thermal gradient. The highest stress is in the MPC-68 fuel basket and is listed in Table 2.AC.51. Using the allowable stress intensity limit for primary plus secondary components per Table 2.1.21, ~~we obtain~~ the following *representative* fuel basket safety factor appropriate to Load Case F1 *is obtained* as "SF", where;

$$SF = 46.2 \text{ ksi} / 15.07 \text{ ksi} = 3.06 \quad (\text{Load Case F1 from Table 2.1.6})$$

It is ~~We~~ concluded that since all reported factors of safety for the fuel basket panels (based on stress analysis) are greater than the DLF, the MPC fuel basket is structurally adequate for its intended functions

during and after a postulated lateral drop event associated with the normal conditions of transport.

Tables 2.6.6 and 2.6.7 report stress intensities and safety factors for the helium retention boundary (enclosure vessel) subject to internal pressure alone and to internal pressure plus the normal operating condition temperature with the most severe thermal gradient (Load Cases E1.a and E1.c in Table 2.1.7). Table 2.6.8 reports safety factors from the finite element analyses of the 1' free drop simulating a normal handling condition of transport. The final values for safety factors in the various locations of the helium retention boundary provide assurance that the MPC enclosure vessel is a robust pressure vessel.

2.6.1.4.2 Overpack

2.6.1.4.2.1 Discussion

The overpack is subject to the load cases listed in Table 2.1.8 for normal conditions of transport. Results from the series of finite element analyses are *tabulated* reported in Appendix 2.AE. Appendix 2.AE reports ~~finite element results~~ for normal heat and cold conditions of transport in Tables 2.AE.1 through 2.AE.8. ~~The tabular results~~ The remaining tables in Appendix 2.AE report results for the hypothetical accident conditions of transport that are discussed in Subsection 2.7. Tables 2.AE.1 to 2.AE.4 include contributions from mechanical and thermal loading and are needed to insure satisfaction of primary plus secondary stress limits for normal conditions of transport. Tables 2.AE.5 through 2.AE.8 contain ~~R~~results are also tabulated from analyses that neglect thermal stresses. These tables are used to check primary stress limits. ~~In order to identify and to locate appropriate regions with limiting safety factors, we note that Appendix 2.AE reports the results for each load case at a select set of nodes identified as "stress report locations". Appendix 2.P defines these node locations in the overpack finite element model that are considered stress report locations. Appendix 2.P also includes tables to convert node numbers to stress report location and stress report locations to node numbers.~~

The following text is a brief description of how the results are presented for evaluation and how the evaluation is organized in final form:

- ~~Appendix 2.AE reports the results of the finite element analyses of the overpack in a series of tables for individual applied loads and for combined load cases associated with normal conditions of transport as prescribed by Table 2.1.8.~~ The stress intensity results are sorted by safety factor in ascending order for each component making up the overpack. In particular, results are *sorted separately* presented for locations in the lid, the inner shell, and the bottom plate that together make up the containment boundary.
- The extensive body of results in Appendix 2.AE is initially summarized in Table 2.6.9 wherein the minimum safety factor for different components of the overpack for each of the load cases is presented. This table lists minimum safety factors for the load cases associated with the normal heat conditions of transport. All safety factors are conservatively computed using allowable stresses

based on the maximum normal operating temperatures (see Tables 2.1.2 and 2.1.21 for temperatures and for allowable stresses).

- The finite element analyses include the stress state induced by bolt preload but do not include the effect of secondary fabrication stresses. Table 2.6.5 presents results of re-calculation of the safety factors for the inner containment shell and *for* the intermediate shells to include the "fabrication stresses" reported in Subsection 2.6.1.3.2.2. Table 2.6.5 summarizes these recomputed safety factors, based on limits for primary plus secondary stresses, and reports the limiting safety factors for the overpack shells for events subject to normal conditions of transport (Level A Service Conditions). The incorporation of the fabrication stress and the computation of revised safety factors ~~is detailed in Appendix 2.AD where we~~ begins with the individual principal stress components ~~listed in Appendix 2.AE for the shells,~~ conservatively adds the circumferential fabrication stress in the inner and intermediate shells to the principal stress having the same sign as the fabrication stress, and *then* re-computes the stress intensity and the safety factor. For the inner shell, the safety factors including fabrication stress are computed from principal stress data ~~in Appendix 2.AE including mechanical and thermal loading.~~ For the intermediate shell, however, the recomputed safety factors are based on principal stresses that only include mechanical loading (no thermal stresses need be evaluated for a component designed in accordance with ASME Code Section III, Subsection NF regardless of Class 1 or Class 3 designation (see paragraph NF-3121.11)).
- Finally, Table 2.6.4 summarizes the minimum values of safety factors (global minima) for the overpack components for the normal conditions of transport.

The modifications summarized in Table 2.6.5 ~~and documented in Appendix 2.AD~~ are briefly discussed below for the normal heat conditions of transport. The same series of modifications are also performed for the normal cold conditions of transport.

Case 1 (Pressure) - ~~Table 2.AE.1 reports results in tabular form for Load Case 1 in Table 2.1.8. Safety factors are summarized in Table 2.6.9 prior to inclusion of fabrication stress. Table 2.6.5 shows the modified safety factor *resulting that results* from "adding" the fabrication stress for the inner containment shell to the appropriate principal stress from Table 2.AE.1 *that includes where results* for the combination of mechanical plus thermal loads are reported. Appendix 2.AD contains the necessary calculations to obtain the correction for safety factor associated with the inner containment shell.~~ The same conservative methodology is applied to modify the safety factor for the intermediate shell to include fabrication stress. However, since the intermediate shells are designed to ASME Code Section III, Subsection NF, no thermal stresses need be included in the strength evaluation. ~~Therefore, to include the effect of fabrication stress in the intermediate shell, we use the results from Table 2.AE.5 that does not contain any stress due to thermal gradients.~~

Case 3 (1 foot drop): *Results are tabulated* ~~Table 2.AE.3 reports results in tabular form for Load Case 03~~

in Table 2.1.8 including both thermal and mechanical loading. Safety factors for the inner containment shell are summarized in Table 2.6.9 prior to inclusion of fabrication stress. Table 2.6.5 shows modified safety factors that are computed in the same manner as reported for Case 1. ~~The calculation details are in Appendix 2.A.D.~~ For the intermediate shell, ~~Table 2.AE.7 provides the principal stress results that do not include thermal stress effects~~ are conservatively modified to include fabrication effects ~~since we need not include thermal stresses.~~

2.6.1.4.3 Result Summary for the Normal Heat Condition of Transport

- Stress Results from Overall Finite Element Models of the MPC and Overpack

Tables 2.6.6 through 2.6.9 summarize minimum safety factors from load cases analyzed using the finite element models of the MPC fuel basket plus canister and the overpack described in Subsections 2.6.1.3.1 and 2.6.1.3.2. All safety factors are greater than 1.0 and are greater than any credible dynamic amplifier for the location. Table 2.6.5 provides a summary table that includes the effect of fabrication stress on safety factors for the intermediate and inner shells of the overpack. Table 2.6.5 reports safety factors based on primary plus secondary allowable strengths.

- Status of Lid Bolts and Seals on the Overpack

The finite element analysis for the overpack provides results at the lid-to-top flange interface. *In particular, tabulated results* ~~Appendix 2.AE presents results~~ for seals and lid bolts *are examined*. The output results for each load combination indicate that all seal springs remain closed (i.e. the loading in the elements representing the seal remains compressive) indicating that the sealworthiness of the bolted joint will not be breached *during normal heat conditions of transport*.

Each load combination *results in a report* ~~reported in Appendix 2.AE lists~~ the total compressive force on the closure plate-overpack interface as well as the total tangential force (labeled as "friction force" ~~in the tables~~). If the ratio "total friction force/total compressive force" is formed for each set of results, the maximum value of the ratio is 0.219. There will be no slip of the closure plate relative to the overpack if the interface coefficient of friction is greater than the value given above. Mark's Handbook for Mechanical Engineers [3.4.9] in Table 3.2.1 shows $\mu_s = 0.74-0.79$ for clean and dry steel on steel surfaces. Therefore, it is concluded that there is no propensity for relative movement.

Based on the results of the finite element analysis for normal heat conditions of transport, the following conclusions are reached.

No bolt overstress is indicated under any loading event associated with normal conditions of transport. This confirms the results of *alternate* closure bolt analyses, performed *in accordance with NUREG/CR-6007 UCRL-ID-110637, "Stress Analysis of Closure Bolts for Shipping Casks", by Mok, Fischer, and Hsu, LLL, 1993.* ~~in Appendix 2.U.~~

The closure plate seals do not unload under any load combination; therefore, the seals continue to perform their function.

- Stress and Stability Results from Miscellaneous Component Analyses in Subsection 2.6.1.3

Tables 2.6.10 and 2.6.11 repeat summary results from additional analyses described and reported on in Subsection 2.6.1.3 for components of the MPC and the overpack. ~~The results have been listed within the text of Subsection 2.6.1.3 or within appendices.~~ The safety factors are summarized in this subsection in accordance with the requirements of Regulatory Guide 7.9. The tables report comparisons of calculated values with allowable values for both stress and stability and represent a compilation of *miscellaneous* analyses ~~detailed in appendices that form an integral part of this chapter.~~

- Overpack Internal Pressure Test

The overpack is considered as an ASME pressure vessel. A hydrostatic test of the overpack under 1.5 times internal pressure must result in no stresses in excess of the material yield strength at room temperature to meet the requirement of 10CFR71.85(b). In the following, ~~we present~~ the necessary results to support ~~the our~~ conclusion that the HI-STAR 100 transport containment boundary meets the requirement ~~are presented~~. Table 2.3.4 gives the material yield strengths of SA350 LF3 and SA 203-E as 37.5 ksi and 40.0 ksi, respectively, at 100 degrees F. ~~Table 2.AE.5 includes stress results for the components of the containment boundary under internal pressure.~~ A survey of the safety factors for the containment boundary reported in Table 2.6.9 gives the following minimum safety factors:

CONTAINMENT BOUNDARY SAFETY FACTORS - Internal Pressure	
Item	Safety Factor
Lid	2.87
Inner Shell	12.1
Baseplate	11.2

These safety factors are determined using allowable stress intensities at the reference temperatures listed in Table 2.1.21 ~~that which~~ are less than the yield stress for the corresponding material at room temperature. From the large safety factors in the above table, ~~it we isean~~ concluded, without further analysis, that an increase in the internal pressure by 50% will not cause stresses in the containment boundary to exceed the material yield stress.

- Summary of Minimum Safety Factors for Normal Heat Conditions of Transport

Tables 2.6.2 through 2.6.4 present a concise summary of safety factors for the fuel basket, the enclosure vessel, and the overpack, respectively. Locations within this SAR from which the summary results are culled are also indicated in the above tables.

Based on the results of all analyses, with results presented or summarized in the text *and in tables*, ~~in tabular form, and in appendices~~, *it is we concluded* that:

- i. All safety factors reported in the text, *and in the summary tables*, ~~and in appendices~~ are greater than 1.0.
- ii. There is no restraint of free thermal expansion between component parts of the HI-STAR 100 System.

Therefore, the HI-STAR 100 System, under the normal heat conditions of transport, has adequate structural integrity to satisfy the subcriticality, containment, shielding, and temperature requirements of 10CFR71.

2.6.2 Cold

The Normal Cold Condition of Transport assumes an ambient environmental temperature of -20 degrees Fahrenheit and maximum decay heat. A special condition of extreme cold is also defined where the system and environmental temperature is at -40 degrees F and the system is exposed to increased external pressure with minimum internal pressure. A discussion of the resistance to failure due to brittle fracture is provided in Subsection 2.1.2.3.

The value of the ambient temperature has two principal effects on the HI-STAR 100 storage system, namely:

- i. The steady-state temperature of all material points in the cask system will go up or down by the amount of change in the ambient temperature.
- ii. As the ambient temperature drops, the absolute temperature of the contained helium will drop accordingly, producing a proportional reduction in the internal pressure in accordance with the Ideal Gas Law.

In other words, the temperature gradients in the cask system under steady-state conditions, will remain the same regardless of the value of the ambient temperature. The internal pressure, on the other hand, will decline with the lowering of the ambient temperature. Since the stresses under normal transport condition arise principally from pressure and thermal gradients, it follows that the stress field in the MPC under a

bounding "cold" ambient would be smaller than the "heat" condition of normal transport, treated in the preceding subsection. Therefore, the stress margins computed in Section 2.6.1 can be conservatively assumed to apply to the "cold" condition as well. ~~Calculations Appendix 2.AL~~ using the methodology outlined in NUREG/CR-6007 UCRL-ID-110637, "Stress Analysis of Closure Bolts for Shipping Casks", by Mok, Fischer, and Hsu, LLL, 1993 demonstrates that the overpack closure bolts will retain the helium seal under the cold ambient conditions.

In addition, allowable stresses generally increase with decreasing temperatures. Safety factors, therefore, will be greater for an analysis at cold temperatures than at hot temperatures. Therefore, the safety factors reported for the hot conditions in Subsection 2.6.1 provide the limiting margins. The overpack, however, is analyzed under cold conditions to ensure that the integrity of the seals is maintained.

As no liquids are included in the HI-STAR 100 System design, loads due to expansion of freezing liquids are not considered.

2.6.2.1 Differential Thermal Expansion

The methodology for determination of the effects of differential thermal expansion in the normal heat condition of transport has ~~ve~~ been presented in Subsection 2.6.1.2. The same methodology is applied to evaluate the normal cold condition of transport.

~~The calculational procedure outlined is presented in Appendices 2.AI and 2.AK for the different fuel baskets, (HI-STAR 100 overpack with MPC 24 and MPC 68, respectively).~~

The results are summarized in the tables given below for normal cold condition of transport.

THERMOELASTIC DISPLACEMENTS IN THE MPC AND OVERPACK UNDER COLD TEMPERATURE ENVIRONMENT CONDITION				
CANISTER - FUEL BASKET				
	Radial Direction (in.)		Axial Direction (in.)	
Unit	Initial Clearance	Final Gap	Initial Clearance	Final Gap
<i>All PWRs MPC-24</i>	0.1875	0.095	2.0	1.524
<i>BWR MPC-68</i>	0.1875	0.101	2.0(min)	1.554 (min)
CANISTER - OVERPACK				
	Radial Direction (in.)		Axial Direction (in.)	
Unit	Initial Clearance	Final Gap	Initial Clearance	Final Gap
<i>All PWRsMP C-24</i>	0.09375	0.069	0.625	0.487
<i>BWRMPC-68</i>	0.09375	0.071	0.625	0.497

It can be verified by referring to the Design Drawings provided in Section 1.4 of this report, and the foregoing table, that the clearances between the MPC basket and canister structure, as well as those between the MPC shell and overpack inside surface, are sufficient to preclude a temperature induced interference from the thermal expansions listed above.

It is We concluded that the HI-STAR 100 package meets the requirement that there be no restraint of free thermal expansion that would lead to development of primary stresses under normal cold conditions of transport.

2.6.2.2 MPC Stress Analysis

The only significant load on the MPCs under cold conditions arises from the postulated 1-foot side drop. Since the allowable stress intensities are higher under the extreme cold condition, results for the MPCs are bounded by the analysis for heat; no additional solutions need to be considered. Since the MPCs are constructed of austenitic stainless steel, there is no possibility of a brittle fracture occurring in any of the MPCs

2.6.2.3 Overpack Stress Analysis

Table 1 of NRC Regulatory Guide 7.8 [2.1.2] mandates load cases at the extreme cold temperature. The overpack may not be bounded by the results of the heat condition load cases for these following conditions:

- increased external pressure with minimum internal pressure, and extreme cold at –40 degrees F.
- minimal internal pressure plus 1 foot drop with extreme cold condition at –20 degrees F.
- rapid ambient temperature change during normal condition of transport (note that this case is not explicitly listed as a load case in Regulatory Guide 7.8).

The first two bulleted items are presented in Table 2.1.8; the results of those analyses are presented here. Structural evaluation for the last bulleted item is performed in this subsection. The structural evaluation uses inputs from thermal transient analyses performed and reported in Chapter 3 subsection 3.4.3.1.

Results of finite element analyses for increased external pressure with minimum internal pressure, and for minimum internal pressure plus 1 foot drop (Load Cases 2 and 4 in Table 2.1.8)

Safety factors for Load Cases 2 and 4 in Table 2.1.8 are computed from the results *tabulated from the archived finite element analyses summarized in Appendix 2.AE, Tables 2.AE.6 and 2.AE.8.* Table 2.6.12 summarizes the safety factors obtained. The finite element analyses does not clearly elucidate the effect of temperature on bolt preload. *Separate calculations, using the methodology outlined in NUREG/CR-6007 UCRL-ID-110637, "Stress Analysis of Closure Bolts for Shipping Casks", by Mok, Fischer, and Hsu, LLL, 1993 Appendix 2.AL* analyzes the closure bolts under extreme cold ambient condition plus pressure and provides the appropriate change in bolt preload expected from operation at the extreme low temperature. A small decrease from the initial preload stress in the bolt results from this operating condition.

The computed change in stress due to the assumption of a severe local low temperature condition is insignificant compared to the initial bolt stress and to the change in the allowable bolt stress because of the lowered temperature. ~~We note that the bolt structural analyses in Appendix 2.U performed for normal heat conditions of transport used bolt allowable stresses at a temperature of 400 degrees F (see Table 2.3.5).~~ It

is ~~We~~ concluded that the small change in bolt preload stress has no effect on structural calculations and safety factors.

The overpack load cases for normal conditions of transport described for the hot condition are re-analyzed for the cold condition in accordance with the requirements of Regulatory Guide 7.9. Since higher allowable stresses apply to the overpack components, it is not expected that the re-analyses will result in lower safety factors than have been already reported for the heat condition. The purpose of the analyses is to demonstrate that the overpack seals remain intact under the cold condition. The results of the analyses for normal cold conditions of transport are presented in Tables 2.AE.1 through 2.AE.8 of Appendix 2.AE (and are summarized in Tables 2.6.12 and 2.6.13).

Stress Analysis for Rapid Lowering of Ambient Temperature from 100 degrees F to -40 degrees F (Load Case 5 in Table 2.1.8)

During transportation, the HI-STAR 100 packaging may experience changes in the ambient temperature. Since the HI-STAR 100 packaging is a passive heat rejection device, a change in the ambient temperature has a direct influence on the temperature of its metal parts. In the preceding sub-sections, all structural integrity evaluations have focused on the steady state thermal conditions using 100°F and -40°F as the limiting upper and lower ambient steady state values. In this sub-section, the structural consequences of a rapid change from the hot (100°F) to cold (-40°F) ambient condition is considered. This scenario is labelled as ASME Code Service Condition A, which requires that the range of primary plus secondary stress intensity must be less than $3 S_m$ (S_m = allowable stress intensity at the mean metal temperature). The loadings assumed to exist coincidentally with the thermal stresses from the transient event are: (i) overpack internal design pressure, P_i ; and (ii) the inertial deceleration load during transport (10g's). The primary plus secondary stress intensity range from the simultaneous action of internal pressure, axial g-load (10 g's), and thermal transient must be shown to be less than $3S_m$.

It should be noted that the reverse transient (i.e. rapid change from cold to hot will produce a less severe thermal stress gradient. Therefore, the magnitudes of the results of a "rapid cooldown" event bound the event".

To perform a bounding evaluation, it is necessary to identify the material locations on the overpack where the thermal stresses are apt to be most adverse. The thick top forging, which is directly exposed to the ambient air during transport is clearly a candidate location. The other location is the planar cross section of the overpack at approximately mid-height where the heat emission rate from the SNF is at its maximum. These locations are identified in Figure 3.4.24 and further explained in sub-section 3.4.3.

To evolve thermal gradient results for the postulated rapid ambient temperature change, a transient temperature problem is formulated and solved in Chapter 3. The thermal problem and finite element model are fully articulated in Chapter 3 (Subsection 3.4.3.1) where a three-dimensional thermal transient analysis of the HI-STAR 100 Package is performed under a postulated rapid drop in ambient temperature (100

degree F to -40 degree F in one hour). The design basis decay heat load is imposed throughout the time span of the transient solution. The temperature profiles through the wall of the overpack and the top forging are determined as functions of time and the change in thermal gradient through the wall of the sections are documented in Chapter 3, Figures 3.4.25-3.4.27. These locations are limiting since there is direct exposure to the ambient temperature on the outer surface of these components. It is shown in the figures that the top forging experiences a change in through-wall thermal gradient of less than 2.5 degrees K (4.5 degrees F) and that other sections of the overpack experience an even weaker change in thermal gradient. The finite element analyses for normal conditions of transport report results and safety factors for all locations for the normal heat and cold conditions of storage (under assumed steady state thermal conditions). The following additional calculation provides the stress state due to the maximum through-wall thermal gradient in the top forging. This stress state is then combined with the stresses from other load cases and stress intensities formed.

Based on the results from the thermal solutions, the material properties for this calculation are obtained for a metal temperature of 150 degrees F. For the top forging material, the Young's Modulus, E, and the coefficient of linear thermal expansion, α , are (at 150 degrees F):

$$E = 27,400,000 \text{ psi}$$

$$\alpha = 6.405 \times 10^{-6} \text{ inch/inch-degree F}$$

As reported in sub-section 3.4.3.1, the maximum change in temperature difference in the top forging material is 4.5°F. The ASME Code, (paragraph NB-3222.4(a)(4)) defines a significant temperature change ΔT_s as

$$\Delta T_s = S/2E\alpha$$

Where S is the value of S_a from the applicable design fatigue curve for 1 million cycles. For the forging material, $S = 18,900$ psi, which yields

$$\Delta T_s = 18,900 / (2 \times 27,400,000 \times 0.00000641) = 53.9 \text{ }^\circ\text{F}$$

It therefore follows that the metal temperature gradient change produced by the rapid cooldown (or heat up event) does not lead to a significant stress adder. Nevertheless, ~~we proceed to quantify~~ the factor of safety under this loading condition *is quantified*.

The linear temperature profile gives a linear stress distribution through the wall thickness with compressive stresses at the inside surface of the top forging. The magnitude of the stress due to the maximum thermal gradient is:

$$\Delta\sigma = E\alpha(\Delta T)/(2(1-\nu))$$

For $\Delta T = (4.5 \text{ degrees F (change)} + 1.5 \text{ degrees F (initial)})$ and $\nu = 0.3$, the stress intensity is computed as:

$$\Delta\sigma = 752 \text{ psi}$$

This stress is now combined with transport longitudinal stress from a 10g deceleration plus longitudinal stress from the normal condition internal pressure. These stresses are computed below:

Pressure stress:

$$\begin{aligned} p &= 100 \text{ psi (internal pressure per Table 2.1.1)} \\ \text{inside radius of top forging} &= a = 34.375'' \\ \text{outside radius of top forging} &= b = 41.625'' \text{ (away from shear ring)} \end{aligned}$$

The magnitude of the longitudinal and circumferential stresses at the inside surface is

$$\sigma_x = (a^2/(b^2 - a^2))p = 2.14 \times p = 214 \text{ psi}$$

$$\sigma_h = ((a^2 + b^2)/(b^2 - a^2))p = 5.289 \times p = 529 \text{ psi}$$

Axial stress from deceleration:

The package weight = 282,000 lb. (Table 2.2.4)

The direct stress due to the axial deceleration is

$$\sigma_d = 10g \times 282,000 \text{ lb/Area} \quad \text{where the cross-section area is Area} = 1731 \text{ sq. inch}$$

Therefore,

$$\sigma_d = 1,629 \text{ psi}$$

Adding the absolute values of the stresses (for conservatism), the maximum surface stress intensity is

$$SI = (\sigma_d + \sigma_x + \Delta\sigma) + p = 2,695 \text{ psi}$$

This value is compared against 3 x the allowable stress intensity since it involves a secondary thermal stress. From Table 2.1.13, the allowable primary plus secondary stress intensity is

$$SI(\text{allowable}) = 3 \times \text{allowable membrane stress intensity} = 69,100 \text{ psi}$$

The safety factor is $69,100/2,695 = 25.64$

Therefore, the HI-STAR 100 overpack is shown to meet the level A stress intensity limits under the rapid ambient temperature change event with a large margin of safety.

Conclusions

Based on the results of the finite element analysis and the calculations carried out within this subsection, the following conclusions are reached for normal cold conditions of transport:

- No bolt yielding is indicated under any loading event.
- The closure plate seal springs do not unload under any load combination; therefore, the seals continue to perform their function.
- The postulated rapid drop in the ambient temperature from hot (-100 degrees F) to cold (-40 degrees F) conditions of transport has no appreciable effect on the stress intensities in the transport overpack. The top forging will experience a small increase in through-wall thermal gradient. Calculations show that the change in thermal stress induced by this through-wall thermal gradient is small; large safety factors are calculated when the secondary thermal stress is combined with the pressure stress and the longitudinal transport stress.

Relative movement between the top flange and the top closure lid has been examined for the normal cold condition of transport. Each load combination reported in ~~Appendix 2.AE provides lists~~ the total compressive force on the lands as well as the total tangential force on the lands (~~labeled as "friction force" in the tables~~). If the ratio "total friction force/total compressive force" is formed for each set of results appropriate to the cold condition of normal transport, the maximum value of the ratio is 0.138. There will be no slip of the closure plate relative to the overpack if the coefficient of friction is greater than the value given above. Mark's Handbook for Mechanical Engineers [2.6.2] shows $\mu = 0.74-0.79$ for clean and dry steel on steel surfaces. Therefore, it is concluded that there is no propensity for relative movement.

Since the results show that all safety factors are greater than 1.0, ~~it is~~ we concluded that the HI-STAR 100 System under the normal cold conditions of transport has adequate structural integrity to satisfy the subcriticality, containment, shielding, and temperature requirements of 10CFR71.

2.6.3 Reduced External Pressure

The effects of a reduced external pressure equal to 3.5 psia, which is required by USNRC Regulatory Guide 7.8 [2.1.2], are bounded by the effects of the accident internal pressure for the overpack (Table 2.1.1). This is considered in Subsection 2.7 for the overpack inner shell. This case does not provide any

bounding loads for other components of the overpack containment boundary. Therefore, the only additional analysis- performed here to demonstrate package performance for this condition is an analysis of the outer enclosure shell panels.

Under this load condition, the outer enclosure shell panels (see Section 1.4, Drawing 1399, sheet 2) deform as long plates under the 3.5 psi pressure that tends to deform the panels away from the neutron absorber material. The stress developed in this situation can be determined by considering the panel as a clamped beam subject to lateral pressure. ~~The~~ Using appropriate dimensions are the dimensions from the drawing, we have:

L = unsupported width of panel = 7.875"

t = panel thickness (from Bill of Materials in Section 1.4) = 0.5"

p = differential pressure = 3.5 psi

The stress is computed from classical strength of materials beam theory as:

$$\sigma = 0.5p \left(\frac{L}{t} \right)^2$$

Substituting the numerical values gives the stress as 434 psi. From Table 2.1.15, the allowable stress is 26.3 ksi for this condition. Therefore, the safety factor is

$$SF = 60.6$$

Clearly, this event is not a safety concern for package performance.

2.6.4 Increased External Pressure

The effects of an external pressure equal to 20 psia on the package, which is required by USNRC Regulatory Guide 7.8 [2.1.2], are bounded by the effects of the large value for the design external pressure specified for the hypothetical accident (Table 2.1.1). Instability of the overpack shells is examined in Section 2.7. Therefore, no additional analyses need be performed here to demonstrate package performance.

2.6.5

Vibration

During transport, vibratory motions occur which could cause low-level stress cycles in the system *due to beam-like deformations*. If any of the package components have natural frequencies in the flexible range (i.e., below 33 Hz), or near the flexible range, then resonance may amplify the low level input into a significant stress response.

As discussed in Section 2.1, there are no "flexible" *beam-like* members in the HI-STAR 100 MPC. The MPC is a fully welded, braced construction over its entire length and it is fully supported by the overpack during transport. Since the MPC is supported by the overpack, and is itself a rigid structure, any vibration problems would manifest themselves in the fuel basket walls.

It is shown below that the lowest frequency of the fuel basket walls and the overpack, acting as a beam, are well above 33 Hz. Therefore, additional stresses from vibration are not expected.

The lowest frequency of vibration during normal transport conditions will occur due to vibrations of a fuel basket cell wall. ~~Appendix 2.K~~ It is demonstrated that the lowest frequency of the component, computed based on the assumption that there is support sufficient to limit vibration to that representative of a clamped beam, is 658 Hz for a PWR basket and 1,200 Hz for a BWR basket.

These frequencies are significantly higher than the 33 Hz transition frequency for rigidity.

When in a horizontal position, the overpack is ~~continuously supported over a considerable~~ *nearly the entire length of the enclosure shell* supported by two saddle supports. Conservatively ~~considering the HI-STAR MPC as a supported beam at only the two ends of the enclosure shell~~ *midpoint of each saddle support*, and assuming the total mass of the MPC moves with the overpack, an estimate of the lowest material frequency of the structure during transport is in excess of 469 Hz (~~Appendix 2.K~~).

Based on these frequency calculations, ~~it is~~ *we* concluded that vibration effects are minimal and no new calculations are required.

2.6.6

Water Spray

The condition is not applicable to the HI-STAR 100 System per Reg. Guide 7.8 [2.1.2].

2.6.7

Free Drop

The structural analysis of a 1-foot side drop under heat and cold conditions has been performed in Subsections 2.6.1 and 2.6.2 for heat and cold conditions of normal transport. As demonstrated in Subsections 2.6.1 and 2.6.2, ~~and Appendix 2.AE~~, safety factors are well over 1.0.

2.6.8 Corner Drop

This condition is not applicable to the HI-STAR 100 System per [2.1.2].

2.6.9 Compression

The condition is not applicable to the HI-STAR 100 System per [2.1.2].

2.6.10 Penetration

The condition is not applicable to the HI-STAR 100 System per [2.1.2].

Table 2.6.1

FINITE ELEMENTS IN THE MPC STRUCTURAL MODELS

MPC Type Element Type	Model Type		
	Basic	0 Degree Drop	45 Degree Drop
MPC-24	1068942	1179050	1178050
BEAM3	1028898	1028898	1028898
CONTAC12	4036	3834	3834
CONTAC26	0	11007	11008
COMBIN14	0	3	2
MPC-32	766	873	872
BEAM3	738	738	738
CONTAC12	28	27	24
CONTAC26	0	106	105
COMBIN14	0	2	5
MPC-68	1234	1347	1344
BEAM3	1174	1174	1174
PLANE82	16	16	16
CONTAC12	44	43	40
CONTAC26	0	112	111
COMBIN14	0	2	3

Table 2.6.1 Continued

FINITE ELEMENTS IN THE MPC STRUCTURAL MODELS

<i>MPC Type</i>	<i>Model Type</i>		
	<i>Basic</i>	<i>0 Degree Drop</i>	<i>45 Degree Drop</i>
<i>MPC-24E/24EF</i>	<i>1070</i>	<i>1183</i>	<i>1182</i>
<i>BEAM3</i>	<i>1030</i>	<i>1030</i>	<i>1030</i>
<i>CONTAC12</i>	<i>40</i>	<i>38</i>	<i>38</i>
<i>CONTAC26</i>	<i>0</i>	<i>112</i>	<i>112</i>
<i>COMBIN14</i>	<i>0</i>	<i>3</i>	<i>2</i>

Table 2.6.2

MINIMUM SAFETY FACTORS FOR THE MPC FUEL BASKET - NORMAL CONDITIONS OF TRANSPORT

Case Number	Load ¹ Combination	Safety Factor	Location in SAR where Details are Provided
F1	T or T'	NA 3.06	2.6.1.4.12.D-2.G 2.AC (thermal stress)
F2			
F2.a	D+H, 1 ft side drop 0°	1.57	2.AC ; Table 2.6.8
F2.b	D+H, 1 ft side drop 45°	1.291.26	2.AC ; Table 2.6.8

¹ The symbols used for loads are defined in Subsection 2.1.2.1.1.

Table 2.6.3

MINIMUM SAFETY FACTORS FOR THE MPC ENCLOSURE VESSEL - NORMAL CONDITIONS OF TRANSPORT

Case Number	Load Combination ¹	Safety Factor	Location in SAR where Details are Provided or Safety Factors Extracted
E1	E1.a	Design internal pressure, P _i	Lid Baseplate Shell
	E1.b	Design external pressure, P _o	Lid Baseplate Shell
	E1.c	Design internal pressure plus temperature	Base Shell
E2	E2.a	(P _i , P _o) + D + H, 1 ft side drop, 0 deg. ²	
	E2.b	(P _i , P _o) + D + H, 1 ft. side drop, 45 deg. ²	
E4	T or T'	Sections show expansion does not result in restraint of free thermal expansion	

¹ The symbols used for loads are defined in Subsection 2.1.2.1.1.

Table 2.6.4

MINIMUM SAFETY FACTORS FOR OVERPACK FOR NORMAL CONDITION OF TRANSPORT

Case Number	Load Combination ¹	Safety Factor	Location in SAR where Details are Provided
1	$T_h + P_i + F + W_s$	1.651.53	Table 2.6.59
2	$T_s + P_o + F + W_s$	3.383.37	Table 2.6.132
3	$T_h + D_{sn} + P_i + F + W_s$	1.681.44	Table 2.6.9
4	$T_c + D_{sn} + P_o + F + W_s$	2.412.97	Table 2.6.132

¹ The symbols used here are defined in Subsection 2.1.2.1.1.

Table 2.6.5

MINIMUM SAFETY FACTORS INCLUDING FABRICATION STRESSES - PRIMARY PLUS SECONDARY
STRESS INTENSITY, NORMAL HEAT CONDITIONS OF TRANSPORT

Case	Inner Shell Exterior Surface	Intermediate Shell
1- (Tables 2.AE.1, 2.AE.5) Internal pressure	1.65	4.12
3 (Tables 2.AE.3, 2.AE.7) 1 ft. Side Drop	1.70	2.42

Note: Thermal stresses are included for inner containment shell per ASME Section III, Subsection NB, but excluded in intermediate shell per ASME Code, Section III, Subsection NF.

Table 2.6.6
STRESS INTENSITY RESULTS FOR CONFINEMENT BOUNDARY -
INTERNAL PRESSURE ONLY (Load Case E1.a in Table 2.1.7)

Component Locations (Per Fig. 2.6.20)	Calculated Value of Stress Intensity(psi)	Category	Table 2.1.19 Allowable Value (psi) [†]	Safety Factor (Allowable/Calculated)
<u>Top Lid^{††}</u>				
A	3,282,164	$P_L + P_b$	30,000	9.1418.3
Neutral Axis	40,420.2	P_m	20,000	495990.1
B	3,210,160	$P_L + P_b$	30,000	9.3418.7
C	1,374,687	$P_L + P_b$	30,000	21.843.7
Neutral Axis	1,462,731	P_m	20,000	13.627.4
D	5,920,296	$P_L + P_b$	30,000	5.0610.1
<u>Baseplate</u>				
E	19,683	$P_L + P_b$	30,000	1.5
Neutral Axis	412	P_m	20,000	48.5
F	20,528	$P_L + P_b$	30,000	1.5
G	9,695	$P_L + P_b$	30,000	3.1
Neutral Axis	2,278	P_m	20,000	8.8
H	8,340	$P_L + P_b$	30,000	3.5

[†] Stress intensity taken at 300 degrees F in this comparison.

^{††} The stresses in the top lid are reported for the dual lid configuration. The stresses for the single lid configuration are 50% less (see Subsection 2.6.1.3.1.2 for further details).

Table 2.6.6 Continued
 STRESS INTENSITY RESULTS FOR CONFINEMENT BOUNDARY -
 INTERNAL PRESSURE ONLY (Load Case E1.a in Table 2.1.7)

Component Locations (Per Fig.2.6.20)	Calculated Value of Stress Intensity (psi)	Category	Table 2.1.19 Allowable Value (psi) [†]	Safety Factor (Allowable/Calculated)
<u>Canister</u>				
I	6,860	P _m	18,700	2.72
Upper Bending Boundary Layer Region	7,189	P _L + P _b + Q	30,000	4.2
	7,044	P _L + P _b	20,000	2.8
Lower Bending Boundary Layer Region	43,986	P _L + P _b + Q	60,000	1.36
	10,621	P _L + P _b	30,000	2.82

† Allowable stress intensity conservatively based at 300 degrees F except for Location I where allowable stress intensity values are based on 400 degree F.

Table 2.6.7

PRIMARY AND SECONDARY STRESS INTENSITY RESULTS FOR
HELIUM RETENTION BOUNDARY - PRESSURE PLUS THERMAL LOADING (Load Case E1.c in Table 2.1.7)

Locations (Per Fig. 2.6.20)	Calculated Value of Stress Intensity (psi)	Category	Table 2.1.19 Allowable Value (psi) [†]	Safety Factor (Allowable/Calculated)
<u>Top Lid^{††}</u>				
A Neutral Axis	4,6342,317	$P_L + P_b + Q$	60,000	12.925.9
B	1,464732	P_L	30,000	20.441.0
C	2,1401,070	$P_L + P_b + Q$	60,000	28.056.1
C Neutral Axis	1,942971	$P_L + P_b + Q$	60,000	30.861.9
D	3,5281,764	P_L	30,000	8.5017.0
	7,0483,524	$P_L + P_b + Q$	60,000	8.5117.0
<u>Baseplate</u>				
E Neutral Axis				
F	22,434	$P_L + P_b + Q$	60,000	2.67
	1,743	P_L	30,000	17.2
G	18,988	$P_L + P_b + Q$	60,000	3.16
G Neutral Axis				
H	5,621	$P_m + P_L$	60,000	10.7
	5,410	P_L	30,000	5.55
	12,128	$P_L + P_b + Q$	60,000	4.95

±

[†] Allowable stresses based on temperature of 300 degrees F.

^{††} The stresses in the top lid are reported for the dual lid configuration. The stresses for the single lid configuration are 50% less (see Subsection 2.6.1.3.1.2 for further details).

Table 2.6.7 Continued

PRIMARY AND SECONDARY STRESS INTENSITY RESULTS FOR
 HELIUM RETENTION BOUNDARY - PRESSURE PLUS THERMAL LOADING (Load Case E1.c in Table 2.1.7)

Locations (Per Fig.2.6.20)	Calculated Value of Stress Intensity (psi)	Category	Table 2.1.19 Allowable Stress Intensity (psi) ¹	Safety Factor (Allowable/Calculated)
<u>Canister</u>				
I	6,897	P _L	28,100	4.07
Upper Bending Boundary Layer Region	6,525 3,351	P _L + P _b + Q P _L	60,000 30,000	9.2 8.95
Lower Bending Boundary Layer Region	40,070 6,665	P _L + P _b + Q P _L	60,000 30,000	1.5 4.5

¹ Allowable stresses based on temperature of 300 degree F except at Location I where the temperatures are based on 400 degrees F.

Table 2.6.8 - FINITE ELEMENT ANALYSIS RESULTS
 MINIMUM SAFETY FACTORS FOR MPC COMPONENTS UNDER NORMAL CONDITIONS

Component - Stress Result	MPC-24		MPC-68	
	1 Ft. Side Drop, 0 deg Orientation	1 Ft. Side Drop, 45 deg Orientation	1 Ft. Side Drop, 0 deg Orientation	1 Ft. Side Drop, 45 deg Orientation
	Load Case F2.a or E2.a	Load Case F2.b or E2.b	Load Case F2.a or E2.a	Load Case F2.b or E2.b
Fuel Basket — Primary Membrane (P_m)	4.123.87 (852) [2.AC.2]	5.645.44 (852) [2.AC.8]	4.42 (1603) [2.AC.52]	6.16 (1603) [2.AC.58]
Fuel Basket - Local Membrane Plus Primary Bending ($P_L + P_b$)	1.731.62 (523) [2.AC.3]	1.871.26 (132) [2.AC.9]	2.42 (793) [2.AC.53]	1.50 (67) [2.AC.59]
Enclosure Vessel - Primary Membrane (P_m)	2.712.70 (1210) [2.AC.4]	2.71 (1232) [2.AC.10]	2.67 (1867) [2.AC.54]	2.72 (1864) [2.AC.60]
Enclosure Vessel - Local Membrane Plus Primary Bending ($P_L + P_b$)	3.302.27 (1237) [2.AC.5]	3.291.97 (1225) [2.AC.11]	2.17 (1816) [2.AC.55]	1.80 (1864) [2.AC.61]
Basket Supports - Primary Membrane (P_m)	N/A5.33 (1079) [2.AC.6]	N/A5.36 (1075) [2.AC.12]	5.33 (1663) [2.AC.56]	5.34 (1680) [2.AC.62]
Basket Supports - Local Membrane Plus Primary Bending ($P_L + P_b$)	N/A8.11 (1079) [2.AC.7]	N/A4.03 (1083) [2.AC.13]	1.67 (1704) [2.AC.57]	2.16 (1649) [2.AC.63]

Notes:

1. Corresponding ANSYS element number shown in parantheses (Appendices 2.W through 2.AB provide element locations).
2. Corresponding appendix table number shown in brackets.

*Table 2.6.8 (Continued) - FINITE ELEMENT ANALYSIS RESULTS
MINIMUM SAFETY FACTORS FOR MPC COMPONENTS UNDER NORMAL CONDITIONS*

<i>Component - Stress Result</i>	<i>MPC-32</i>		<i>MPC-24E/EF</i>	
	<i>1 Ft. Side Drop, 0 deg Orientation Load Case F2.a or E2.a</i>	<i>1 Ft. Side Drop, 45 deg Orientation Load Case F2.b or E2.b</i>	<i>1 Ft. Side Drop, 0 deg Orientation Load Case F2.a or E2.a</i>	<i>1 Ft. Side Drop, 45 deg Orientation Load Case F2.b or E2.b</i>
<i>Fuel Basket - Primary Membrane (P_m)</i>	4.05	5.65	4.05	5.56
<i>Fuel Basket - Local Membrane Plus Primary Bending (P_L + P_b)</i>	1.57	1.29	1.69	1.83
<i>Enclosure Vessel - Primary Membrane (P_m)</i>	2.55	2.69	2.71	2.71
<i>Enclosure Vessel - Local Membrane Plus Primary Bending (P_L + P_b)</i>	1.41	1.63	3.05	3.14
<i>Basket Supports - Primary Membrane (P_m)</i>	3.96	5.33	N/A	N/A
<i>Basket Supports - Local Membrane Plus Primary Bending (P_L + P_b)</i>	3.49	3.12	N/A	N/A

Table 2.6.9 - FINITE ELEMENT ANALYSIS RESULTS
 MINIMUM SAFETY FACTORS FOR OVERPACK COMPONENTS UNDER NORMAL CONDITIONS (Hot Environment)

Component - Stress Result	Hot Environment	1 Ft. Side Drop
	Load Case 1	Load Case 3
Lid - Local Membrane Plus Primary Bending ($P_L + P_b$)	2.87 (501) [2.AE.5]	2.14 (501) [2.AE.7]
Inner Shell - Local Membrane Plus Primary Bending ($P_L + P_b$)	12.1 (280) [2.AE.5]	3.24 (280) [2.AE.7]
Inner Shell - Primary Membrane (P_m)	13.7 (281) [2.AE.5]	3.53 (281) [2.AE.7]
Intermediate Shells - Local Membrane Plus Primary Bending ($P_L + P_b$)	17.3 (282) [2.AE.5]	2.51 (53) [2.AE.7]
Baseplate - Local Membrane Plus Primary Bending ($P_L + P_b$)	11.2 (4) [2.AE.5]	6.28 (27) [2.AE.7]
Enclosure Shell - Primary Membrane (P_m)	35.2 (11031) [2.AE.5]	3.24 (55) [2.AE.7]

Notes:

1. ~~Corresponding ANSYS node number shown in parentheses.~~
2. ~~Corresponding appendix table shown in brackets.~~

Table 2.6.9 (continued) - FINITE ELEMENT ANALYSIS RESULTS

MINIMUM SAFETY FACTORS FOR OVERPACK COMPONENTS UNDER NORMAL CONDITIONS (Hot Environment)

Component - Stress Result	Hot Environment	1 Ft. Side Drop
	Load Case 1	Load Case 3
Lid - Local Membrane Plus Primary Bending Plus Secondary ($P_L + P_b + Q$)	2.14 (479) [2.AE.1]	1.90 (479) [2.AE.3]
Inner Shell - Local Membrane Plus Primary Bending Plus Secondary ($P_L + P_b + Q$)	2.69 (47) [2.AE.1]	2.84 (10790) [2.AE.3]
Intermediate Shells - Local Membrane Plus Primary Bending Plus Secondary ($P_L + P_b + Q$ excluding thermal stress)	34.5 (53) [2.AE.5]	5.01 (10796) [2.AE.7]
Baseplate - Local Membrane Plus Primary Bending Plus Secondary ($P_L + P_b + Q$)	1.81 (27) [2.AE.1]	1.68 (27) [2.AE.3]
Enclosure Shell - Local Membrane Plus Primary Bending Plus Secondary ($P_L + P_b + Q$)	1.97 (55) [2.AE.1]	1.88 (10798) [2.AE.3]

Notes:

1. ~~Corresponding ANSYS node number shown in parentheses.~~
2. ~~Corresponding appendix table shown in brackets.~~

Table 2.6.10

SAFETY FACTORS FROM MISCELLANEOUS MPC CALCULATIONS - NORMAL CONDITIONS OF TRANSPORT - HOT ENVIRONMENT

Item	Loading	Safety Factor	SAR Appendix or Text Location <i>in SAR</i> Where Details are Provided
Fuel Support Spacers	1' Drop (Load Case F2 in Table 2.1.6)	2.76	2.O; Subsection 2.6.1.3.1.3
MPC Stability	Code Case N-284 (Load Case E1.b in Table 2.1.7)	1.2	2.J; Subsection 2.6.1.3.1.3

Table 2.6.11

MINIMUM SAFETY FACTORS FROM MISCELLANEOUS OVERPACK CALCULATIONS
NORMAL HOT CONDITIONS OF TRANSPORT

Item	Loading	Safety Factor	SAR Text or Appendix Location in SAR Where Details are Provided
Fabrication Stress in Inner Shell	Fabrication	4.3	2.Q; Subsection 2.6.1.3.2.2
Closure Bolt	Average Tensile Stress Including Pre-Load	1.441.08	2.U; Subsection 2.6.1.3.2.3

Table 2.6.12 - FINITE ELEMENT ANALYSIS RESULTS

MINIMUM SAFETY FACTORS FOR OVERPACK COMPONENTS UNDER NORMAL CONDITIONS (Cold Environment)

Component - Stress Result	Super-Cold Environment	1 Ft. Side Drop
	Load Case 2	Load Case 4
Lid - Local Membrane Plus Primary Bending ($P_L + P_b$)	4.55 (501) [2.AE.6]	2.97 (501) [2.AE.8]
Inner Shell - Local Membrane Plus Primary Bending ($P_L + P_b$)	14.4 (280) [2.AE.6]	3.37 (280) [2.AE.8]
Inner Shell - Primary Membrane (P_m)	16.5 (11024) [2.AE.6]	3.53 (48) [2.AE.8]
Intermediate Shells - Local Membrane Plus Primary Bending ($P_L + P_b$)	21.7 (282) [2.AE.6]	2.48 (53) [2.AE.8]
Baseplate - Local Membrane Plus Primary Bending ($P_L + P_b$)	722.8 (1) [2.AE.6]	7.84 (1) [2.AE.8]
Enclosure Shell - Primary Membrane (P_m)	50.2 (5661) [2.AE.6]	3.21 (55) [2.AE.8]

Notes:

1. Corresponding ANSYS node number shown in parentheses.
2. Corresponding appendix table shown in brackets.

Table 2.6.12 (continued)

FINITE ELEMENT ANALYSIS RESULTS
 MINIMUM SAFETY FACTORS FOR OVERPACK COMPONENTS UNDER NORMAL CONDITIONS (Cold Environment)

Component - Stress Result	Super-Cold Environment	1 Ft. Side Drop
Lid - Local Membrane Plus Primary Bending Plus Secondary ($P_L + P_b + Q$)	Load Case 2 8.79 (\$04) [2.AE.2]	Load Case 4 5.79 (\$04) [2.AE.4]
Inner Shell - Local Membrane Plus Primary Bending Plus Secondary ($P_L + P_b + Q$)	15.5 (10792) [2.AE.2]	6.36 (49) [2.AE.4]
Intermediate Shells - Local Membrane Plus Primary Bending Plus Secondary ($P_L + P_b + Q$ excluding thermal stress)	43.24 (10792) [2.AE.6]	4.95 (\$3) [2.AE.8]
Baseplate - Local Membrane Plus Primary Bending Plus Secondary ($P_L + P_b + Q$)	83.8 (+) [2.AE.2]	15.1 (+) [2.AE.4]
Enclosure Shell - Local Membrane Plus Primary Bending Plus Secondary ($P_L + P_b + Q$)	21.4 (\$5) [2.AE.2]	7.67 (\$5) [2.AE.4]

Notes:

1. Corresponding ANSYS node number shown in parentheses.
2. Corresponding appendix table shown in brackets.

Table 2.6.13

MINIMUM SAFETY FACTORS INCLUDING FABRICATION STRESS - PRIMARY PLUS SECONDARY STRESS INTENSITY, NORMAL COLD CONDITIONS OF TRANSPORT

Case	Inner Shell Exterior Surface	Intermediate Shell
2 (Tables 2.AE.2, 2.AE.6) Pressure (Secondary Stress)	3.38	4.22
4 (Tables 2.AE.4, 2.AE.8) 1 ft. Side Drop (Secondary Stress)	2.58	2.41

Note: Thermal stresses are included for inner containment shell per ASME Section III, Subsection NB, but excluded in intermediate shell per ASME Code, Section III, Subsection NF.

Table 2.6.14

MISCELLANEOUS SAFETY FACTOR FOR OVERPACK			
Item	Loading	Safety Factor	<i>Location in SAR Appendix or Text Where Details are Provided/Located</i>
Outer Enclosure Panels	Reduced External Pressure	60.6	Subsection 2.6.3

Temperature Distribution for MPC Thermal Stress Analysis

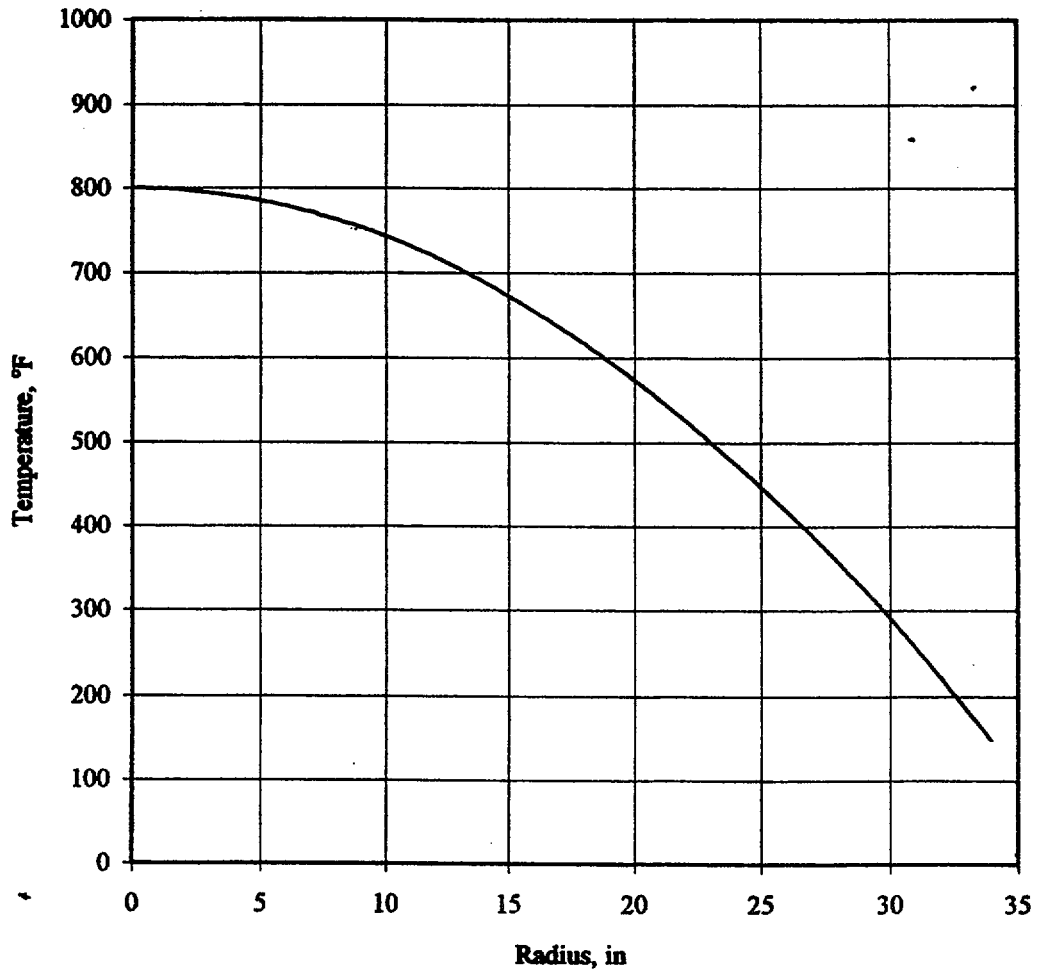


FIGURE 2.6.1; TEMPERATURE DISTRIBUTION FOR MPC THERMAL STRESS ANALYSIS

Temperature Distribution for Overpack Thermal Stress Analysis

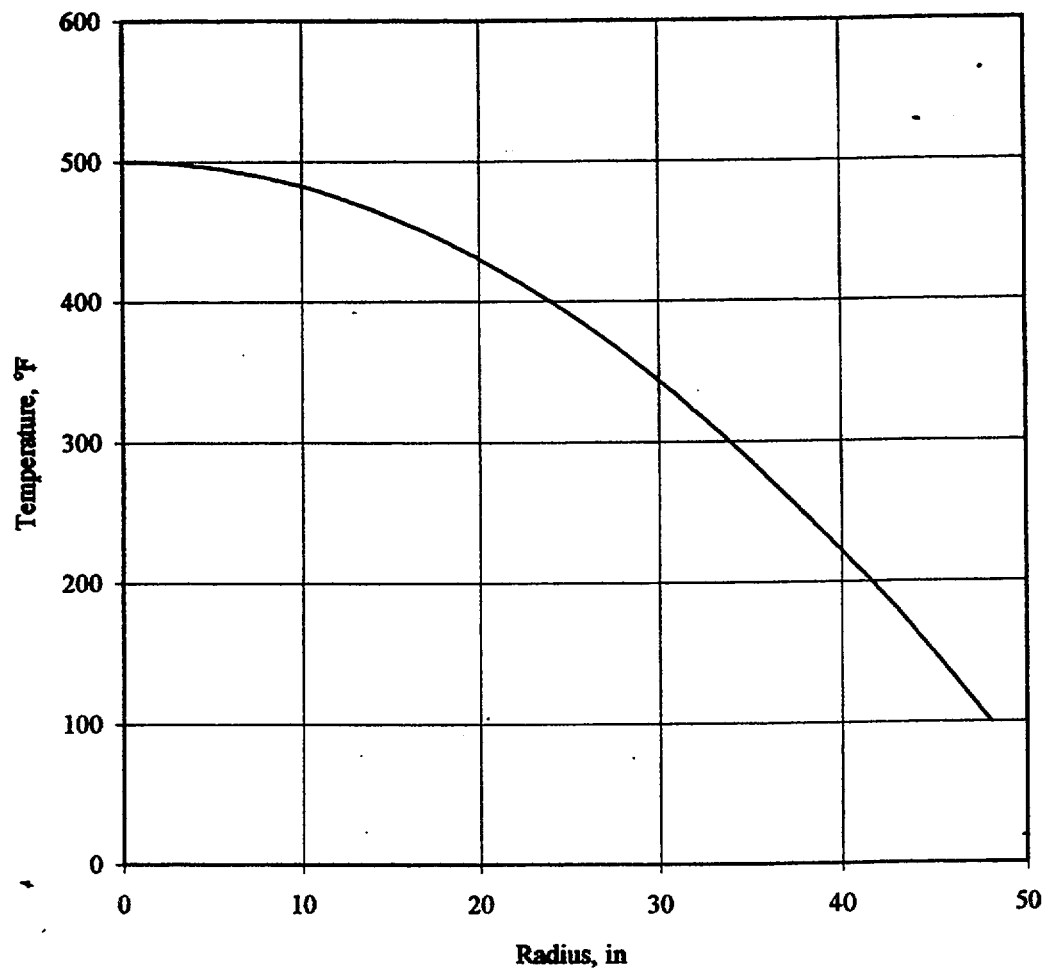
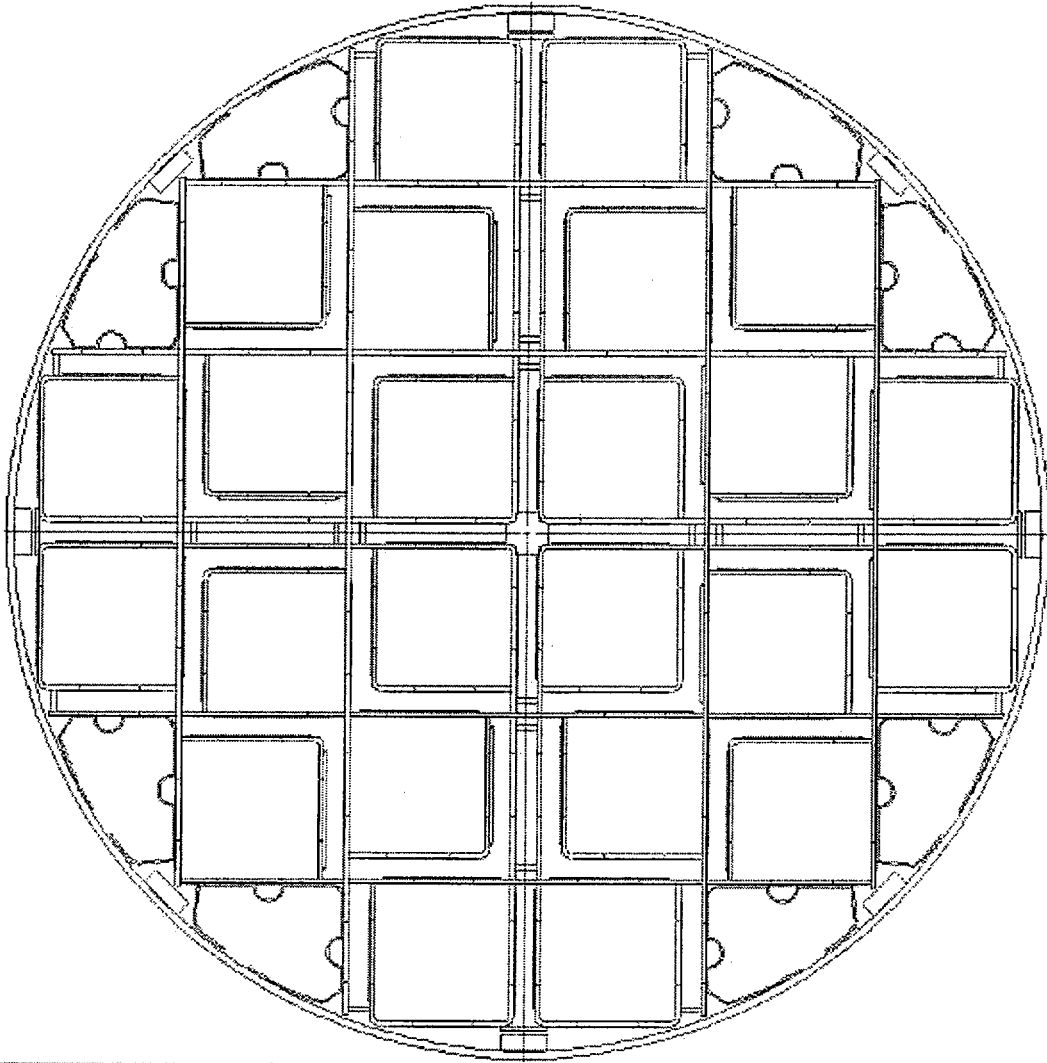
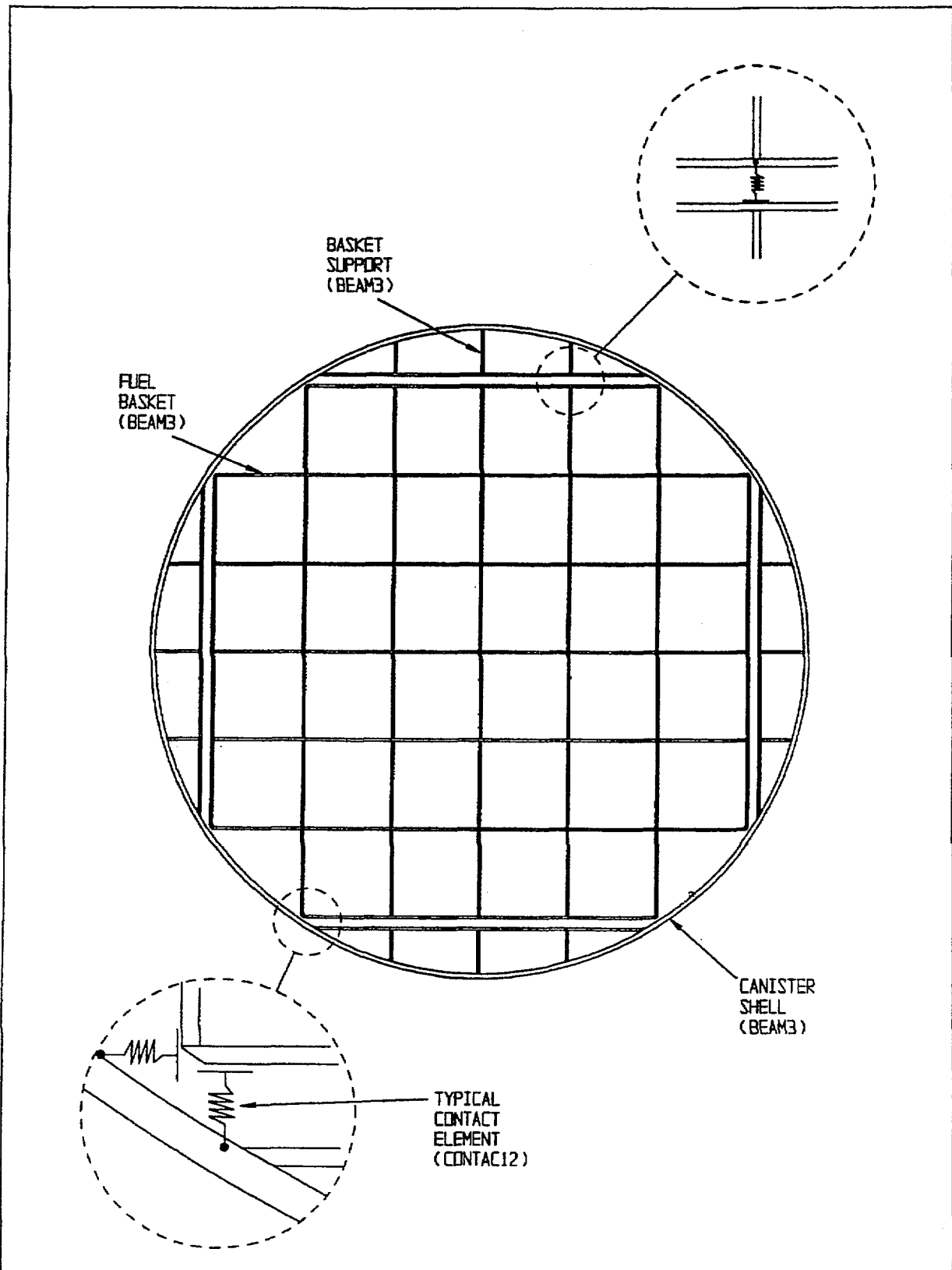


FIGURE 2.6.2; TEMPERATURE DISTRIBUTION FOR OVERPACK THERMAL STRESS ANALYSIS



**FIGURE 2.6.3; FINITE ELEMENT MODEL OF MPC24/24E/24EF
(BASIC CONSTRUCTION)**



**FIGURE 2.6.4; FINITE ELEMENT MODEL FOR MPC-32
(BASIC MODEL)**

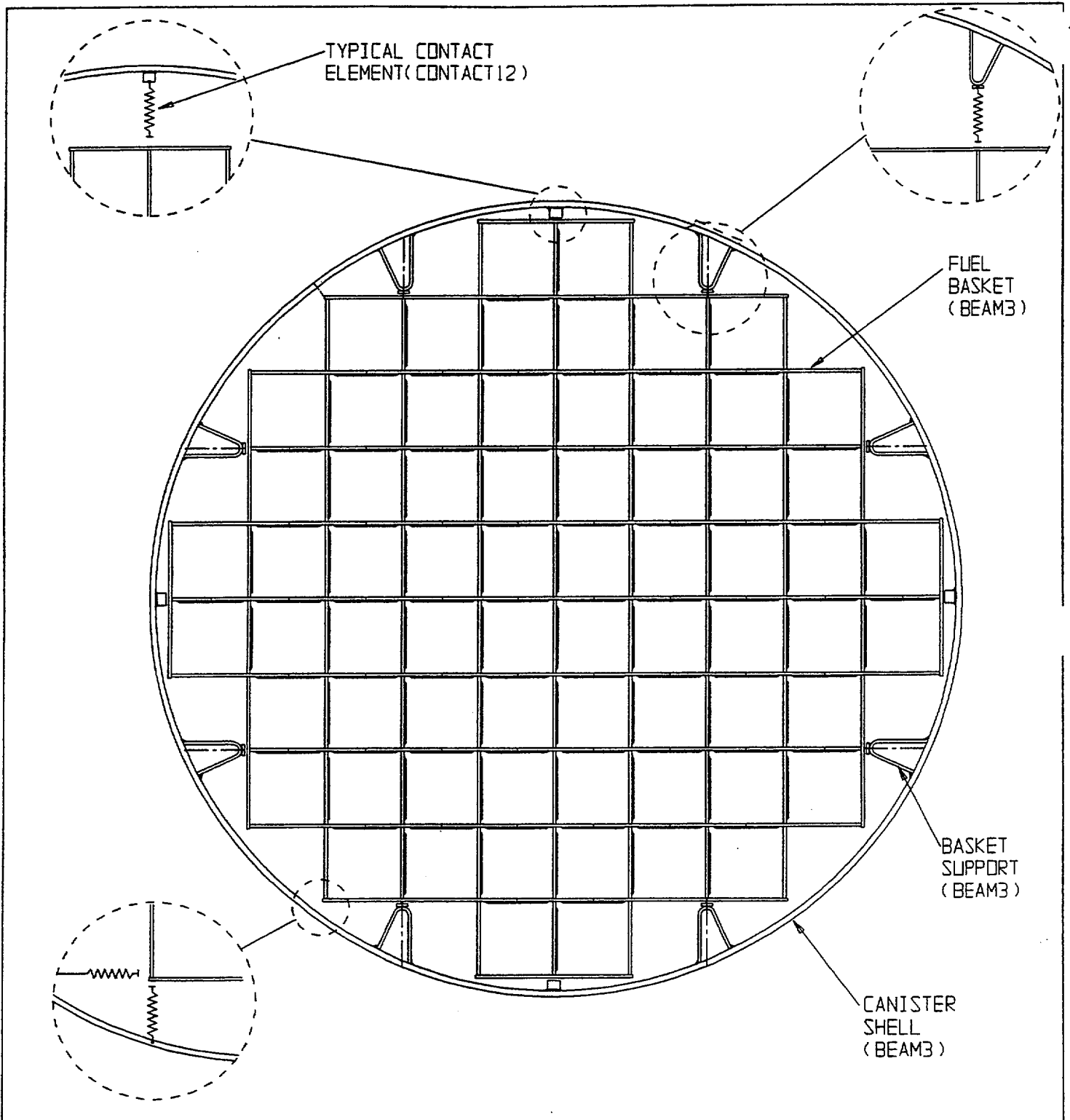
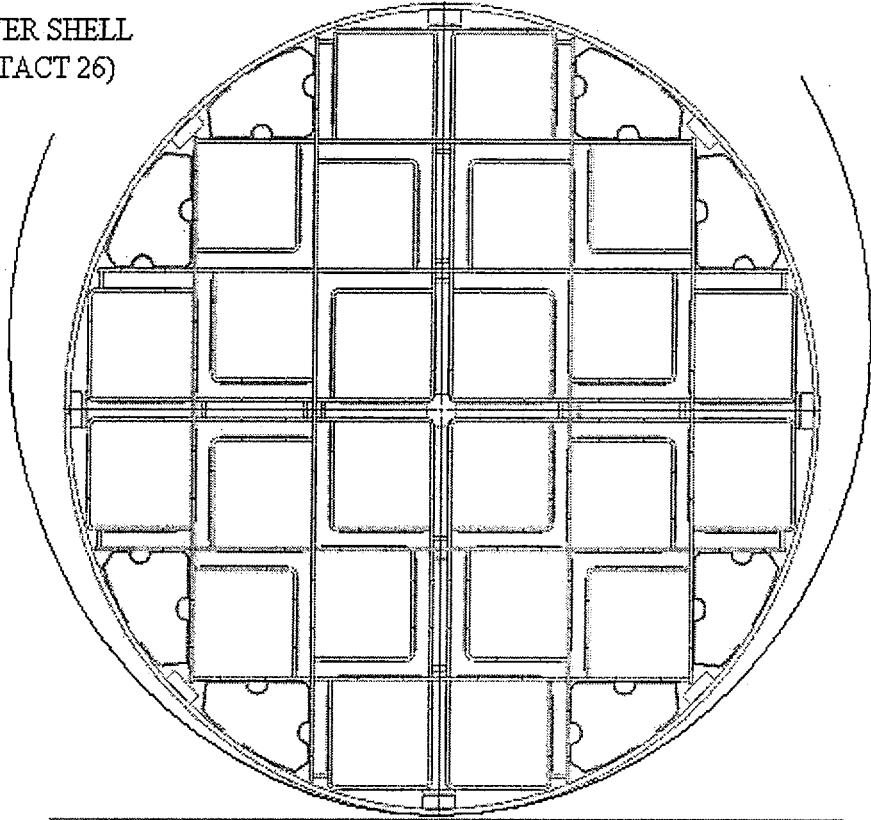


FIGURE 2.6.5; FINITE ELEMENT MODEL OF MPC-68

(BASIC MODEL)

OVERPACK INNER SHELL
SURFACE (CONTACT 26)



**FIGURE 2.6.6; FINITE ELEMENT MODEL OF MPC-24/24E/24EF
(0 DEGREE DROP MODEL)**

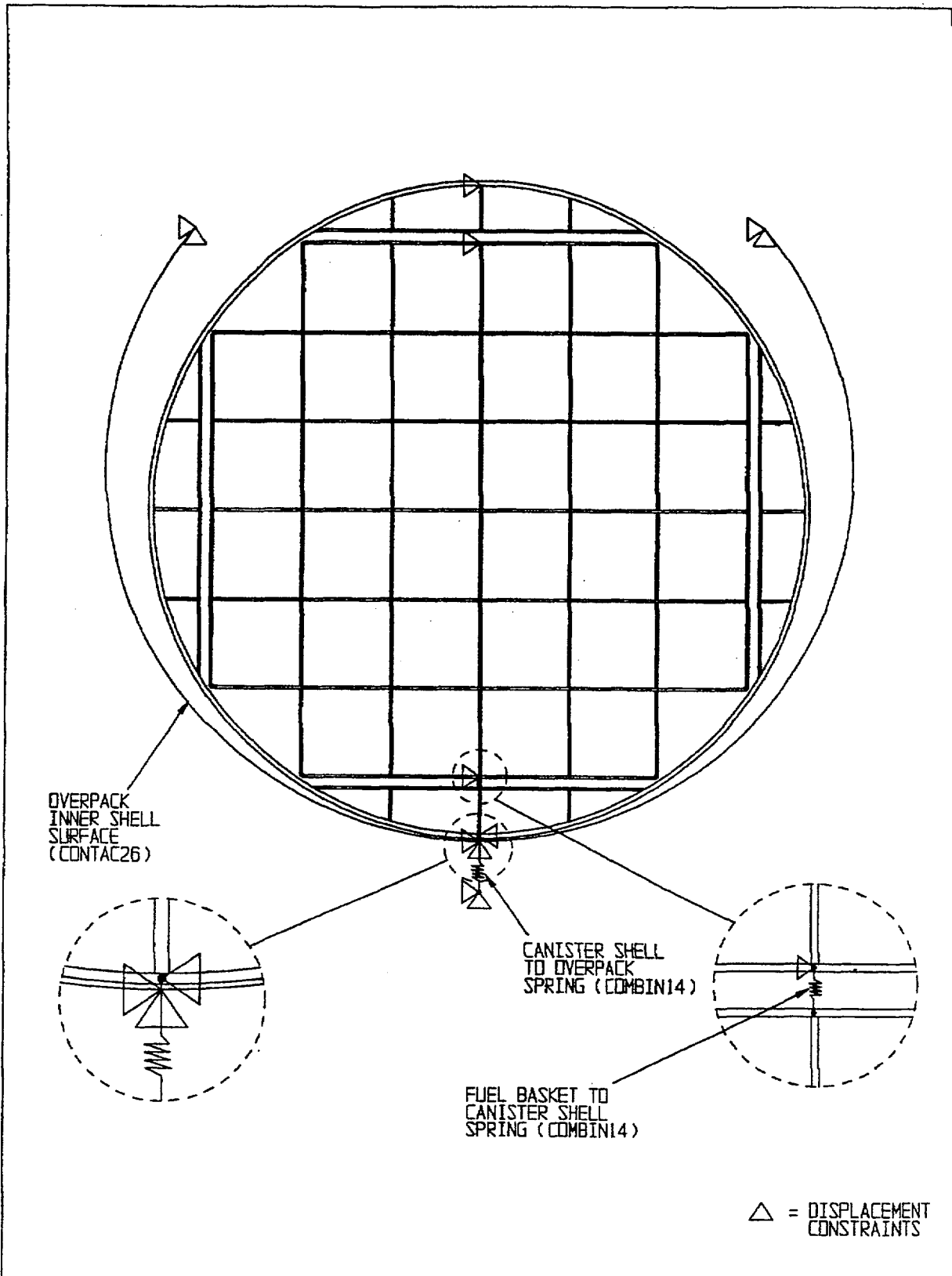
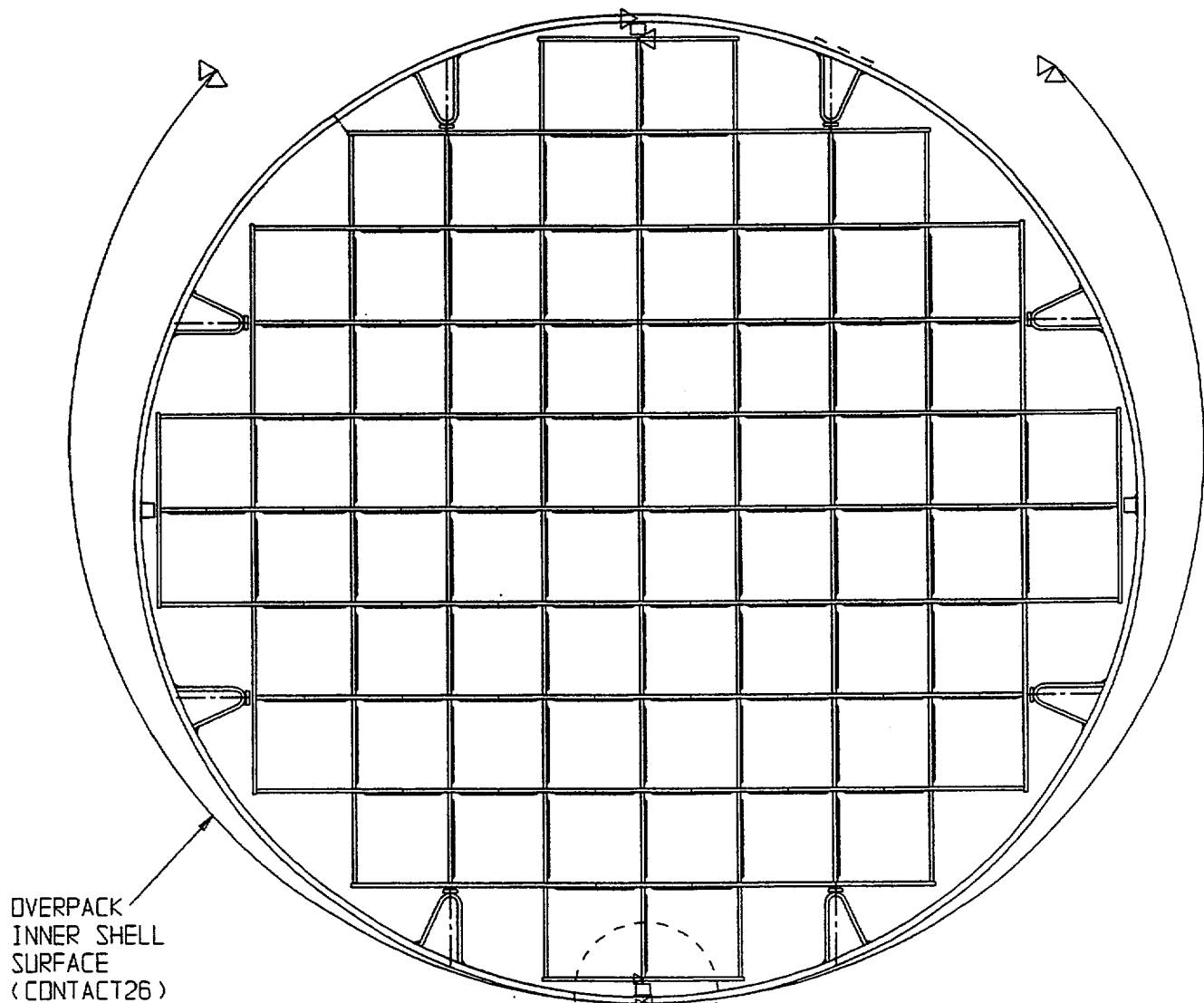
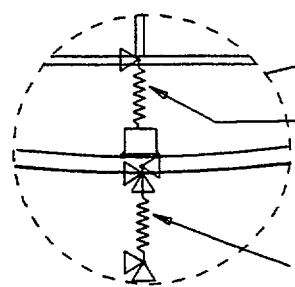


FIGURE 2.6.7; FINITE ELEMENT MODEL FOR MPC-32



OVERPACK
INNER SHELL
SURFACE
(CONTACT26)



FUEL BASKET TO
CANISTER SHELL
SPRING (COMBIN14)

CANISTER SHELL TO
OVERPACK SPRING
(COMBIN14)

△ = DISPLACEMENT
CONSTRAINTS

FIGURE 2.6.8; FINITE ELEMENT MODEL OF MPC-68

(0 DEGREE DROP MODEL)

OVERPACK INNER SHELL
SURFACE (CONTACT 26)

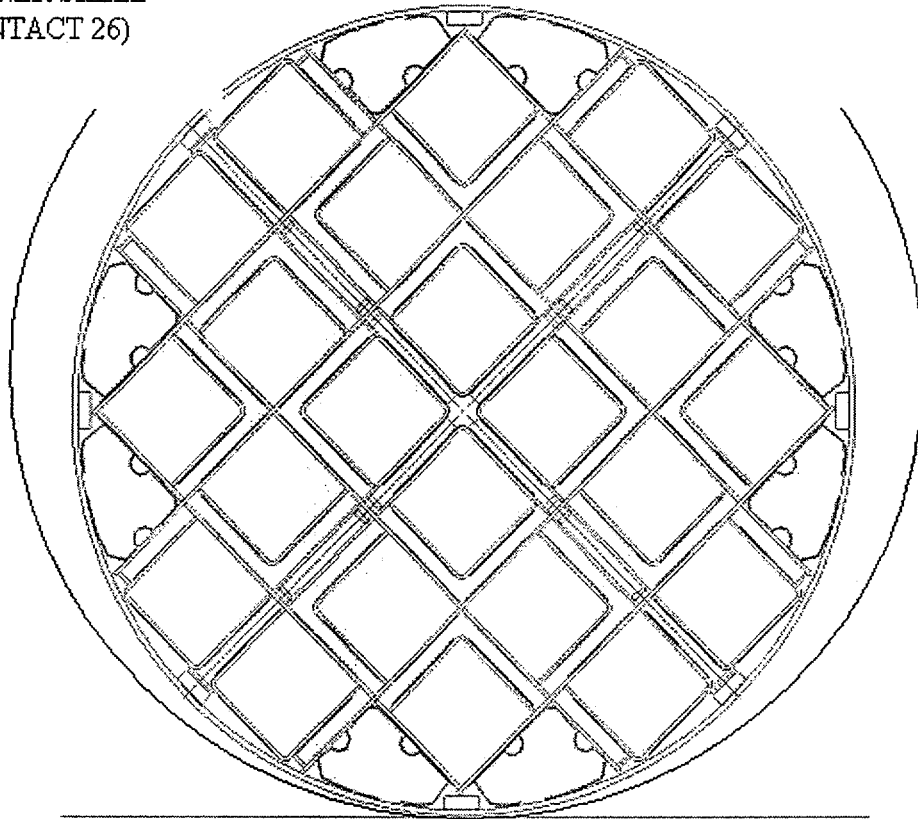


**FIGURE 2.6.9; FINITE ELEMENT MODEL OF MPC-24/24E/24EF
(45 DEGREE DROP MODEL)**

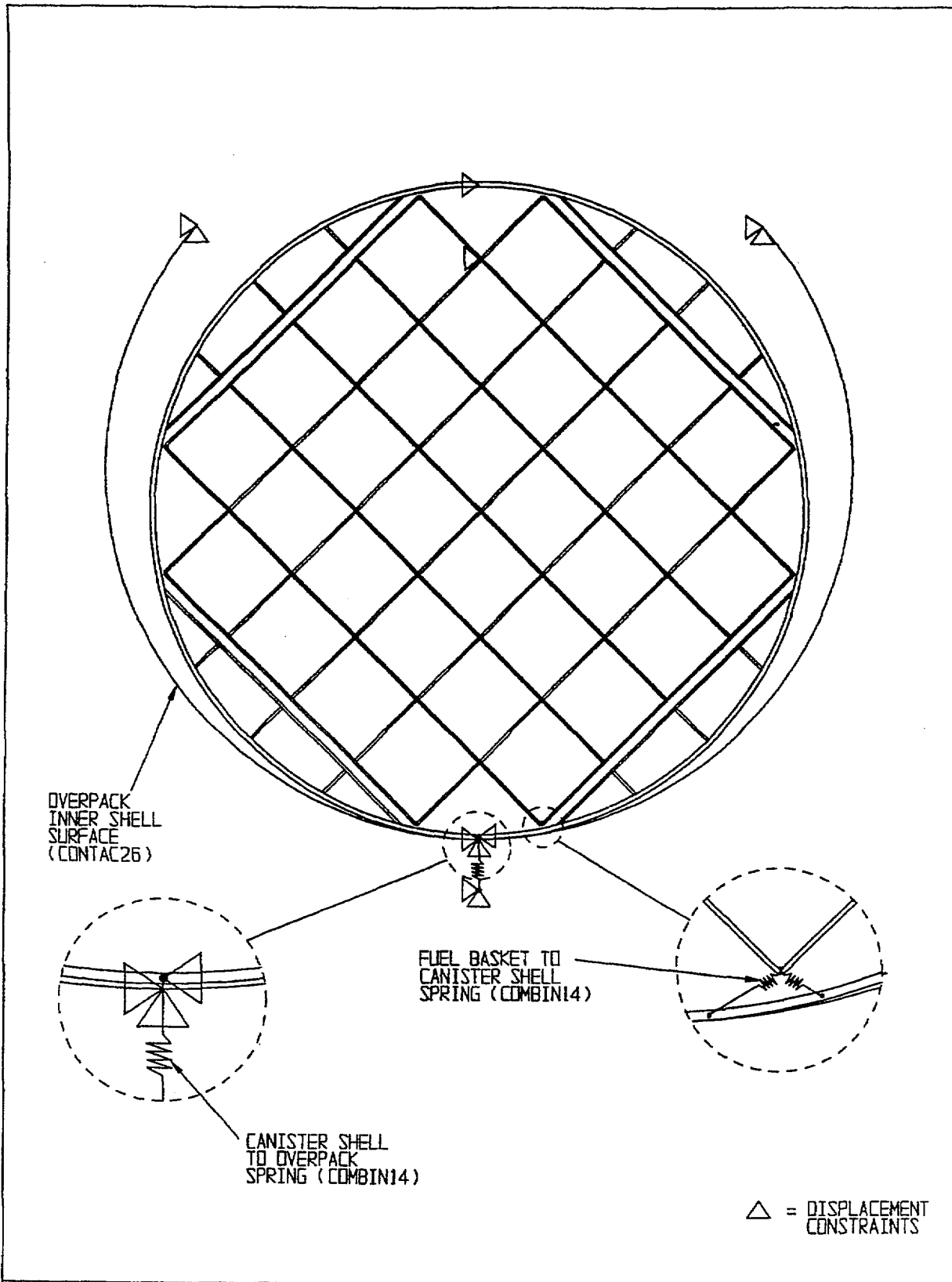


FIGURE 2.6.10; FINITE ELEMENT MODEL FOR MPC-32

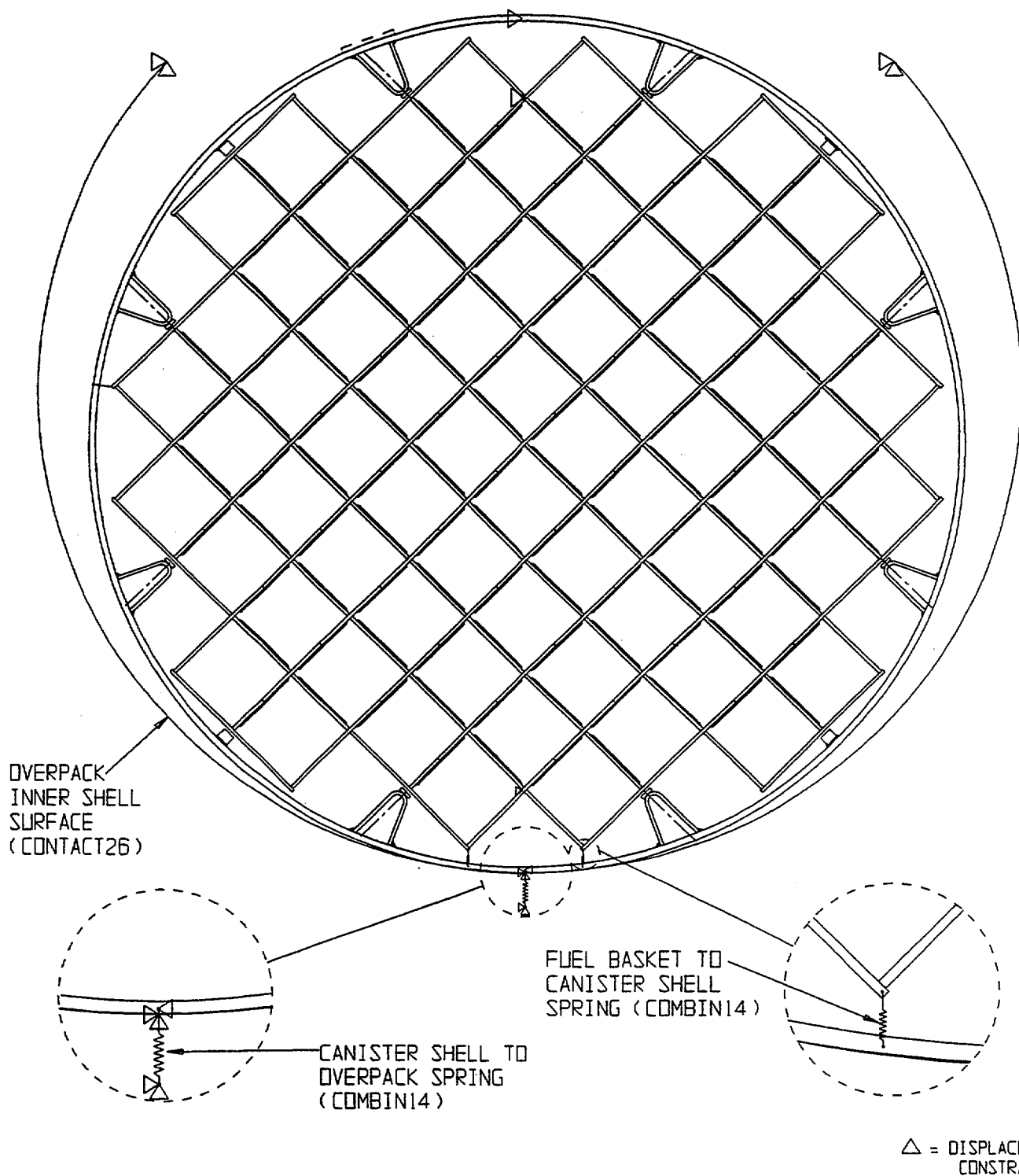
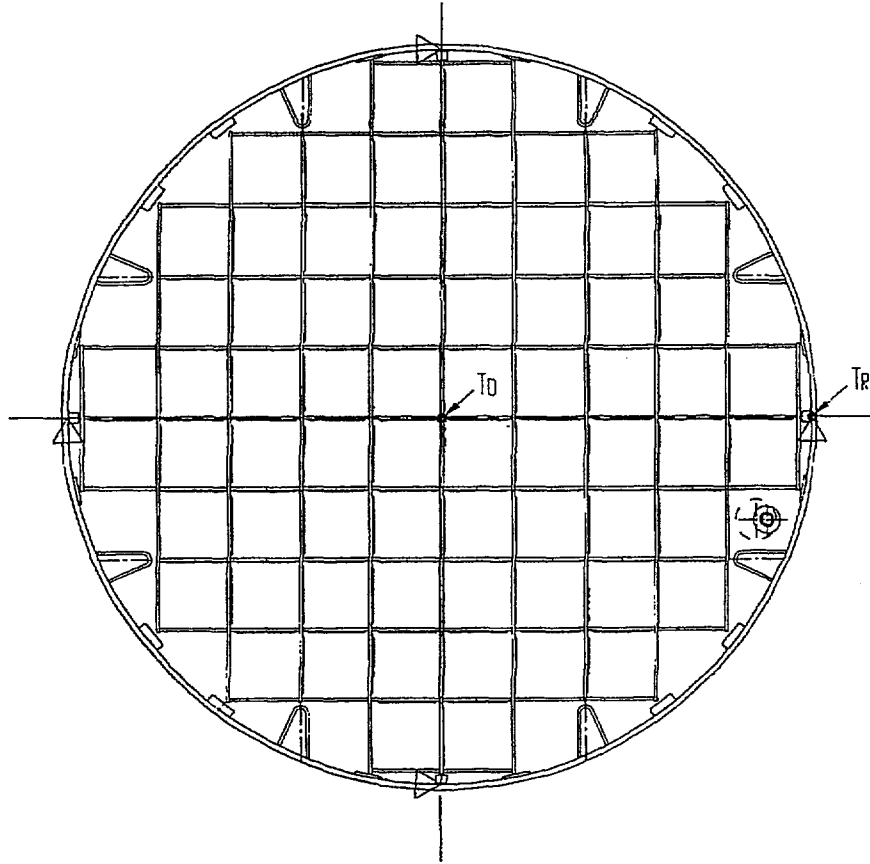
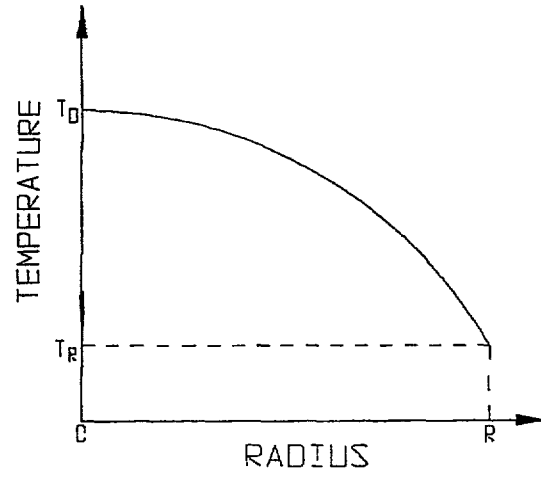


FIGURE 2.6.11; FINITE ELEMENT MODEL OF MPC-68

(45 DEGREE DROP MODEL)



\triangle = DISPLACEMENT CONSTRAINTS

FIGURE 2.6.12; MPC THERMAL LOAD

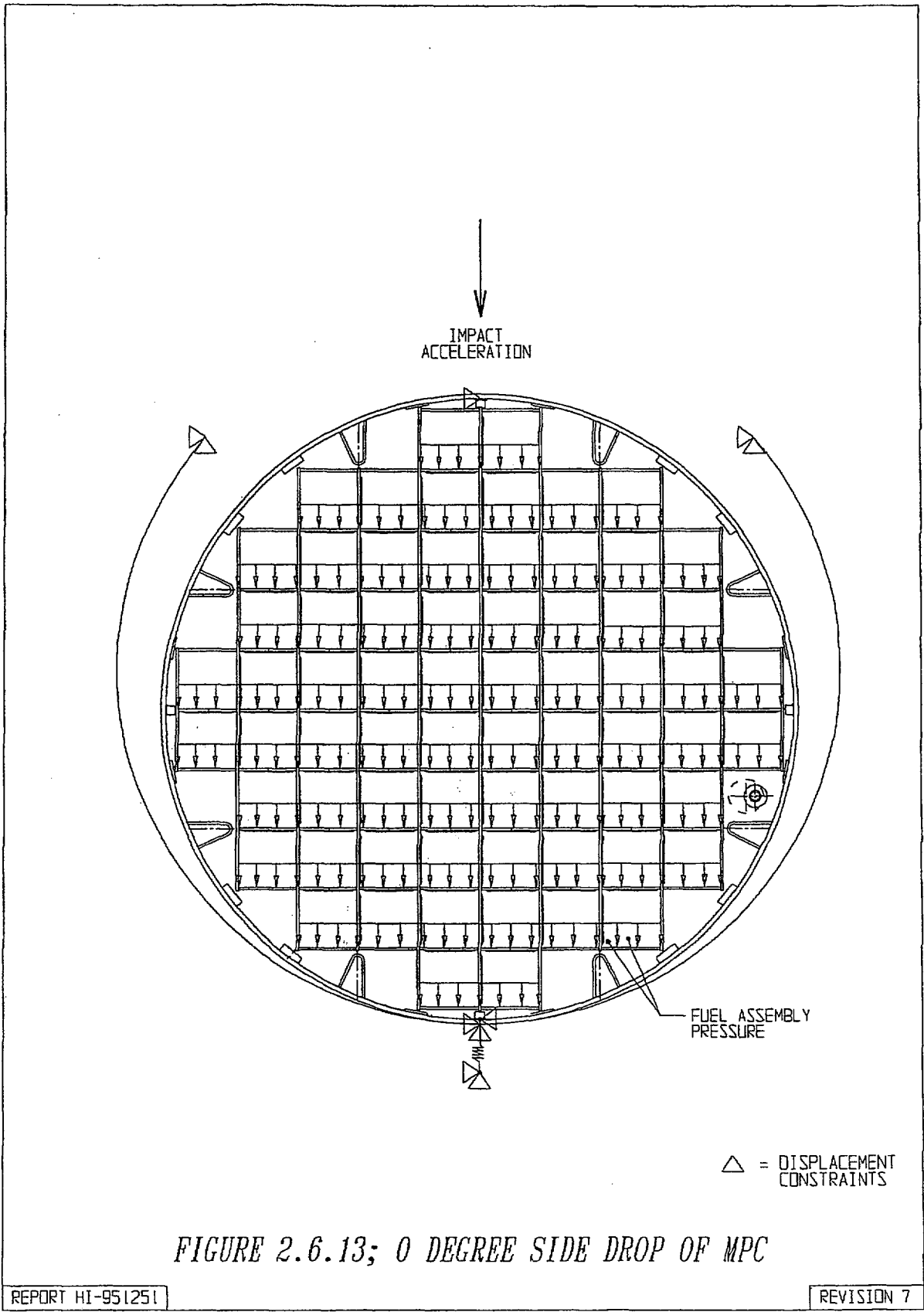


FIGURE 2.6.13; 0 DEGREE SIDE DROP OF MPC

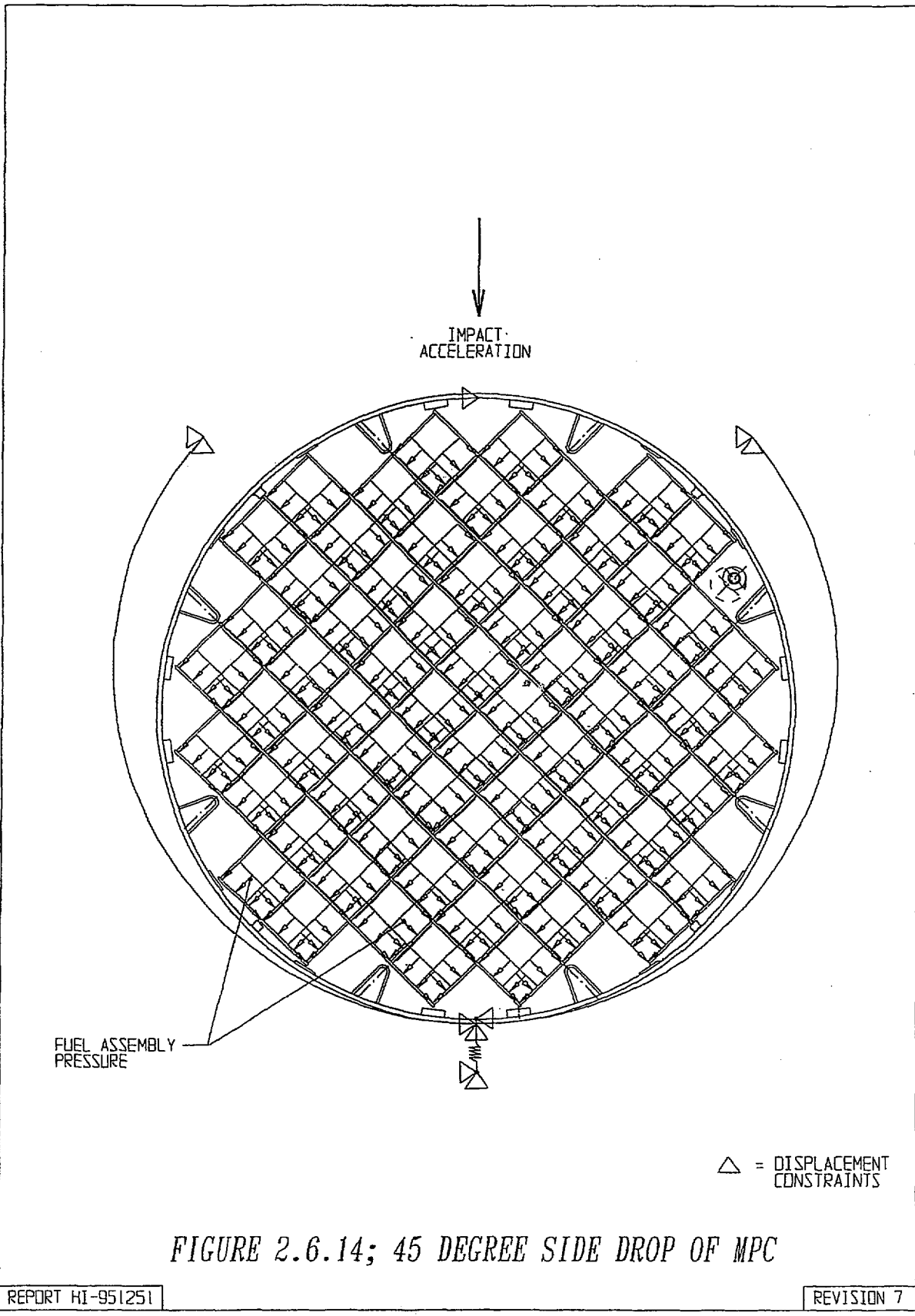
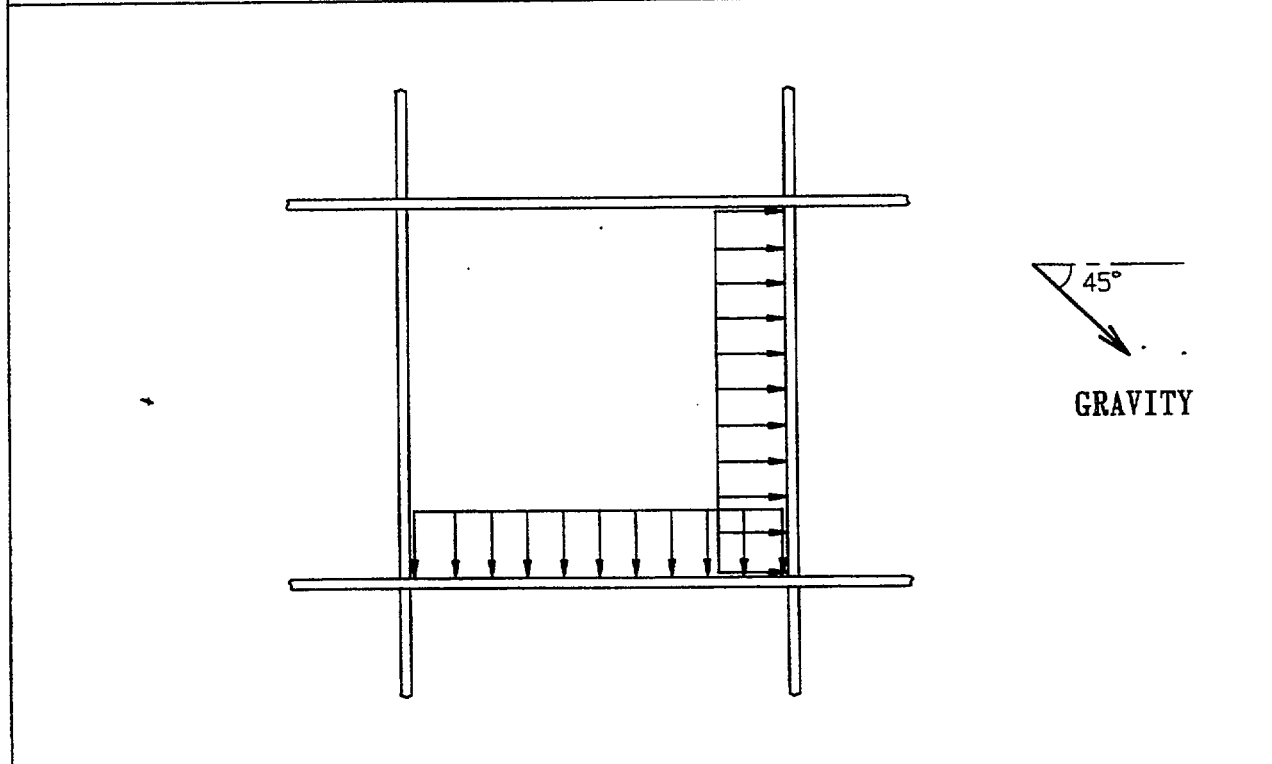
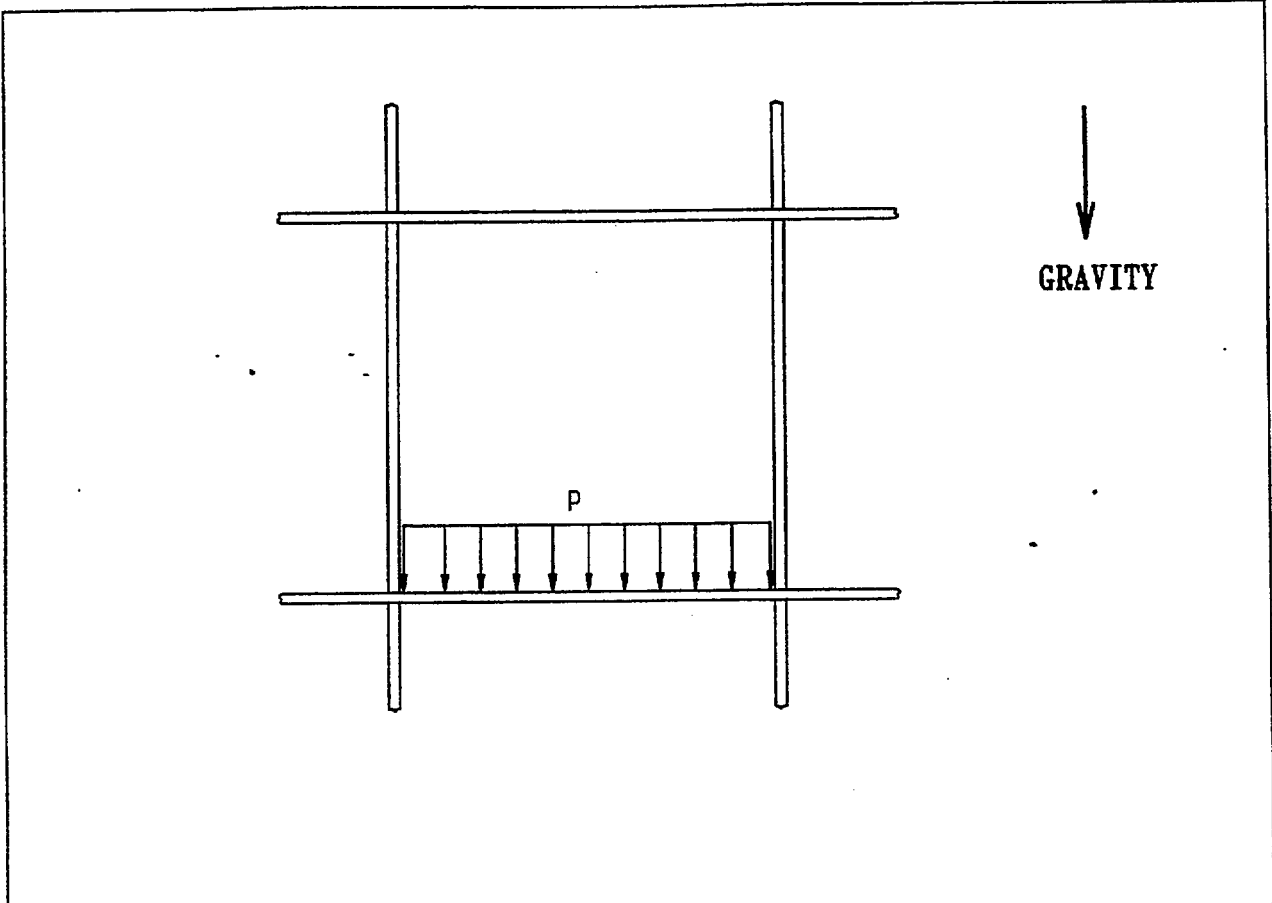


FIGURE 2.6.14; 45 DEGREE SIDE DROP OF MPC



**FIGURE 2.6.15; DETAIL OF FUEL ASSEMBLY PRESSURE
LOAD ON MPC BASKET**

Z
X

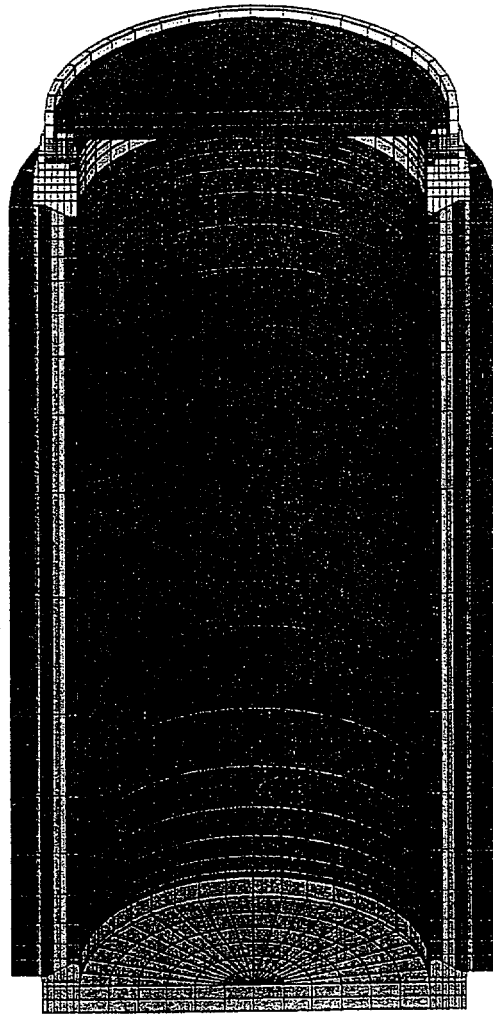


FIGURE 2.6.16 OVERPACK FINITE ELEMENT MODEL

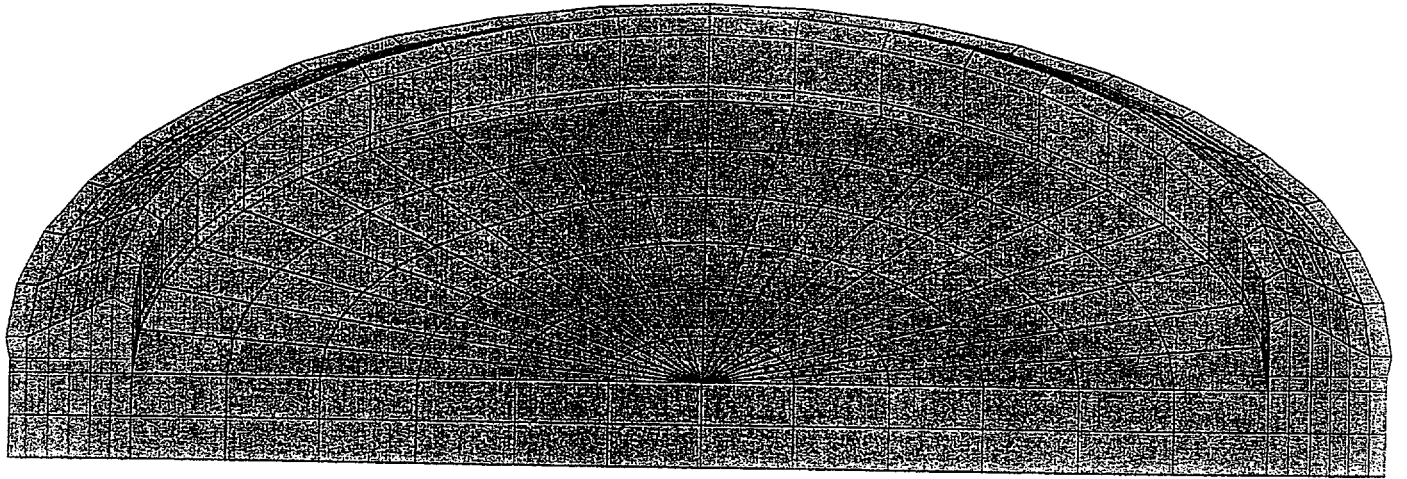


FIGURE 2.6.17 OVERPACK BOTTOM PLATE

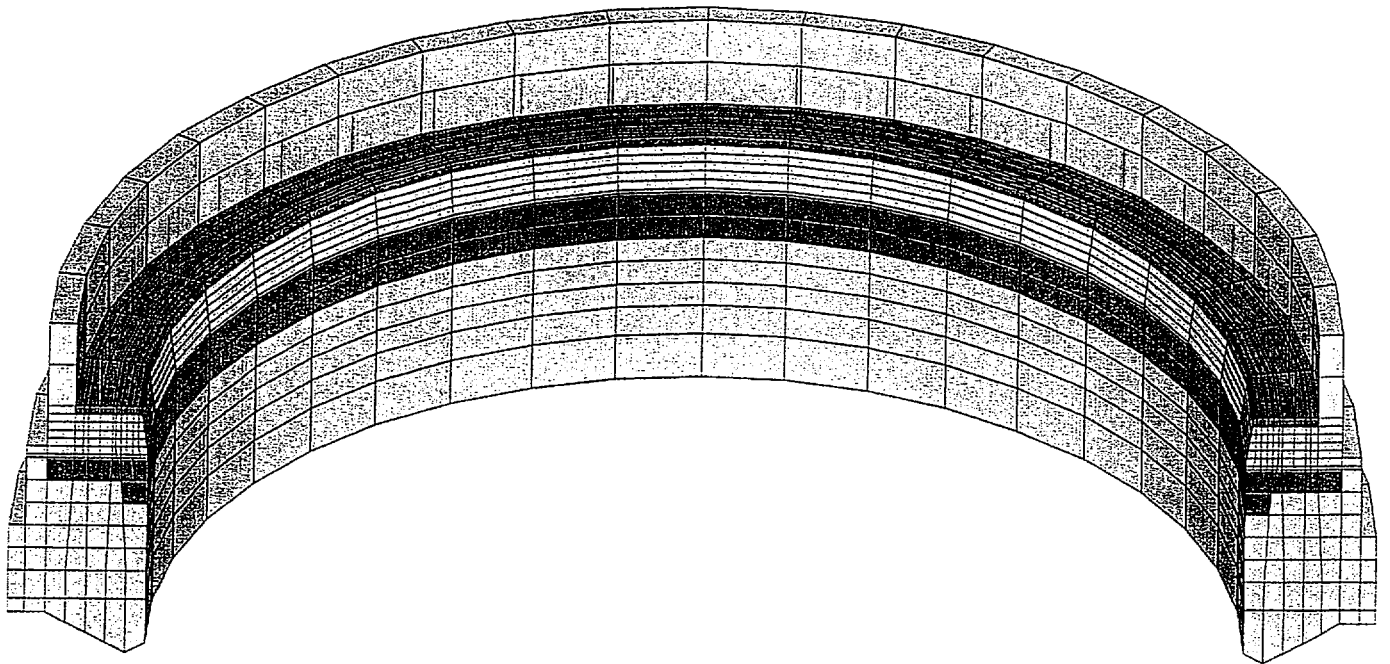
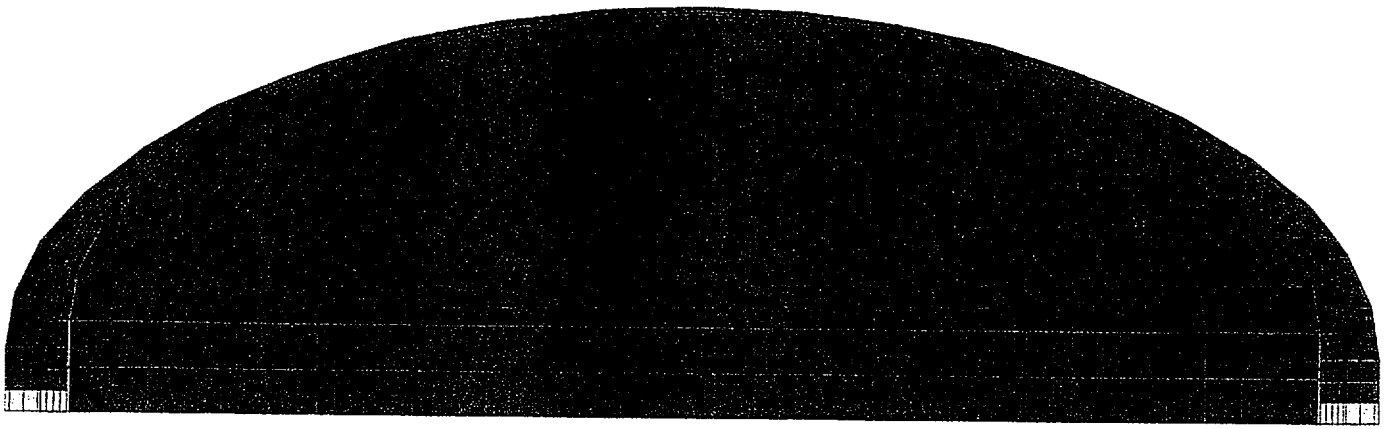


FIGURE 2.6.18 OVERPACK TOP FORGING



Z
X

FIGURE 2.6.19 OVERPACK LID

x
z

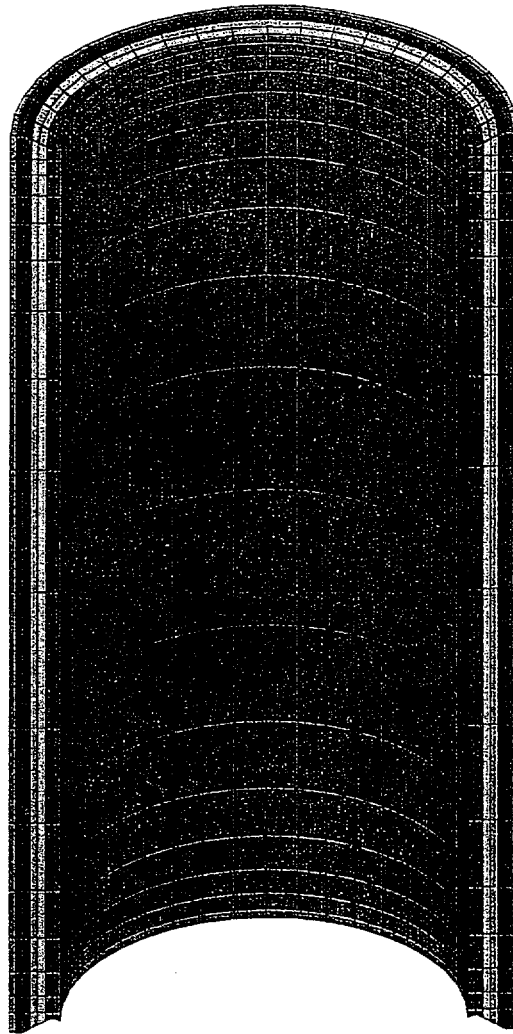


FIGURE 2.6.19A OVERPACK INNER AND INTERMEDIATE SHELLS

Z
X

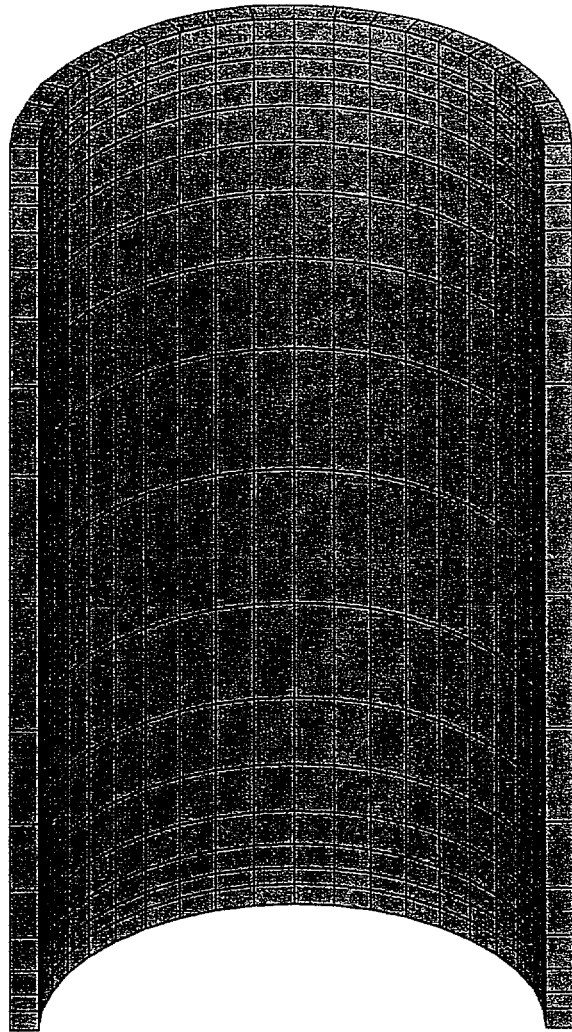
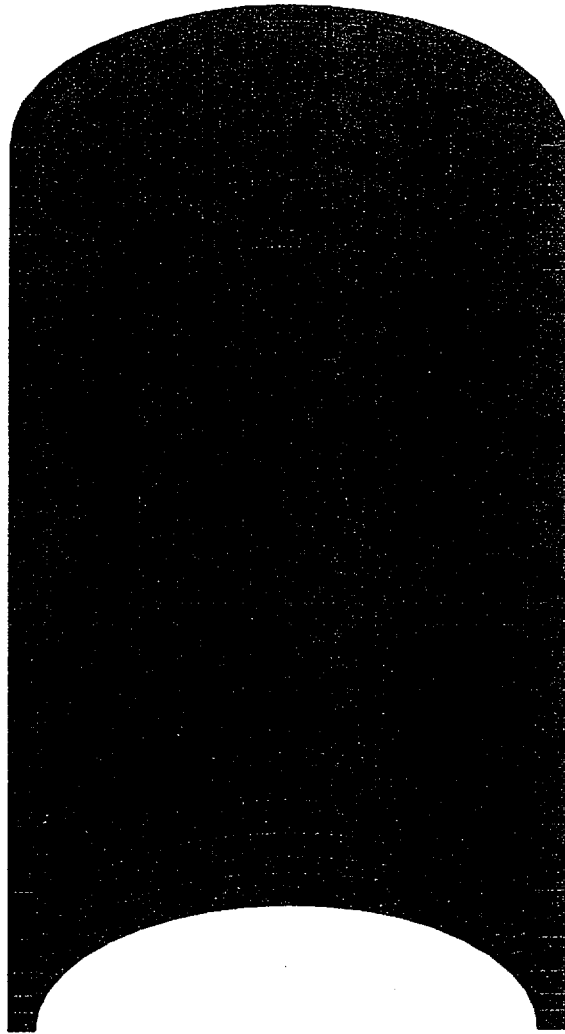


FIGURE 2.6.19B OVERPACK HOLTITE A ELEMENTS



Z
X

FIGURE 2.6.19C OVERPACK OUTER ENCLOSURE

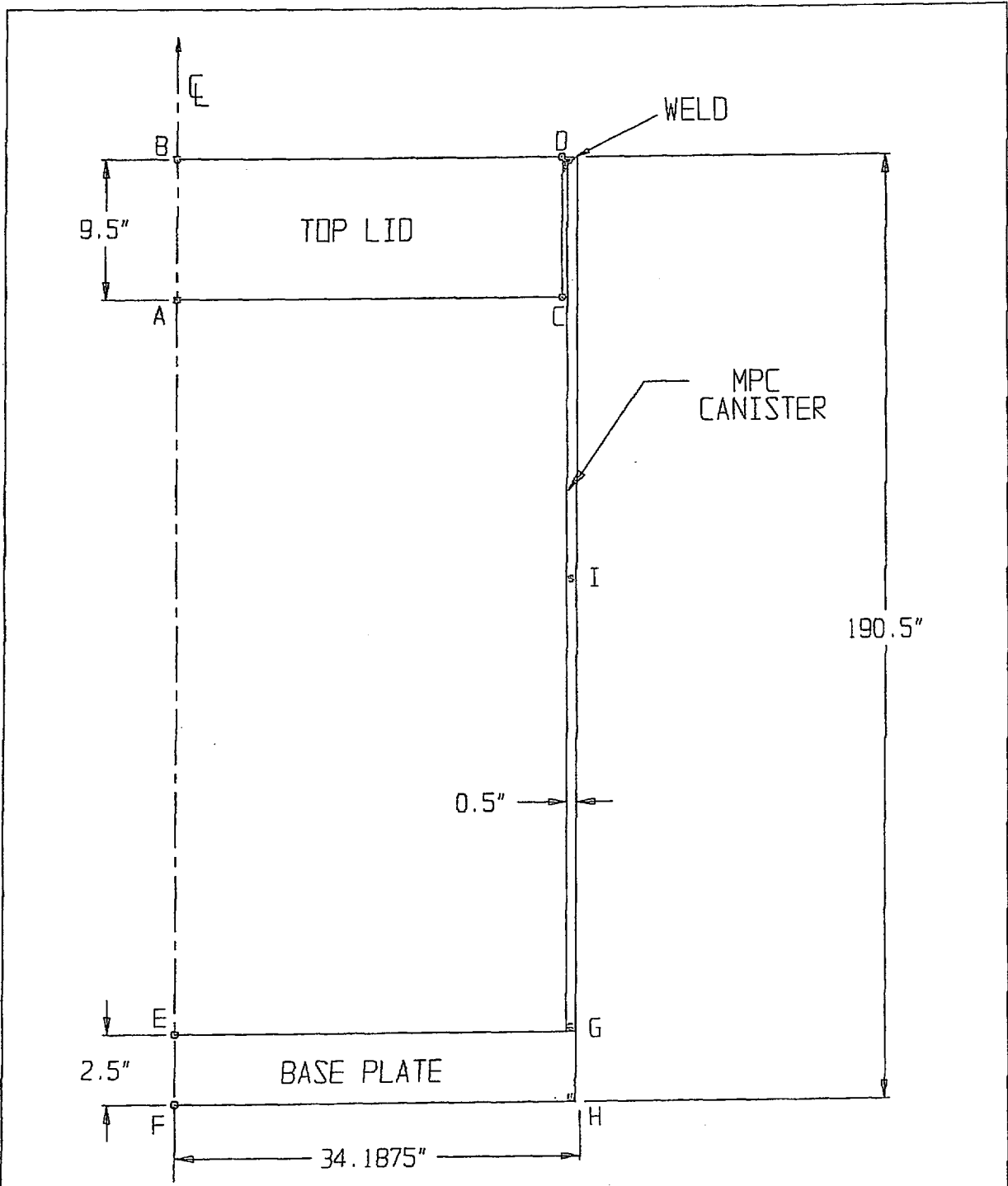


FIGURE 2.6.20 CONFINEMENT BOUNDARY MODEL SHOWING TEMPERATURE DATA POINTS

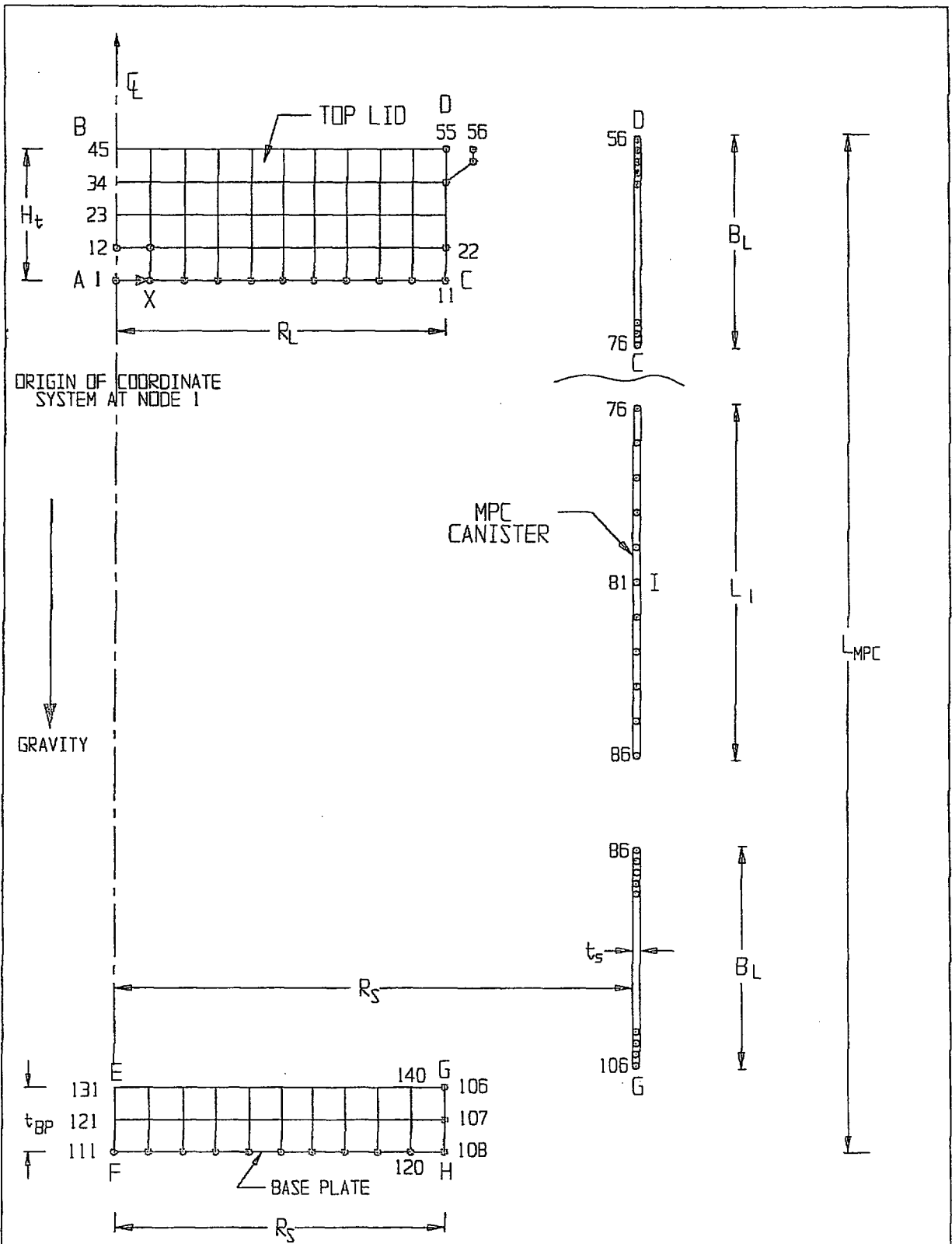


FIGURE 2.6.21 MPC - CONFINEMENT BOUNDARY
 FINITE ELEMENT GRID (EXPLODED VIEW)

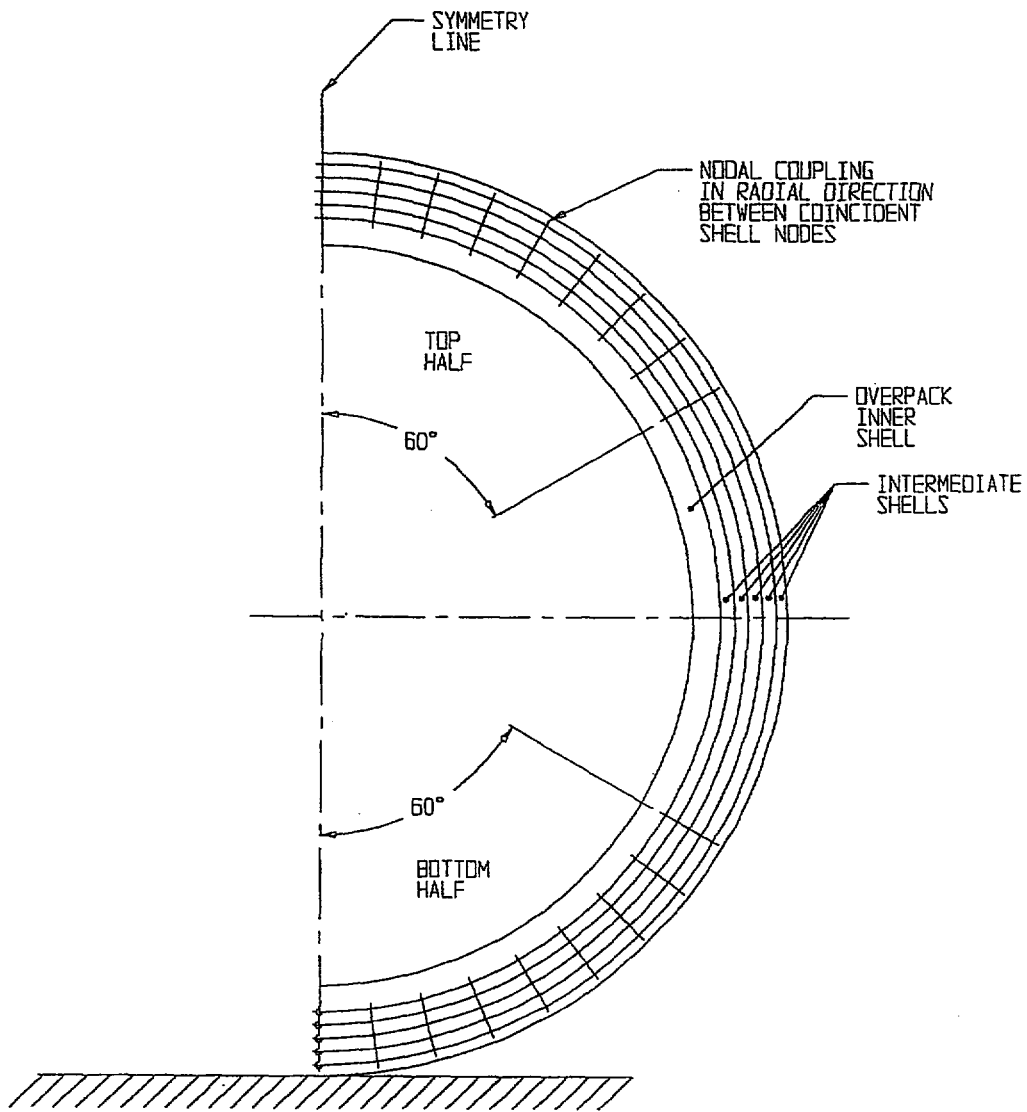


FIGURE 2.6.22; NODAL COUPLING IN OVERPACK
FINITE ELEMENT MODEL

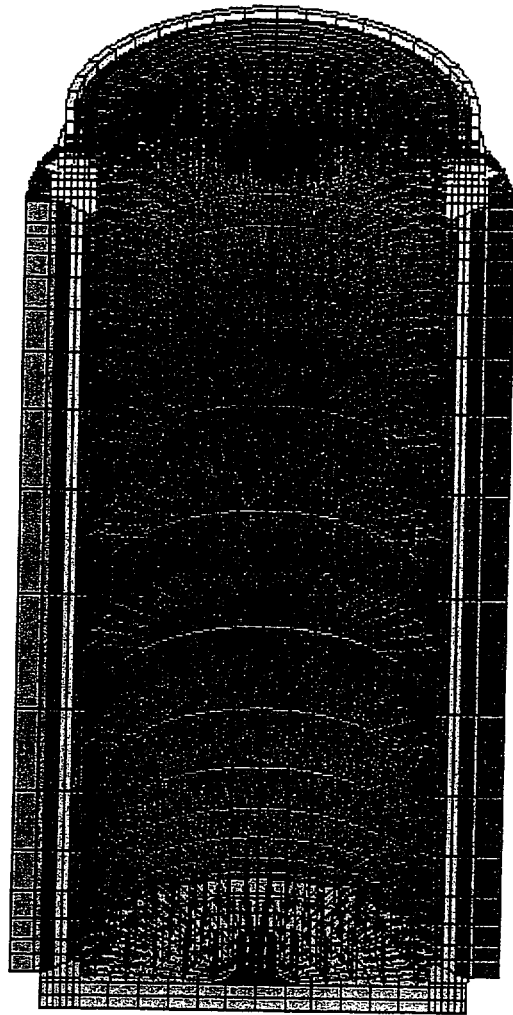


FIGURE 2.6.23 OVERPACK INTERNAL PRESSURE LOADING

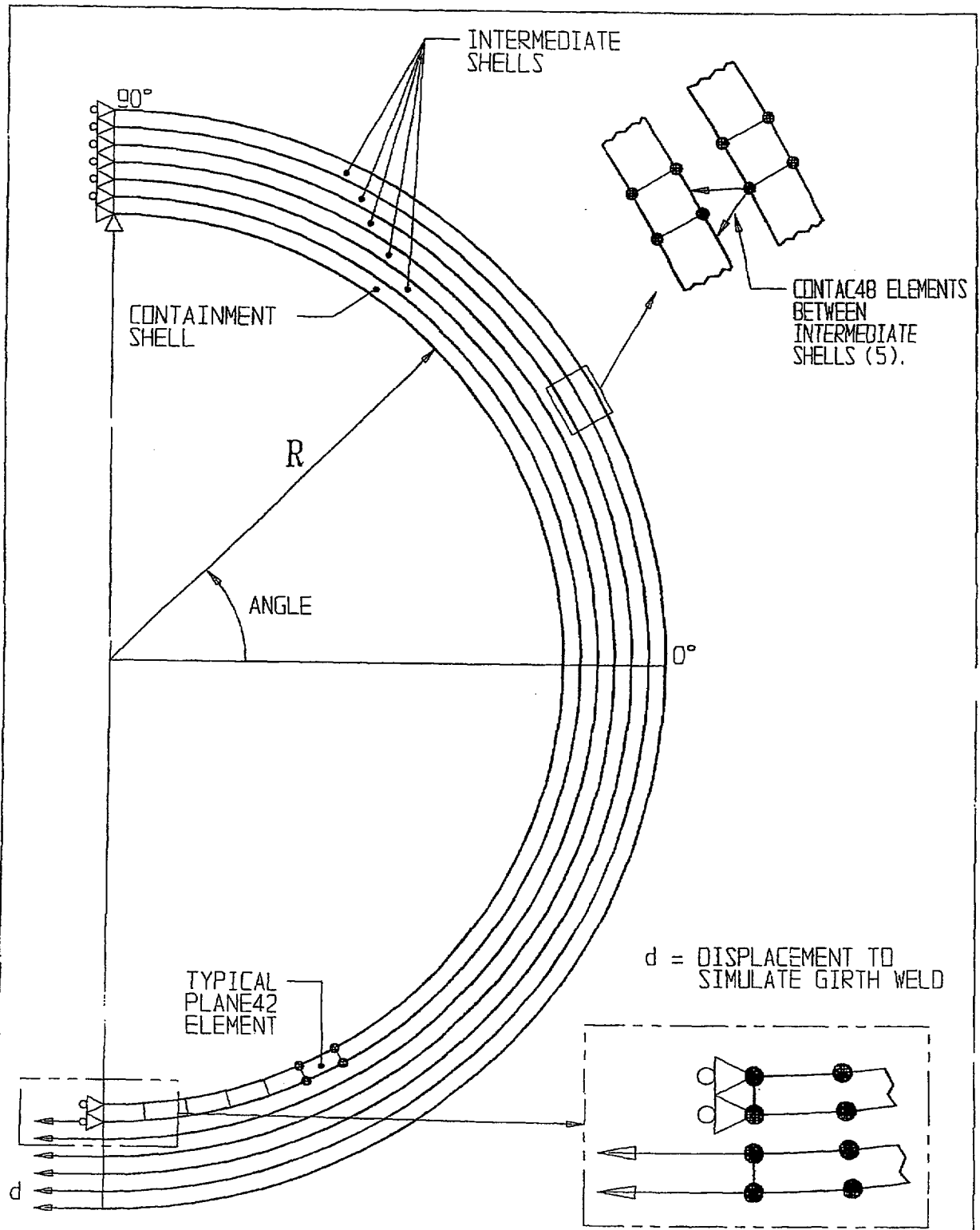
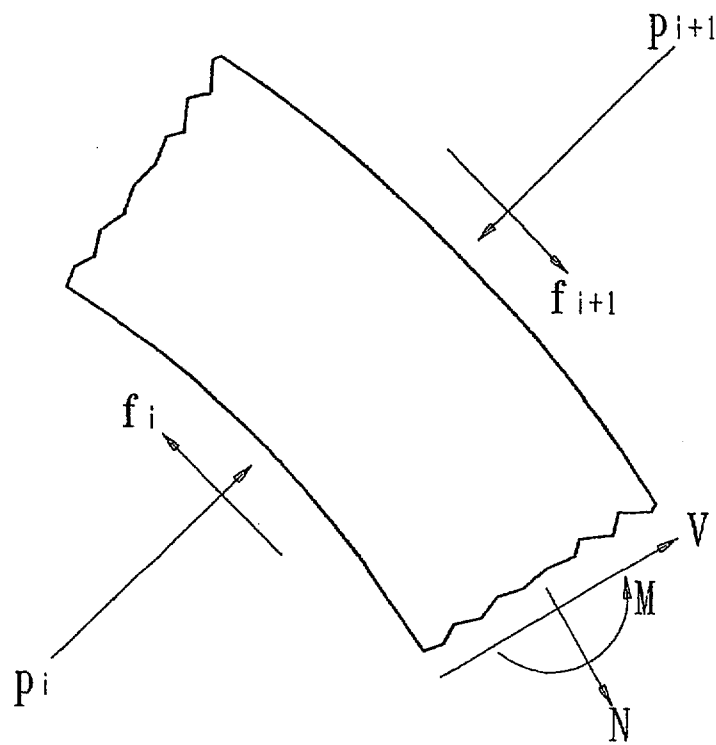


FIGURE 2.6.24 ; SIMULATION MODEL FOR FABRICATION STRESSES IN THE OVERPACK



$$|f_i| \leq \text{COF} * |p_i|$$

COF = COEFFICIENT OF FRICTION

FIGURE 2.6.25 PARTIAL FREE BODY DIAGRAM OF A SHELL SECTION